Polyelectrolyte Complex Micelles as Wrapping for Enzymes

Promotoren
Prof. dr. M. A. Cohen Stuart,
Hoogleraar Fysische Chemie en Kolloïdkunde

Prof. dr. ir. W. Norde,
Hoogleraar Bionanotechnologie

Copromotor
Dr R. J. de Vries
Universitair docent bij de leerstoelgroep
Fysische Chemie en Kolloïdkunde

Promotiecommissie

Prof. Dr. ir. I. M. C. M. Rietjens	Wageningen Universiteit
Prof. Dr. R. v. Klitzing	Technische Universität Berlin
Prof. Dr. M. Schönhoff	Westfälische Wilhems-Universität Münster
Prof. Dr. K. U. Loos	Rijksuniversiteit Groningen

Dit onderzoek is uitgevoerd binnen de onderzoeksschool VLAG

Polyelectrolyte Complex Micelles as Wrapping for Enzymes

Saskia Lindhoud

Proefschrift
ter verkrijging van de graad van doctor
op gezag van de Rector Magnificus
van Wageningen Universiteit,
Prof. dr. M.J. Kropff,
in het openbaar te verdedigen
op woensdag 16 september 2009
des namiddags te half twee in de Aula

ISBN: 978-90-8585-438-8

ψυχῆς πείρατα ἰών οὐκ ἂν
εξεύροιο πάσαν ἐπιπορευόμενος ὁδόν
οὕτω βαθὺν ἔχει

You would not find out the boundaries of the psyche,
even by traveling along every path: so deep a measure does it have

Heraklitus

Contents

Chapter 1

General Introduction

1.1. Enzymes are Proteins.

Nature is able to design molecules with specific functionality. Proteins are striking examples of such molecules which can have various functions and make life possible as it is. The trick to make these intriguing molecules is that nature makes use of 20 different building blocks, called amino acids. These amino acids have different properties, *e.g.,* some dislike water (hydrophobic), some like water (hydrophilic) and some are (electrically) charged. Because of the characteristics of the amino acids, proteins fold in a very specific way, depending on the sequence of amino acids in the protein molecule. This enables the formation of an enormous amount of 3D-structures. These structures are used either as building blocks, or as smart molecules that are able to perform mechanical actions *e.g.,* transmembrane pumps or transport proteins, or so-called enzymes that can catalyse specific chemical reactions. The molecule upon which an enzymes acts is called its "substrate."

Two examples of enzymes that are studied in this thesis are lysozyme and lipase. Lysozyme is a very ancient protein; its origin is estimated to go back for 400 to 600 million years.[1] The original function of this protein was to act as bacteriolytic defense agent. Most of the lysozyme molecules that are known nowadays still have this function. In our body lysozyme molecules are found, *e.g.,* in tears and saliva. Lysozyme is a very well studied enzyme and is easy to handle, therefore it was chosen to use this enzyme as a model protein. The lysozyme used in this thesis is the so-called Hen-Egg White Lysozyme, which is commonly available.

Lipase is an enzyme that assists the digestion of fatty acids. It is widely found in the animal kingdom, as well as in microorganisms and plants. In our bodies lipases are mainly found in the pancreas, where digestive fluids are produced that are injected in the duodenum.[2] The specific reaction which is carried out by lipases is the hydrolysis of the ester-bonds of triacylglycerol molecules. The best studied lipases are water-soluble, but their natural substrates are water insoluble. Hence, the optimum location for lipases to be active is at the lipid-water interface. This makes determination of the enzymatic activity rather complicated.[3] The lipase used in this thesis is Lipolase™, derived from the fungus *Humicola ℓanuginosa*, and was a gift from Novozymes (Bagsvaerd, Denmark).

1.1.1. Enzyme stabilisation

The 3D-structure of an enzyme is very important to perform its biological task. Small changes in the environment, *e.g.,* temperature change or changes of the electrostatic forces (due to changes in pH or salt concentration), can have an effect on the functioning of enzymes. When the three-dimensional structure is irreversibly damaged it is called denaturation. An example of everyday life denaturation of proteins is the boiling of eggs. After cooking, the egg white will not become liquid again due to denaturation, followed by the aggregation of the proteins in the egg white. All the protein molecules have formed a large aggregate together, and return to the native (liquid) state is completely blocked.

Industrial applications require a certain stability of the enzymes, but since enzymes are rather fragile, and may denature when the environmental circumstances change, it is desired to protect enzymes. There are several possible solutions to achieve such protection. Here, we will restrict ourselves to stabilisation protocols where physical driving forces are used, *i.e.,* chemical modifications of proteins or chemical attachment of proteins to substrates will not be discussed.

There exist numerous ways to physically stabilise enzymes in solution by using a support of some sort. On close inspection, they all come down to two principles: (I) adsorption onto a substrate (of any size) and (II) incorporation in a pre-made or self-assembling structure. By adsorption of an enzyme to a support the physical driving forces that one can make use of are Van der Waals forces, hydrophobic interactions and electrostatic interactions. Figure 1a is a simple picture of enzymes adsorbed to a particle. Whether or not this is a suitable method for the enzyme to be stabilised depends on the nature of the substrate and the enzyme itself. When the interaction between the enzyme and the surface is such that the structure of the enzyme is not affected, this may be a very useful procedure.[4] Moreover, the enzyme molecules that are closely adsorbed should not influence each other in a negative way, for instance, by forming biologically inactive aggregates.

A way to achieve deposition of isolated enzymes on a solid support is to make use of a porous material. This also has the advantage of increasing the amount of deposited enzyme per unit mass (see figure 1b). Traditional porous materials have a wide range of pore sizes. The polydispersity of the pore sizes is disadvantageous for enzyme immobilisation, since in larger pores the enzymes can still adsorb closely to each other which, in turn may effect their activity. By making use of surfactant templates, ordered mesoporous materials can be produced with a precisely controlled pore size, varying from $2 - 30$ nanometer.[5] A major advantage of this material is its high specific surface area;[6–8] in addition, the confinement effect may improve the enzyme stability and activity.[6,9,10] The uniform surface chemistry

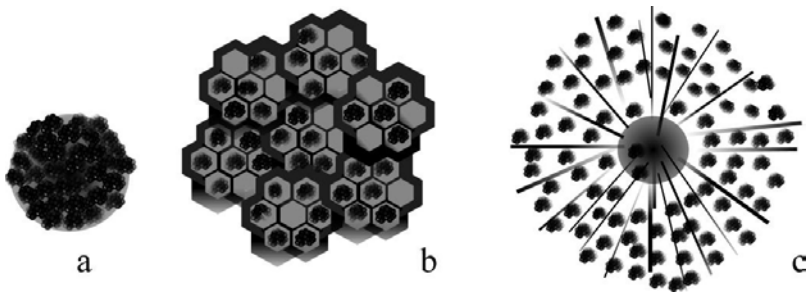

FIGURE 1. **Different ways to stabilise enzymes. a).** solid support, **b).** in porous material and **c).** in the shell of a core-shell particle.

offers predictable enzymatic behaviour, and the method is rather simple.

Another requirement a support should fulfil when it is used for industrial applications is the accessibility to the substrate. One can imagine that within these pores not all the enzymes are equally accessible. Therefore, one could think of other structures to circumvent this problem. An example is shown in figure 1c. Here, a core-shell particle is shown with enzymes incorporated in the shell via, *e.g.,* electrostatic interactions. These specific particles are studied extensively by Ballauff *et al.,*.[11] It has been shown that enzymes incorporated in these brushes retain their secondary structure[12] and remain active.[13] Moreover, enzymes can fairly easily be released by raising the salt concentration.[14] Another advantage of using core-shell particles is that the core may be made of some sort of magnetic material, allowing for recycling of these structures.

In this thesis the incorporation of enzymes in a new kind of assembly, namely polyelectrolyte complex micelles will be investigated. The main difference between the previously discussed structures and these polyelectrolyte complexes micelles is that the micelles are formed in the presence of the enzymes, whereas the other structures are synthesised before the enzymes are introduced. Preparing the structures in presence of the enzymes requires a certain gentleness, because the procedure should not destabilise the 3D structure of the enzyme molecule. The basis of the polyelectrolyte micelle formation is electrostatic co-assembly of two oppositely charged macromolecules. Therefore, it will first be explained what polyelectrolytes are and how polyelectrolyte complexes and polyelectrolyte complex micelles (with and without enzymes in the core) are formed. Subsequently, some possible applications of these micelles with enzymes in the core will be discussed.

1.2. Polyelectrolytes and polyelectrolyte complexes.

A polymer is a macromolecule consisting of repeating structural units ("monomers") that are connected by chemical bonds. Polymers are ubiquitously present in every day-life. Most plastics are polymers, most food contains polymeric substances, and our body largely consists of polymers. The polymers in plastics are mostly polymers that are made petrochemically. There are all sorts of synthetic polymers each having different physical and chemical properties. The polymers in food are made by nature, or are derived from natural polymers. These polymers are (also) called biopolymers. An example of a biopolymer which is present in food is starch. The polymers we have in our body are also biopolymers. We can make these polymers ourselves from what we eat. Examples of polymers that are found in our body are DNA and proteins. So, the polymers we make in our body are very smart functional polymers.

In this thesis polymers are used that bear charge. These polymers are called polyelectrolytes and their main feature is that they are charged in an aqueous environment. This means that polyelectrolytes consist of repeating structural units that can be charged. When a polyelectrolyte consists of only one type of monomers it will be referred to as a homopolymer; this polymer is either negatively or positively charged. In solution polyelectrolytes are accompanied by counterions: a positively charged polyelectrolyte is accompanied by negatively charged small ions (*e.g.,* Cl^-) and a negatively charged polyelectrolyte is accompanied by positively charged small ions (*e.g.,* Na^+). This is because systems have to be (or become) electroneutral: substantial separation of charges is energetically very costly and cannot occur.

When oppositely charged homopolymers are mixed under the right conditions, *e.g.,* mixing ratio, salt strength, *etc.,* they form polyelectrolyte complexes, because positive and negative charges attract each other. One may now wonder why that is, because it was just said that the polyelectrolyte and its counterions are together electroneutral. There is however, a very important thermodynamic law which tells us that systems try to increase their entropy. Simply said, it is favourable to reach as much disorder as possible. This is depicted in figure 2 where a polyelectrolyte complex is formed between to oppositely charged polyelectrolytes. It can be seen that before the "reaction" there are two electroneutral objects (the 2 polyelectrolytes that are accompanied by their counterions). After the reaction there are 21 objects: 1 electroneutral polyelectrolyte complex and 20 free counterions. So the disorder after the reaction has increased. This counterion release is a major (but not the only) driving force of polyelectrolyte complex formation.

In the previous section, it was stated that proteins may have charged amino acids, both positively and negatively. This means that proteins can also act as a polyelectrolyte. Proteins are polyampholytes *i.e.,* they carry

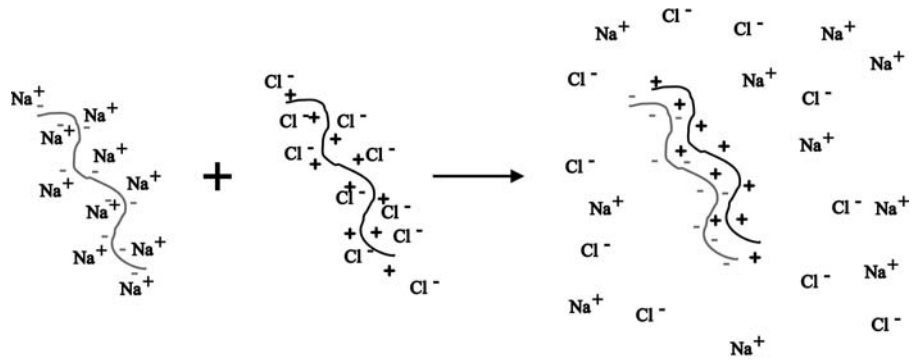

FIGURE 2. Polyelectrolyte complex formation.

both positive and negative groups. These groups can undergo proton exchange and therefore their net charge, and charge sign, is dependent on the pH of the solution. At low pH proteins are positively charged, and at high pH they are negatively charged. This means that there must be a pH at which a protein is electroneutral; the pH at which this happens is called the iso-electric point. This iso-electric point is a property of the protein. In this thesis we have studied proteins at pH 7. Lipase has its iso-electric point at pH= 4.3 and is therefore negatively charged at neutral pH whereas lysozyme, the iso-electric point of which is at pH= 11, is positively charged.

Because proteins are charged at pH-values other than their iso-electric point, they are able to form complexes with oppositely charged polymers. There are two classes of protein-complexes that are formed at close to stoichiometric charge ratio. Like polyelectrolyte complexes consisting of homopolyelectrolytes, these complexes can be solid-like precipitates, which may have a well-defined structure,[15–18] but it may also be that a liquid-like phase is formed. This liquid-like phase is called a complex coacervate phase.[19] Complex coacervation has often been observed when a charged polysaccharide and an oppositely charged natural polyelectrolyte are mixed under the right conditions.[20–22] The relatively low charge density of these polymers is the reason that complex coacervation occurs rather than precipitation. When protein molecules and homopolymers are mixed in such a way that one of the two is in excess, soluble complexes may be formed.

1.3. Polyelectrolyte complex micelles.

For *e.g.,* biomedical applications it is desirable to make a stable solution which contains polyelectrolyte complexes of nanometer size. A way to achieve this is to make use of special polyelectrolytes, of which at least one

is attached to a non-charged, water soluble block. Upon mixing such a so-called diblock copolymer at stoichiometric charge ratio with an oppositely charged homopolymer, particles appear consisting of a relatively compact (complex) core, and are surrounded by a dilute corona of the neutral water soluble block. In the literature these kind of structures are given various names: Polyion Complex Micelles (PIC-micelles),[23] Block Ionomer Complexes (BIC),[24] and Complex Coacervate Core Micelles (C3M's).[25] In this thesis these objects will mainly be referred to as Polyelectrolyte Complex Micelles. A schematic representation of the polyelectrolyte complex micelle formation is given in figure 3.

Because proteins can be regarded as (special) polyelectrolytes, these molecules may also form micelles when they are mixed at stoichiometric charge ratio with oppositely charged diblock copolymers. Figure 4 is an illustration of this micelle formation. Over the last ten years this type of bionanostructures has attracted a lot of attention.[26,27] These micelles may be applicable as controlled release systems for *e.g.,* functional components, or as bionanoreactors.

When one considers figure 4, one can imagine that the enzyme molecules in the middle of the core are hardly accessible to substrate molecules. This would make such a particle very inefficient as a bionanoreactor. To overcome the problem of accessability to the substrate it was decided to "dilute" the core with homopolyelectrolyte. In such a three component system the amount of enzyme in the core of the micelles can be controlled by varying the ratio between homopolymer and protein. In figure 5 a sketch of the micelle formation of such a three component system is shown. An additional advantage is that the micelles become more stable against disintegration by salt.

1.4. Possible applications of these enzyme-containing micelles.

Scientific work (always) requires a certain context, such as a practical application, in order to make it appealing to the general public. Knowledge about enzymes wrapped in polyelectrolyte complex micelles, which is generated by the work described in this thesis, could be applicable in different fields. Enzymes are used in many industrial processes, *e.g.* brewery, cheese production, baking, cosmetics, laundry, *etc.,*. Whenever it is possible to somehow control or influence the enzymatic activity of incorporated enzymes, these micelles may be very useful in biotechnology.

One aspect may be the specific protection of an enzyme in mixtures of different enzymes. As an example one could think of enzymes used in liquid laundry detergents. Here, fat degrading (lipases) and protein degrading enzymes (proteases) are present in the same solution. The shelf-life of such a solution may be very short, because the proteases are able to degrade the

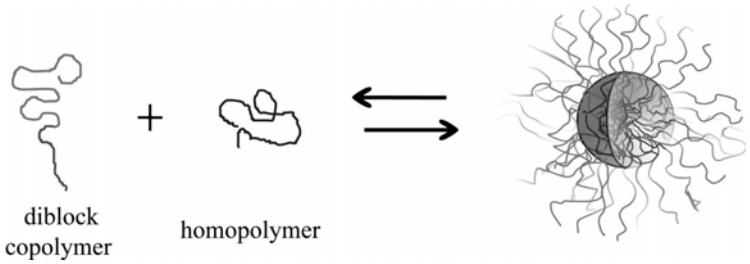

FIGURE 3. Complex formation between a charged diblock copolymer and oppositely charged homopolymer.

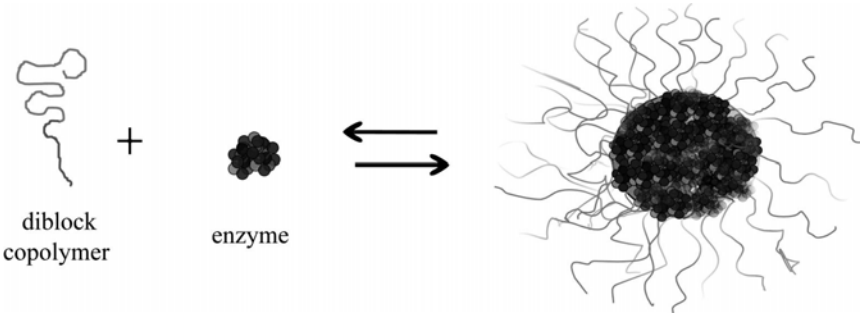

FIGURE 4. Complex formation between a charged diblock copolymer and oppositely charged enzyme.

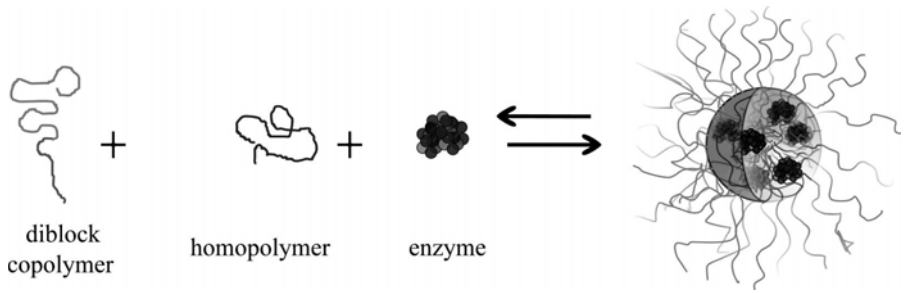

FIGURE 5. Complex formation between a charged diblock copolymer and an oppositely charged homopolymer and protein.

lipases. Incorporation of one of these enzymes in polyelectrolyte complex micelles may solve this problem.

Also in food and pharma applications these nanostructures may be of use. In food, one could think of wrapping badly tasting, yet healthy substances, in micelles. When the micelles arrive in the stomach, the acid environment will induce disintegration of the micelles and the functional component will be released.

For pharmaceutical applications several aspects are relevant. These micelles are so small that they are not attacked by phagocytes in the immune

system.[28] Because of this, the micelles might be applicable for targeted release. Another application is the storage of therapeutical proteins. When these proteins are incorporated in the micelles the colloidal stability of the protein-containing solution may be increased. Increased shelf-life is also one of the properties pharmaceutical companies are trying to achieve nowadays.

The information that is obtained by this research is also relevant from a fundamental point of view. Polyelectrolyte complex formation is an extensively studied phenomenon of which the thermodynamics is not (yet) fully understood. Correlations are observed between relaxation time and the enthalpy of the complex formation, but the details are still lacking. This research may also contribute to a better understanding of the dynamics and thermodynamics of polyelectrolyte complex formation.

Another interesting aspect is that the behaviour of enzymes in these polyelectrolyte complexes may contribute to a better understanding of the behaviour of proteins in multicomponent systems. An example of a multicomponent system is the cytosol, found within cells. In cells many different types of molecules coexist, all having their own sophisticated task. Since in cells a certain amount of these molecules is charged (RNA, proteins), studying enzymes in polyelectrolyte complexes may contribute to the understanding of the behaviour of enzymes in crowded environments such as cells.

1.5. How to study these polyelectrolyte complex micelles.

Objects with nano dimensions are difficult to study, because one cannot simply see them. The smallest objects we can see by eye are approximately 200 micron (0.2 mm). Using a light microscope one may see objects up to 200 nm (0.0002 mm). The micelles we are studying have a radius of approximately 25 nm (0.000025 mm). By using an electron microscope objects with these dimensions can be seen. Because deep vacuum must be maintained, electron microscopy requires samples to be in the solid state but we want to study these micelles in solutions. Using a special technique which is called cryogenic transmission electron microscopy (Cryo-TEM), very quickly frozen samples can be seen. It is assumed that rapid cooling down does not affect the structure of the complex. An example of a Cryo-TEM image of a complex consisting of lysozyme and a negatively charged diblock copolymer (PAA_{42}-$PAAm_{417}$) is shown in figure 6; only the core of the objects can be seen.

Because it is desired to also obtain dynamical and structural information about the formation of the micelles and the behaviour of the micelles in solution, scattering techniques are useful. The techniques which were mostly used in this thesis are Dynamic and Static Light Scattering (DLS and SLS). When light hits a particle, the light is scattered in all directions.

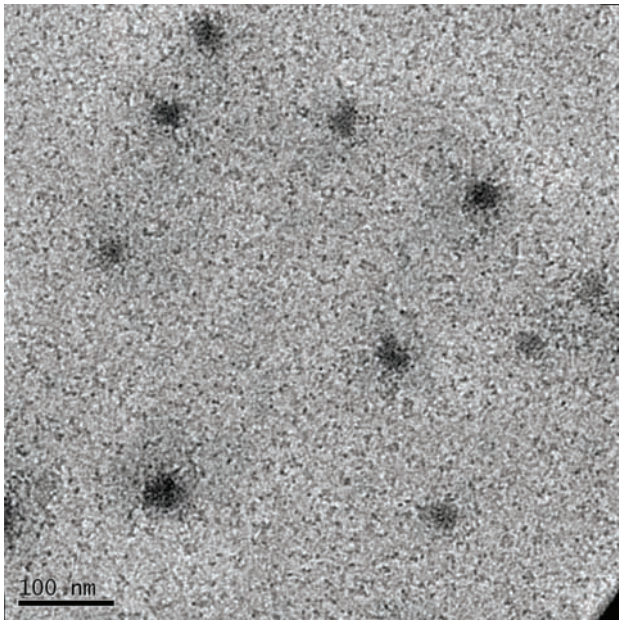

FIGURE 6. CryoTEM image of a complex consisting of lysozyme and a negatively charged diblock copolymer (PAA_{42}-$PAAm_{417}$)

If the light source is a monochromatic laser and the particles are smaller than the wavelength of the light that is used (< 250 nm) one can derive structural information about the scattering objects. This is illustrated in figure 7. In the first figure one can see a primary beam hitting a sample and the scattered intensity at a certain angle θ, is followed in time. One can see that the intensity fluctuates in time because there is a certain contrast between the solvent and the particle. The fluctuations in intensity are due to the (Brownian) motion of the particles. From the autocorrelation of the fluctuations (measured with DLS), the diffusion coefficient can be determined. Via the Stokes-Einstein relation this diffusion coefficient gives information about the size of the particles. Thus, from dynamic scattering one can obtain information about the size of the particles.

In the second sketch in figure 7, scattering intensity is studied as a function of the angle θ. Using this technique, which is called static scattering, structural information may be obtained. If one is able to accurately perform such an experiment, it is also possible to determine the mass of the particles. When such an experiment is performed with a laser (light), it is called Static Light Scattering (SLS), but other radiation sources can be used as well. In this thesis, Small Angle Neutron Scattering (SANS) has been used. Unlike light scattering, neutron scattering originates from differences in scattering length density between the solvent and the particles. The scattering length density is a property of the nucleus of an atom, *i.e.,*

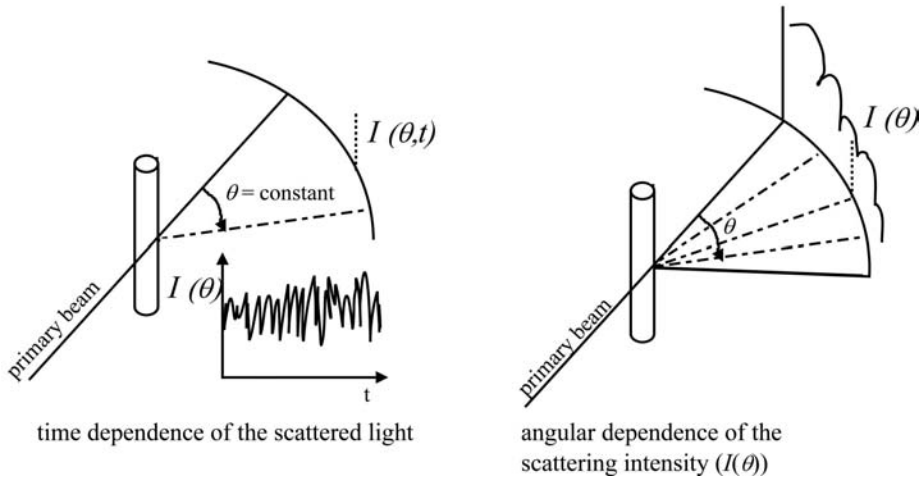

FIGURE 7. Dynamic and static scattering.

this is a specific number for each individual atom.

1.6. Aim and outline of this thesis.

This thesis is about enzymes wrapped in polyelectrolyte complex micelles. The final goal was to study the activity of incorporated enzymes. In order to achieve such a goal various aspects of the formation and stability of the micelles have to be known. Therefore, the formation of the micelles has been studied in detail first. When the best protocol for the micelle formation is known, the behaviour of the micelles as function of the salt concentration is important. Several applications require a certain salt strength, *e.g.,* it is important to know whether the micelles are stable under physiological conditions.

The following three chapters (2-4) will deal with this micelle formation. In chapter 2 we shall discuss how to obtain stable micelles with enzymes in the core and how the amount of incorporated enzymes can be tuned. From this we learnt that three components are needed to prepare stable micelles: diblock copolymers, homopolymers and enzymes.

Since three components are needed for the micelle formation, the sequence in which these components are mixed may be important. Chapter 3 deals with relaxation phenomena observed during polyelectrolyte micelle formation. In this chapter two micellar systems are studied: (A) negatively charged diblock copolymers (PAA_{42}-$PAAm_{417}$), positively charged homopolymers ($PDMAEMA_{150}$) and positively charged protein molecules (lysozyme); (B) positively charged diblock copolymers ($P2MVP_{41}$-PEO_{205}), negatively charged homopolymers (PAA_{139}) and negatively charged protein

molecules (α-lactalbumin). From this chapter it became clear that sample history may be an important aspect to take into account.

In chapter 4 micelle formation of diblock copolymers and like-charged proteins and oppositely charged homopolymers was studied. Incorporation of different enzymes in these micelles resulted in some sort of packaging problem, and it was decided not to use homopolymers and protein molecules that are oppositely charged.

The disintegration of micelles as function of salt is under consideration in chapter 5 and 6. Here again, two different micellar systems are studied using DLS, SLS and SANS. In chapter 5 the salt-induced release of lipase from PAA_{139} + $P2MVP_{41}$-PEO_{205} micelles is discussed. The disintegration of lysozyme-filled PAA_{42}-$PAAm_{417}$ + $PDMAEMA_{150}$ micelles is considered in chapter 6.

Chapter 7 deals with self-consistent field calculations of "polyelectrolyte" complex micelle formation and the incorporation of enzyme molecules. From these calculations the free energy of enzyme incorporation could be estimated. The results of the calculations are compared to experimental data. The calculations further provide evidence for the salt-induced release of enzymes which was experimentally observed in chapter 5.

In chapter 8, finally, the enzymatic activity of lipase is studied. Several aspects were considered: the activity of lipase in micelles, in the presence of micelles and partly in micelles. The lipase activity in these systems was compared to the activity of free lipase. Furthermore, the activity of lipase as function of the polyelectrolyte complex composition is discussed. Also the influence of the salt concentration on the activity of lipase in, out and in presence of polyelectrolyte complexes is discussed in this chapter.

Chapter 2

Structure and Stability of Complex Coacervate Core Micelles with Lysozyme

Abstract.
Encapsulation of enzymes by polymers is a promising method to influence their activity and stability. Here, we explore the use of complex coacervate core micelles for encapsulation of enzymes. The core of the micelles consists of negatively charged blocks of the diblock copolymer PAA_{42}-$PAAm_{417}$ and the positively charged homopolymer $PDMAEMA_{150}$. For encapsulation, part of the positively charged homopolymer was replaced by the positively charged globular protein lysozyme. We have studied the formation, structure, and stability of the resulting micelles for three different mixing ratios of homopolymer and lysozyme: a system predominantly consisting of homopolymer, a system predominantly consisting of lysozyme, and a system where the molar ratio between the two positively charged molecules was almost one. We also studied complexes made of only lysozyme and PAA_{42}-$PAAm_{417}$. Complex formation and the salt-induced disintegration of the complexes were studied using dynamic light scattering titrations. Small angle neutron scattering was used to investigate the structures of the cores. We found that micelles predominantly consisting of homopolymer are spherical but that complex coacervate core micelles predominantly consisting of lysozyme are nonspherical. The stability of the micelles containing a larger fraction of lysozyme is lower.

published as: Saskia Lindhoud, Renko de Vries, Willem Norde and Martien. A. Cohen Stuart in Biomacromolecules 2007, Volume 8, page 2219-2227

2.1. Introduction

Complex coacervates are viscous liquids consisting of oppositely charged macromolecules. The classical example is phase separation between gum arabic and gelatin at acidic conditions, studied by Bungenberg de Jong.[19] More recently, complex coacervation is gaining interest. Since biomacromolecules, such as DNA, proteins, and polysaccharides, often are charged, complex coacervation can be used to construct particles for encapsulation, targeting, and delivery of functional ingredients in food[29] and pharmaceutics.[30] Furthermore, in food science the influence of complex coacervation on the structure and texture of food[20–22] is studied.

Previously, we have investigated block copolymer micelles with cores consisting of complex coacervates. These consist of diblock copolymers having both an electroneutral hydrophilic and a charged block mixed with either oppositely charged homopolymer or diblock copolymer.[31–34] At equal charge ratios electrostatic complexes of finite size are obtained that are stabilised by a hydrophilic corona. We call these complexes "complex coacervate core micelles."[25] Stable micelles are formed when the neutral block is 3 times longer than the charged block.[31] It has also been found that a minimum block length is required for the formation of the complexes. Micelles made of an oppositely charged homopolymer and diblock copolymer are more resistant against salt than micelles made of two oppositely charged diblock copolymers.[32] Other authors have studied similar polymer micelles and called them polyion complex micelles (PIC micelles)[23] or block ionomer complexes (BICs).[24]

Complex coacervate core micelles can be used for different applications. It has been found that they spontaneously adsorb on substrates[35] and therewith may give the substrate protein resistant antifouling properties. Other applications can be the encapsulation of nanoparticles in the core of these micelles. There are already micellar aggregates available with "soft" nanoparticles such as DNA and proteins in the core[26,27,36–43] and with "hard" nanoparticles such as oxide nanoparticles.[44–47] We are interested in using these micelles primarily for encapsulating enzymes.

When using these complex coacervate core micelles to encapsulate enzymes, there are a number of potential difficulties. Because electrostatics, which includes electrostatic attraction and entropy gain due to counterion release, is the main driving force of complexation, pH and ionic strength influence the stability of the micelles. The pH can influence the electrostatic attraction since the charge on, for example, proteins and other (bio)polymers usually originates from dissociation or association with protons and therefore varies with pH. As electrostatic interactions are screened by low-molecular-weight electrolytes in solution, one has to think about "tricks" to make structures at physiological ionic strength stable. Enzymes, *i.e.,* globular proteins, have a charge density that is much lower than the

charge densities of the homopolymers and diblock copolymers used. Therefore the ionic strength at which these structures disintegrate is expected to be lower than that for micelles without proteins in the core. Kataoka *et al.,* solved this problem by increasing the hydrophobic interactions[39] and by cross-linking[40,43] the core with glutaraldehyde.

We use a different approach. To regulate the number of enzyme molecules in the cores of the complex coacervate core micelles, we mix proteins with like-charged homopolymers and let this solution form a complex with oppositely charged diblock copolymers. By changing the ratio between protein and homopolymer we are able to control the number of enzyme molecules in the cores of the particles. This also results in micelles that are more stable against disintegration by increases in ionic strength.

Our system consists of the negatively charged diblock copolymer PAA_{42}-$PAAm_{417}$, the positively charged homopolymer $PDMAEMA_{150}$, and the positively charged globular protein lysozyme. We studied three systems with varying protein to homopolymer ratios. These systems are compared with the formation of complex coacervate core micelles without lysozyme, studied by Hofs *et al.,*[32] and complexes that are formed when lysozyme and PAA_{42}-$PAAm_{417}$ are mixed.

We use dynamic light scattering (DLS) titration measurements to study the formation of micelles. Starting with one of the charged species, we are able to study the existence and size of the complex coacervate core micelles as a function of the composition, expressed as a ratio between the concentrations of charges of one sign, divided by the total concentration of charges. Dynamic light scattering titrations can also be used to determine the ionic strength at which the complexes disintegrate. Dynamic light scattering only gives information about the hydrodynamic radius, which is mainly determined by the corona of the micelles. The corona thickness is larger than the double layer of the core, and therefore electrostatics does not influence particle diffusivity. To obtain information about the shape, structure, and the size of the core of the micelles, small angle neutron scattering (SANS) experiments were performed.

2.2. Experimental

2.2.1. Materials.

Lysozyme (L6876) was purchased from Sigma and used without further purification. The poly(acrylic acid)-*block*-poly(acryl amide) (PAA_{42}-$PAAm_{417}$, where the numbers refer to the number averaged degree of polymerisation) diblock copolymers were a gift from Rhodia, Auberville, France. For details of the synthesis see Taton *et al.,*.[48] The positively charged homopolymer used was poly(N,N dimethylaminoethyl methacrylate) ($PDMAEMA_{150}$),

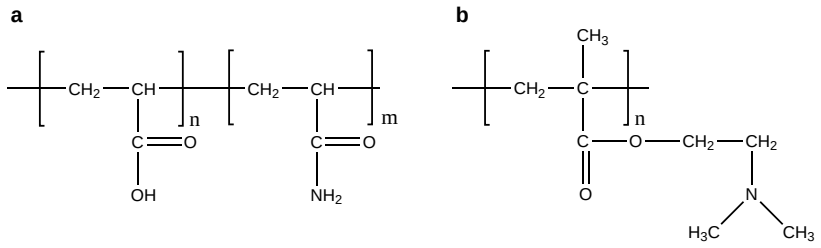

FIGURE 1. Structures of **a)** PAA_n-$PAAm_m$ and **b)** $PDMAEMA_n$

purchased from Polymer Source, *Inc.,* Canada.

2.2.2. Sample Preparation.

Lysozyme was dissolved in demineralised water. The pH was adjusted to 6.5. Solutions were filtered (pore size, 0.1 μm), and the protein concentration was determined by UV (281.5 nm, 2.635 L g^{-1} cm^{-1}).[49] Diblock copolymer and homopolymer solutions were prepared by dissolving the molecules in demineralised water. The pH was adjusted to 6.5. The solutions were diluted to the desired concentration and a salt concentration of 5 mM NaCl. For the light scattering titrations of the three-component systems, the solutions containing the like-charged molecules, *i.e.,* lysozyme and PDMAEMA, were mixed first. This solution was always optically clear. There was no indication of the presence of aggregates in this solution during DLS measurements.

2.2.3. Dynamic Light Scattering Titrations.

Dynamic light scattering was performed with an ALV5000 multiple τ digital correlator and an argon ion laser with a wavelength of 514.5 nm. All measurements were performed at a scattering angle of 90°. The laser power used was 200 mW. Temperature was kept constant at 25 °C by means of a Haake C35 thermostat, providing an accuracy of ± 0.1 °C. Titrations were performed using a Schott-Geräte computer-controlled titrations setup to control the addition of titrant, the cell stirring, and the delay times. The pH was recorded with a calibrated Mettler Toledo InLab pH electrode filled with a 3 M KCl solution.

Two different types of titrations were performed: composition titrations and salt titrations. For the composition titrations the measurement cell contains macromolecules of the same charge sign. The titrant is a solution containing macromolecules of opposite charge. After every titration step the pH is measured and a light scattering run is started; the typical number of light scattering runs per titration step is five. The scattered intensity, the pH, and the hydrodynamic radius are recorded as a function of the composition F^- (equation 1).

$$F^- = 1 - F^+ = \frac{[-]}{[-] + [+]} \quad (1)$$

Effective average hydrodynamic radii of the complexes were determined by analysing the autocorrelation function using the methods of cumulants and using the Stokes-Einstein equation for spherical particles. The composition was calculated in the following way: We know from proton titration curves that at pH 6.5 the net charges of the diblock copolymer and homopolymer are -29 and $+105$, respectively. But, because in these experiments pH is not fixed, for the calculation of F^-, we used the maximal amount of chargeable groups of the polymers.

PAA_{42}-$PAAm_{417}$ has 42 chargeable groups per molecule, and $PDMAEMA_{150}$ has 150 chargeable groups per molecule. For lysozyme we used +8 charges, based on a titration curve measured by Van der Veen *et al.*,;[50] the number of net positive charges on the protein is almost constant in the pH interval between 6 and 8.5.

To determine the ionic strength at which the complex coacervate core micelles disintegrate we carried out light scattering titrations with salt. For the salt titration solutions with a composition at $F^-_{micelle}$ (figure 2) were prepared. The typical volume of these solutions was 9 mL. To these solutions a 4 M NaCl solution was titrated in steps of 10 or 20 μL. Both the intensity and the hydrodynamic radius were plotted as a function of the salt concentration. When the error in the average radius of five measurements was larger than 2 nm, the measurement is said to be unreliable, and its value is not plotted.

2.2.4. Small Angle Neutron Scattering.

Small angle neutron scattering measurements were performed at the time-of-flight instrument LOQ at ISIS (Rutherford Appleton Laboratory). The incident wavelengths are $2.2 - 10.0$ Å, giving a scattering vector q between 0.008 and 0.287 $Å^{-1}$. For these measurements D_2O was used as a solvent, taking the difference in pH and pD into account.[51] All measurements were performed at 25 °C. Samples were prepared with a concentration of 10 g/L, having the solution composition $F^-_{micelle}$ (figure 2). Solutions were kept in quartz cells with a path length of 5 mm. All samples were corrected for sample transmission, background scattering, and thickness. From the raw spectra absolute intensities were determined using a polymer standard (a solid blend of protonated and deuterated polystyrene with a known scattering cross-section), which was provided by ISIS. Small angle neutron scattering measurements were analysed using the generalized indirect Fourier

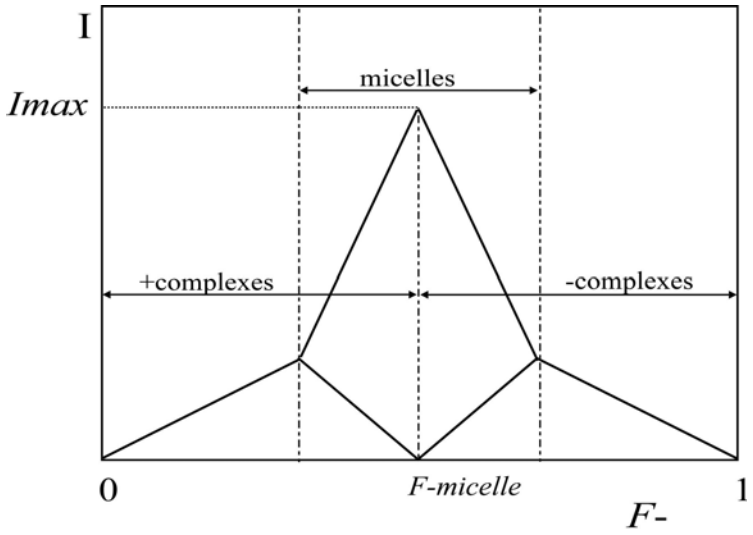

FIGURE 2. Schematical representation of the light scattering intensity as function of the composition F^- for complex coacervate core micelle formation.

transformation (GIFT) method. This is a model-independent way to extract information about the size and shape of the particles.[52–54]

2.3. Results and Discussion

Complexation of oppositely charged macromolecules is strongly dependent on the composition of the system. Light scattering titration is a useful tool to study the complex formation as function of the composition. During a light scattering titration measurement, charged macromolecules are titrated to a solution with macromolecules of opposite charge. Van der Burgh *et al.*,[31] postulated a diagram of the various species formed due to complexation in such a titration. This diagram is shown in figure 2. At low F^- positive soluble complexes are formed. Adding more titrant to this solution one arrives at a value of F^- where electroneutral aggregates first appear. These we call "complex coacervate core micelles." At the peak I_{max} in the aggregation diagram these micelles are the dominating species; we call this composition $F^-_{micelle}$. For $F^- > F^-_{micelle}$ overcharging will result in the disintegration of micelles into negatively charged soluble complexes.

In the following section, light scattering titrations as a function of the composition F^- (equation 1) will be discussed. First we will focus on two-component systems, complexes formed when PAA_{42}-$PAAm_{417}$ and $PDMAEMA_{150}$ (figure 3) or lysozyme and PAA_{42}-$PAAm_{417}$ are mixed (figure 4). Then the three component systems will be discussed (figure 5).

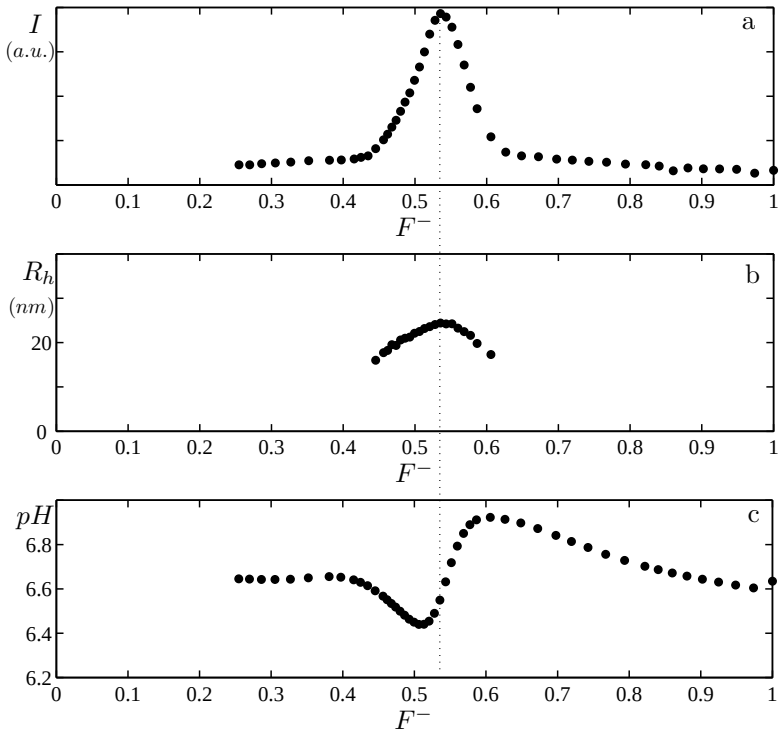

FIGURE 3. Light scattering titrations of complex coacervate core micelles made of diblock copolymer and homopolymer: **a)** intensity *versus* composition, **b)** hydrodynamic radius *versus* composition, and **c)** pH *versus* composition. Raw data were provided by Hofs *et al.*[32]

2.3.1. Complex Coacervate Core Micelles without Lysozyme.

Figure 3 shows the light scattering titration results for PAA_{42}-$PAAm_{417}$ and $PDMAEMA_{150}$ at pH 6.7 and 10 mM $NaNO_3$, taken from Hofs *et al.*,.[32] The intensity versus composition curve (figure 3a) shows a very sharp peak at $F^- \approx 0.5$. The hydrodynamic radius (figure 3b) at the peak composition ($F^-_{micelle}$) is about 25 nm. The pH versus composition curve (figure 3c) gives information about the protein uptake and release during the complex formation. The behaviour of the pH during the light scattering titration measurement is rather complicated. This behavior will be discussed in more detail in the section below.

2.3.2. pH during the Light Scattering Titrations.

The change in the proton concentration is due to the proton uptake or release by the macromolecules involved in the complexation process. It gives rise to a typical curve for the pH, shown in figure 3c. This kind of curve, with pH values that are the same at $F^- = 0$, $F^- = F^-_{micelle}$, and $F^- = 1$, will be found when the pH at which the complexation process is studied is in between the pKs of the different macromolecules.

In our system all the components have a charge that varies with pH. The degree of ionisation, α, of these groups can be expressed [55] by (equation 2):

$$\alpha_{\pm} = \frac{1}{1 + 10^{((pH - pK_0 + e\psi)/kT)}} \tag{2}$$

where pH is the measured pH, pK_0 is the intrinsic pK value of the ionisable groups of the macromolecule, ψ is the electrostatic potential, k is the Boltzmann constant, and T is the temperature. First, consider the extremes of the titration curve. When a positively charged macromolecule is introduced into a solution containing mainly negatively charged macromolecules ($F^- = 1$), the pH increases (figure 3c). Because the macromolecule experiences a negative potential (equation 2), proton uptake by the polycation is favoured. However, protons are released by the polyanion, because the negatively charged macromolecules experience the positive potential of the polycations. Since an increase in pH is measured, it means that the polycation also takes up protons from the solvent. This gives rise to an increase of the pH. At the other extreme of the titration curve, when a negatively charged macromolecule is brought into a solution of mainly positively charged macromolecules ($F^- = 0$), the opposite effect will be seen. Protons are then released, and the bulk pH will decrease.

In the intermediate regime the increasing and decreasing extremes are connected by a curve that crosses the initial pH value. The slope of the curve is steepest at $F^-_{micelle}$ and is actually the "isoelectric point" of the complex; the number of positive charges and negative charges at this composition are the same. Depending on the potential, the negatively charged groups deprotonate, and the positively charged groups protonate. The net effect depends on the differences between the pH and the pK values of the charged groups. For two isolated oppositely charged species, the effect is exactly symmetric for pH values halfway between the two pKs. In that case the extra protonation of the positive species cancels deprotonation of the negative species, and the pH will stay the same. In short, for a symmetric system, at pH=$\frac{1}{2}$(pK$_{anion}$ + pK$_{cation}$), we expect the pH to be the same at $F^- =$, $F^- = 0.5$, and $F^- = 1$. If the pH is not the average of the pKs of the system, then the pH curve of a titration experiment can be totally different, but at $F^-_{micelle}$ the slope of the curve is the steepest.

Various complications make a quantitative analysis of these effects rather difficult. [56] In complexes formed by polyelectrolytes or polyampholytes, the

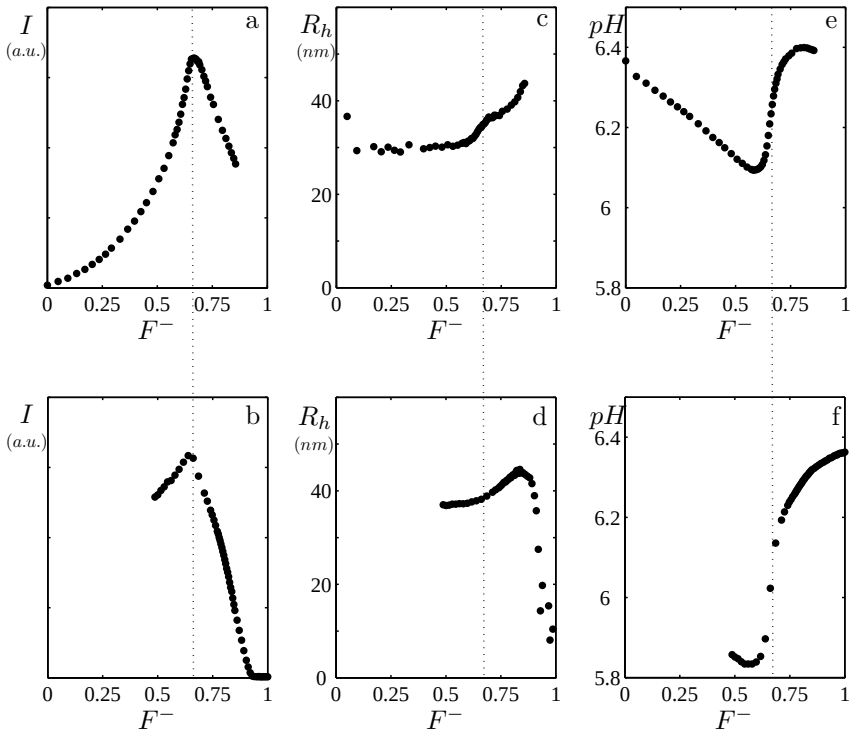

FIGURE 4. **a)** Intensity *versus* composition (titrating PAA_{42}−$PAAm_{417}$ to lysozyme) and **b)** (titrating lysozyme to $PAA_{42}PAAm_{417}$). **c)** Hydrodynamic radius *versus* composition (PAA_{42}−$PAAm_{417}$ to lysozyme) and **d)** (lysozyme to $PAA_{42}PAAm_{417}$) and **e)** pH *versus* composition (PAA_{42}−$PAAm_{417}$ to lysozyme) and **f)** (lysozyme to $PAA_{42}PAAm_{417}$).

effects are not so easy to predict. The potential is already nonzero before complexation, and the potentials felt by groups in the complex are a complicated function of the structure of the complex and the salt concentration. For an amphoteric species, such as a protein, charges may occur in patches. In complexes with such molecules, the distance between attracting charges will be smaller than the distance between repelling charges. The protonation and deprotonation will be complicated in such a system. The titration curve does not just shift, but can change in shape as well. Nevertheless, figure 3c nicely confirms the situation that we have described, because we know that the starting pH in this experiment is pH= $\frac{1}{2}(\mathrm{pK}_{anion} + \mathrm{pK}_{cation})$.

2.3.3. Complex Formation of Lysozyme and $PAA_{42}-PAAm_{417}$.

Figure 4 shows the results of the light scattering titrations for the system where all of the homopolymer is replaced by lysozyme. Titrations were performed both by increasing F^- (figure 4a, 4c, and 4e) as well as by decreasing F^- (figure 4b, 4d, figure 4f).

There is a limited, but significant difference between the "up" (increasing F^-) and "down" (decreasing F^-) titrations. Starting with lysozyme in the cuvette (figures 4a, 4c and 4e), micelles are directly formed. The hydrodynamic radius of these particles is about 30 nm. At $F^- \approx 0.67$ the peak is found. The radius of the particles at this composition is about 37 nm. After the peak (the intensity *versus* composition), the radius of the particles increases. Since the intensity decreases, the best explanation for this observation is that the aggregates disintegrate partly and become less dense.

The aggregation of the particles in the opposite titration (figure 4b, 4d, 4f) follows a different pattern; before micelle formation, first, soluble complexes are formed. During the first titration steps there is no increase in the light scattering intensity (figure 4b). A peak in the intensity *versus* composition plot is found at the same position as for the diblock copolymer to lysozyme titration. The hydrodynamic radius *versus* composition (figure 4d) shows the formation of large structures with a radius of 45 nm at $F^- \approx 0.85$. The size of the particles decreases to about 37 nm; this is the size of the aggregates found at the position of the main peak. The pH *versus* composition curve for both systems (figure 4e and 4f) only shows the disintegration of one single type of particle.

Plotting figure 4a and 4b on top of each other it becomes clear that the formation of the structures is slightly different than the disintegration. It is noticed directly that the curves are asymmetric. When the protein solution is the solution that one starts with (figure 4a), micelles are directly formed. Similar behaviour has been found previously when lysozyme and an oppositely charged chemical analogue of lysozyme are mixed; directly precipitates are formed,[57] and no soluble complexes were formed. Starting from the other side, when the protein solution is the titrant (figure 4b), first soluble complexes are formed, and only after reaching a certain composition micelles are formed.

Irreversibility of the aggregation process is reflected in the intensity *versus* composition curves (figure 4a and 4b) of $F^- = 1$ or $F^- = 0$, respectively; the intensity will be much higher than the starting intensity. A reason for this could be that one diblock copolymer is attached to about five proteins. The electrostatic attraction between diblock copolymer and protein will not be the same for the different protein molecules. For a non-stoichiometric charge ratio this could imply that the proteins that are loosely attached can leave the complex easily, resulting in complexes that are less dense and have

a lower light scattering intensity. These structures have a radius that is the same or larger than that of the original micelles.

A similar system was already studied by Kataoka *et al.*,.[26,27] They mixed lysozyme and PEG-p(ASP) at different mixing ratios and determined the size of their complexes with DLS. They never found an asymmetry or irreversibility of their system. A reason that we find this could be that we do not wait long enough after every light scattering titration step. The system might therefore not be in equilibrium, which is a disadvantage of our measuring method. However, an advantage of the light scattering titrations is that the maximal light scattering intensity indicates at which composition our neutral complexes are formed. In this system $F^-_{micelle}$ is found at 0.67, whereas one would expect to find neutral particles at $F^- = 0.5$ (equation 1). For the calculation of F^- fully charged PAA_{42}-$PAAm_{417}$ was taken into account. We know however that the number of charges on this diblock copolymer is pH-dependent. Lysozyme is an amphoteric molecule; the sign and the number of its charges depend on the pH. Therefore we chose to use the titration curve measured by Van der Veen[50] to determine the number of charges at the pH region at which our measurements are performed. The way that we calculate F^- is therefore the reason for this deviation from 0.5. When pH dependent molecules are involved in complex formation, one should be careful to calculate the composition of the neutral complexes. By using light scattering titrations, we avoid miscalculations for our neutral complexes, because we can simply determine the composition $F^-_{micelle}$ at I_{max}. This makes it a more accurate way to study these structures than to calculate the stoichiometric composition of the micelles by taking the maximum number of positive charges on the protein molecule.[26,27]

2.3.4. Complex Formation at Different Lysozyme/PDMAEMA Ratios.

Figure 5 contains the light scattering titration results for three different systems with different lysozyme to $PDMAEMA_{150}$ molar ratios: 83:17, 3:2, and 7:13. The curves in figure 5a, 5d, and 5g show the intensity as function of the composition F^- (equation 1). In figure 5b, 5e, and 5h the radius of the particles that are formed during the titrations can be found. In figure 5c, 5f, and 5i the pH of the solution during the measurement is plotted. The data are individually discussed for the three different systems.

In figure 5a it is seen that $F^-_{micelle} \approx 0.5$. Particles at this composition have a hydrodynamic radius of about 28 nm (figure 5b). In the intensity *versus* composition curve a shoulder is found at $F^- \approx 0.4$, suggesting the formation of another structure with a radius of about 25 nm. The same was observed starting at $F^- = 0$ (results not shown). A possible explanation for this phenomenon is that the attraction between the homopolymer and the diblock copolymer is stronger than the attraction between the diblock

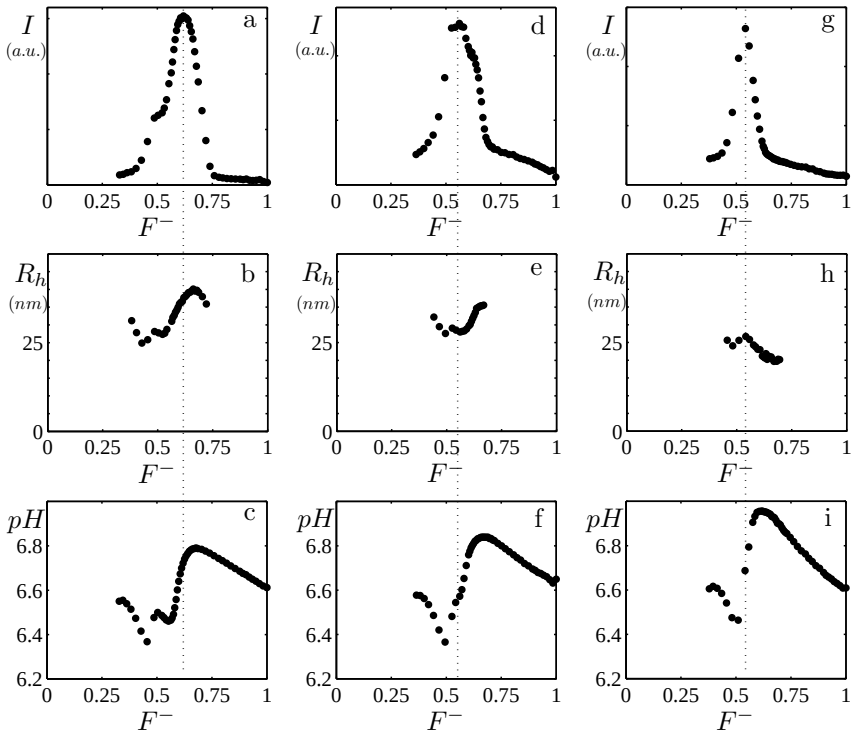

FIGURE 5. Intensity (I), hydrodynamic radius (R_h), and pH *versus* composition with three different lysozyme/PDMAEMA molar ratios: **(a), b) and c)**) 83:17, (**d), e), and f)**) 3:2, and (**g), h), and i)**) 7:13. In all measurements a mixture of lysozyme and PDMAEMA was added to the $PAA_{42}-PAAm_{417}$ solution.

copolymer and the protein, because of the difference in charge density between the homopolymer and the lysozyme molecule. Therefore the homopolymer will be preferably taken up in the micelles, and when a small amount of positively charged components is needed (low F^- value) lysozyme will be expelled from the complexes. The new particles that are formed contain a lower lysozyme to PDMAEMA ratio. Those complexes are expected to have a lower light scattering intensity and a smaller radius. This observation is confirmed by the pH *versus* composition curves.

Because the intensity, hydrodynamic radius, and pH as function of the composition all suggest the formation of a second particle, we tried to analyse the light scattering autocorrelation functions more extensively. Both bi-exponential fitting these curves and a CONTIN analysis did not give

indications of multiple species being present at the same time. The concentration of individual protein molecules is too low to be determined using light scattering.

Like the system where lysozyme is in excess (figure 5a-c), the 3:2 system also seems to have a shoulder at $F^- \approx 0.62$. The radius *versus* composition curve (figure 5e) shows that in this system most likely another particle is formed. The particle formed at $F^-_{micelle}$ has a hydrodynamic radius of about 28 nm; the second particle has a hydrodynamic radius of about 35 nm. In the pH *versus* composition plot (figure 5f) only a small kink is seen, which could correspond to the formation of this second particle as well.

The last system considered is the system where the positively charged component predominantly consists of homopolymer (figure 5g-i). One single sharp peak at $F^- \approx 0.56$ is found in the intensity *versus* composition plot. The formation of one type of particle is confirmed by the hydrodynamic radius *versus* composition and the pH *versus* composition plots. These results strongly resemble the results of the light scattering titration of the homopolymer to the diblock copolymer (figure 3). The radius of the particles formed at the composition of the peak is about 22 nm.

Summarising the light scattering titrations, we can say that the broader intensity *versus* composition curves are obtained at higher lysozyme to homopolymer ratios. When lysozyme is in excess more than one type of particle seems to be formed, but these structures might not exist simultaneously. The system predominantly consisting of homopolymer shows only one kind of micelle.

2.3.5. Titrations with NaCl Solution.

Since electrostatics is the main driving force of the complex formation, the stability of the complexes will depend on the ionic strength. Therefore, a second type of light scattering titration was performed to determine the resistance of the micelles toward salt. Solutions with composition $F^-_{micelle}$ were prepared, and a 4 M NaCl solution was titrated to these solutions. The intensity and the radius as a function of NaCl concentration are shown in figure 6 for the four different systems studied.

For all of the systems the intensity as function of the salt concentration decreases. This is to be expected since the electrostatic interactions become weaker when the salt concentration is increased due to screening of the charges. The particles are expected to swell when salt is added, resulting in larger radii. Salt resistance is markedly different for the different systems. For micelles containing only lysozyme (figure 6a), the salt concentration at which the particles fall apart can accurately be determined. At 0.12 M NaCl the radius of these complex coacervate core micelles is increasing. The error at higher salt concentrations is very largely increased compared to the error at lower salt concentrations.

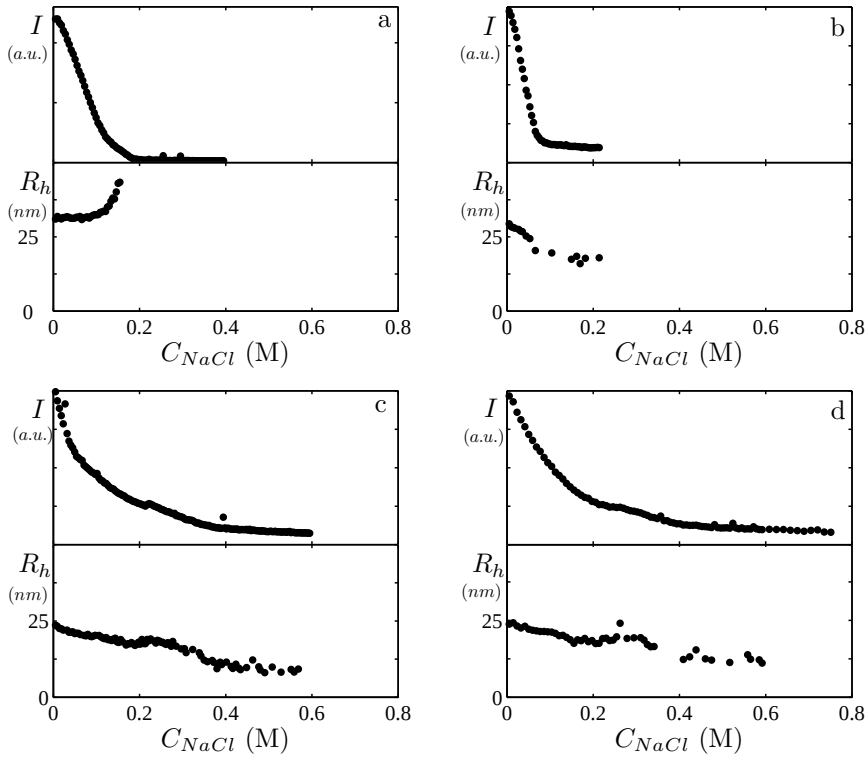

FIGURE 6. Salt titrations: **a)** intensity (I) and radius (R_h) *versus* salt concentration for micelles containing only lysozyme, **b)** intensity (I) and radius (R_h) *versus* salt concentration for 83:17 micelles, **c)** intensity (I) and radius (R_h) *versus* concentration for 3:2 micelles, and **d)** intensity (I) and radius (R_h) *versus* concentration for 7:13 micelles.

For the micelles predominantly consisting of lysozyme (figure 6b), the intensity as function of the salt concentration drops off much steeper than that for the system with only lysozyme. The radius as function of the salt concentration decreases. The error in the radius does not increase as much as for the micelles containing only lysozyme. A possible explanation could be that the proteins are expelled from the micelles and complexes of homopolymer and diblock copolymer are favoured. These complexes are expected to have a smaller radius and have a lower light scattering intensity.

Figure 6c and 6d are very much alike. The salt resistance of the micelles predominantly consisting of homopolymer (figure 5c) seems to be slightly better than the salt resistance of the 3:2 system (figure 6c). In summary, the results in figure 6 show that the salt resistance increases when the cores

of the complex coacervate core micelles contain more homopolymer. For micelles with mixed cores, it seems that at a certain salt concentration lysozyme seems to be expelled from this core. The particles that are formed then have smaller radii.

It is known that the number of charges and the charge density on the molecules that are participating are relevant parameters in complex formation.[31] For instance, complex coacervate core micelles made of oppositely charged block copolymers are less salt resistant than complex coacervate core micelles made of a diblock copolymer and oppositely charged homopolymer.[32] Therefore, it is not surprising that the structures made of protein and diblock copolymers are more sensitive to increases of the ionic strength than the complexes with mixed cores.

2.3.6. Small Angle Neutron Scattering.

From the dynamic light scattering titration measurements we know the hydrodynamic radius of the complex coacervate core micelles, but we are also interested in the structure and composition of the core. A method to obtain this information is SANS. The relatively densely packed cores of the micelles have a much higher contrast with the surrounding medium than the dilute corona. Figure 7 shows the scattering curves of five different systems with different amounts of lysozyme in the cores. The first remark about the scattering curves is that no distinct minima are observed. If the micellar cores had been monodisperse, then, given the instrument setup, we would certainly have been able to observe form factor minima.

Unfortunately, for the present data the q-range does not extend to low enough q-values ($qR \ll 1$) such that we could do a Guinier analysis to extract the radii of gyration and to extrapolate to $q = 0$ to obtain the core contrast, which should be indicative of the water content. Also, form factors of homogeneous spheres fit very poorly, presumably because the core inhomogeneities contribute significantly to the scattering at higher q.[58] Therefore, instead we have used the GIFT method. This method gives a model-free representation of the scattering data, which is called the pair distance distribution function (PDDF), $p(r)$. Even for inhomogeneous particles the $p(r)$ function is proportional to the number of pairs of electrons separated by the distance r. This is the distance that is found in combination of any volume element i with any volume element k of the same particle. The shape of the $p(r)$ function gives an indication about the shape of the particles.[52–54]

The scattering curves of the different systems are clearly different. The micelles containing only protein have a high scattering intensity at low $q$compared to those of the other systems. The function $p(r)$ of this system tells us that the shape of the cores of these types of micelles is most likely ellipsoidal.[54] The pair distance distribution function of micelles predominantly consisting of lysozyme does not indicate a well-defined structure.

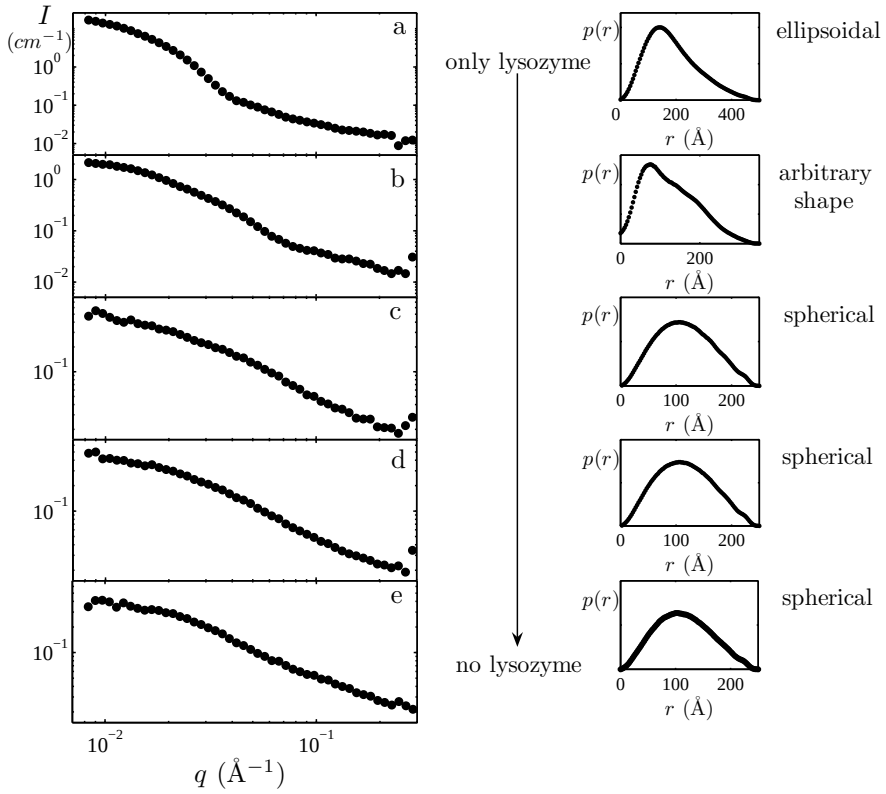

FIGURE 7. Neutron scattering intensity (I) curves as function of scattering vector q for the five different systems. From **a)** to **e)** the ratios betweenlysozyme/homopolymer are 1:0, 83:17, 3:2, 7:13, and 0:1, respectively. The corresponding pair distance distribution functions as function of r (in Å) for these systems are plotted on the right side.

Light scattering titrations for this system as function of the composition and the salt titration already showed the presence of a second particle. Comparing the $p(r)$ function to the $p(r)$ functions of the other systems, one could say that it seems to be an intermediate between the $p(r)$ of an ellipsoid and a sphere. The $p(r)$ function of the average scattering curve of the micelles with only lysozyme and the micelles with only homopolymer does not give a similar pair distance distribution function.

The last three scattering curves for the systems with lysozyme/ homopolymer ratios of 3:2 and 7:13 and the complex coacervate core micelles made of homopolymer only are quite similar. The pair distance distribution functions of these systems show that the shape of the structures is spherical. The radius of the spheres is however much smaller than the hydrodynamic

radius measured with light scattering. This suggests that the core scattering dominates.

At high q the intensity in the scattering curves of the complex coacervate core micelles with proteins (figure 7b, 7c, and 7d) seems to increase whereas a curve without protein (figure 7e) decreases. This could be an indication that at higher q it should be possible to find a structure peak of the protein molecules. Berret *et al.,* found structure peaks of micelles in the neutron scattering curves of core-shell structures made of micelles and oppositely charged diblock copolymers.[58] This structure peak is found at $q > 0.15$ Å^{-1}, which is within the q-range of our neutron scattering experiment, but the micelles that Berret used were larger than our protein molecules. It would be worthwhile for a next SANS experiment to go to higher q and try to find out whether this increase in intensity is caused by the structure peak of the protein molecules.

From the SANS data we tried to determine the number of proteins inside the cores of our micelles. In the absence of a more precise determination by fitting the SANS data over much wider q-range, we here estimate the number of proteins inside the cores of the micelles based on the results of the GIFT analysis. As a first estimation of the number of lysozyme molecules in the core of the spherical complexes, we use the radius of the sphere (the top of the PDDF) to calculate the total volume of the micelles. Since we know the composition of the complexes and we know the radius of the proteins, we can calculate the number of lysozyme molecules. For the 3:2 system this is about 38, and for the 7:13 system this results in 15 lysozyme molecules per micelle.

The number calculated in this way would only be correct if there were not any water in the cores of the complexes. Since it is known that complex coacervates contain a large fraction of water, the actual number of proteins in the cores is expected to be lower. Weinbreck *et al.,*[21] determined the amount of water by freeze-drying the complex coacervate phase. They determined for their system that the water content was about 67 percent. If we now correct the calculated numbers using this information, then this would mean that for the 3:2 micelles the number of enzymes inside the core is about 13, and for the 7:13 micelles this would result in 5 protein molecules per core.

2.4. Conclusions

We have shown the possibility to encapsulate proteins in complex coacervate core micelles. We are able to control the number of lysozyme molecules in the cores of the micelles by changing the mixing ratio between lysozyme and the like charged homopolymer. The shape and stability of these micelles also depend on this mixing ratio. The most stable micelles are formed

when homopolymer is in excess over lysozyme. The estimated number of protein molecules in the cores of these micelles is $5 - 15$. This suggests that the enzymes in the core are accessible, which would make them suitable for enzymatic applications.

Chapter 3

Reversibility and Relaxation Behaviour of Polyelectrolyte Complex Micelle Formation.

Abstract.
In this chapter the formation and disintegration of polyelectrolyte complex micelles is studied by Dynamic Light Scattering titrations with the aim to assess the extent to which these complexes equilibrate. Also, the time evolution of samples at fixed (electroneutral) composition was followed to obtain information about the relaxation time of the complex formation. We find that, in 3.5 mM phosphate buffer with pH 7, polyelectrolyte complex micelles consisting of the positively charged homopolymer $PDMAEMA_{150}$, the negatively charged diblock copolymer PAA_{42}-$PAAm_{417}$ (both having a pH-dependent charge) as well as the positively charged protein lysozyme, slowly equilibrate with a relaxation time of about two days. The same structures were obtained, independent of the way the polymers and proteins had been mixed. In contrast, polyelectrolyte complex micelles (at the same pH) consisting of (pH-dependent) negatively charged homopolymer PAA_{139}, the pH-independent positively charged diblock copolymer $P2MVP_{41}$-PEO_{205}, and the negatively charged protein α-lactalbumin did not equilibrate. The way solutions containing these macromolecules were mixed, yielded different results that did not change over the period of at least a week.

published as: Saskia Lindhoud, Willem Norde and Martien A. Cohen Stuart in The Journal of Physical Chemistry B 113(15), 5431-5439, 2009

3.1. Introduction

Nanopackaging of biomacromolecules, in particular enzymes, may be desired for several reasons, *e.g.*, protection, stabilisation, enhancing biological activity and controlled delivery. The properties of the enveloping structure should be well understood and designed for its particular application. Sometimes the application requires very robust structures which are stable under a wide range of conditions; sometimes it is necessary to build in triggers to allow for opening of the enveloping structure, enabling the release of the enzyme. This makes encapsulation of enzymes a challenging task. Understanding the enveloping structure and its properties in detail is crucial for designing functional structures.

To protect the enzyme molecule from adverse environmental influences some sort of self-assembly may be very useful. This may be combined with very mild chemical reactions, if necessary. Self-assembly of proteins with oppositely charged polyelectrolytes is commonly employed. Most proteins are polyampholytes, carrying both positive and negative charges, enabling them to interact with negatively and positively charged polyelectrolytes. This leads to the formation of (polyelectrolyte) complexes, not only in cases where polyelectrolyte and protein are oppositely charged, but also to some extent on the "wrong" side of the isoelectric point due to charge regulation processes that may occur.[59] Depending on the nature and mixing ratio of the protein and the polyelectrolyte, charged soluble complexes, precipitates[15,18] or complex coacervates are formed.[19]

Over the last two decades, extensive research has been performed on charge-driven associative phase separation which leads to complex formation between two oppositely charged macromolecules. Well-studied themes are the complex coacervate formation between proteins and polysaccharides[19–22] (because of its application in food systems *e.g.*, food texture and structure) and polyelectrolyte multilayers (obtained by exposing a charged surface in an alternating fashion to solutions of oppositely charged polyelectrolytes[60–62]).

Employing appropriate polymer architectures, one can also prepare nanoparticles from charged polymers. An example is a diblock copolymer, consisting of a neutral water soluble block and a charged block. This polymer is mixed with an oppositely charged species at stoichiometric charge ratio. In such a mixture micelles appear that have an electroneutral core consisting of the charged block of the diblock copolymer and the oppositely charged macromolecule, stabilised by a corona consisting of the neutral block. Numerous examples have been reported: diblock copolymers with (a) oppositely charged diblock copolymers,[23,24,33,34,63,64] with (b) homopolymers,[25,31] with (c) DNA[41,42] and (d) with proteins.[26,27] Each of these cases corresponds to a type of so-called polyelectrolyte complex micelles.

It has been shown that enzymes may be incorporated in the electroneutral core of the micelles using a similar procedure.[26,27] However, mixing just diblock copolymers with oppositely charged proteins will typically result in particles containing of about 1000 protein molecules. For application as enzymatic bio-nanoreactors such a large number is expected to be inappropriate, because only a small number of so many enzyme molecules in a particle may be accessible for the substrate. Therefore, we decided to dilute the protein with a like-charged homopolymer. Accordingly, a solution of appropriate protein/homopolymer composition is mixed with a solution containing the oppositely charged diblock copolymer. In this way the number of enzyme molecules in the micelles can be controlled just by changing the ratio between protein and homopolymer. Moreover, the stability against the disintegration by salt increases when the micelles contain less protein, but a substantial fraction of homopolymer (chapter 2).

The formation of two-component systems, consisting of a diblock copolymer and an oppositely charged diblock or a homopolymer has been extensively studied,[31–34,63–65] often by means of light scattering titrations. During such an experiment one charged component is titrated to the component of opposite charge, and the light scattering intensity, as well as the hydrodynamic radius is measured as a function of the composition. These measurements were always performed in such a way that the highest charged component was titrated to the other component, since that is the most economical way to perform an experiment. It has been tacitly assumed that the formation of the micelles is independent of the way in which the two components are mixed *i.e.,* whether the positively charged macromolecule is titrated to the negative one, or *vice versa*. It should be realised, however, that the two cases represent entirely different sample histories.

In the present study, we address the question what the effect of sample history is. Obviously, the complexes with incorporated enzymes, are three component systems. Now, the sequence in which the molecules are mixed might become more important. During a light scattering titration one can study the effect of sample history on complex formation. This is done by performing two titrations for each system, namely one where the negatively charged component(s) is (are) added to the positive one(s), and another in the reverse direction. This protocol allows us to check whether the way the components are mixed, will give the same results (independent of the order of mixing) or not. In another experiment, solutions having the optimal (micellar) composition were prepared in three different ways, and light scattering intensity and the particle size after mixing was studied as a function of time. In this way the kinetics of the complex formation can be probed to some extent.

One investigated system (system A) consisted of the positively charged homopolymer $PDMAEMA_{150}$, the positively charged protein lysozyme and

the negatively charged diblock copolymer PAA_{42}-$PAAm_{417}$ (the subscript numbers refer to the degrees of polymerisation). It has already been shown that micelles are formed by mixing these three components (chapter 2). If it is possible to make micelles using a negatively charged diblock copolymer and a mixture of positively charged homopolymer and protein, it should in principle also be possible to make micelles by mixing a negatively charged homopolymer, a negatively charged protein and a positively charged diblock copolymer. Therefore, a second system was chosen as well (system B), consisting of the negatively charged protein α-lactalbumin, the negatively charged homopolymer PAA_{139} and the positively charged quarternised diblock copolymer $P2MVP_{41}$-PEO_{205}.

Systems A and B should in principle enable us to incorporate both negatively and positively charged enzymes. For possible applicability of these micellar systems on industrial scale information about the relaxation times of these micelles is crucial with respect to the final structure the micelles adopts. When sample history is influential, one has to take this into account when designing a protocol for making the particles.

3.2. Experimental

3.2.1. Materials.

Lysozyme (L6876) and calcium depleted α-lactalbumin (L6010) were purchased from Sigma and used without further purification. The positively charged homopolymer Poly(N,N-dimethyl amino ethyl methacrylate) ($PDMAEMA_{150}$), and the negatively charged homopolymer Poly(acrylic acid) (PAA_{139}), were purchased from Polymer Source *Inc.,* Canada.
The Poly(acrylic acid)$_{42}$-*block*-poly(acryl amide)$_{417}$ (PAA_{42}-$PAAm_{417}$, the numbers refer to the number-averaged degree of polymerisation)) diblock copolymers were a gift from Rhodia, Auberville, France; for details of the synthesis see Taton *et al.*.[48] The positively charged diblock copolymer Poly(2-methyl vinyl pyridinium iodide)$_{41}$-*block*-Poly(ethylene oxide)$_{205}$, was obtained by quarternisation of Poly(2-vinyl pyridinium)$_{41}$-*block*-Poly(ethylene oxide)$_{205}$) purchased from Polymer Source *Inc.,* Canada, using the following protocol. In a typical reaction, 1 g of diblock copolymer containing P2VP was dissolved in 35 mL DMF. Iodomethane (3 mL) was added, and the reaction was stirred under nitrogen flux for 48h at 60°C. Ether (110 mL) was added to precipitate the polymer (add until no more precipitation occurs). The precipitate was filtered and washed with ether ($5x$10 mL) to yield a light yellow powder. (At each washing step the polymeric product became less yellow, less sticky, and more powdery). Subsequently, the polymer was placed in an oven at 50°C to dry overnight.

3.2.2. Sample Preparation.

Solutions of the macromolecules were prepared in a 3.5 mM phosphate buffer. The pH of these solutions was adjusted to 7 with NaOH or HCl after dissolving the macromolecules. Mixtures of like charged macromolecules were prepared in such a way that the molar ratio between lysozyme and $PDMAEMA_{150}$ was 2:8 and the molar ratio between α-lactalbumin and PAA_{139} was 1:9. In this study we examine three systems: A, B and C. Typically the *charge* concentrations are in the $1-10$ micromolar range. During the titration 3 mL of titrant is added and beforehand it is calculated that the F^- value (see equation 3) at the end of the titration is 0.3 for a titration starting at $F^- = 1$ or 0.7 for a titrations starting at $F^- = 0$.

System A: lysozyme, PAA_{42}-$PAAm_{417}$ and $PDMAEMA_{150}$
System B: α-lactalbumin, $P2MVP_{41}$-PEO_{205} and PAA_{139}
System C: lysozyme or α-lactalbumin, PAA_{42}-$PAAm_{417}$ and $P2MVP_{41}$-PEO_{205}

3.2.3. Dynamic Light Scattering Titrations.

Dynamic Light Scattering Titrations were performed with an ALV5000 multiple tau digital correlator and an argon ion laser with a wavelength of 514.5 nm. All measurements were performed at a scattering angle of 90°. Temperature was kept constant at 25 °C by means of a Haake C35 thermostat, providing an accuracy of ±0.1 °C. Titrations were performed using a Schott-Geräte computer controlled titrations set-up to control the addition of titrant, the cell stirring and delay times. The typical time for a titration measurement is four hours. All measurements were performed in a 3.5 mM phosphate buffer at pH 7. Effective average hydrodynamic radii of the complexes were determined by analysing the autocorrelation function using the method of cumulants and applying the Stokes-Einstein equation for spherical particles.

Dynamic light scattering titrations are plotted as a function of the composition F^-, defined by:

$$F^- = \frac{[n_-]}{[n_-] + [n_+]} \tag{3}$$

in this equation $[n_-]=c_-N_-$ and refers to the total negative charge concentration and $[n_+]=c_+N_+$ is the total positive charge concentration. The number of chargeable groups on the polyelectrolytes (N_- and N_+) is used to calculate $[n_-]$ or $[n_+]$, which is $+150$ for $PDMAEMA_{150}$, -139 for PAA_{139}, -42 for PAA_{42}-$PAAm_{417}$ and $+41$ for $P2MVP_{41}$-PEO_{205}. For the number of charges on the proteins we used proton titration curves,[66] for lysozyme this is $+8$, and for α-lactalbumin -8. Since the molar ratio between

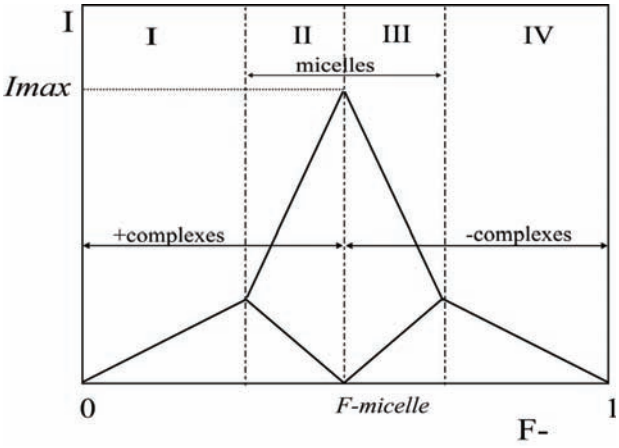

FIGURE 1. Schematical representation of the light scattering intensity as function of the composition ($I(F^-)$) for polyelectrolyte complex micelle formation.

$PDMAEMA_{150}$ and lysozyme is 8:2, the lysozyme contribution to the positive charge in system A is about 1.2%. For system B the contribution to the negative charge of α-lactalbumin is about 0.6%. The data in figures 2, 3 and 4 are normalised on the intensity at $F^-_{micelle}$.

3.2.4. Dynamic light scattering relaxation experiments.

Time-resolved dynamic light scattering measurements were performed with an ALV5000 multiple tau digital correlator and an Oxxius DPSS solid state laser with a wavelength of 532 and a power of 150 mW. All measurements were performed at a scattering angle of 90°. The measurements were performed at room temperature, using the following protocol. First, two components were mixed and left for equilibration overnight. For this sample light scattering was measured with (10 runs of 30 s), giving the first point in the curve. Then, the missing component was added, and the composition of the system became the theoretical $F^- = 0.5$, and immediately 120 light scattering runs of 10 s and subsequently 80 runs of 30 s were taken. The sample was subsequently monitored at appropriate time up to hours or days; always 10 light scattering measurements of 30 s were performed. Two different systems were studied: $PDMAEMA_{150}$, lysozyme and PAA_{42}-$PAAm_{417}$ (system A), and PAA_{139}, α-lactalbumin and $P2MVP_{41}$-PEO_{205} (system B). The autocorrelation functions were analysed by CONTIN-analysis and the method of cumulants. Radii determined by CONTIN are shown.

3.3. Results

3.3.1. Dynamic Light Scattering Titrations.

Plots of light scattering intensity as function of the composition ($I(F^-)$) have been first reported and discussed by Van der Burgh *et al.*[31] They concluded that one finds a symmetrical pattern consisting of four regions (I-IV), schematically shown in figure 1. Starting at $F^- = 0$, a slight increase in intensity is seen first upon the addition of titrant (I). This increase has been argued to be due to the formation of small soluble complexes having a positive charge. At a certain composition the slope ($\frac{dI}{dF^-}$) becomes more pronounced. At this point micelles start to form (II). The system is electroneutral at $F^- \approx 0.5$, and here the maximum intensity is found. This composition will be referred to as $F^-_{micelle}$. Addition of more negatively charged macromolecules to the system results in disintegration of the polyelectrolyte complex micelles, leading to a similar (but negative) slope on $I(F^-)$ as for the formation of the micelles (III). When all the micelles are disintegrated the slope becomes less pronounced and the solution contains again soluble complexes, now with negative charge (IV).

3.3.2. Composition titrations of system A.

The intensity *versus* composition plot reported by Van der Burgh was for a two component polymer system. In our study two three component systems are considered: systems A and B. System A consists of a negatively charged diblock copolymer (PAA_{42}-$PAAm_{417}$), a positively charged homopolymer ($PDMAEMA_{150}$) and the positively charged protein lysozyme. Figure 2 shows composition titrations for this system. Figure 2a presents the scattered intensity $I(F^-)$ and figure 2b the hydrodynamic radius $R_h(F^-)$. Two data sets are shown: one for increasing F^- (closed symbols) and one for decreasing F^- (open symbols). The shape $I(F^-)$ is qualitatively similar to the one discussed by Van der Burgh *et al.*, but there is a clear effect of the direction followed: the maxima of the intensity are found at different compositions. For the titration that started at $F^- = 0$, the maximum is at $F^-_{micelle} = 0.58$, whereas for the titration that started at $F^- = 1$, the maximum is at $F^-_{micelle} = 0.48$.

The fact that the position of the maximum is direction dependent indicates that the system does not reach equilibrium within the time span of a measurement. This implies that the duration of a titration experiment (≈ 4 hours) is shorter than the relaxation time of the system. As a result, equilibrium is not maintained throughout the titration, and $F^-_{micelle}$ is not found at the expected value of 0.5. The polyelectrolytes used have a charge which is pH-dependent. It could be that the actual number of charges on the polyelectrolytes during a titration depends on the history of the sample,

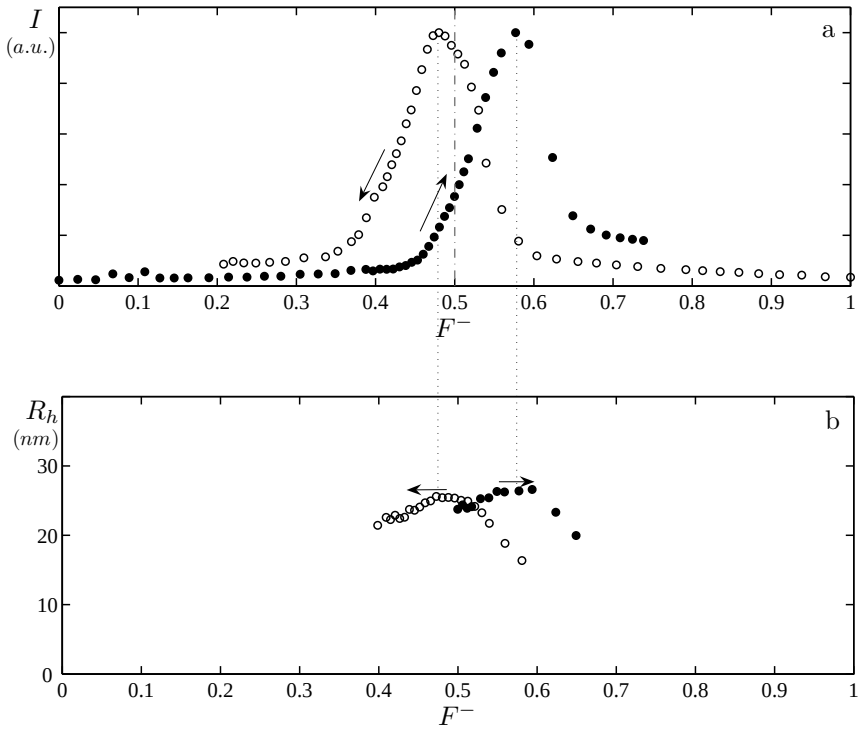

FIGURE 2. **Composition titrations of system A. a)** $I(F^-)$ **b)** $R_h(F^-)$, • titrant is PAA_{42}-$PAAm_{417}$ ○ titrant is mixture of $PDMAEMA_{150}$ and lysozyme.

i.e., whether the negative charged polyelectrolytes are titrated to the positive ones or *vice versa*. One could imagine that when *e.g.,* a few negatively charged macromolecules are thrown in a solution full of positively charged ones, more positively charged molecules try to form a complex with this negatively charged one than are needed to compensate the charge. This induces the formation of positively charged complexes. When the equilibrium time is too short, addition of more negatively charged macromolecules may lead to positive charges being trapped inside the complex at an inaccessible place. As a consequence more titrant is needed to achieve electroneutrality and I_{max} is shifted. Of course the same process may occur when titrating positively charged macromolecules to negative ones. When the charges are also pH-dependent, this process can be even more complicated, since the oppositely charged polymers influence each others dissociation behaviour. [67–71]

The effects, described above, may also be reflected in the hydrodynamic radius. When the delay time of a titration step is too short, the micelles do

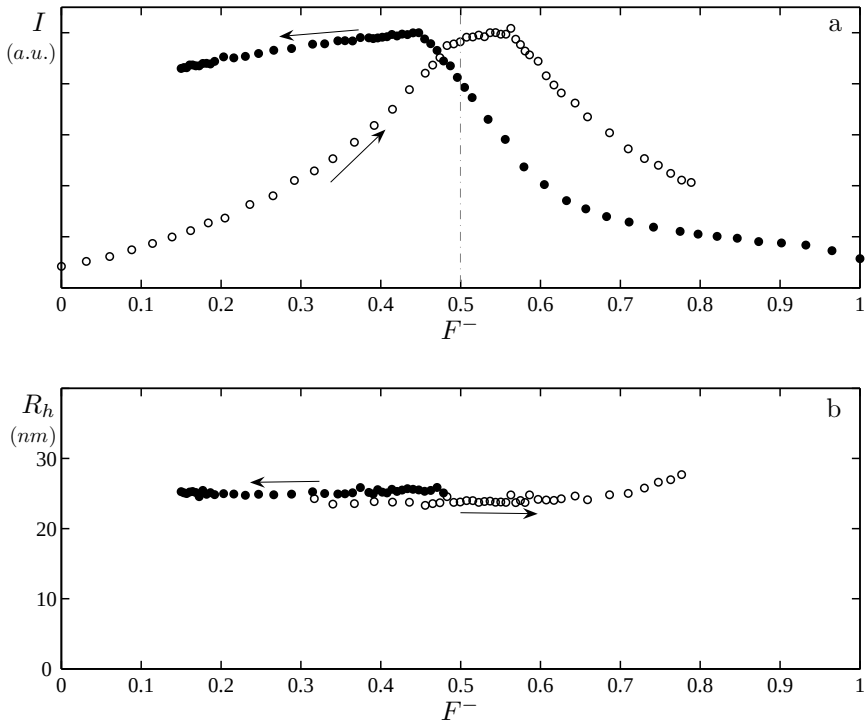

FIGURE 3. **Composition titrations of system B. a)** $I(F^-)$ **b)** $R_h(F^-)$, ∘ titrant is a mixture of PAA_{139} and α-lactalbumin • titrant is $P2MVP_{41}$-PEO_{205}.

not reach equilibrium and therefore do not attain their thermodynamically most favourable form and size. For complexes consisting of weak polyelectrolytes that are not fully charged the size might deviate as well, since the actual charge on the polyelectrolytes is responsible for their aggregation number, *i.e.,* the number of molecules per micelle. Differences in R_h of the micelles between the two directions are clearly seen in figure 2b. Apparently, coming from the $F^- = 0$ site, that is starting the titration with a solution of positively charged molecules, leads to a maximum at larger F^- (like in the $I(F^-)$ plot). Also, there is a slight difference in height of the maximum, meaning a difference in size of the complexes.

3.3.3. Composition titrations of system B.

The second system, system B, consists of the positively charged diblock copolymer $P2MVP_{41}$-PEO_{205}, negatively charged homopolymer PAA_{139} and

the (at pH= 7) negatively charged protein α-lactalbumin. Systems A and B are charge inverse copies of each other: system A consists of a positively charged protein, a positively charged homopolymer and a negatively charged diblock copolymer; system B consists of a negatively charged protein, a negatively charged homopolymer and a positively charged diblock copolymer. In figure 3 the results of the composition titrations for system B are plotted. The open data points again refer to protein and homopolymer (now both being negatively charged) being titrated to positively charged diblock copolymer.

The shapes of $I(F^-)$ of system B are markedly different from those for system A. It seems that when the titrant contains PAA_{139} and α-lactalbumin, $I(F^-)$ shows a gradual non-linear increase over the entire range from $F^- = 0$ to $F^- = 0.5$. No clear difference is observed between region I and II (see figure 1). A maximum is found at composition $F^-_{micelle} = 0.52$, but this maximum is less pronounced than for system A. Addition of more titrant induces the disintegration of the micelles ($\circ$ figure 3a). When $P2MVP_{41}$-PEO_{205} is the titrant ($\bullet$), the intensity as function of F^- can be divided in three regions. Starting at $F^- = 1$ the intensity first slightly increases. At $F^- = 0.62$ the slope becomes more steep, until the maximum, found at $F^-_{micelle} = 0.45$ is reached. This part of the curve somewhat resembles the diagram proposed by Van der Burgh (figure 1). Unexpectedly for $F^- < 0.45$, the intensity does not decrease; it stays almost constant. Apparently additional negative charge (PAA_{139} and α-lactalbumin) is not able to destroy the nanoparticles.

The hydrodynamic radii of the micelles during the two titrations (figure 3b) show a behaviour similar to system A (figure 2b). The hydrodynamic radius is smaller when the protein and homopolymer are the titrant as compared to the reverse titration. The difference between system A and B is the composition range in which micelles can be detected: this range is much broader for system B.

3.3.4. Composition titrations of system C.

Systems A and B, each contained (apart from proteins) homopolymer and oppositely charged diblock copolymer. To study the influence of the molecular architecture on the reversibility of the complex formation, the homopolymer was replaced by a diblock copolymer. Two cases were considered: the positively charged diblock copolymer mixed with lysozyme (figure 4a) and the negatively charged diblock copolymer mixed with α-lactalbumin (figure 4b).

For these double diblock systems $I(F^-)$ can be divided in the previously described four regions (I-IV), which were also found for system A (see figure 2), but the chemical nature of the charged blocks is the same as for system

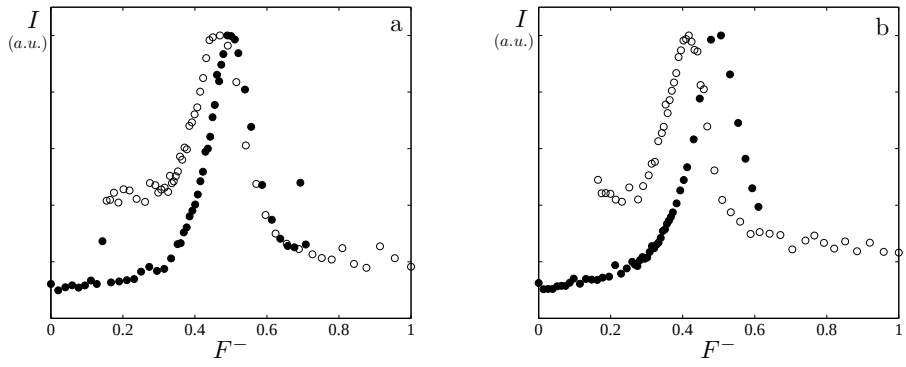

FIGURE 4. **Composition titration system C a)** $I(F^-)$ for • titrant is PAA_{42}-$PAAm_{417}$ ∘ titrant is a mixture of $P2MVP_{41}$-PEO_{205} and lysozyme. **b)** Intensity and as function of the composition • titrant is a mixture of PAA_{42}-$PAAm_{417}$ and α-lactalbumin ∘ titrant is $P2MVP_{41}$-PEO_{205}.

B. Apparently the molecular architecture is important for the complex formation.

3.3.5. Size relaxation at fixed composition

The light scattering titrations revealed differences between the complex formation of system A and B. Such differences might be caused by different relaxation times. A way to study the relaxation time of a system is to monitor solutions with composition $F^-_{micelle}$ as a function of time. Since the systems contain three components the experiments were performed in the following way. First, two components were mixed and this solution was kept in a refrigerator overnight. Where possible, the intensity and hydrodynamic radius were determined with light scattering, yielding the first data point. Subsequently, the third component was rapidly added and the intensity and hydrodynamic radius were measured as a function of time, keeping the composition fixed.

In figure 5 the intensity and hydrodynamic radius as function of time is displayed for system A. Directly after the addition of the third component the intensities of the three systems are markedly different. For the system where lysozyme was added to a mixture of PAA_{42}-$PAAm_{417}$ and $PDMAEMA_{150}$ the intensity and hydrodynamic radius remain constant as a function of time. For the other two systems the intensity just after mixing is lower, then it slightly decreases for about 10 minutes, after which it increases in time to obtain the same value after about 1 day. The same trend is seen for their hydrodynamic radii.

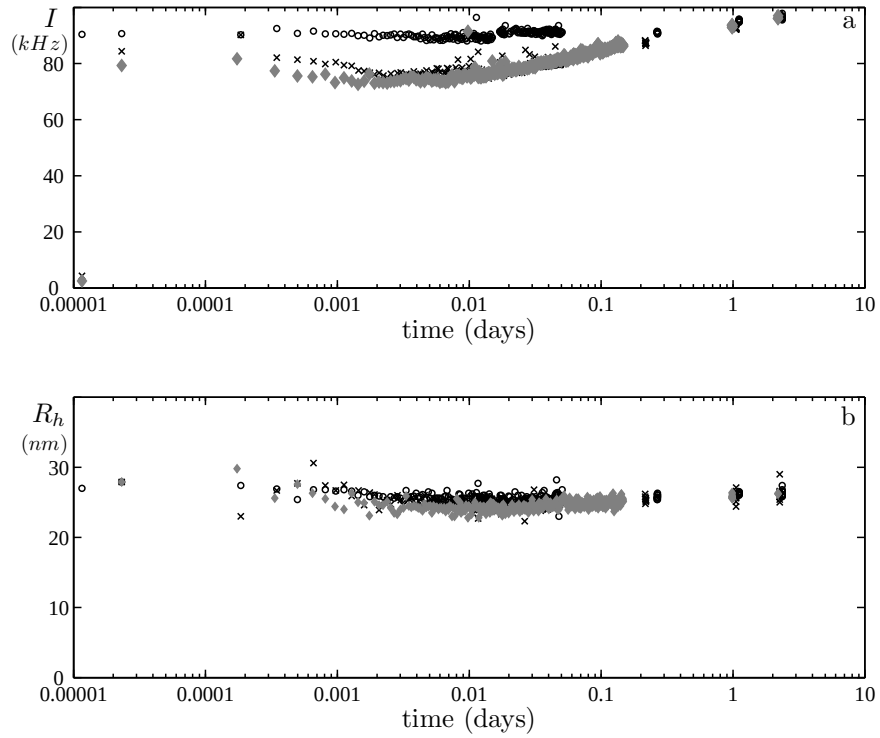

FIGURE 5. **Relaxation of system A. a)** Intensity and **b)** Hydrodynamic radius as function of time for ∘ PAA_{42}-$PAAm_{417}$ and $PDMAEMA_{150}$ mixed with lysozyme, grey ⋄ PAA_{42}-$PAAm_{417}$ and lysozyme mixed with $PDMAEMA_{150}$ and x $PDMAEMA_{150}$ and lysozyme mixed with PAA_{42}-$PAAm_{417}$. The micelle concentration was 1 g L^{-1}, the composition was the theoretical $F^- = 0.5$ (dashed line in figure 2).

The difference in intensity between starting at $F^- = 0$ and $F^- = 1$ and the maximal intensity (grey line in figure 2a) directly may be compared to the intensities shown in figure 5a. When starting at $F^- = 1$, the difference between maximal and measured intensity, is comparable to the difference in initial intensities (seen in figure 5). Starting at $F^- = 0$, a larger difference between the maximal and the measured intensity is observed.

Figure 6 shows the light scattering intensity and the hydrodynamic radius as a function of time for system B, having composition $F^-_{micelle}$, obtained by mixing in three different ways. Now the intensity of each of the three different systems is constant in time up to about six days. The system where $P2MVP_{41}$-PEO_{205} and PAA_{139} are mixed and then α-lactalbumin

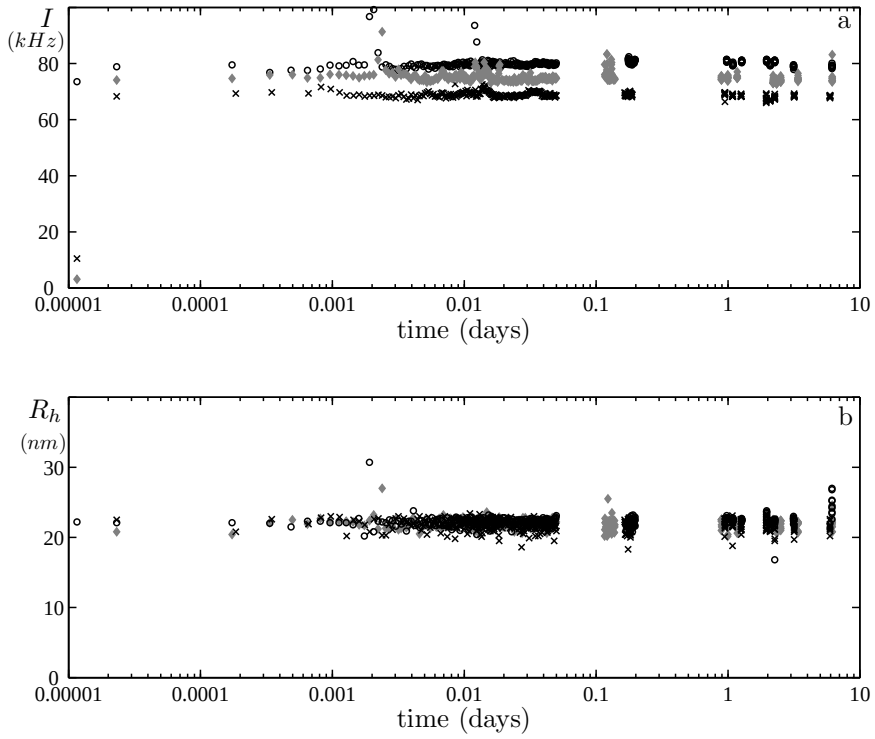

FIGURE 6. **Relaxation of system B. a)** Intensity and **b)** Hydrodynamic radius as function of time for composition ∘ PVP-PEO and PAA_{139} mixed with α-lactalbumin, grey ⋄ $P2MVP_{41}$-PEO_{205} and α-lactalbumin mixed with PAA_{139} and x PAA_{139} and α-lactalbumin mixed with $P2MVP_{41}$-PEO_{205}. The micelle concentration was 1 g L^{-1}, the composition was the theoretical $F^- = 0.5$ (dashed line in figure 3).

is added has the highest intensity of ≈ 80 kHz. The system where first PAA_{139} and α-lactalbumin are mixed and then $P2MVP_{41}$-PEO_{205} is added has an intensity of ≈ 74 kHz. The system where $P2MVP_{41}$-PEO_{205} and α-lactalbumin are mixed and PAA_{139} is added has the lowest intensity of ≈ 68 kHz. The hydrodynamic radii for the three systems are approximately the same.

3.4. Discussion

In this research we are dealing with a three component system. However, the shape of $I(F^-)$ for a two component system (diblock copolymer and homopolymer) and the corresponding three component system (diblock copolymer, homopolymer and protein) are remarkably similar. This can be seen when comparing figure 2 to figure 8 and figure 3 to figure 9 (see Appendix for figure 8 and 9). The similarity suggests that the highly charged components, *i.e.,* the homopolymer and diblock copolymer mainly determine the relaxation behaviour of the polyelectrolyte micelle formation. In the following, we will therefore focus on the oppositely charged polymers.

In this section we will try to explain the differences between system A and B. To avoid misunderstanding we will distinguish between the following three scenarios that apply for relaxation behaviour. In the first scenario, the relaxation time (τ) is shorter than the experimental time scale (τ_{exp}). Here, equilibrium complex formation is observed. For the titration experiments discussed here it would mean that the maximum is found at the same position independent of the direction of the titration. Moreover, systems satisfying this criterion show the same result independent of the way of mixing. None of our systems belongs to this category. In the second scenario $\frac{\tau}{\tau_{exp}} \approx 1$. For systems in this class the relaxation behaviour can be observed during the experiment. System A is an example of a system where this is the case. It was found that the shapes of $I(F^-)$ are similar, but the composition at which the maximum occurs, is direction-dependent, indicating that the measurement was performed in a shorter period (≈4 hours) than the system needed for its relaxation. By following the light scattering intensity and hydrodynamic radius of solutions of the same composition, but mixed in different ways, we found that it takes about 2 days for the system to equilibrate. The last case is when $\frac{\tau}{\tau_{exp}} \gg 1$. Here, the structures that are obtained are quenched. This is the behaviour found in system B. For this system the shape of $I(F^-)$ differed strongly between starting at $F^- = 0$ or $F^- = 1$, respectively. Moreover, the light scattering intensity and hydrodynamic radius of solutions of the same composition, but mixed in different ways, where clearly different, and did not change over a period of six days.

Apparently, systems A and B have a different relaxation rates. In the following we will try to explain why this is the case. Let us first consider the process of polyelectrolyte complex formation. It consists of two steps. Upon mixing a solution containing positively and negatively charged polymers, random aggregates of these oppositely charged molecules are initially formed. The first step is diffusion controlled, the rate of the complex formation is determined by collisions between the compounds, which, in turn, depends on the polyelectrolyte concentrations and the temperature. The typical time for this process is in the μs range. The initial aggregates are

fluffy, dilute structures, that do not have the optimal packing. These structures rearrange towards their equilibrium state, via polyelectrolyte exchange reactions between the chains within the complex or with free polyelectrolytes in the solution during the second step of the relaxation process.[72,73]

An example of this rearrangement of initial aggregates was observed by Cohen Stuart *et al.,*.[25] They did stopped-flow experiments to study the complex formation of two weakly charged polyelectrolytes, and found a strong scattering immediately upon mixing, which subsequently disappeared. Hence, directly upon mixing large structures are formed that reorganise into smaller ones. It might be that for system A a remnant of this process is seen in our size relaxation measurements (see figure 5). For two of the three ways of mixing, the intensity initially decreased for about ten minutes, which could indicate the rearrangement of these structures.

The rearrangement of the initial aggregates towards their equilibrium state, depends on molecular properties of the complex forming molecules. Several aspects of this rearrangement have been addressed, mainly by studying polyelectrolyte multilayer formation. It has been found that chain length differences between the complexing molecules,[74] molecular architecture, hydrophobicity[75,76] of the polymeric backbone and charge density[61,77–80] influence the mobility of the polymers in a complex, and hence the rate of relaxation. Also solvent properties, such as pH and salt concentration, are influential factors.

Differences in mobility also show up prominently in multilayer formation. For polyelectrolyte multilayers two growth regimes are found: exponential[81–83] and linear growth. Linear growth is typically observed when multilayers are formed by the complexation of two strongly charged polyelectrolytes, or by two weakly charged polyelectrolytes, at pH= $\frac{1}{2}$(pK_{anion} + pK_{cation}), and very low salt ionic strength ($<$ 5 mM).[69,84] Addition of salt often induces exponential growth, before it leads to the disintegration of the multilayer because of the formation of soluble complexes.[84] Changing the pH of a weakly charged polyelectrolyte containing multilayer may also induce exponential growth. For multilayers consisting of strongly charged polyelectrolytes, the addition of salt may lead to exponential growth in some cases. In other cases the multilayer thickness increment is a function of the ionic strength. What scenario will apply to a certain kind of polyelectrolyte pair depends on the chemical nature of the polyelectrolytes.

The explanation proposed for the switching from linear to exponential growth in polyelectrolyte multilayers is that the strength of electrostatic attraction decreases, leading to enhanced mobility of at least one of the components. As a result, all polyions of a certain kind in the layer can participate in complex formation (reservoir effect), so that the thickness increment becomes proportional to the thickness.[85] This is the hallmark of exponential growth.

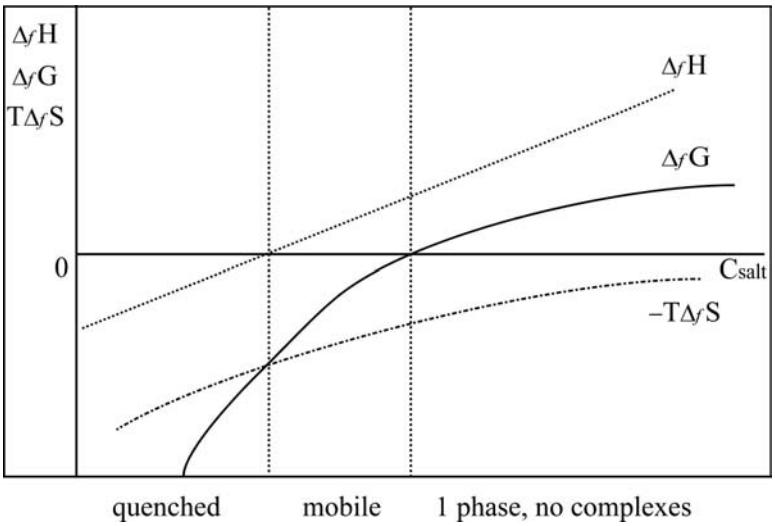

FIGURE 7. Schematical picture of $\Delta_f H$, $\Delta_f G$ and $\Delta_f S$ of polyelectrolyte complex formation as function of the salt concentration.

An important observation concerning the enthalpy of polyelectrolyte complex formation ($\Delta_f H$) was made by Laugel *et al.,*.[86] It appears that the sign of the enthalpy correlates with the growth behaviour of the multilayers. A negative $\Delta_f H$, *i.e.,* an exothermic process, is measured in cases of linear growth. Upon addition of salt to these systems the enthalpy becomes weakly negative or positive and the growth behaviour switches to exponential. Positive values of $\Delta_f H$ (endothermic process) and exponential growth are typically found for complexes consisting of two weakly charged polyelectrolytes at salt concentration of > 150 mM. Hence, it seems that dynamic properties of complexes (such as mobility and structural rearrangement) correlate strongly with the thermodynamical property $\Delta_f H$, in particular with its sign.

The change from exothermic to endothermic behaviour is found when the salt concentration increases. Hence, at low salt, the complex formation is enthalpically favourable, but it becomes entropically driven when the salt concentration is increased. This may be understood when the following reaction is considered:

$$Pol^+Pol^- + A^+B^- \leftrightarrows Pol^+B^- + Pol^-A^+ \tag{4}$$

where $Pol^{+/-}$ refers to different polyelectrolytes and A^+, B^- to the simple salt ions. Addition of salt, screens electrostatic repulsion within each polyelectrolyte layer, allowing for a less compact structure[87] and eventually an increased mobility of the polyelectrolytes within the multilayer.

A qualitative picture of the thermodynamic properties, $\Delta_f H$, $\Delta_f G$ and $\Delta_f S$, of polyelectrolyte complex formation, as function of salt, is sketched

in figure 7. In this figure the changes in enthalpy, entropy and free energy as a function of salt are shown. At low ionic strength, counterion release leads to a large positive $\Delta_f S$, hence $-T\Delta_f S$ is strongly negative. The main contribution to the entropy as a result of this counterion release decreases as a function of salt because at higher salt concentrations there are already plenty of salt ions present in the solution. A mobility increase of the polymer chains within the complex upon the addition of salt will also contribute to the change in entropy. In figure 7 $-T\Delta_f S$ is plotted, which increases with increasing salt concentration. It remains a negative contribution over the entire salt range. $\Delta_f H$ arises from the change in potential energy associated with the inter ionic distances:

$$\Delta_f H = \Delta_f(\sum_{ij} \frac{e^2}{4\pi\varepsilon r_{ij}}) \tag{5}$$

At low ionic strength this is also negative because of the tight ion pairs in the complex. Upon increasing C_{salt}, due to screening of the charges, the ion pairs become less tight, causing $\Delta_f H$ to increase and eventually turn positive. Now, we can predict the trend for the change in the free energy ($\Delta_f G$), because $\Delta_f G = \Delta_f H - T\Delta_f S$.

In principle the influence of pH on the polyelectrolyte complex formation can be explained in a similar way, the only difference being that now we are dealing with protons instead of salt ions. Protons are present in water and it is known that water occurs abundantly in polyelectrolyte complexes (chapter 5).[21,88–92] This makes the pH a rather special interaction parameter for tuning the growth behaviour. The reaction that occurs is:

$$PolH^+PolO^- \leftrightarrows Pol + PolOH \tag{6}$$

where $PolH^+/Pol$ is the polybase pair and $PolO^-/PolOH$ is the polyacid pair.

Figure 7 is a sketch for the complex formation of two fully charged polyelectrolytes. Complex formation between a weak polyacid and a weak polybase is rather complicated because they are only fully charged at high and low pH, respectively. Moreover, these polyelectrolytes influence each others dissociation behaviour, and therefore each others charge density.[67–71] Laugel *et al.,* measured the $\Delta_f H$ for weak polyelectrolytes only at pH= $\frac{1}{2}(pK_{cation}+pK_{anion})$.[86] Under this condition and at salt concentrations, say below <5 mM, two weakly charged polyelectrolytes act as two fully charged polyelectrolytes. In this case, linear multilayer growth is found.[69,84] Increasing the salt concentration for PAA/PDMAEMA[84] or PGA/PAH[86] to 10 mM already changes the growth from linear to exponential. Apparently, for these systems the mobility of the polyelectrolytes drastically increases upon the addition of salt. A reason for this increase may be that at this low salt concentration the distance between the charges is just enough for protons to "jump" from one place to the next and thereby increasing the

mobility of the polyelectrolytes. At other pH values it is difficult to predict the behaviour of $\Delta_f H$ and $\Delta_f S$. They will also become a function of the pH (or charge density) and graphical representation of $\Delta_f H$, $\Delta_f G$ and $\Delta_f S$, in figure 7 would require an additional pH-axis.

Within this framework, we can rationalise the different relaxation processes found for systems A and B. System A contains two weakly charged polymers (PDMAEMA and PAA). For these two polymers it is known that the multilayer growth regime changes upon the addition of salt.[84] Hofs *et al.,* studied the $\Delta_f H$ for complex formation of these polymers and found that, at 10 mM $NaNO_3$, this enthalpy is slightly negative.[32] It indicates that it is in the regime where the driving force switches from enthalpically favourable to enthalpically unfavourable. We performed our experiments in a 3.5 mM phosphate buffer, which is in the $5-10$ mM salt range. Therefore we observe relaxation of system A during the course of the experiment, *i.e.,* $\frac{\tau}{\tau_{exp}} \approx 1$.

In system B we are dealing with a strongly charged polyelectrolyte (P2MVP) and a weakly charged polyelectrolyte (PAA). We do not have any information on multilayer growth and interaction enthalpy, of this polyelectrolyte couple. However, since the relaxation time is much longer than the experimental time scale ($\frac{\tau}{\tau_{exp}} \gg 1$), we conclude that the sign of $\Delta_f H$ is very likely negative at our experimental conditions (3.5 mM phosphate buffer).

A question which remains to be addressed is why the double diblock system C behaves as system A in the light scattering titrations, whereas the charged groups of the polyelectrolytes are the same as system B (P2MVP and PAA). One possible reason is that the neutral water soluble blocks (PAAm and PEO) are incompatible. It is known that this may lead to particles with demixed coronas.[33] Apparently, this segregative force between the two neutral soluble blocks enhances mobility and results in the disintegration of micelles upon addition of more titrant. As a consequence, the four regions of figure 1 are found. Hence, additional segregative forces between the diblock copolymers may influence the relaxation behaviour of the charged blocks. Another reason could be that the relaxation rate of these complexes is different is the chain lengths are different: compare the number of chargeable groups on the diblock compolymers ($+42$ and -41) to the number of chargeable groups on the homopolymers have ($+150$ and -139).

Finally, we return to the final goal of this study, which is to determine optimal conditions for using these micelles as wrapping for enzymes. In order to understand the activity of the enzymes incorporated in the micelles, there are two aspects which we have to take into account. First, for system A, after approximately two days the resulting average composition and structure of the micelles are independent of the way of mixing. However,

since these structures are slightly dynamical, the number of protein molecules which are enclosed in the micelles might fluctuate. On the other hand, using the more quenched system B, one has to follow one and the same procedure of micelle preparation, to make a fair comparison between different samples possible. An advantage of this system is that in a period of at least a week no measurable rearrangements in the micelles occur, which suggests that the proteins are really trapped in the micelles and cannot leave them.

3.5. Concluding Remarks

Light scattering titrations and size relaxation measurements at fixed composition revealed a difference between the relaxation behaviour of systems A and B. The main difference between system A and system B is that system A consists of two weakly charged polyelectrolytes and system B of a strongly and a weakly charged polyelectrolyte. System B is quenched ($\frac{\tau}{\tau_{exp}} \gg 1$) at the chosen experimental conditions. For system A, the relaxation is observed during the measurement ($\frac{\tau}{\tau_{exp}} \approx 1$). Differences in relaxation behaviour arise from differences in molecular properties and environmental conditions such as salt concentration and pH.

Laugel *et al.,* have measured the enthalpy of the complex formation.[86] Combining their results with our findings about the relaxation behaviour it seems that when $\frac{\tau}{\tau_{exp}} \gg 1$ the complexation is an exothermic process. When $\frac{\tau}{\tau_{exp}} \ll 1$ the complexation is endothermic and therefore driven by an increase of entropy in the system. For systems with $\frac{\tau}{\tau_{exp}} \approx 1$, Δ_fH switches from favouring to opposing the complex formation.

The relaxation time of a polyelectrolyte couple can be altered by the addition of salt. When the salt concentration is increased the relaxation switches from quenched to mobile and when more salt is added the complexes dissolve. The salt concentration at which this happens is system dependent. When one is dealing with two weakly charged polyelectrolytes at pH= $\frac{1}{2}$(pK$_{anion}$ + pK$_{cation}$), this salt concentration is expected to be very low.

The main consequence of these differences in relaxation times is that the structure and composition of polyelectrolyte complexes consisting of a weakly and a strongly charged polyelectrolyte are history dependent. Therefore, to study the influence of recipe and environmental variables on the composition and structure of micelles belonging to system B, a given preparation route has to be followed.

Appendix

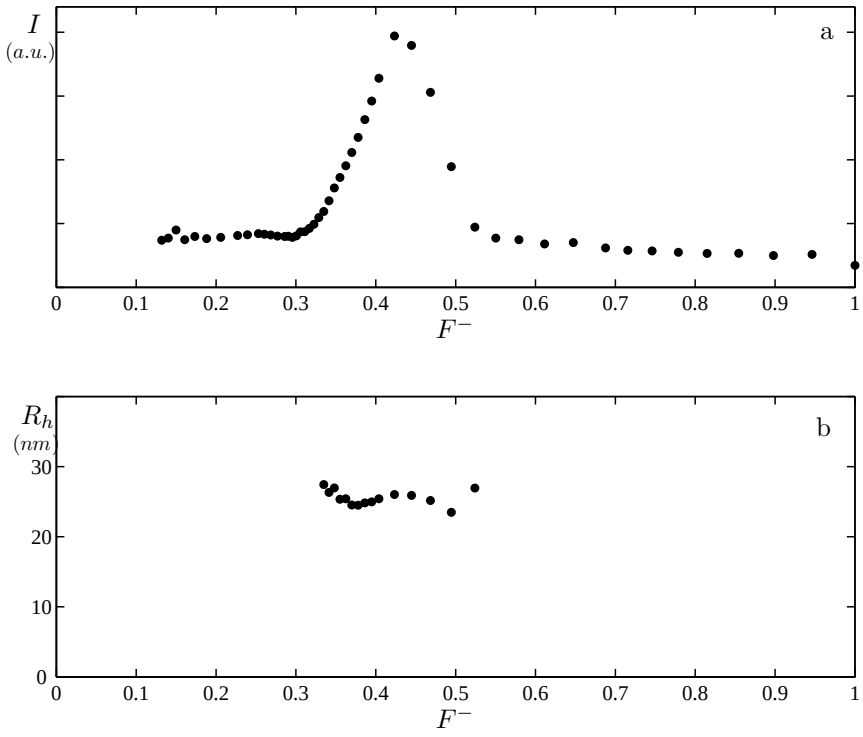

FIGURE 8. Light scattering titrations of $PDMAEMA_{150}$ titrated to PAA_{42}-$PAAm_{417}$: **a)** $I(F^-)$ **b)** $R_h(F^-)$, pH 7, 3.5 mM phosphate buffer.

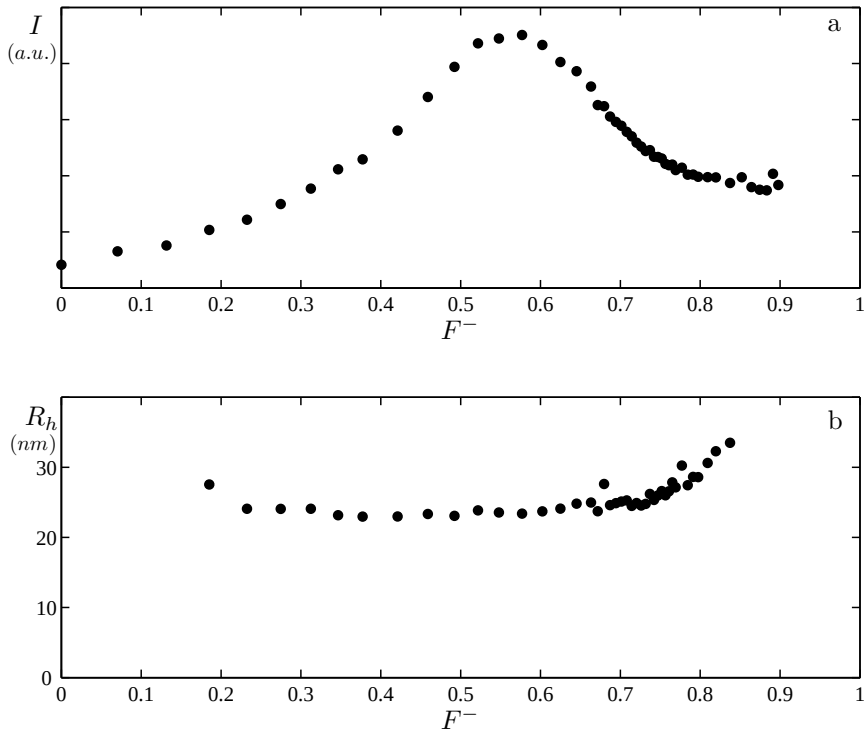

FIGURE 9. Light scattering titrations of $P2MVP_{41}$-PEO_{205} and homopolymer PAA_{139}: **a)** $I(F^-)$ **b)** $R_h(F^-)$, pH 7, 3.5 mM phosphate buffer.

Chapter 4

Packaging problems of enzymes in polyelectrolyte complex micelles.

Preface.
This chapter is important in the context of this thesis; it is about why (apart from a diblock copolymer) it is better to use a like charged homopolymer and a protein, rather than an oppositely charged homopolymer and protein. It therefore merely serves to illustrate the issues; the variety of data is too diverse to justify an article. Yet, this chapter will not be submitted as a regular publication.

4.1. Introduction

Proteins may be regarded as polyelectrolytes that are weakly charged and have a low charge density. Moreover, these biomacromolecules are amphoteric, meaning that at pH values below their isoelectric point they are positively charged and they become negatively charged above their isoelectric point. Because these biomacromolecules are charged, mixing them with oppositely charged macromolecules will result in the formation of polyelectrolyte complexes. Several protein-polyelectrolyte complexes have been prepared and studied.[11,15–18,20,26,27,93–95]

Polyelectrolyte-protein complexes are interesting for all sorts of applications. In food science these complexes may be used to improve texture and structure of, *e.g.,* dairy products.[21,22] In industry these complexes might be used to increase the shelf-life of protein formulations. One could also think of pharmaceutical applications of these complexes, for instance for the delivery of therapeutical proteins and peptides.

In the context of application the size of a complex is important. It is known that for targeted delivery nanometer dimensions are required, because larger objects will be removed by the immune system, *e.g.,* by phagocytes. Preparing protein containing nanoparticles requires the use of special polyelectrolytes. These polyelectrolytes must at least have one non-charged hydrophilic block. At stoichiometric charge ratio electroneutral structures will form having this neutral block at the periphery of the polyelectrolyte complex. It has been shown that diblock copolymers having one neutral hydrophilic block and a charged block indeed form micellar structures with oppositely charged proteins. Also charged triblock copolymers or charged graft copolymers will form structures with nanometer dimensions, when mixing with oppositely charged macromolecules.

The present chapter deals with three component polyelectrolyte complex micelles. These micelles consist of diblock copolymers, homopolymers and protein molecules. In our previous studies the homopolymer and protein always bear the same charge. For these systems we found that stable micelles are formed when the homopolymer is in excess with respect to the protein (see chapter 2). This procedure further allows us to control the amount of proteins in the core of the polymeric micelles.

The protocol we have used so far to prepare the micelles was always as follows: we made a mixture of like-charged homopolymers and protein molecules and subsequently mixed this with oppositely charged diblock copolymers. In principle, it should also be possible to make micelles with like-charged diblock copolymer and protein, and oppositely charged homopolymer. The latter protocol was tried several times. We have experienced certain difficulties when using this preparation method. The reason why this method is unsuitable is the subject of this chapter. First, peculiar experimental results will be shown and then discussed.

In this chapter six different systems are under investigation. Five of the six systems are based on $PDMAEMA_{150}$ + $PAA_{42}PAAm_{417}$ and one is based on PAA_{139} + $P2MVP_{41}$-PEO_{205}. From the previous chapter it is known that the relaxation behaviour is different for these two systems, and that the PAA_{139} + $P2MVP_{41}$-PEO_{205} system has a relaxation time $\frac{\tau}{\tau_{exp}} \gg 1$, which means that the sample history strongly influences the characteristics of the polyelectrolyte complexes. $PDMAEMA_{150}$ + $PAA_{42}PAAm_{417}$ micelles have a shorter relaxation time *i.e.,* these micelles are more dynamical.

4.2. Experimental

4.2.1. Materials.

Six systems will be discussed in this chapter:

System 1: α-Lactalbumin, PAA_{42}-$PAAm_{417}$ and $PDMAEMA_{150}$
System 2: Lipase, PAA_{42}-$PAAm_{417}$ and $PDMAEMA_{150}$
System 3: Glucose Oxidase, PAA_{42}-$PAAm_{417}$ and $PDMAEMA_{150}$
System 4: HRP, PAA_{42}-$PAAm_{417}$ and $PDMAEMA_{150}$
System 5: GFP, PAA_{42}-$PAAm_{417}$ and $PDMAEMA_{150}$
System 6: Lysozyme, $P2MVP_{41}$-PEO_{205} and PAA_{139}

Lysozyme (L6876), calcium depleted α-Lactalbumin (L6010), Glucose Oxidase (GOx) from *Aspergillus niger* and Horseradish Peroxidase (HRP) from *Armoracia rusticana* were purchased from Sigma and used without further purification. The lipase was Lipolase™, derived from the fungus *Humicola ℓanuginosa*, was a gift from Novozymes (Bagsvaerd, Denmark). The Green Fluorescent Protein (GFP-S65T) was provided by the Biochemistry Department of Wageningen University. The positively charged homopolymer Poly (N,N-dimethyl amino ethyl methacrylate) ($PDMAEMA_{150}$) and the negatively charged homopolymer Poly(acrylic acid) (PAA_{139}) were purchased from Polymer Source *Inc.,* Canada). The Poly(acrylic acid)$_{42}$-*block*-poly(acryl amide)$_{417}$ ($PAA_{42}PAAm_{417}$, the numbers refer to the number-averaged degree of polymerisation)) diblock copolymers were a gift from Rhodia (Auberville, France); for details of the synthesis see Taton *et al.,*.[48] The positively charged diblock copolymer Poly(2-methyl vinyl pyridinium iodide)$_{41}$-*block*-Poly(ethylene oxide)$_{205}$, was obtained by quarternisation of Poly(2-vinyl pyri-dinium)$_{41}$-*block*-Poly(ethylene oxide)$_{205}$ (see chapter 3 and 5).

4.2.2. Sample Preparation.

Solutions of the macromolecules were prepared in 3.5 mM phosphate buffer. The pH of these solutions was adjusted to 7 (for system 1, 2, 5 and 6) and 6.5 (system 3 and 4) with NaOH or HCl, after dissolving the macromolecules.

Mixtures of like charged macromolecules were prepared in such a way that the homopolymer was in excess.

4.2.3. Dynamic Light Scattering Titrations.

Dynamic light scattering titrations were performed with an ALV5000 multiple tau digital correlator and an argon ion laser with a wavelength of 514.5 nm. All measurements were performed at a scattering angle of 90°. Temperature was kept constant at 25 °C by means of a Haake C35 thermostat, providing an accuracy of ±0.1 °C. Titrations were performed using a Schott-Geräte computer controlled titrations set-up to control the addition of titrant, the cell stirring and delay times. All measurements were performed in a 3.5 mM phosphate buffer at pH 7. Effective average hydrodynamic radii of the complexes were determined by analysing the autocorrelation function using the method of cumulants and applying the Stokes-Einstein equation for spherical particles.

Dynamic light scattering titrations are plotted as a function of the composition F^-, defined by:

$$F^- = \frac{[n_-]}{[n_-] + [n_+]} \tag{7}$$

In this equation $[n_-]=c_-N_-$ refers to the total negative charge concentration and $[n_+]=c_+N_+$ is the total positive charge concentration; c_i is the molar concentration of species i and the number of chargeable groups per chain on the polyelectrolytes is denoted as N_i.

4.3. Results

System 1. In the previous chapters complex formation between positively charged lysozyme, positively charged $PDMAEMA_{150}$ and negatively charged PAA_{42}-$PAAm_{417}$ has been discussed. It was shown that complex formation is reversible. At pH 7 lysozyme is a positively charged molecule. In principle it should also be possible to put a negatively charged protein molecule in these micelles. The (at pH 7) negatively charged α-lactalbumin was mixed with the negatively charged diblock copolymer PAA_{42}-$PAAm_{417}$ and subsequently the complex formation with positively charged $PDMAEMA_{150}$ was studied.

In figures 1a and b the intensity and hydrodynamic radius as function of the composition are shown for a light scattering titration of system 1 including α-lactalbumin. As in chapter 3, the titration was performed twice, starting from both ends of the composition axis ($F^- = 0$ and $F^- = 1$, respectively). The intensity plots are similar to the intensity plots found for the complex formation of lysozyme, $PDMAEMA_{150}$ and PAA_{42}-$PAAm_{417}$

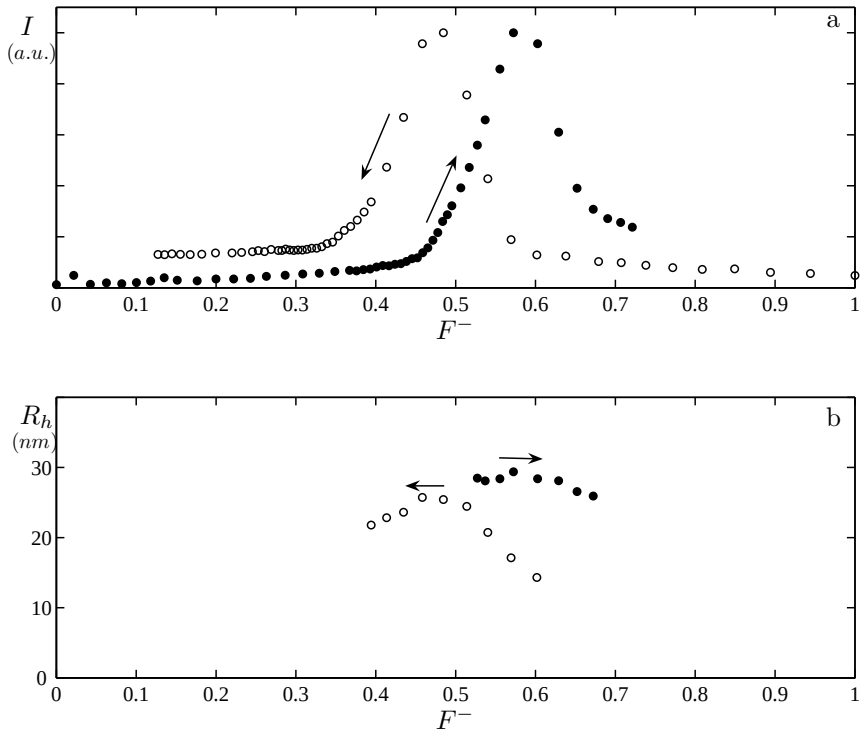

FIGURE 1. **Composition titration of system 1**. **a)** Intensity and **b)** hydrodynamic radius as function of the composition. ○ $PDMAEMA_{150}$ titrated to PAA_{42}-$PAAm_{417}$ and α-lactalbumin and • PAA_{42}-$PAAm_{417}$ and α-lactalbumin titrated to $PDMAEMA_{150}$, molar ratio between $PDMAEMA_{150}$ and α-lactalbumin 9:1.

(see figure 2 and chapter 3). For this lysozyme-containing system it was also found that the composition at which the maximum intensity is found is direction dependent; equilibrium is not reached throughout the titration and, hence, the state of the sample is not uniquely defined by composition alone. Since the micelles do disintegrate, the relaxation time and the experimental time scale are expected to be of the same order (see chapter 3). Because of its similarity to the lysozyme-containing system the relaxation behaviour of the α-lactalbumin system shown in figure 1 is expected to be similar.

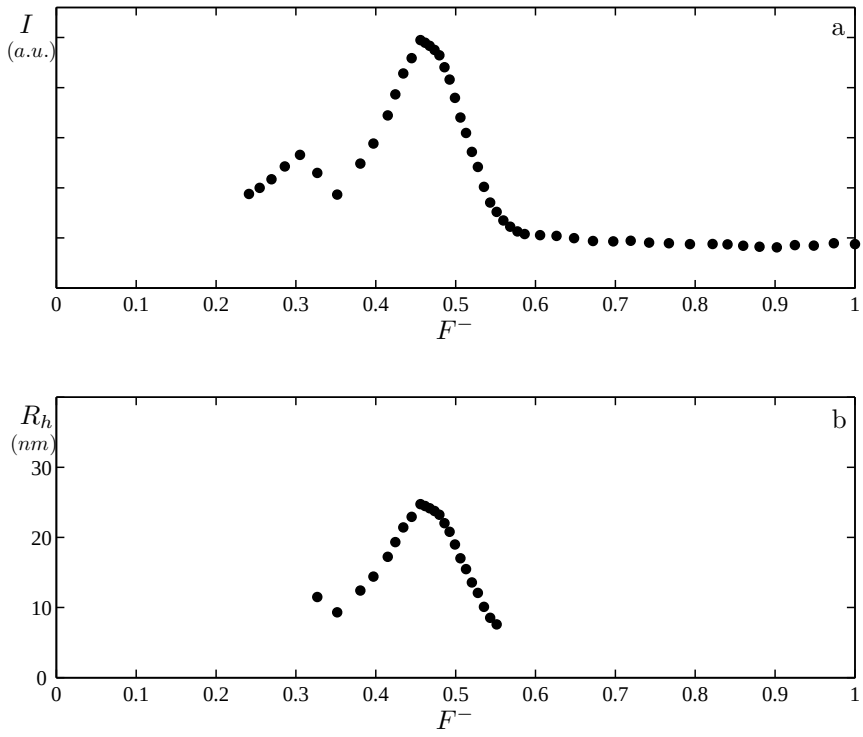

FIGURE 2. **Composition titration of system 2**. **a)** Intensity and **b)** hydrodynamic radius as function of the composition. Molar ratio between $PDMAEMA_{150}$ and lipase 9:1.

System 2. The second system is the complex micelle formation of lipase, PAA_{42}-$PAAm_{417}$ and $PDMAEMA_{150}$. Like α-lactalbumin lipase is negatively charged at pH= 7, but this protein molecule is twice as big as α-lactalbumin. The aim of making these micelles was to have another lipase system to study enzymatic activity measurements (the other system will be discussed in chapter 5). Figure 2a and b contain the LS titration results for the complex formation of lipase, PAA_{42}-$PAAm_{417}$ and $PDMAEMA_{150}$. In this case only one titration was performed, starting at composition $F^- = 1$. This means that a polymer solution (containing the positively charged homopolymer $PDMAEMA_{150}$) was titrated to a mixture of lipase and negatively charged diblock copolymer PAA_{42}-$PAAm_{417}$.

In the intensity plot not only a maximum at $F^- = 0.5$ is found (as expected), but there is a second maximum at $F^- = 0.3$. This second maximum may be due to the formation of another polyelectrolyte complex. Because the protein and the homopolymer are oppositely charged these molecules

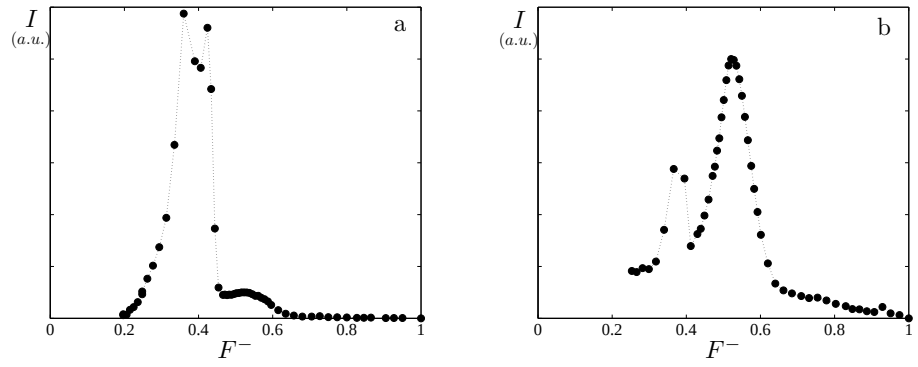

FIGURE 3. **a)** Composition titration of system 3 and **b)** system 4. In both systems the homopolymer was titrated to a mixture of diblock copolymer and protein.

are able to form a complex and this may be reflected by the maximum at $F^- = 0.3$. Since eventually we are interested in the enzymatic activity of lipase in polyelectrolyte complex micelles, the possible formation of complexes consisting only of lipase and $PDMAEMA_{150}$ is undesired. Therefore, we have chosen not to use these micelles for enzymatic activity measurements.

Systems 3 and 4. Some enzymes catalyse cascade reactions. This means that the product made by one enzyme can be used by the other enzyme. A well known enzyme couple performing such a cascade reaction consists of Glucose Oxidase (GOx) (system 3) and Horseradish Peroxidase (HRP) (system 4):

- Glucose + oxygen $\xrightarrow{GOx}$ H_2O_2 + gluconic acid
- H_2O_2 + electron donor $(2e-)$ + $2H^+$ $\xrightarrow{HRP}$ 2 H_2O + oxidised donor

Both enzymes were incorporated in $PAA_{42}PAAm_{417}$ + $PDMAEMA_{150}$ micelles. If successful the next obvious step would be to incorporate both enzymes together in the same micelles, to see whether the enzymatic activity was affected by the mode of incorporation. However, due to time constraints we have limited ourselves to the individual incorporation of the enzymes.

The results for the light scattering titrations for both proteins with PAA_{42}-$PAAm_{417}$ and $PDMAEMA_{150}$ are presented in figures 3a and b. Figure 3a shows one prominent maximum at $F^- \approx 0.4$, and a smaller one at $F^- = 0.5$ which would normally be the preferred micellar composition. The intensity *vs* composition plot for the horseradish peroxidase containing system (figure 3b) is very similar to figure 2, both having the maximal

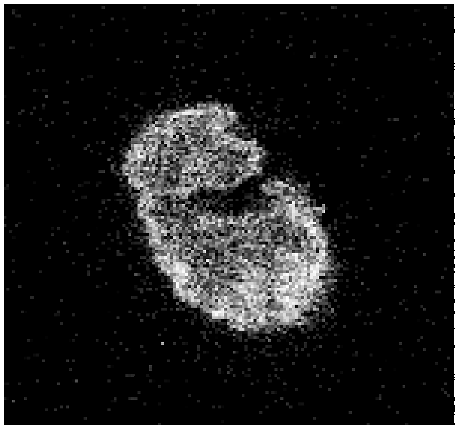

FIGURE 4. CLSM picture of a Green Fluorescent Protein/PDMAEMA complex, height: 8 μm, width 5 μm.

intensity at $F^- \approx 0.5$ and a smaller maximum at $F^- \approx 0.35$. For lipase (figure 2), GOx (figure 3a) and HRP (figure 3b) multiple maxima are observed at similar compositions, *i.e.,* between $F^- = 0.3$ and $F^- = 0.35$. The maximum intensity of the glucose oxidase containing system is higher than for the lipase and horseradish peroxidase containing systems probably because glucose oxidase has a molecular weight of 160 kDa, whereas the molecular weights of lipase and horseradish peroxidase are 27 and 44 kDa, respectively.

System 5. Light scattering is commonly used throughout this thesis for studying micelle formation. Using this technique it is very difficult to check what amount of proteins in the system is actually incorporated in the micelles and what amount of enzymes is free. This is because the mass of the micelles is much higher than the mass of the individual protein molecules and it is therefore difficult to probe free enzyme molecules using light scattering. Fortunately, nature is able to make fluorescent proteins. Incorporation of such a protein allows for using fluorescent techniques. By using a naturally fluorescent protein one overcomes probable difficulties by labeling with fluorescent probes and possible (negative) effects of the label on the protein structure. Therefore it was chosen to incorporate the the negatively charged green fluorescent protein (GFP) in PAA_{42}-$PAAm_{417}$ and $PDMAEMA_{150}$ micelles.

A fluorescence method which is similar to Dynamic Light Scattering is Fluorescence Correlation Spectroscopy (FCS). This technique requires a well-defined focal volume in which the diffusion time of fluorescent molecules is probed. Larger objects will diffuse slower than smaller ones. Therefore, one is able to discriminate between free (small particles) and incorporated

(large particles) protein molecules. Moreover, the intensity of the fluorescence may provide information about the number of proteins that are in the cores of the micelles.

During the FCS measurements, it was found that $\approx 96\%$ of the GFP had disappeared out of the solution. This could indicate that precipitation between the oppositely charged PDMAEMA and GFP had occurred. To check whether such aggregates where present in the measurement cell a confocal microscope was used. Figure 4 is a picture of the aggregates which were found at the bottom of the measurement cell. After discussions with the students it appeared that the composition of the system was $F \approx 0.35$ (instead of $F \approx 0.5$) , indicating that the system contained an excess of positively charged homopolymer. Moreover, this is the same composition at which a maximum was found in figure 2, 3a and b.

System 6. In chapter 3 we studied the complex formation between α-lactalbumin, PAA_{139} and $P2MVP_{41}$-PEO_{205}. It was also tried to incorporate lysozyme in these micelles. Here we also chose to perform a titration starting in two directions *i.e.,* from both ends of the composition axis. The results of these titration are shown in figure 5.

Like system B in chapter 3, the intensity plots are not symmetrical. As expected, the relaxation behaviour of this system is the same as system B. By comparing the shapes of the $I(F^-)$ plots of system B (see figure 3, chapter 3) and system 6 there is a clear difference. For the titration starting at $F^- = 0$ a shoulder appears at $F^- = 0.48$. A similar shoulder was also found for a system where the homopolymer to protein ratio (PDMAEMA: Lysozyme) was 17:83 (see chapter 2, figure 5a). For this system a plausible explanation was that a second structure is formed, because a different hydrodynamic radius was found, and also the pH as function of the composition suggested the formation of a second structure. From SCF calculations (chapter 7), it became clear that the most favourable place of the enzyme in the micelles is in the core-corona interface. It may be that micelle formation of system 6 consist of two steps: first micelles are formed at the composition of the shoulder and subsequently enzyme molecules are incorporated, resulting in micelles with a higher mass, and hence, a higher intensity at $F^-_{micelle}$. However, a detailed experimental analysis whether this the case for system 6 is currently missing.

4.4. Discussion

In this chapter complex formation between a like charged diblock copolymer and protein, and an oppositely charged homopolymer was studied. For complex formation of PAA_{42}-$PAAm_{417}$ + $PDMAEMA_{150}$ and a negatively charged protein molecule five systems where studied, using light scattering

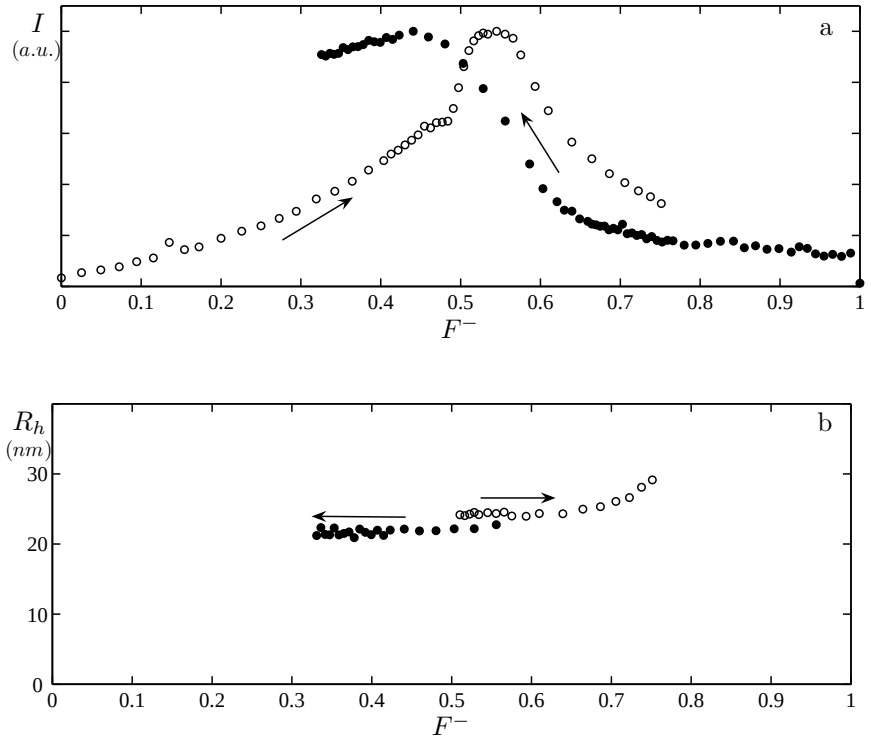

FIGURE 5. **Composition titration of system 6**. **a)** Intensity and **b)** hydrodynamic radius as function of the composition. ○ PAA_{139} titrated to P2MVP$_{41}$-PEO$_{205}$ and lysozyme and ● P2MVP$_{41}$-PEO$_{205}$ and lysozyme titrated to PDMAEMA$_{150}$, molar ratio between PAA_{139} and lysozyme 9:1.

titrations (systems 1-4) and fluorescence spectroscopy (system 5). For three (systems 2-4) of these five systems, two intensity maxima were observed: a maximum at $F^- \approx 0.5$ and a second maximum at $F^- \approx 0.35$. The system where no second maximum was observed contained α-lactalbumin, which is (in comparison to the other proteins lipase, horseradish peroxidase and glucose oxidase) rather small (14.2 kDa, *versus* 27, 44 and 160 kDa, respectively).

An explanation of the appearance of the maximum at $F^- \approx 0.35$ may be the formation of a complex between the oppositely charged homopolymers and protein molecules. In that case, the intensity of the second maximum is expected to depend on the molecular weight of the protein. For the glucose oxidase containing system the maximum at $F^- \approx 0.35$ was even higher than

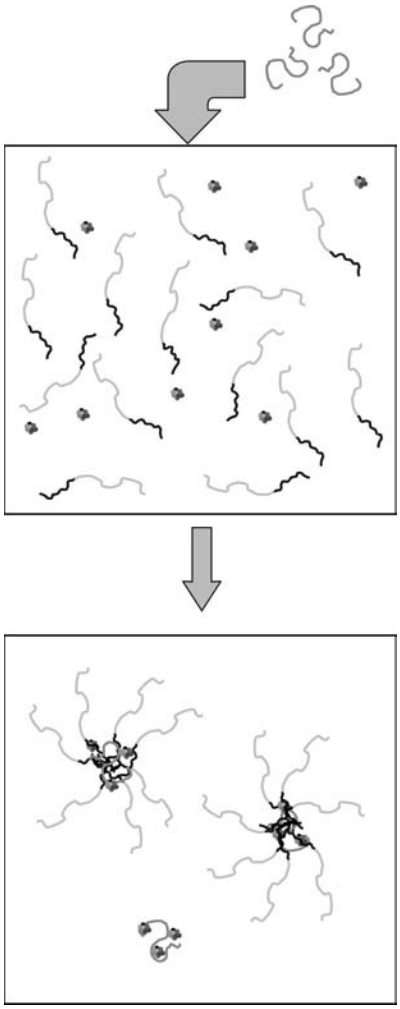

FIGURE 6. Sketch of the formation of polyelectrolyte complex micelles and protein-homopolymer polyelectrolyte complexes.

the maximum at the $F^-_{micelle}$. Other evidence for the formation of this homopolymer/protein complex was obtained by studying GFP incorporation with FCS. Here, the fluorescent protein had disappeared from the solution. The GFP seemed to be present in a precipitate which had settled at the bottom of the FCS measurement cell and could be imaged by CSLM (see figure 4). A schematic overview of the two types of polyelectrolyte complexes formed for system 2-5 is shown in figure 6.

During a titration experiment starting at $F^- = 1$, *i.e.,* adding positively charged homopolymer to negatively charged diblock copolymer and negatively charged protein molecules, three different complexes may be formed: (I) complexes between homopolymers and diblock copolymers, (II)

complexes between homopolymers and protein molecules and (III) complexes between al three: homopolymers, diblock copolymers and protein molecules. Because the attraction between the homopolymer and diblock copolymer is larger than the attraction between the homopolymer and the protein, it is expected that micellar structures are predominantly formed (both with and without protein molecules) and the typical maximum in the $I(F^-)$ plot is found at $F^- = 0.5$. These micelles disintegrate when more positively charged homopolymers are added. This leads to conversion of micelles into soluble complexes; the added homopolymers "steel" diblock copolymers from the micelles. Micelles containing both protein molecules and diblock copolymers as negatively charged components may disintegrate into soluble complexes consisting of diblock copolymers and homopolymers and complexes contains mainly homopolymers and protein molecules. These latter aggregates may be responsible for the maximum found at $F^- \approx 0.35$.

From the experiments described in chapter 3, it was found that the PAA_{42}-$PAAm_{417}$ + $PDMAEMA_{150}$ system has a relaxation time which is of the same order as the experimental time scale and rearrangements of the polyelectrolyte complexes may be observed during a titration experiment. In systems 1-5, the same polyelectrolytes are used (PAA_{42}-$PAAm_{417}$ + $PDMAEMA_{150}$) and thus the same relaxation behaviour may be expected. This may have an effect on the particles that are formed during the complex formation. When the homopolymer and protein are oppositely charged it may be that there is a coexistence between micelles and protein-homopolymer complexes. Moreover, when complexes are prepared by first mixing the homopolymer and protein, and subsequently adding the diblock copolymer, complexes between the homopolymers and protein molecules already are formed (see "size relaxation at fixed composition," chapter 3). This results in large precipitates; micellar structures containing enzymes will be hardly present in the solution.

The shape of the PAA_{139}, $P2MVP_{41}$-PEO_{205} and lysozyme titrations shown in figure 5 are different from the titrations of PAA_{139}, $P2MVP_{41}$-PEO_{205} and α-lactalbumin, shown in figure 3 of chapter 3. Starting at $F^- = 1$ the shapes of the titration with lysozyme and α-lactalbumin are the same. Starting at $F^- = 0$, however, first a gradual increase in the intensity is found. At $F^- = 0.45$ a shoulder shows up, whereafter the intensity increases again and a maximum is observed at $F^- = 0.55$. At higher F^--values the intensity decreases. The shoulder may be an indication of a two-step process: first, formation of micelles consisting of diblock copolymers and homopolymer and, second, incorporation of proteins in these micelles.

A similar shoulder has also been observed when the molar ratio between lysozyme and $PDMAEMA_{150}$ is 83:17 (chapter 2, figure 5b). The difference between these two titrations is the direction of the titration path. The shoulder found in this system may be explained by the presence of micelles

consisting only of homopolymer-diblock copolymer. At the composition at I_{max}, micelles may be present with enzymes in the core. We will come back to this in chapter 7.

Another difference between system 6 in this chapter and system B in chapter 3 is the size of the micellar objects during the titration (compare figure 5b to figure 3b in chapter 3. For system 6 the objects in the titration starting at $F^- = 0$ are slightly bigger than starting at $F^- = 1$. This is the opposite for system B in chapter 3. It is difficult to give a reason for this difference, because the PAA_{139} + P2MVP$_{41}$-PEO_{205} micelles are kinetically frozen and the way of preparation strongly affects the final structure of the complexes.

4.5. Concluding Remarks

There are strong indications that systems containing like-charged protein and diblock copolymer molecules mixed with oppositely charged homopolymer molecules phase separate into a mixture of micelles and protein-homopolymer complexes. Therefore, for incorporation of enzymes in polyelectrolyte complex micelles, it is recommended to choose a system such that the homopolymer and protein molecule have the same charge, and the diblock copolymer is oppositely charged.

Acknowledgements Most of the results in this chapter were obtained by BSc-students during the subject: "Bachelor Completion Molecular Sciences." I therefore would like to thank: Leon Jong, Marre Schäfer, Leonie Driessen, Bojk Berghuis, Frank Leavis and Jacky Flipse and their co-supervisors Willem van Berkel, Jan Willem Borst, Adrie Westphal and Jasper van der Gucht for their contributions to this chapter.

Chapter 5

Salt-induced Release of Lipase from Polyelectrolyte Complex Micelles

Abstract.
With the aim to gain insight in the possible applicability of protein-filled polyelectrolyte complex micelles under physiological salt conditions, we studied the behaviour of these micelles as function of salt concentration. The micelles form by electrostatically driven co-assembly from strong cationic block copolymers poly(2-methyl vinyl pyridinium)$_{41}$-*block*- poly(ethylene oxide)$_{205}$, weak anionic homopolymers poly(acrylic acid)$_{139}$, and negatively charged lipase molecules. The formation and disintegration of these micelles were studied with Dynamic Light Scattering (DLS), by means of composition and salt titrations, respectively. The latter measurements revealed differences between disintegration of lipase-filled and normal polyelectrolyte complex micelles. These data, together with Small Angle Neutron Scattering (SANS) measurements provide indications that lipase is gradually released with increasing salt concentration. From the SANS data a linear relation between the intensity at $q = 0$ and the volume of the cores of the micelles at different salt concentrations was derived, indicating a loss of volume of the micelles due to the release of lipase molecules. It was estimated that beyond 0.12 M NaCl all lipase molecules are released.

published as: Saskia Lindhoud, Renko de Vries, Ralf Schweins, Martien A. Cohen Stuart and Willem Norde in Soft Matter, 2009, 5, 242-250

5.1. Introduction

Functional ingredients, *e.g.*, proteins may be encapsulated to enhance their stability or to prevent external attack. This is beneficial in various applications. In industry and food technology[22,96] encapsulation might provide ways to protect enzymes against loss of activity or could even enhance the activity. Stabilisation of enzymes might significantly increase the shelf-life of bioactive formulations. Moreover, it might enable recycling of the enzymes on industrial scale. In pharmaceutics one could think of controlled delivery and release of therapeutic proteins.[30,97–99]

Several difficulties have to be overcome before proteins can usefully be incorporated in actual applications. The biological functioning of a protein is directly related to its molecular three-dimensional structure. This structure can very easily be destabilised, either physically, *e.g.,* by changing the environmental conditions,[100,101] or (bio)chemically, *e.g.,* by proteolytic attack. Obtaining a self-assembled structure in which protein molecules can be safely stored is a complicated challenge. The main problem to be solved is how to design the architecture and structure of this protein containing particle. Difficulties arise from the requirement that the protein to be incorporated should not suffer from any irreversible damage either during the packaging procedure or due to interactions with the packaging material.

Because proteins have a structure that is very sensitive to changes in the environment, *e.g.*, in temperature, polarity of the medium, pH, *etc.*, use of organic reactions during the incorporation procedure may be hazardous. Alternatively, nearly all proteins have charges, therefore one could use oppositely charged polyelectrolytes as package material.[93] Protein/polyelectrolyte mixtures are known to form dense liquid-like phases, called complex coacervates.[19] One advantage of using polyelectrolytes is that one can work in aqueous environment and avoid the use of organic solvents that may damage the protein.

Depending on the charge ratio between the polyelectrolyte and the protein, either charged soluble complexes are formed or, at stoichiometric charge ratio, precipitation or complex coacervation occurs.[20] Well-defined structures with specific distances between the proteins molecules have been obtained by protein/polyelectrolyte complexation.[15–18] However, not all polyelectrolyte/protein combinations will result in well-defined structures.

An extensively studied procedure to make encapsulating structures using polyelectrolytes is the layer-by-layer technique. Encapsulation of functional charged molecules can be achieved by exposing it in an alternating fashion to a solution containing polyanions and then to a solution containing polycations or *vice versa*. In this way layers of oppositely charged polymers are formed around the molecule. Since proteins are charged they can be encapsulated by this technique[102] or they may be incorporated within these layers.[103] Because of the electrostatic nature of the cohesive interactions,

changes in ionic strength and/or pH can induce the disintegration of the structure. It is also possible to incorporate permeability in the layer-by-layer shell, thereby enabling protein molecules to leave the capsule.[104]

Depending on the type of application, the size of a structure is important. In food systems particles may have micrometer dimensions; for medical applications sizes from $10 - 100$ nm are desired, since larger structures are known to be caught by the immune system (*e.g.*, phagocytes) and accumulate in the liver and the spleen.[28] For the nanopackaging and controlled delivery of hydrophobic drugs, promising results have been obtained[105–107] by making use of micelles. Kataoka *et al.*, synthesised amphiphilic block copolymers having a folate group attached to the water soluble block. These folate-conjugated micelles were used to encapsulate hydrophobic anti-cancer drugs, by conjugating them to the hydrophobic part of the block copolymer linkers that are sensitive to acidic pH. The micelles thus obtained, showed lower *in vivo* toxicity and higher anti-tumor activity than conventional anti-cancer formulations.[108–110]

The use of micelles seems to be very promising for pharmaceutical applications, because micelles are nanostructures with a well-defined architecture. The core of micelles consisting of amphiphilic block copolymers is relatively hydrophobic which could have a damaging effect on the native structure of the protein. A gentle way to incorporate proteins in micellar structures is the use of polyelectrolyte complex micelles. These micelles consist of a diblock copolymer (having a charged and a neutral hydrophilic block) and an oppositely charged homopolymer or a diblock copolymer.[23–25] At stoichiometric charge ratio, micellar structures with a polyelectrolyte complex core are formed. These structures are stabilised by a corona made of the hydrophilic block of the block copolymers. Since proteins are charged at pH other than their isoelectric point it is possible to incorporate them in the complex core by mixing them with an oppositely charged diblock copolymer.[26,27]

In our approach a protein solution is added to a solution containing like-charged homopolymers. This solution is subsequently mixed with a solution containing oppositely charged diblock copolymers (chapter 2). In this way micelles are obtained of which the stability against disintegration by salt and the number of protein molecules in the core can be controlled by changing the homopolymer-to-protein ratio (see figure 1 for a schematic illustration). It was found that stable micelles are formed when the homopolymer is in excess. This can be explained by the much higher charge density on the polyelectrolytes compared to that on the protein.

In line with this, one could imagine that by reducing the strength of the electrostatic attraction, proteins are the first molecules to leave the micelle. It has been shown that it is possible to weaken electrostatic interactions between the proteins and oppositely charged polyelectrolytes by

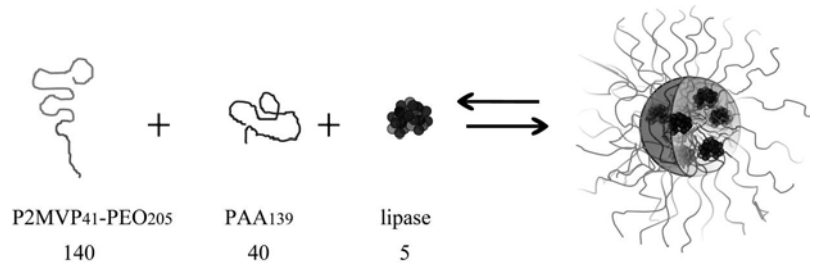

FIGURE 1. Schematic illustration of the formation of a polyelectrolyte complex micelle with proteins. The aggregation number of the micelles is estimated from Small Angle Neutron Scattering data.

salt,[36] pH,[111,112] external electric field,[38] and composition of the system. Hence, this would provide various ways to release protein molecules from their capsule.

To test whether proteins are indeed released from these polyelectrolyte complex micelles, we incorporated the (at pH 7) negatively charged lipase in micelles made of negatively charged homopolymer poly(acrylic acid)$_{139}$ (PAA_{139}) and the positively charged diblock copolymer poly(2-methylvinyl pyridinium)$_{41}$-*block*-poly(ethylene oxide)$_{205}$ ($P2MVP_{41}$-PEO_{205}). Lipase is a protein with a molar mass of 27000 g mol^{-1}. At pH 7 it has a net charge of -8e.[113] Clearly, the number of charges on the protein is fairly low, especially compared to the number of charges on the homopolymer ($-139e$) and on the charged block of the diblock copolymer ($+41e$). In this study we try to make use of this difference in charge density for the controlled release of the proteins. The addition of salt causes screening of the charges on the (bio)polymers. Since lipase is a very big molecule compared to the polyelectrolytes and has only 8 charges and, hence, a low charge density, one would expect these molecules to be released from the micelles first because the electrostatic attraction between lipase and $P2MVP_{41}$-PEO_{205} is much weaker than that between $P2MVP_{41}$-PEO_{205} and PAA_{139}.

The topic of disintegration of polyelectrolyte complexes by addition of salt has already been addressed by other groups. In most cases the polyelectrolyte complex systems were not electroneutral, *e.g.*, polyelectrolyte multilayers[114,115] or non-stoichiometric complexes in solutions.[72] The latter investigation by Zinchenko *et al*,. was performed on systems containing highly aggregated complexes of nearly stoichiometric charge ratio and free excess polyelectrolyte. They describe in detail the disintegration process of the complexes and report a shift in the equilibrium between large aggregates and smaller soluble complexes towards the latter with increasing salt concentration.

Kataoka *et al.*, have shown that it is possible to "unpack" proteins from

polyelectrolyte complex micelles by the addition of salt. They made complexes with lysozyme and oppositely charged diblock copolymers and studied the enzymatic activity during and after encapsulation.[36] Information about the disintegration of the micelles as a function of salt is very important for possible future applications. In our study lipase was chosen, because it is a commonly used industrial enzyme. This enzyme is *e.g.,* used in detergent formulations. We are interested in the enzymatic activity of lipase in the micelles. To study the lipase activity, before, during and after nanopackaging, the salt concentration at which all lipase molecules are released has to be known. Therefore we investigate the behaviour of the micelles as function of salt.

The techniques used to study the disintegration of the micelles as a function of salt were Dynamic Light Scattering (DLS) and Small Angle Neutron Scattering (SANS). Two types of DLS-titrations were performed: composition and salt titrations. During a composition titration like charged molecules are titrated to oppositely charged molecules, and information is obtained on the hydrodynamic radius and the intensity as function of the composition of the micelles. From these titrations one can determine the preferred micellar composition ($F^-_{micelle}$). Solutions with this composition are used for the salt titration and the neutron scattering experiments.

5.2. Experimental

5.2.1. Materials

The homopolymer used was Poly(acrylic acid)$_{139}$ (Polymer Source Inc., Canada), Mw= 10000 g mol^{-1}, PDI= 1.15, when fully charged this anion contains 139 charges. The lipase used in this study was Lipolase™, derived from the fungus *Humicola ℓanuginosa*, and was a gift from Novozymes (Bagsvaerd, Denmark). The positively charged diblock copolymer Poly(2-methylvinyl pyridinium iodide)$_{41}$-*block*-Poly(ethylene oxide)$_{205}$, obtained by quarternisation of Poly(2-vinyl pyridinium)$_{41}$-*block*-Poly(ethylene oxide)$_{205}$, PDI= 1.05, purchased from Polymer Source *Inc.*, Canada, and using the following protocol. In a typical reaction, 1 g of diblock copolymer containing P2VP was dissolved in 35 mL DMF. Iodomethane (3 mL) was added, and the reaction was stirred under nitrogen flux for 48 h at 60 °C. Ether (110 mL) was added to precipitate the polymer (add until no more precipitation occurs). The precipitate was filtered and washed with ether (5 × 10 mL) to yield a light yellow powder. (After each washing step the polymeric product was less yellow, less sticky, and more powdery). Subsequently, the polymer was placed in an oven at 50 °C to dry overnight. The mass after quarternisation was 19100 g mol^{-1}.

5.2.2. Dynamic Light Scattering Titrations

For the DLS-titrations we used an ALV5000 multiple tau digital correlator and an argon ion laser with a wavelength of 514.5 nm. All measurements were performed at a scattering angle of 90°. Temperature was kept constant at 25 °C by means of a Haake C35 thermostat, providing an accuracy of ± 0.1 °C. Titrations were performed using a Schott-Geräte computer-controlled titration set-up to control the addition of titrant, the cell stirring, and delay times. Effective average hydrodynamic radii of the complexes were determined by analysing the autocorrelation function using the methods of cumulants and using the Stokes-Einstein equation for spherical particles. From previous work we found that spherical particles are obtained when micelles contain more homopolymer molecules than protein molecules. Although a certain polydispersity is expected.

In the composition titrations a mixture of negatively charged PAA and lipase were titrated to the positively charged P2MVP$_{41}$-PEO$_{205}$. The pH was kept constant by using a 3.5 mM sodium phosphate buffer of pH 7. Scattered intensity and hydrodynamic radius are typically presented as a function of the composition F^-:

$$F^- = \frac{[n_-]}{[n_-] + [n_+]} \tag{8}$$

where n_+ is the total number of charges on the P2MVP$_{41}$-PEO$_{205}$ in solution, and n_- is the total number of chargeable groups of PAA$_{139}$ plus the number of charges on lipase in solution. The number of charges of lipase was estimated from the titration curve determined by Duinhoven *et al.*,.[113] The molar ratio between the homopolymer (PAA$_{139}$) and the protein was 9 : 1, since we know from previous experiments that stable micelles are formed when the homopolymer is in excess (chapter 2). Moreover, in this case it was estimated that there are about 10 protein molecules inside a micelle. Titrations were performed at two conditions of ionic strength: no added salt and 50 mM NaCl. For the normal micelles (without lipase) the PAA$_{139}$ was added to P2MVP$_{41}$-PEO$_{205}$. The stirring time in these measurements was 60 s, waiting time after stirring varied from $10 - 120$ s. After every titration step, five light scattering runs each of 30 s were performed.

For the salt titrations 9 mL solution (in 3.5 mM phosphate buffer, pH= 7) of micelles containing lipase and without lipase were prepared. The starting concentration of both solutions was 1 g L^{-1}. Micelles with lipase were prepared in the following way: first lipase and PAA$_{139}$ were mixed and then P2MVP$_{41}$-PEO$_{205}$ was added. This solution was kept in a refrigerator overnight. To this solution a 5 M NaCl solution was titrated in small steps of 20 μL. After every addition a delay time of 150 seconds (60 stirring, 90 s of waiting) was used.

5.2.3. Small Angle Neutron Scattering

Small Angle Neutron Scattering experiments were performed at the Institut Max von Laue- Paul Langevin (ILL), Grenoble, France, on the D22 beam line. Measurements were performed at two detector distances; 4 and 17.6 m, resulting in a q-range of $0.0023 - 0.137$ Å^{-1}. The wavelength was 8 Å. Spectra were treated according to ILL standard procedures, and put on an absolute scale using the known absolute scattering intensity of H_2O.

Samples were prepared from a stock solution of micelles at their preferred micellar composition $F^-_{micelle}$, in a 3.5 mM phosphate buffer in D_2O, pH= 7 (pD=6.56). After 6 hours of equilibration of the micellar stock solution, the NaCl concentrations were set using a concentrated solution of NaCl in D_2O, to give final NaCl concentrations in the samples of 0, 0.1, 0.3, 0.5 and 0.7 M, respectively, and a micelle concentration of 8 g l^{-1} (polymers and proteins combined).

For particles of volume V_{part} and number density n_{part}, the absolute scattering intensity, $I(q)$, (cm^{-1}) can be written as:

$$I(q) = n_{part}\Delta\varrho^2 V_{part}^2 P(q)S(q) \tag{9}$$

where $\Delta\varrho$ is the contrast, *i.e.,* the difference between the solvent scattering length density and the average scattering length density of the particles (cm^{-2}), $P(q)$ the form factor and $S(q)$ the structure-factor. We use low concentrations of micelles such that, to a good approximation, the structure-factor $S(q) \approx 1$.

From previous work (chapter 2) we know that at low protein content the micelles are spherical, and rather monodisperse, hence we expect scattering curves to satisfy the $P(q)$ for a sphere with radius R:

$$P(q) = \left[\frac{3[sin(qR) - qRcos(qR)]}{(qR)^3} \right]^2 \tag{10}$$

At higher values of q, the internal structure of the polyelectrolyte core contributes to the form factor, and a simple sphere model no longer fits. Therefore, equation 10 is only used to fit the data up to $q \leq 0.024$ Å^{-1} (which is sufficient to obtain a reliable estimate of the micellar core radius R_c). At higher salt concentrations, the scattering intensity drops rapidly. As a consequence, the statistics of the low-q data for the higher salt concentrations is not sufficient to allow for a form factor fit, even though we can still use the data for a rough estimate of the scattering intensity for $q \to 0$.

The PEO corona of the polyelectrolyte core micelles is rather dilute (see Results and Discussion) and may be expected to hardly contribute to the scattered intensity. Therefore, the scattering intensity is to a good approximation due to the polyelectrolyte complex core of the micelles, and the

radius R_{core} from the form factor fit is the radius of the micellar core. If we know both the scattering at zero angle and the core radius R_{core}, we can estimate the degree of solvent-swelling of the micellar cores. The zero angle scattering $I(0)$ is:

$$I(0) = n_{part}(\Delta\varrho)^2 V_{part}^2 \tag{11}$$

For a given global volume fraction Φ of swollen core material in the system, the number density of the micelles is:

$$n_{part} = \frac{\Phi}{V_{part}} \tag{12}$$

However, from the system composition we can only calculate the global volume fraction Φ_0 of unswollen core material. The two are related by the local volume fraction φ of dry core material inside a swollen micelle,

$$\Phi_0 = \varphi\Phi \tag{13}$$

Swelling and deswelling also changes the contrast of the micellar cores, according to:

$$\Delta\varrho = \varphi\Delta\varrho_0 \tag{14}$$

where $\Delta\varrho_0$ is the scattering length density contrast between the unswollen core material and the solvent. Combining everything, the zero angle scattering can be written as:

$$I(0) = \Phi_0\varphi(\Delta\varrho_0)^2 V_{part} \tag{15}$$

Given values for $\Delta\varrho_0$, Φ_0, and R, and using $V_{part} = \frac{4}{3}\pi R_c^3$, this equation can be used to obtain a rough estimate for φ, the total volume fraction of macromolecules in the micellar cores.

5.3. Results and Discussion

5.3.1. Dynamic light scattering composition titration.

Previously it has been shown that DLS-titration is a useful tool to obtain information about polyelectrolyte complex micelle formation (chapter 2 and 3).[31,32] During a composition titration like-charged molecules are titrated to molecules of opposite charge. This allows to simultaneously study the hydrodynamic radius and light scattering intensity as function of the composition F^- (equation 8). By changing the composition upon addition of titrant, the intensity increases until a maximum is found. The initial intensity increase is ascribed to the formation of soluble complexes, of which it is not possible to accurately determine the hydrodynamic radius. After

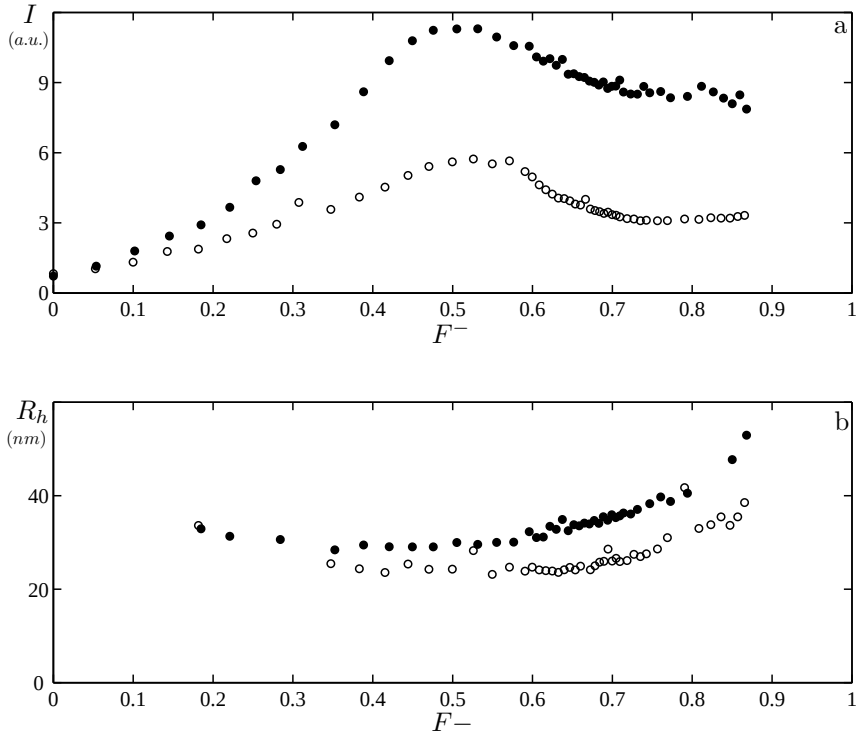

FIGURE 2. **DLS composition titration**. **a)** Light scattering intensity and **b)** hydrodynamic radius as function of the composition of solutions prepared with no salt (•) and 50 mM NaCl(○). Typically a 10 g L^{-1} solution of of PAA_{139} and lipase with a molar ratio of 9:1 titrated to a 1 g L^{-1} solution of P2MVP$_{41}$-PEO$_{205}$, pH= 7.

reaching a certain composition micelles are formed. The maximum in the intensity corresponds to the preferred micellar composition $F^-_{micelle}$. Typically this maximum is at the electroneutral composition $F^- = 0.5$ (equation 8).[31] Maxima deviating from $F^- = 0.5$ have been found in systems where polymers with a pH dependent charge or proteins are used (chapter 2 and 3).

The results of the DLS composition titration are shown in figure 2. In these measurements the starting solution contained P2MVP$_{41}$-PEO$_{205}$ to which a 9:1 mixture (molar ratio) of PAA_{139} and lipase was titrated. Figure 1 shows a schematic representation of the formation of these micelles. The intensity (figure 2a) and hydrodynamic radius (figure 2b) of the micelles as function of the composition are plotted. According to equation 8

electroneutral particles are expected at $F^-_{micelle} = 0.5$. The hydrodynamic radius of the micelles consisting of PAA_{139}, lipase and $P2MVP_{41}$-PEO_{205} at $F^- = F^-_{micelle}$ is about 25 nm. From $F^-_{micelle}$ the mixing ratio of the different components can be derived. Solutions with this optimal composition (for micelles with no extra salt added) are used in the salt titrations and the neutron scattering experiments. The intensity as function of the complex formation is asymmetric along F^-. Similar asymmetry has been found in other systems (chapter 2),[65] but there are also examples of symmetric intensity distributions around $F^- = 0.5$.[31,32]

The polyelectrolyte complex formation was studied at two different ionic strengths, 3.5 mM phosphate buffer with no extra salt added and 3.5 mM phosphate buffer with 50 mM NaCl, respectively. The light scattering intensity of the system without extra addition of salt is higher than the intensity of the system containing 50 mM NaCl, for all values of F^-. The hydrodynamic radius is also larger. Anticipating the discussion of the DLS salt titrations (figure 3) and the SANS data (figure 4), it is mentioned that, at 50 mM NaCl less protein molecules are incorporated, resulting in a lower scattered intensity and smaller hydrodynamic radius.

There may be several reasons for the asymmetry of the intensity as function of the composition. Apparently, there is a difference in the formation of the micelles ($F^- < 0.5$) and disintegration of the micelles ($F^- > 0.5$). In the case of the complex formation between a homopolymer and diblock copolymer similar asymmetry was found when at least one of the components was a strong polyelectrolyte (having a charge which is pH independent). Symmetric curves have been found when both polyelectrolytes had a pH dependent charge. The titrations performed at 50 mM NaCl indeed suggest that the micelles more readily disintegrate ($F^- > 0.5$), indicating that the differences in disintegration between the two systems are electrostatic in nature. At higher salt concentration electrostatic forces are weaker, allowing for faster rearrangements.

Another explanation for the asymmetry of figure 2a could be that the system itself is not symmetrical, because it contains three components. However, in our previous work we have seen that the intensity as function of the composition for a system containing only (positively charged) lysozyme and (negatively charged) PAA_{42}-$PAAm_{417}$ was asymmetric and became more symmetric when the protein molecules were partly replaced by the positively charged homopolymer $PDMAEMA_{150}$, yielding a symmetric curve for three component systems where homopolymer was in excess of the protein (chapter 2).

The hydrodynamic radii (figure 2b) as function of the composition shows a minimum at $F^-_{micelle}$. At this composition electroneutral particles are obtained. The somewhat larger radii together with the lower light scattering intensity at compositions other than $F^-_{micelle}$ indicate, larger, less dense

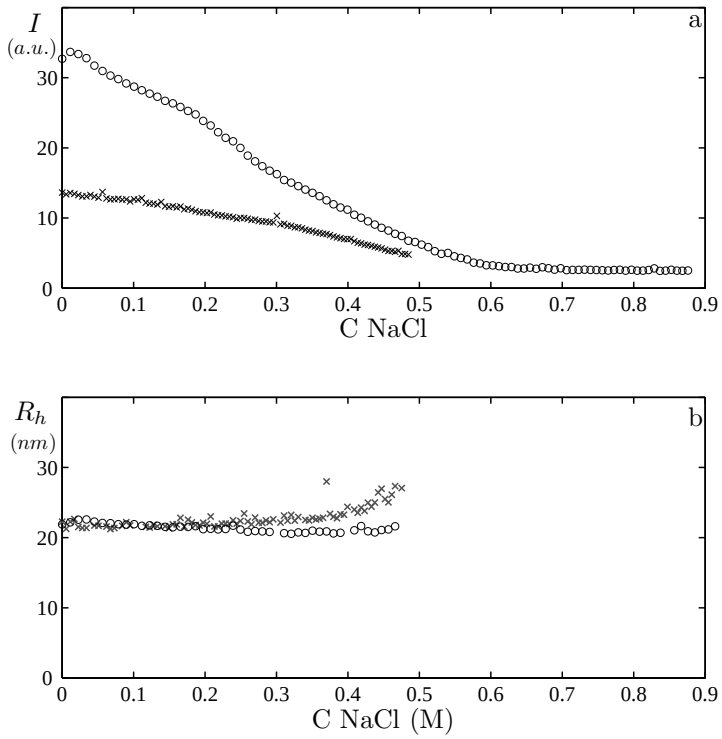

FIGURE 3. **DLS salt titration**. **a)** Light scattering intensity and **b)** hydrodynamic radii of light scattering titrations. Micelles with lipase (○), micelles without lipase (x). Starting solution contained 9 mL of 1 g L^{-1} micelles, the titrant was 5 M NaCl, pH= 7, titration steps were 20 μL.

structures. Under these conditions the micelles (or soluble complexes) are expanded due to repulsion between the charged groups within these structures.

5.3.2. Dynamic light scattering titrations with salt.

To study the disintegration of the micelles by weakening of electrostatic interactions a DLS-titration with salt was performed. During this measurement a concentrated NaCl (5 M) solution was titrated to a solution with composition $F^{-}_{micelle}$. In figure 3a and b the results of the salt titration are shown. In this figure data for both the micelles with and without lipase are plotted. The composition of the normal micelles is the $F^{-}_{micelle}$ ($F^{-} = 0.5$) resulting from a titration with only PAA_{139} and P2MVP$_{41}$-PEO$_{205}$. Hence,

these micelles are different structures than the lipase-filled micelles. At the same concentration of the micelles and no NaCl added, the light scattering intensity of the micelles with lipase is much higher than the light scattering intensity of the normal micelles.

The scattering intensity is found to decrease with increasing salt concentration. This could have several reasons. First, it may be that addition of salt causes a shift in the equilibrium between small soluble complexes (consisting of a few polyelectrolytes) and micelles. Such a shift in equilibrium towards smaller soluble complexes was found to occur during the disintegration of non-stoichiometric polyelectrolyte complexes.[72] Second, the number of polymer or protein molecules in the micelle *i.e.*, aggregation number of the micelles, may be affected by salt. This will result in a population of micelles with a salt dependent aggregation number and free polyelectrolytes or proteins. This is most likely the case for the micelles with proteins. The less densely charged protein molecules might be expelled from the micelles resulting in a different aggregation number. It is also possible that all these processes take place simultaneously.

Comparing the micelles with and without proteins reveals a few differences. The decrease in light scattering intensity with increasing NaCl concentration is more pronounced for micelles with lipase than for the micelles without lipase. The effect of salt on the hydrodynamic radius (figure 3b) is different for the micelles with and without lipase as well. For the micelles without protein the radius slightly increases between 0.2 and 0.5 M NaCl. This is consistent with swelling of the micelles because of screening of the charges. The hydrodynamic radius of the micelles with lipase decreases slightly upon the addition of salt. Above 0.5 M NaCl all the micelles, both with and without lipase, are disintegrated.

Since both systems show a decrease in light scattering intensity and a hydrodynamic radius that is approximately constant up to a salt concentration of 0.2 M NaCl, the mass of the micelles changes upon the addition of salt. The decrease in intensity of the micelles without lipase may result from an aggregation number which is dependent on the salt concentration. The decrease in intensity of the micelles with lipase is likely to be caused by either proteins or polyelectrolytes being expelled from the micelles. Previous work showed that complexes of lysozyme and PAA_{42}-$PAAm_{417}$ disintegrated at a salt concentration of 0.12 M NaCl (chapter 2). Kataoka *et al.*, used a salt concentration of 0.15 M NaCl to unpack lysozyme from polyelectrolyte complex micelles.[36] So it could be that $0.12 - 0.15$ M NaCl is a typical salt strength at which protein/polyelectrolyte complexes disintegrate.

One might expect that, when all proteins are released the micelles with and without lipase are similar, implying that both the intensity and hydrodynamic radius are the same at NaCl concentrations beyond 0.2 M. According to figure 3 this is clearly not the case and the dissimilarity may

be explained as follows. The micelles without lipase are electroneutral structures. Lipase-release from the lipase-filled micelles will induce the formation of slightly charged micelles. However, since the charge density of a lipase molecule is much lower than the charge density of the poly(acrylic acid) the resulting micellar charge is negligibly small. The deviating characteristics of these micelles is most likely due to the fact that lipase has an influence on the packing of the micelles and, hence, on their internal structure. Lipase is rather big compared to the polyelectrolytes. By addition of salt, the electrostatic interaction between the lipase and positively charged diblock copolymer can easily be weakened, inducing the release of the lipase. The departing lipase molecules may leave behind some holes in the micellar core. It may be that rearrangement of the macromolecules in the micellar core is slow. Of course the addition of salt will enhance the rearrangement kinetics, but in figure 2 it is seen that their is only a small difference in terms of disintegration of the micelles between no salt and 50 mM NaCl. The normal micelles and micelles which have released all their lipase are two different structures, at least within the time frame of a salt titration measurement.

5.3.3. Small Angle Neutron Scattering.

The information, notably R_h, derived from dynamic light scattering reflects the whole micelles, *i.e.*, the core and corona. Because of our interest in what is happening during the disintegration of the micelles, it would be desired to get more information on the fate of the core of the micelles. To study the structure of the core of the micelles we used SANS. This technique provides information about the internal structure of the micelles, since it probes at a smaller scale than light scattering. Differences in contrast between the particles and the solvent are measured. At low scattering vector q, information about the size of the particles is obtained. At high q, information about the internal structure of the micelles is derived. For micelles made of charged diblock copolymers and oppositely charged surfactant micelles a peak was found at high q, giving insight in the distances between the surfactant micelles within the complexes.[58] Similar peaks were also found in systems consisting of a protein and oppositely charged polyelectrolyte.[15,16,18] In the following, first the intensity at $q = 0$ will be discussed. This is followed by the fitting of the curves and the scattering at high q. In the next section a detailed analysis of the structure of the micelles and the release of lipase is presented.

Figure 4 shows that the intensity of the neutron scattering at $q = 0$ strongly decreases as function of the salt concentration. By either fitting (0, 0.1 and 0.3 M NaCl) or taking the intensity of the lowest accurate q-value (0.5 and 0.7 M NaCl) the intensity at $q = 0$ can be estimated. This intensity can directly be compared to the light scattering titration as function of salt. In figure 5 it is seen the changes in light and neutron scattering intensity as

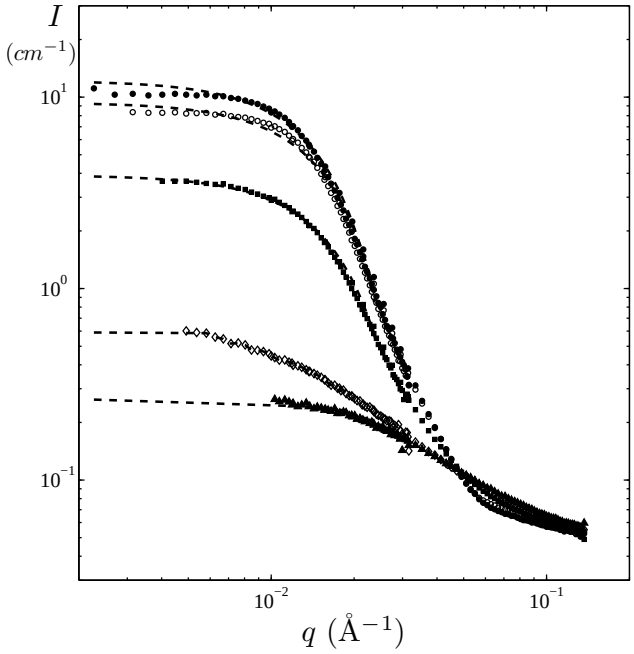

FIGURE 4. Small Angle Neutron Scattering as a function of salt concentration: • 0 M NaCl, ○ 0.1 M NaCl, ■ 0.3 M NaCl, ◇ 0.5 M NaCl and ▲ 0.7 M NaCl. The micellar concentration was 8 g L^{-1}. The dashed lines of 0, 0.1 and 0.3 M NaCl are form factor fits for monodisperse spheres. The dashed lines of 0.5 and 0.7 indicate the estimated intensity at $q = 0$.

function of salt are proportional; at the lower salt concentrations a decrease of the intensity as function of salt is found. From 0.5 to 0.9 M NaCl with both scattering techniques the intensity levels off to reach a constant value.

Knowledge of $I(0)$ is also useful for another reason. In equation 15 it is shown that the intensity scales with the volume. Knowing the radius, which can be determined by fitting of the scattering curves, and calculation of the contrast ($\Delta\varrho_0$) and density (see table 2), one can determine the mass and aggregation number of the particles. Since the only difference between the curves in figure 4 is the salt concentration, this figure directly suggests that the volume of the particles varies with the salt concentration. The signal-to-noise ratio for the scattering curves of the 0, 0.1 and 0.3 M NaCl samples allow for a detailed analysis, but the signal-to-noise ratio of the 0.5 and 0.7 M NaCl samples is not good enough for this purpose. The data quality could have been improved by increasing the concentration of the micelles or use a longer measuring time. However, from the DLS-titration with salt

it became clear that at 0.5 and 0.7 M NaCl one is most likely dealing with soluble complexes and individual micellar building blocks rather than with micelles. A very detailed analysis of the curves obtained at these conditions is therefore less relevant for our understanding of the enzyme-filled micelles.

The scattering curves of 0, 0.1 and 0.3 M NaCl allow to characterise the structure of the micelles. These scattering curves were fitted to the form factor for homogeneous spheres (equation 10). The dashed lines in figure 4 are the fits to the data (the dashed lines of the 0.5 and 0.7 M NaCl samples are simply the intensity at the lowest q-value measured). Scattering curves at 0, 0.1 and 0.3 M NaCl could only be fitted to $q \leq 0.024$ Å^{-1}. At higher q the internal structure of the micelles starts contributing to the scattering. Therefore, this form factor fit could only be used to obtain an approximate core radius. Generalised Indirect Fourier Transformation (GIFT) is a model-free method to analyse small angle scattering data, which could be used over the total q-range. This method gave the same R_{core},[52,53] indicating validity of our approach. Table 1 summarises an overview of the radii determined by light- and neutron scattering. In the next section we will come back to these results.

As mentioned before, information about the internal structure of the micelles is extracted from the remaining part of the scattering curve at q-values > 0.024 Å^{-1}. The five scattering curves cross each other around $q = 0.05$ Å^{-1} and the order of the scattering curves inverts at this point. Iso-scattering was also found during heat-induced gelation of globular proteins and was interpreted in terms of microphase separation between native proteins and aggregates.[116] Such a point may be found when there are two distinct populations of different species present. Another reason for the existence of an iso-scattering point is a change in solvent quality for one or more components. For instance, it is known that the solubility of PEO decreases as function of salt concentration.[117] Similar iso-scattering points are therefore also found in PEO-PPO-PEO micellar systems at different salt concentrations.[118] Both explanations could be valid for our system. On one hand, two populations of species could be present in the system *e.g.* micelles *versus* single components. On the other hand, the lower solubility of PEO with increasing salt concentration could as well give rise to the iso-scattering point.

At higher q-values we expected to find a correlation peak due to scattering by the proteins.[15,16,18,58] Correlation peaks are found when very distinct distances are present within a structure, *e.g.*, protein molecules. In our data such peaks are not found, indicating that there is no well-defined characteristic distance between the protein molecules. Anticipating the discussion in the next section, the absence of such a characteristic distance and, hence, ordered packing of the protein molecules in the micellar core, could be due

to a too small amount of protein in the micelles.

Table 1: Radii of the Complexes

$\mathbf{C}_{salt}$ **(M)**	$\mathbf{R}_H$ **(nm) (DLS)**	$\mathbf{R}_{core}$ **(nm) (SANS)**
0	22	13.8
0.1	21	13.0
0.3	20	12.2

Table 2: Densities and scattering length densities components of the micelles

Component	**density (g cm^{-3})**	**SLD cm^{-2}**
PAA	1.15	2.09^{10}
Lipase	1.41	3.20^{10}
P2MVP	1.05	1.33^{10}
PEO	1.13	6.46^{10}

values were taken from [64,119–122] and www.isis.rl.ac.uk

5.3.4. Lipase release from the micelles.

In the paragraph 5.2.3 it has been described how to derive characteristics of the micelles from the neutron scattering data. From the fitting of the SANS curves the radii of the cores (see table 1) and $I(0)$ have been determined. Using equation 15 and the values from table 2, the total volume fraction of macromolecules in the core (φ) can be established. If we assume that all the protein molecules are encapsulated in the micelles when no salt is added, the scattering length density of the core material is $\Delta\varrho_0 = 1.73 \times 10^{10}$ cm^{-2} and the global volume fraction Φ_0 of unswollen core material is 2.8×10^{-3}. This results in $\varphi \approx 0.17$ implying that 83% of the core of the micelles consist of water. This gives a molar mass of the core of approximately 1.2×10^6 g mol^{-1}. Since the ratio between the various components is known, we can estimate the number of different molecules in the micelles: approximately 140 diblock copolymers, 40 homopolymers and 5 proteins. The area per block copolymer at the core-corona interface ($\sigma = \frac{4\pi R_{core}^2}{\sharp diblock}$) is about 17 nm^2. The volume of five lipase molecules is about 2% of the core volume, and

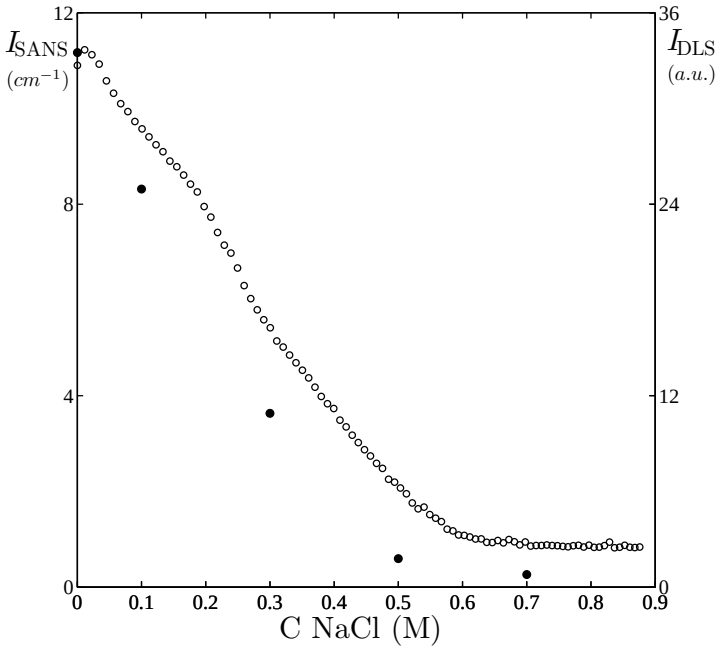

FIGURE 5. • I(0) (SANS) and ∘ I (light scattering) as function of the salt concentration.

about 11% of its dry mass.

It has been stated in paragraph 5.2.3 that the PEO corona is rather dilute and is expected to hardly contribute to the neutron scattering. Indeed, there is a clear difference between the radii of the micelles measured with light-and neutron scattering, see table 1. The hydrodynamic radius (R_H) is much larger than the fitted SANS radius (R_{core}). To estimate the corona contribution (r) to the neutron scattering we use the following expression:

$$r = \left[\frac{(\varphi_{corona}\Delta\varrho_{0,corona}V_{corona})}{(\varphi\Delta\varrho_0 V_{core})}\right]^2 \tag{16}$$

in this expression the scattering length densities of all the components and the solvent, as well as the densities of the components are needed in this equation (see table 2 for these values). Furthermore, the volumes of (what is assumed to be) the core and the corona are required. The volume of the corona (V_{corona}) was calculated in the following way: the core volume ($V_{core} = \frac{4}{3}\pi R_{core}^3$) was subtracted from the hydrodynamic volume ($V_H = \frac{4}{3}\pi R_H^3$). In equation 16 φ_{corona} is the volume fraction of PEO in the corona and $\Delta\varrho_{0,corona}$ is the scattering length density of the corona. The corona contribution r to the scattering was less than 0.1% indicating

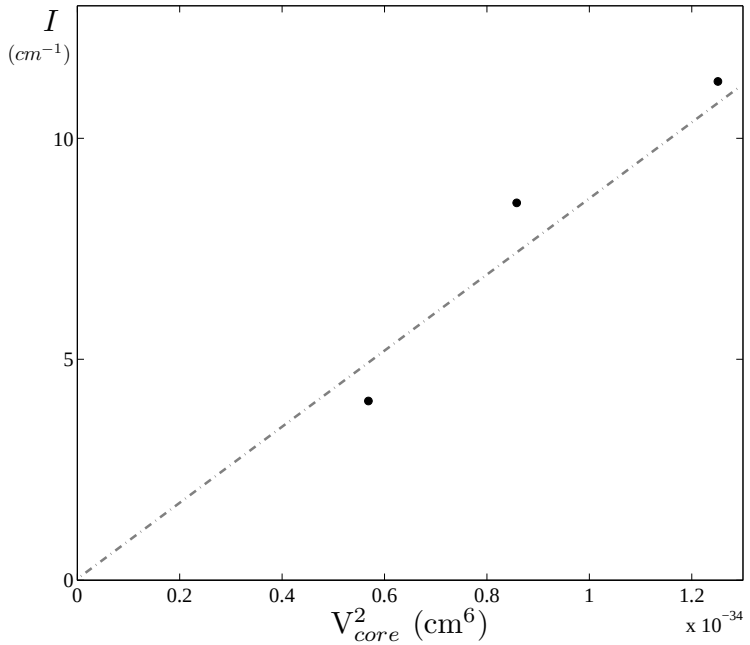

FIGURE 6. • I(0) (SANS) as function of V^2_{core}. Where V_{core} was calculated from the fitted radii of the 0, 0.1 and 0.3 M NaCl scattering curves.

that essentially the core radius is measured.

As discussed above, the micelles with and without protein behave differently during the light scattering salt titrations (figure 3). For both systems the intensity decreases upon increasing salt, but for the lipase-filled micelles the influence of salt is more pronounced. Because the two systems are both electroneutral, the different sensitivities for salt mean that the systems are not the same. For the lipase-filled-micelles the charge of the proteins is needed to obtain electroneutrality, whereas the normal micelles at stoichiometric charge ratio consist of polyelectrolytes only. Also the hydrodynamic radii measured during light scattering titrations of micelles with and without lipase are slightly different. This could mean that lipase molecules are released, yielding smaller micelles because of the volume loss due to the released proteins. Please note, that the differences in hydrodynamic radii are masked by the large corona.

If upon the addition of salt only lipase molecules are released from the micelles, it would mean that the number of polyelectrolytes in the micelles remains constant. Changes in the volume of the micelles, the volume fractions of the polymers and the amount of water are expected to occur. Figure

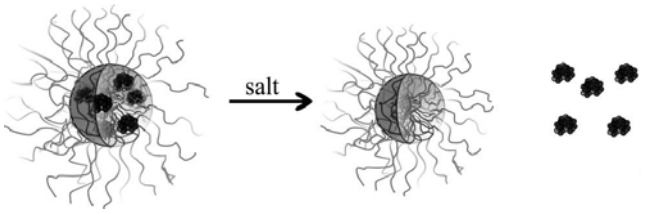

FIGURE 7. Artistic impression of the release of lipase from polyelectrolyte complex micelles as function of salt.

7 is an artistic impression of this process. The neutron scattering curves of five systems at different salt concentrations show a reduced scattering intensity and radius of the micelles at higher salt concentration. In (neutron) scattering $I(0) \sim V^2$ (see also equation 9), because $n\Delta\varrho^2$ is approximately constant at 0, 0.1 and 0.3 M NaCl. This means that plotting $I(0)$ as a function of V_{core}^2, where V_{core}^2 is derived from the form factor fit ($V_{core} = \frac{4}{3}\pi R_{core}^3$, see table 1), should have a linear relationship if the core volume reduction is a function of salt concentration. In figure 6 it is seen that a linear relation between $I(0)$ and V_{core}^2 exists. Thus, the decrease in volume is likely to be caused by the release of the lipase.

A change in volume may also be caused by other components leaving the micelles. One could imagine that diblock copolymers or homopolymers or small soluble complexes consisting of both these polymers, are leaving the complex. However, considering the differences in charge density of the different components (-8 per lipase molecule *versus* -139 per PAA_{139} molecule) this scenario is rather unlikely. The charge density of the polymers is much higher than that of the proteins. Whenever a polymer would leave, the complex is no longer electroneutral and rearrangement of micelles has to occur, resulting in total re-organisation of the system. This could lead to the formation of other complexes and influence the size and/or number of micelles in the system. Hence, in other scenarios a linear relation between $I(0)$ and V^2 is not necessarily the case. Moreover, to be electroneutral the charges of the lipase are not really needed; the poly(acrylic acid) is a weak polyelectrolyte and is therefore able to take up protons or release them. Micelles made of only polyelectrolytes seem to swell slightly upon the addition of salt and there is no indication of release of components from these micelles or a reduction in the number of micelles (see figure 3).

In conclusion, expulsion of polyelectrolytes from the complexes seems highly unlikely. Assuming that only lipase molecules are released, it should in principle be possible to estimate the number of incorporated proteins as function of the salt concentration. This can be calculated by defining $\Delta V = V_0 - V_{salt}$ and $\Delta V / V_{lipase}$ = number of free lipase molecules. (A lipase molecule is ellipsoidally shaped with dimensions $5.3 \times 5.0 \times 4.1$ nm^3).

If we assume that in a 3.5 mM phosphate buffer all the proteins are encapsulated, the number of protein molecules per micelle core can be derived from the neutron scattering, using equation 15. Since the mass of the micelles can be calculated and the ratio between the components is known, the aggregation number of the micelles can be determined and, hence, the number of protein molecules per core. Furthermore, it is assumed that the number of polyelectrolytes in the micelles and therefore also the number of micelles remain unaltered. In this way it is possible to model the lipase release as a function of salt. Table 3 shows the results for different salt concentrations.

Interpolating the data in table 3 reveals that at 0.12 M NaCl all the lipase molecules are released from the micelles. From previous DLS-titrations with salt we know that all complexes made of only diblock copolymer ($PAA_{42}PAAm_{417}$) and protein (lysozyme) are disintegrated at 0.12 M NaCl (chapter 2). Apparently, for these two systems the electrostatic interactions between a protein and oppositely charged polyelectrolyte vanish at this salt concentration. This salt concentration is lower than the physiological salt strength (150 mM), and therefore these systems are not suitable for drug-delivery applications.

Table 3: Properties of the Complexes

$\mathbf{C}_{salt}$ **(M)**	**number of proteins**
0	4.6
0.05	2.6
0.1	0.4
0.3	0

5.4. Concluding Remarks

This study shows a difference in disintegration between lipase-filled and normal polyelectrolyte complex micelles upon the addition of salt, studied with dynamic light scattering titrations. Combination of DLS measurements and Small Angle Neutron Scattering allowed for a structural analysis of the lipase-filled complexes. It was determined that without the addition of salt, five lipase molecules are incorporated in the micelles. Furthermore, the micellar core consists of 83% of water. This implies the enzymes are quite well accessible for substrate molecules.

Increasing the salt concentration of a solution containing lipase-filled polyelectrolyte complex micelles, induces the release of lipase. This release

can be explained in terms of charge density difference between the proteins and the polyelectrolytes. Around a salt concentration of 0.12 M all the lipase molecules are released. This is a rather low salt concentration and indicates that these micellar systems are not very useful for pharmaceutical applications, because they have released most of their proteins at physiological salt strength (150 mM). To make these systems applicable under these conditions, other interaction forces between the protein molecules and the polyelectrolytes have to be incorporated, such as, for instance, increasing the hydrophobic interactions.[39] This may be achieved by designing polyelectrolytes that have repeating charged and hydrophobic groups, provided that the native three-dimensional structure of the protein is maintained. Another procedure could be to covalently attach the proteins to one of the polyelectrolytes and make this bond sensitive to an external trigger which induces the release of the protein molecules. One could for instance think of a similar kind of pH trigger that was used by Kataoka *et al.*, to release anti-cancer drugs from folate-conjugated micelles.[108–110]

In the future we intent to investigate the activity of lipase in the micelles. The knowledge that at 0.12 M NaCl all the enzymes have been released will enable us to study the activity of lipase before, during and after incorporation.

Chapter 6

Salt-induced Disintegration of Lysozyme-containing polyelectrolyte complex micelles

Abstract.
The salt-induced disintegration of lysozyme-filled polyelectrolyte complex micelles, consisting of positively charged homopolymers ($PDMAEMA_{150}$) negatively charged diblock copolymers (PAA_{42}-$PAAm_{417}$) (and lysozyme), has been studied with Dynamic Light Scattering (DLS) and Small Angle Neutron Scattering (SANS). These measurements show that, from 0 to 0.2 M NaCl, both the hydrodynamic radius (R_h) and the core radius (R_{core}) decrease with increasing salt concentration. This suggests that the micellar structures rearrange. Moreover, from $\approx$ 0.2 to 0.4 M NaCl the light scattering intensity is constant. In this salt-interval the hydrodynamic radius increases, has a maximum at 0.3 M NaCl and subsequently decreases. This behaviour is observed in both a lysozyme-containing system and a system without lysozyme. The SANS measurements on the lysozyme-filled micelles do not show an increased intensity nor a larger core radius at 0.3 M NaCl. This indicates that from 0.2 to 0.4 M NaCl another structure is formed, consisting of just the diblock copolymer and the homopolymer, since at 0.12 M NaCl lysozyme$-$$PAA_{42}$-$PAAm_{417}$ have been disintegrated. One may expect that the driving force for the formation of the complex in this salt-range is other than electrostatic.

accepted in Langmuir

6.1. Introduction

Polyelectrolyte complexes are commonly employed packaging material for functional biomacromolecules.[22,102,123] Proteins are incorporated in such complexes to be protected, stabilised and structured. These protein containing structures can be used to control the structure and texture of food, but can also be used for targeted and controlled delivery of therapeutic proteins.[30] A reason why polyelectrolytes are chosen as wrapping material is that at pH-values other than their iso-electric point proteins are charged and may therefore form polyelectrolyte complexes with oppositely charged polyelectrolytes.

Since different polyelectrolyte architectures are available, numerous polyelectrolyte complex structures can be formed. When using linear polyelectrolytes and oppositely charged protein molecules, depending on the mixing fraction, either nano-sized soluble complexes or macroscopic precipitates are formed. These precipitates may be either liquid-like or solid-like. Liquid-liquid phase separation in polyelectrolyte complexation is called complex coacervation and it often occurs in systems containing proteins and weakly charged polyelectrolytes with low charge densities *e.g.,* charged polysaccharides.[19–21,124] Strongly charged polyelectrolytes may form more solid-like precipitates with oppositely charged protein molecules. In these precipitates there often is a characteristic distance between the protein molecules within the complex, which has been determined by Gummel *et al.,*[15,16,18] for lysozyme containing complexes.

By changing the architecture of the polyelectrolyte, protein-containing nanoparticles may be formed. The change in the architecture should be such that a hydrophilic stabilising mechanism is introduced. Examples of such polymers are graft-copolymers, having a hydrophilic backbone and charged side-chains[125] and diblock copolymers of which one block is uncharged and hydrophilic and one block is charged.[26,27] Using these diblock copolymers, core-shell structures are obtained, having a polyelectrolyte complex core and a corona consisting of the neutral block of the diblock copolymer.

Here, we study polyelectrolyte complex micelles consisting of negatively charged diblock copolymers (PAA_{42}-$PAAm_{417}$), positively charged homopolymers ($PDMAEMA_{150}$) and positively charged protein molecules (lysozyme). It has been shown that micelles made of these three components are less easily destabilised by added salt in comparison to micelles consisting of just PAA_{42}-$PAAm_{417}$ and lysozyme (chapter 2).

Various applications of enzymes wrapped in polyelectrolytes, require a certain robustness towards *e.g.,* changes in the salt concentration. Therefore, knowledge of the stability of protein-polyelectrolyte complexes as function of salt is relevant. From previous work we know that polyelectrolyte complex micelles consisting of $P2MVP_{41}$-PEO_{205}, PAA_{139} and lipase show

a salt induced release of lipase, prior to disintegration of the micelles themselves (chapter 5).

A main difference between these lipase-containing micelles and the micelles considered in the present study (PAA_{42}-$PAAm_{417}$, $PDMAEMA_{150}$ and lysozyme) is their relaxation behaviour. It was found that micelles consisting of $P2MVP_{41}$-PEO_{205} and PAA_{139} and negatively charged protein molecules are kinetically quenched for at least seven days. In contrast, micelles consisting of PAA_{42}-$PAAm_{417}$, $PDMAEMA_{150}$ and lysozyme seem to equilibrate entirely on a timescale of approximately two days (chapter 3). Hence, the salt-induced disintegration of the lysozyme-filled micelles may also be different from the previously studied lipase-filled micelles. In this study we will therefore compare the disintegration of the lysozyme-filled micelles to the previously studied disintegration of the lipase-containing micelles (chapter 5).

Light scattering titrations and neutron scattering experiments, similar to those that were used to unravel the salt-induced release of lipase, are used in this study to gain insight in the disintegration of the lysozyme-filled micelles. The light scattering titration with salt will be compared to a light scattering titration of polyelectrolyte complex micelles without lysozyme (consisting only of homopolymers and diblock copolymers). These latter micelles will be referred to as "normal micelles."

6.2. Methods

6.2.1. Materials

Lysozyme (L6876) was purchased from Sigma and used without further purification. The poly(acrylic acid)-*block*-poly(acryl amide) ($PAA_{42}PAAm_{417}$, where the numbers refer to the number averaged degree of polymerisation) diblock copolymers were a gift from Rhodia, Auberville, France. For details of the synthesis see Taton *et al.,*.[48] The positively charged homopolymer used was poly(N,N dimethylaminoethyl methacrylate) ($PDMAEMA_{150}$), purchased from Polymer Source, *Inc.,* Canada.

6.2.2. Dynamic Light Scattering (DLS) Titrations

For the DLS-titrations we used an ALV5000 multiple tau digital correlator and an argon ion laser with a wavelength of 514.5 nm. Measurements were performed at a scattering angle of 90°. Temperature was kept constant at 25 °C by means of a Haake C35 thermostat, providing an accuracy of ± 0.1 °C. Titrations were performed using a Schott-Geräte computer-controlled titration set-up to control the addition of titrant, the cell stirring, and delay times. Effective average hydrodynamic radii of the complexes were determined by analysing the autocorrelation function using the methods of

cumulants and using the Stokes-Einstein equation for spherical particles. The viscosity and refractive index of water were used for this particle size determination.

In the composition titrations a mixture of positively charged lysozyme and $PDMAEMA_{150}$ was added to the negatively charged PAA_{42}-$PAAm_{417}$. The pH was kept constant by using a 3.5 mM sodium phosphate buffer of pH 7 Scattered intensity and hydrodynamic radius are presented as a function of the composition F^-:

$$F^- = \frac{[n_-]}{[n_-] + [n_+]} \tag{17}$$

where n_- is the total number of charges on the $PAA_{42}PAAm_{417}$ in solution, and n_+ is the total number of chargeable groups of $PDMAEMA_{150}$ plus the number of charges on lysozyme in solution. The number of charges of lysozyme was estimated from the proton charge (pH) curve determined by Van der Veen *et.al.*,.[50] The molar ratio between the homopolymer ($PDMAEMA_{150}$) and the protein was 8:2; this ratio was chosen since we know from previous experiments that stable micelles are formed when the homopolymer is in excess (chapter 2). It was estimated that there are about 10 protein molecules inside a micelle. For the normal micelles (without lysozyme) $PDMAEMA_{150}$ was added to $PAA_{42}PAAm_{417}$. The stirring time in these measurements was 60 s, waiting time after stirring varied from $10 - 120$ s. After every titration step, five light scattering runs of 30 s each were performed. From these composition titrations the preferred micellar composition ($F^-_{micelle}$) can be determined.

For the salt titrations a solution (in 3.5 mM phosphate buffer, pH= 7) of 1 g L^{-1} micelles containing lysozyme was prepared. The micelles, having composition $F^-_{micelle}$, were prepared by adding $PAA_{42}PAAm_{417}$ to a mixture of lysozyme and $PDMAEMA_{150}$. This solution was kept in a refrigerator overnight. Then, a 5 M NaCl solution was titrated to 9 mL of micellar solution, in small steps of 20 μL. Between additions a delay time of 150 seconds (60 stirring, 90 s of waiting) was maintained. These salt titration measurements were performed with an ALV5000 multiple tau digital correlator and an Oxxius DPSS solid state laser with a wavelength of 532 and a power of 150 mW.

6.2.3. Small Angle Neutron Scattering

SANS experiments were performed on the D22 beam line at the Institut Max von Laue-Paul Langevin (ILL), Grenoble, France. Measurements were performed at two detector distances, 4 and 17.6 m, resulting in a q-range of $0.0023 - 0.137$ Å^{-1}. The wavelength was 8 Å. Spectra were treated according to ILL standard procedures and put on an absolute scale using the

known absolute scattering intensity of H_2O.

Samples were prepared from a stock solution of micelles having composition $F^-_{micelle}$, in a 3.5 mM phosphate buffer in D_2O, pH= 7 (pD= 6.56). After 6 hours of equilibration of the micellar stock solution, the NaCl concentrations were set using a concentrated solution of NaCl in D_2O, to give final NaCl concentrations in the samples of 0, 0.1, 0.3, 0.5 and 0.7 M, respectively, and a micelle concentration of 8 g L^{-1} (polymers and proteins combined).

The analysis of the scattering curves is done in the same way as for the previously studied lipase-containing micelles (chapter 5). Here, the procedure is briefly summarised as follows:

For a dispersion of (randomly dispersed) particles of volume V_{part} and number density n_{part}, the absolute scattering intensity, $I(q)$, (cm^{-1}) can be written as:

$$I(q) = n_{part}\Delta\varrho^2 V_{part}^2 P(q)S(q) \tag{18}$$

where $\Delta\varrho$ is the contrast, *i.e.,* the difference between the solvent scattering length density and the average scattering length density of the particles (cm^{-2}), $P(q)$ the form factor and $S(q)$ the structure-factor. The concentration of micelles is chosen such that, to a good approximation, the structure-factor $S(q) \approx 1$.

From previous work (chapter 2) we know that at low protein content the micelles are spherical, and rather monodisperse, hence, we expect scattering curves to satisfy the $P(q)$ for a sphere with radius R:

$$P(q) = \left[\frac{3[sin(qR) - qRcos(qR)]}{(qR)^3} \right]^2 \tag{19}$$

At higher values of q, the internal structure of the polyelectrolyte core contributes to the form factor, and a simple sphere model no longer fits. Therefore, equation 19 is only used to fit the data in the range from 0.0076 up to $q \leq 0.028$ $Å^{-1}$ (which is sufficient to obtain a reliable estimate of the micellar core radius R_{core}). The scattering intensity drops rapidly at higher salt concentrations (0.5 – 1.0 M). As a consequence, the statistics of the low-q data for the higher salt concentrations is not sufficient to allow for a form factor fit, even though we can still use the data for a rough estimate of the scattering intensity for $q \to 0$.

The polyacrylamide corona of the polyelectrolyte core micelles is rather dilute (see Results and Discussion) and may be expected to hardly contribute to the scattered intensity, like the PEO corona, discussed in previous work (chapter 5). Therefore, the scattering intensity is to a good approximation due to the polyelectrolyte complex core of the micelles, and the

radius R_{core} derived from the form factor fit is the radius of the micellar core. If both the scattering at zero angle and the core radius R_{core} are known, an estimate of the degree of solvent-swelling of the micellar cores can be made. The zero angle scattering $I(0)$ is:

$$I(0) = n_{part}(\Delta\varrho)^2 V_{part}^2 \tag{20}$$

For a given global volume fraction Φ of swollen core material in the system, the number density of the micelles is:

$$n_{part} = \frac{\Phi}{V_{part}} \tag{21}$$

However, only the global volume fraction Φ_0 of unswollen core material can be calculated from the system composition. The two are related by the local volume fraction φ of dry core material inside a swollen micelle,

$$\Phi_0 = \varphi\Phi \tag{22}$$

Swelling and deswelling also influence the contrast of the micellar cores, according to:

$$\Delta\varrho = \varphi\Delta\varrho_0 \tag{23}$$

where $\Delta\varrho_0$ is the scattering length density contrast between the unswollen core material and the solvent. Combining everything, the zero angle scattering can be written as:

$$I(0) = \Phi_0\varphi(\Delta\varrho_0)^2 V_{part} \tag{24}$$

Given values for $\Delta\varrho_0$, Φ_0, and R, and using $V_{part} = \frac{4}{3}\pi R_{core}^3$, this equation can be used to obtain a rough estimate for φ, the total volume fraction of macromolecules in the micellar cores.

6.3. Results and Discussion

The polyelectrolyte complex micelles in this study consist of three components: positively charged homopolymers ($PDMAEMA_{150}$), negatively charged diblock copolymers (PAA_{42}-$PAAm_{417}$) and the (at pH= 7) positively charged lysozyme molecules. First, the optimal ratio between these three components is determined by performing a dynamic light scattering composition titration. The optimal ratio is the composition ($F^-_{micelle}$) at which the light scattering intensity is maximal (figure 1). Disintegration of micelles (having this composition) by salt are studied by means of dynamic

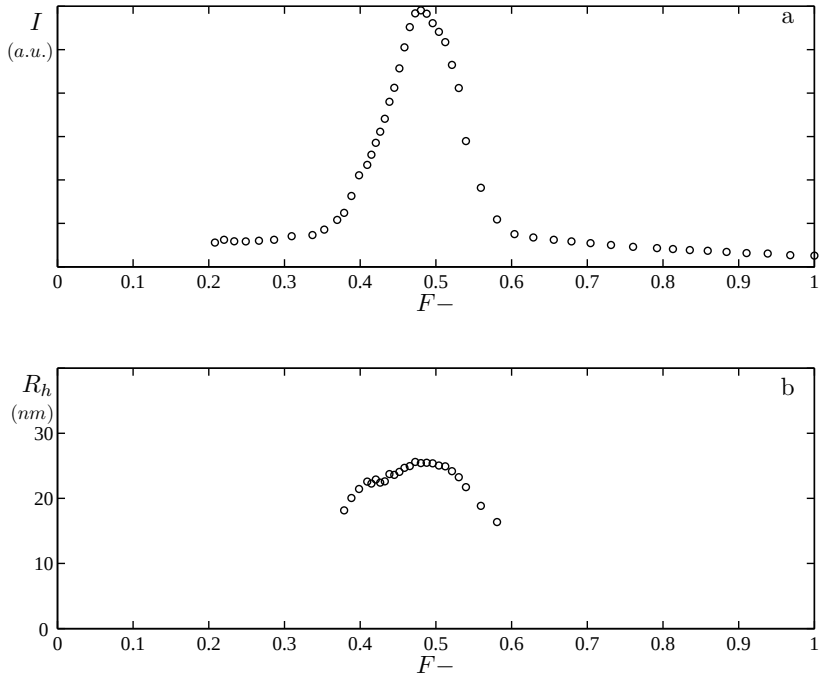

FIGURE 1. **a)** Light scattering intensity (I) and **b)** hydrodynamic radius (R_h) as function of the composition. Only radii having a standard deviation of less than 1 nm are shown. A 8:2 mixture of $PDMAEMA_{150}$ and lysozyme (10 g L^{-1}) was titrated to a PAA_{42}-$PAAm_{417}$ solution (1 g L^{-1}).

light scattering (figure 2) and small angle neutron scattering (figure 3).

6.3.1. Dynamic Light Scattering titrations

Composition titrations. During a DLS-composition titration a mixture of the positively charged homopolymer ($PDMAEMA_{150}$) and protein (lysozyme), with a molar ratio of 8:2, is titrated to a solution containing the negatively charged diblock copolymer (PAA_{42}-$PAAm_{417}$). After every titration step a light scattering measurement is performed and the profile of the intensity and the derived hydrodynamic radius are plotted as a function of the composition F^- (equation 17). The results of this titration are presented in figure 1a and b.

The plots shown in figure 1a and b are typical plots for systems containing two weakly charged polyelectrolytes. In such a system the intensity plot can be divided in four regions. These regions have first been described by

Van der Burgh *et al.*,.[31] The maximum in intensity is found at $F^- = 0.48$ (figure 1a), which is close to the theoretical value of 0.50. The hydrodynamic radius of the micelles (figure 1b) can only be determined between $F^- > 0.38$ and $F^- < 0.58$. At $F^-_{micelle}$ (where the scattered intensity has a maximum) the size of the micelles is 25 nm.

Salt titrations. From the composition titrations $F^-_{micelle}$ has been determined, and solutions having this composition have been prepared for the salt titration. During a (DLS) salt titration a concentrated solution containing 5 M NaCl is slowly titrated to 9 mL of a micellar solution (1 g L^{-1}) in steps of 20 μL. After every addition a light scattering measurement is started and the light scattering intensity and hydrodynamic radius are measured.

In figures 2a and b the result of the salt titration is shown. In these graphs the results for normal micelles without lysozyme (consisting of only PAA_{42}-$PAAm_{417}$ and $PDMAEMA_{150}$) are plotted as well. The composition of these micelles is determined using the same protocol as described in the previous section. Note that these protein-free micelles are also electroneutral particles and are slightly different from the lysozyme-filled micelles, since they only contain homopolymers and diblock copolymers. At electroneutrality the ratio between the two polyelectrolytes is slightly different from the ratio within polyelectrolyte complexes consisting of diblock copolymers, homopolymers and lysozyme molecules.

For both micellar systems, the intensity (figure 2a), first gradually decreases over the range from 0 to 0.22 M NaCl. The slope of the lysozyme-filled micelles is slightly steeper than that of the normal micelles. From 0.22 to 0.3 M NaCl for the lysozyme-filled micelles and from 0.22 M to 0.4 M NaCl for the normal micelles the light scattering intensity remains more or less constant. For both systems the light scattering intensity decreases and levels off; this occurs at 0.42 M NaCl for the lysozyme-filled micelles and at 0.5 M NaCl for the normal micelles. This indicates that disintegration of normal micelles occurs at a higher salt concentration, implying that the lysozyme-filled micelles are less resistent towards the addition of salt.

For both systems the trends in hydrodynamic radius and intensity as function of salt are similar up to a salt concentration of 0.22 M NaCl (figure 2b). From 0 to 0.25 M NaCl the size of the lysozyme-filled micelles decreases from about 28 nm to about 20 nm. The size of the normal micelles decreases from 27 to 21 nm over this salt interval. Further raising of the NaCl concentration induces an increase of the size of the micelles for both systems, with a maximum of about 28 nm for the lysozyme-filled micelles at 0.32 M NaCl. The hydrodynamic radii of the normal micelles cannot be determined accurately above a salt concentration of 0.35 M NaCl, because of the large standard deviation of the radii. Further addition of salt induces

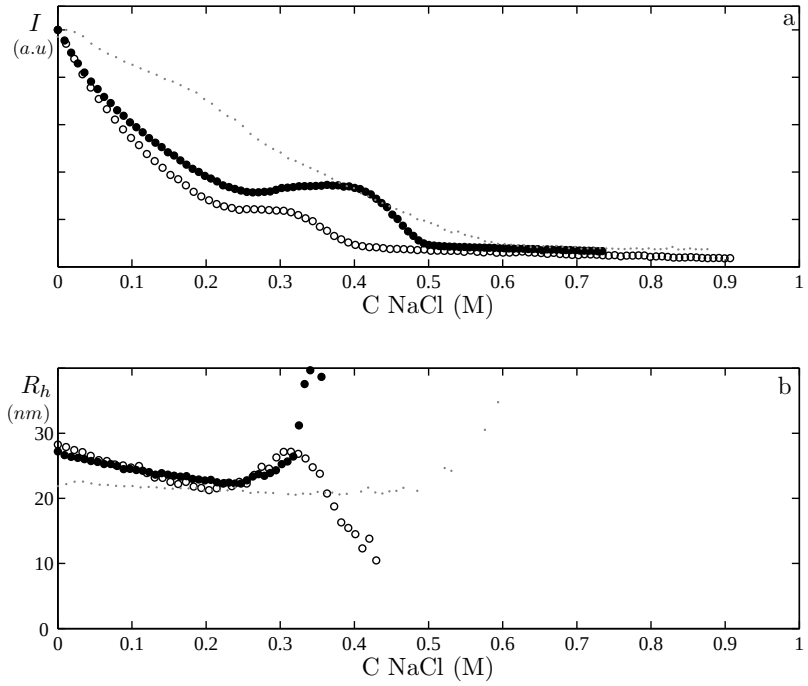

FIGURE 2. **Salt titration. a)** Light scattering intensity (I) and **b)** hydrodynamic radius (R_h) as function of salt concentration for ○ lysozyme-filled micelles and ● normal micelles. Only radii having a standard deviation of less than 1 nm are shown. Light grey dots are the results for the salt titration of the lipase-filled micelles consisting of P2MVP$_{41}$-PEO$_{204}$. The concentration of micelles is 1 g L^{-1}, the starting volume was 9 mL.

a decrease in micelle size of the lysozyme filled micelles, until no micelles are detected anymore at a NaCl concentration of 0.42 NaCl. This is the same concentration at which the intensity of the lysozyme-filled micelles levels off (see figure 2a).

Similar measurements performed on the PAA$_{42}$-PAAm$_{417}$/ lysozyme/ PDMAEMA$_{150}$ micelles reported above, have also been performed with PAA$_{139}$/ lipase/ P2MVP$_{41}$-PEO$_{205}$ micelles. That study also included a salt titration with normal micelles (consisting of PAA$_{139}$ and P2MVP$_{41}$-PEO$_{205}$) (chapter 5). Comparing the present results to those for the lipase-containing micelles and the normal micelles that were studied in chapter 5 (consisting of PAA$_{139}$ and P2MVP$_{41}$-PEO$_{205}$), reveals an important difference in the shape of the intensity as function of the salt concentration. The previously studied lipase-containing micelles and the normal micelles

showed a gradual decrease in intensity as function of the salt concentration (chapter 5) and no plateau was observed as seen in figure 2a for the lipase-containing micelles, (the light grey dots). The hydrodynamic radii of the lipase-filled and normal micelles remained almost constant up to a salt concentration of 0.4 M NaCl. An explanation for the difference between the salt-induced disintegration of the lysozyme-containing and lipase-containing micelles in the light scattering titrations with salt will later be provided.

The decrease in light scattering intensity for the previously studied lipase-containing micelles (chapter 5) indicates that the core of the micelle was losing contrast-rich material. Small Angle Neutron Scattering on this system revealed that with increasing salt concentration the effective core radius R_{core} decreases. For the lysozyme-filled micelles studied here, both the light scattering intensity and the hydrodynamic radius decrease as function of salt. Therefore, it was decided to do similar SANS measurements with the lysozyme-filled micelles.

Table 1: Densities and scattering length densities

Component	**density (g cm^{-3})**	**SLD (cm^{-2})**
PDMAEMA	0.92 *	8.00^{9} (126)
Lysozyme	1.41 (127)	3.20^{10} (127)
PAA	1.15 *	2.09^{10} (121)
PAAm	1.30 (128)	6.46^{10} (121)

* values were taken from handbook of Chemistry and Physics 85th edition

6.3.2. Small Angle Neutron Scattering.

Light scattering provides information about the size of the whole micelles, *i.e.,* the core and the corona. To obtain information on the core of the micelles, Small Angle Neutron Scattering (SANS) may be used as it probes distances that are smaller than can be measured by light scattering and, hence, it may provide details of the internal structure of the micelles. Differences in contrast between the particles and the solvent are measured. For the lipase containing micelles it has been shown that the contribution to the scattering intensity by the corona was less than 0.1% (chapter 5). At low scattering vector q, information about the size of the particles can be derived. At high q (> 0.15 Å^{-1}), information about the internal structure of the micelles may be obtained. High q peaks, from which characteristic distances within a complex can be derived, have been observed in polyelectrolyte complex micelles with surfactant micelles in the core [58] and in protein/polyelectrolyte complexes. [15,16,18] From previous experiments we know,

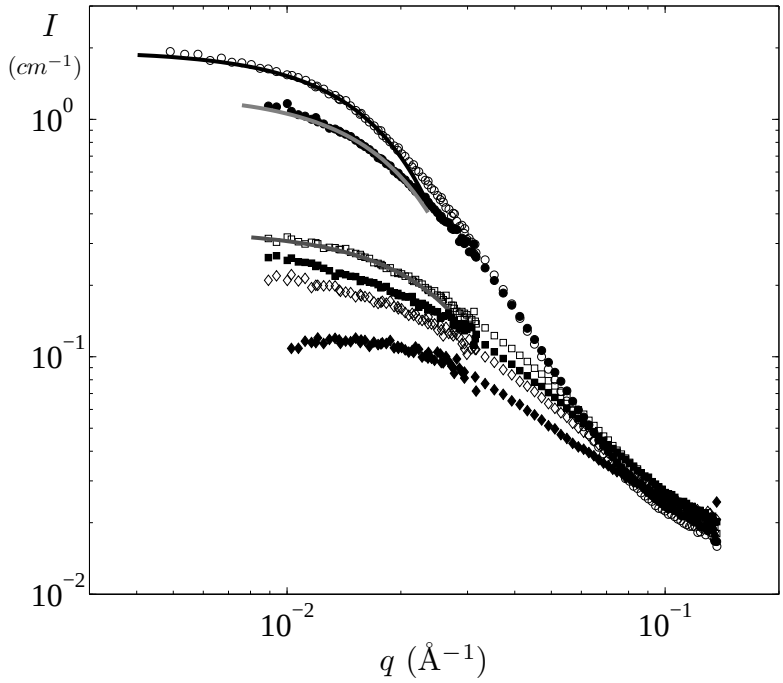

FIGURE 3. Small Angle Neutron Scattering as a function of salt concentration ○ 0 M, ● 0.1 M, □ 0.3 M, ■ 0.5 M, ◊ 0.7 M and ♦ 1 M NaCl. The dashed lines in this figure are the form factor fits. The composition of the solutions is $F^{-}_{micelle}$, derived from figure 1, the micelle concentration is 8 g L^{-1}.

however, that in our systems, the number of protein molecules in the core of the micelles is too low to obtain such a high q peak (chapter 5).

SANS curves of the polyelectrolyte complex micelles at various salt concentrations are shown in figure 3. With increasing salt concentration the scattering decreases, which was also observed by DLS during the salt titration. Figure 4 shows that the intensity of both the light- and neutron scattering levels off at high salt concentration. However, we do not have enough neutron scattering intensity points to obtain information about the core between 0.2 and 0.3 M NaCl.

From the fitting of the SANS curves the radii of the cores (see table 2) and $I(0)$ have been determined and it is seen that R_{core} decreases upon increasing NaCl concentration. Using equation 24 and the values of table 1, the total volume fraction of macromolecules in the core (φ) can be established. If we assume that in the absence of salt all the protein molecules are incorporated in the micelles, the scattering length density of the core material is $\Delta\varrho_0 = 1.19 \times 10^{10}$ cm^{-2} and the global volume fraction Φ_0 of

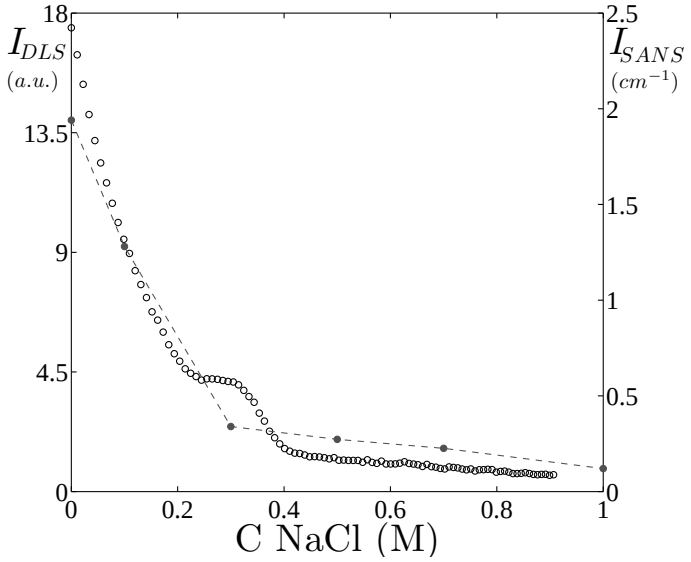

FIGURE 4. DLS intensity ∘ and (0, 0.1 and 0.3 M NaCl) and estimated (0.5, 0.7 and 1 M NaCl) SANS intensity ($I(0)$) intensity • as function of salt concentration.

unswollen core material is 2.8×10^{-3}. This results in $\varphi \approx 0.08$ implying that 92% of the core of the micelles consists of water. This gives a molar mass of the core of approximately 2.8×10^5 g mol^{-1}. Since the ratio between the various components is known, we can estimate the number of different molecules in the micelles: approximately 29 diblock copolymers, 8 homopolymers and 2 lysozyme molecules. The volume taken by these two lysozyme molecules is about 2% of the core volume and approximately 5% of the dry mass of the core.

The core mass of this lysozyme-micelle is significantly smaller than for the lipase containing micelle (1.2×10^6 g mol^{-1}). A possible explanation may be that the length of the water soluble block of the diblock copolymer is approximately twice as long for the lipase-filled micelles. The ratio between the corona-block and core forming block is determining for the kind of micelles that are formed. When the corona-forming block is very long in comparison to the charged block, star-like micelles will form.[129] The aggregation number of these micelles is smaller in comparison to the aggregation numbers of micelles with shorter corona-blocks. Hence, their core mass is also smaller. The polymers on the core-corona interface occupy a certain surface area. For the lysozyme-containing micelles the area per block copolymer ($\sigma = \frac{4\pi R_{core}^2}{\sharp diblock}$) is about 51 nm^2.

The hydrodynamic radius of the lipase-containing micelles remained

more or less constant during the salt titration and the light scattering intensity decreased gradually. Furthermore, the SANS intensity and the core volume decreased, which points to a reduction of the core mass. For the lysozyme-containing micelles in this study, both the initial ($0-0.2$ M NaCl) hydrodynamic radius and the light scattering intensity decreased as function of salt. In the SANS measurements both the intensity and the core radius decreased, which was also observed for the lipase-containing micelles. These data, together, suggest that the disintegration of the lysozyme-filled micelles is more complicated; both the hydrodynamic volume and the core volume change upon the addition of salt. The simple model of lipase-release cannot be applied to these lysozyme containing micelles.

The dissimilarity in disintegration behaviour between the lysozyme-filled micelles and the lipase-filled micelles may be caused by a different relaxation rate for the polyelectrolyte complex formation. Experiments were performed in which the three different components of the micelles were mixed in three different ways. It has been shown that the lysozyme-filled micelles have a relaxation time of approximately two days. Polyelectrolyte complex micelles consisting of the same polyelectrolytes as the lipase-filled micelles (PAA_{139} and $P2MVP_{41}$-PEO_{205}) and α-lactalbumin are kinetically quenched for a period of at least six days (chapter 3). The relaxation rate of polyelectrolyte complex formation is influenced by the addition of salt: the relaxation rate of polyelectrolyte complex formation is decreased by salt. Therefore, one may expect that effect of the addition of salt to the two lysozyme-containing micelles changes the relaxation behaviour more drastically than for the lipase-containing micelles; their relaxation time will become shorter.

Table 2: Hydrodynamic radius and Core radius at different NaCl concentrations

$\mathbf{C}_{salt}$ **(M)**	$\mathbf{R}_H$ **(nm) (DLS)**	$\mathbf{R}_{core}$ **(nm) (SANS)**
0	29	10.9
0.1	25	9.7
0.3	29	7.1

The question that remains, is whether this difference in relaxation behaviour is responsible for the plateau in the light scattering intensity which was observed at $0.22-0.3$ M NaCl, during the salt titration (see figure 2). It was expected that the neutron scattering measurements shed some light

on this feature. However, neutron scattering intensity and the fitted core radius at 0.3 M NaCl do not feature a plateau; rather both seem to decrease monotonically upon increasing salt. This suggests that the plateau-value in the light scattering intensity is caused by event(s) occurring in the corona, which cannot be traced by SANS because the corona is practically invisible by neutron scattering.

In previous work, polyelectrolyte complex micelle formation and salt-induced disintegration was studied for micelles with different ratios of lysozyme and $PDMAEMA_{150}$ (chapter 2). Micelles consisting of just lysozyme and PAA_{42}-$PAAm_{417}$ disintegrated at a salt concentration of 0.12 M NaCl. If for the micelles in this study the lysozyme molecules are all released at 0.12 M NaCl, above this salt concentration these complexes would only contain $PDMEAMA_{150}$ and PAA_{42}-$PAAm_{417}$. The decrease in intensity beyond 0.12 M NaCl suggests that the polymers are released from the micelles, *i.e.,* implying a reduction in the aggregation number of the micelles. The released $PDMAEMA_{150}$ may interact with the water soluble (corona-forming) block of the diblock copolymer (polyacrylamide). This polymer can form hydrogen bonds with $PDMAEMA_{150}$.[130,131] Further proof that the shape of the intensity *versus* salt concentration and the increase in hydrodynamic radius is due to some sort of interaction between the two polymeric species is that the effect becomes more pronounced when the core of the micelles consists predominantly of $PDMAEMA_{150}$. Previously studied micelles, where the ratio between $PDMAEMA_{150}$ and lysozyme was 13:7, hardly showed a plateau in the intensity or an increase in the hydrodynamic radius (chapter 2). In the present study, the ratio between $PDMAEMA_{150}$ and lysozyme was 8:2 and for this ratio a pronounced plateau in the intensity and an increase in hydrodynamic radius was observed (figure 2a and b). When the system contained no lysozyme the effect is the most prominent (figure 2a and b).

Another reason for the plateau may be the approach of the critical point of the polyelectrolyte complex formation. Similar observations, *i.e.,* an increase of the light scattering intensity and hydrodynamic radius at a certain ionic strength have been observed.[132] Moreover, not only upon increasing ionic strength, but also upon decreasing ionic strength this behaviour has been found (data not published).

6.4. Conclusions

The salt-induced disintegration of lysozyme-filled polyelectrolyte complex micelles (consisting of $PDMAEMA_{150}$ and PAA_{42}-$PAAm_{417}$) was studied by DLS and SANS and compared to previously presented results on the disintegration of lipase-containing polyelectrolyte complex micelles (consisting of PAA_{139} and $P2MVP_{41}$-PEO_{205}). For the light scattering measurements a

decrease in hydrodynamic radius and light scattering intensity upon increasing NaCl concentration was observed, whereas the hydrodynamic radius of lipase-filled micelles remained constant and only the light scattering intensity decreased. The neutron scattering intensity at $q = 0$ as well as the core radius, for both the lysozyme-filled and lipase-filled micelles decreased. This difference indicates that the aggregation number of the lysozyme-filled micelles depends on the salt concentration. An explanation may be the difference in relaxation rate between the polyelectrolyte complex micelles, containing lysozyme and lipase, respectively.

From the SANS measurements with no additional NaCl added, the aggregation numbers of the lysozyme-filled micelles have been derived. These micelles contain approximately 29 diblock copolymers, 8 homopolymers and 2 lysozyme molecules. The volume fraction of water in the core is approximately 92%.

The size of polyelectrolyte complex micelles consisting of lysozyme, $PDMAEMA_{150}$ and PAA_{42}-$PAAm_{417}$ strongly depends on the salt concentration. From previous work[133] we know that these systems are quite dynamical and we expect that enzymes can move easily in and out these micelles. Interpretation of the enzymatic activity measurements of enzymes in these micelles will therefore be very difficult.

Chapter 7

SCF calculations of protein incorporation in polyelectrolyte complex micelles

Abstract.
Self-consistent field theory is applied to model the structure and stability of polyelectrolyte complex micelles with incorporated protein (molten globule) molecules in the core. The electrostatic interactions that drive the micelle formation are mimicked by nearest-neighbour interactions using Flory-Huggins χ-parameters. The strong qualitative comparison with experimental data proves that the Flory-Huggins approach is reasonable. The free energy of insertion of a protein-like molecule into the micelle is non-monotonic: there is (i) a small repulsion when the protein is inside the corona; the height of the insertion barrier is determined by the local osmotic pressure and the elastic deformation of the core, (ii) a local minimum occurs when the protein molecule is at the core-corona interface; the depth (a few k_BT's) is related to the interfacial tension at the core-corona interface and iii) a steep repulsion (several k_BT) when part of the protein molecule is dragged into the core. Hence, the protein molecules reside preferentially at the core-corona interface and the absorption as well as the release of the protein molecules has annealed rather than quenched characteristics. Upon an increase of the ionic strength it is possible to reach a critical micellisation ionic strength (CMI). With increasing ionic strength the aggregation numbers decrease strongly and only few proteins remain associated with the micelles near the CMI.

submitted to Physical Review E

7.1. Introduction

Incorporation of proteins in nanostructures is of interest for food, pharmaceutical and industrial applications. Polyelectrolyte complex micelles that are formed by attractive electrostatic forces between chains with opposite charge,[23–25] have successfully been used to incorporate proteins (chapter 2).[26,27] Many proteins have multiple charges at their surface (even near their iso-electric point). These charges provide the proteins with a weak cooperative binding mechanism (much weaker than simple 1:1 electrolyte) to oppositely charged chains that are abundantly present in the core of such micelles. This binding mechanism is generic and may be modified by other non-generic interactions (specific binding).

To model the electrostatic driving force is a major challenge for state-of-the-art self-consistent field (SCF) modeling, because the core that is composed of two oppositely charged species is in essence electroneutral. In the mean-field SCF theory, the chains in the bulk (*i.e.,* in the reference state) are modeled as quasi-neutral Gaussian chains, with small ions compensating the charge of the electrolyte chains. When such chains are forced to pack in an electroneutral core, they again do not feel electrostatic interactions. As a result, on the level of the SCF theory, there is no driving force for the assembly. The attractive force between plus and minus (requiring ion correlation) is not captured. The high packing density in the core is against the assembly. In the absence of any other attractive forces the micelles should fall apart spontaneously.

Recently, however, it was shown that, to first order, one may replace the electrostatic correlation force by a negative (attractive) Flory-Huggins parameter.[134] It is rather common that the Flory-Huggins parameters are used to account for a complex underlying interaction. For example in alkyl surfactants, the SCF model features a simple χ-parameter for the interaction between hydrocarbon segment and water, completely ignoring the H-bonding structure of water and how this is affected by the alkyl segment. In doing so, the SCF model obviously cannot predict temperature dependencies for such systems, but structural features on a micellar level are reasonably accounted for. For the current problem, it is expected that the electrostatic forces inside the core are short ranged, because the electrostatic attraction is only felt locally between nearby positively and negatively charged units and it may hence be reasonable to invoke a short-range parameter to capture this. In doing so, one may, *e.g.,* loose detailed information on entropic and energetic contributions hidden in such an effective parameter, but importantly, one can still use the classical self-consistent field method to obtain relevant structural information.

The particles of interest in this study are inter-polyelectrolyte complex

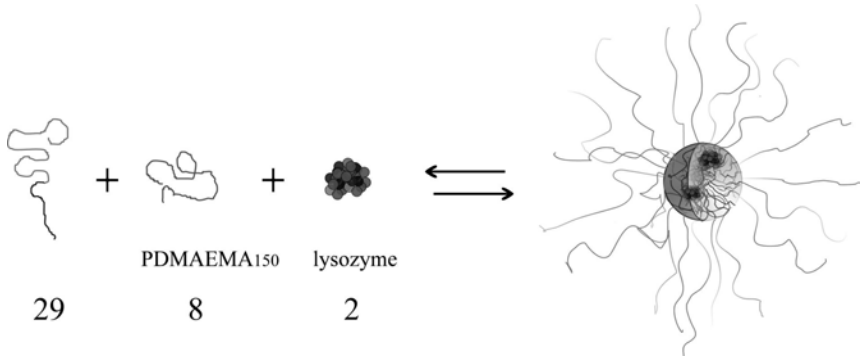

FIGURE 1. Artistic impression of the formation of lysozyme-filled polyelectrolyte complex micelles. The numbers indicate the aggregation number of the different components of the lysozyme-filled micelle (derived from SANS data (chapter 6)).

micelles.[23–25] These association colloids are formed when a diblock copolymer, having a charged as well as a neutral hydrophilic block, and an oppositely charged macromolecule are mixed at about equal charge ratio. The oppositely charged macromolecules may be diblock copolymers,[23,24,33,34,63,64] homopolymers,[25,31,32] DNA,[41,42] and proteins (chapter 2),[26,27] *etc.*,. The micelles have a core-corona structure: the core consists of the two oppositely charged polyelectrolyte species, the corona is formed by the (uncharged) hydrophilic block(s) of the diblock copolymer(s).

Previous experimental work revealed that, in order to obtain stable micelles with a protein-containing core, one can dilute the core of the micelles with a certain amount of homopolyelectrolyte, which has the same charge sign as the protein (chapter 2). When the ratio between protein molecules and homopolymers is such that the homopolymer is in excess (see figure 1), the polyelectrolyte complex micelles persist up to a salt concentration of 0.5 M NaCl. Above this salt concentration the micelles disintegrate due to the screening of the charges within the polyelectrolyte complex core (chapter 2). One of the aims of the theoretical modeling presented here, is to get deeper understanding of the entire co-assembly process as presented in figure 1.

Quite generally, micelles form, rather suddenly upon exceeding a certain (polymer) concentration, which is called the "critical micelle concentration" (CMC). The sharpness of this threshold is a consequence of the cooperative character of micelle formation. The equilibrium between free molecules and micelles can be affected by environmental conditions. Classical (surfactant or block copolymer) micelles often have, for a given polymer concentration, a critical micellisation temperature (CMT), micelles usually form at $T >$ CMT. For polyelectrolyte complex micelles the equilibrium between micellar and polymer species is a function of the salt concentration. In this study we are therefore interested in a limiting salt concentration

below which, for given overall polymer concentration, micelles form; by analogy this concentration will be referred to as the critical micellisation ionic strength (CMI).

The micellar system in this study consists of three components: a homopolymer, a diblock copolymer and lysozyme. The addition of salt may affect the equilibrium between incorporated and free lysozyme, because the charge density of most protein molecules is relatively low in comparison to the charge density of the polyelectrolytes, *i.e.,* the attraction between the positively charged homopolymers and negatively diblock copolymers is expected to be stronger than the attraction between the negatively charged diblock copolymers and positively charged lysozyme molecules. From Small Angle Neutron Scattering (SANS) on lipase-filled micelles a decrease in core volume has been observed when the salt concentration was increased. Assuming this decrease to be caused solely by a gradual release of the protein molecules, we could estimate that beyond a salt concentration of 0.12 M NaCl, all the protein molecules were released (chapter 5).

In the following, our interest is in structural and thermodynamical aspects of protein uptake in polyelectrolyte complex micelles. The approach involves the following three steps. First "empty" (*i.e.,* protein free) micelles consisting of homopolymer and diblock copolymer only, were studied. The model is designed to closely match the polymers that were used in experiments. The second step is to find a suitable model for the selected protein molecule lysozyme. Lysozyme is modeled as a linear copolymer where each amino acid in the primary sequence is represented by either a polar, an apolar, a negatively or a positively charged (amino acid) segment. The modeling of the empty micelles, as well as that of the molten globule lysozyme was performed in a one-gradient SCF calculation, using spherical geometry. In the third step we probe the free energy landscape associated with bringing a lysozyme molecule from a large distance into the micelle. These calculations call for a two-gradient SCF analysis using a cylindrical coordinate system. For all the systems, our interest is in studying the effect of the salt concentration. We now argue that this information can be obtained even when explicit electrostatic effects are not accounted for.

Consider, for the sake of argument, a pair of oppositely charged polyions, featuring negatively charged units A, and positively charged C units. In charge driven self-assembly it is natural to expect that the attractive interactions (A-C) can be screened by the addition of salt. We now introduce monomeric components, generically named D_1 and E_1, which (in 'charge language') have charges corresponding to those of A and C, respectively. In the FH language we obtain attractive (correlation) whenever interactions $\chi_{DE} = \chi_{DC} = \chi_{AE} = \chi_{AC} << 0$. In the presence of D_1 and E_1 a process which may be referred to as screening of A-C interactions occurs. Instead of making many A-C contacts, a sufficient concentration of "salt" (D_1 and

E_1) prompts the system to predominantly makes A-E and C-D contacts that are not productive in the sense that they give a driving force for self-assembly. Hence, the addition of D_1 and E_1 eventually causes the micelles to disintegrate, similarly as is known to occur upon the adding salt to the experimental systems.

For polyelectrolyte complex micelles one often invokes the "entropy release" (of the 1:1 electrolyte) argument to rationalise their formation. Screening of interactions, as discussed above, is a very similar entropic effect. Only when these ions cannot gain enough translational entropy (*i.e.,* at high salt concentrations) they will not contribute to the formation of micelles, in other cases they apparently support the formation of micelles.

The protein insertion in polyelectrolyte complex micelles discussed below comes from the correlation attraction, but as stated already, our method cannot treat the ionic interactions in the system explicitly. We nevertheless keep small ions as a component in order to mimic the screening of the electrostatic attraction. It therefore makes sense to continue using "electrostatic language" to describe the homopolymers, diblock copolymers and the small ions. This will make the following discussion more transparent.

In this chapter we like to mimic an experimental system on which one diblock copolyelectrolyte, a homopolyelectrolyte, lysozyme, and 1:1 electrolyte are present (see figure 1). Before we will give information on the model that is used, we will first mention important thermodynamic quantities that are used to evaluate the micelles seen in an SCF analysis. This is followed by a short introduction to the SCF machinery.

7.2. Theoretical preliminaries

Classical thermodynamics fails to give detailed information on the formation of association colloids. In a macroscopically homogeneous system the internal energy U is a function of entropy (S), volume (V) and $\{n\}$ only, $\{n\}$ is the number of molecules of various types in the system. There is no external parameter linked, to *e.g.,* the number of micelles in the system. On the level of the classical thermodynamics this number is irrelevant. Even if there would be a hidden parameter representing this number, say $\mathcal{N}$, its corresponding intensive variable must necessarily remain zero, $\varepsilon = 0$; in words, there is no excess free energy associated with the formation of micelles.

The approach to study association colloids in a molecular (SCF) model is fundamentally different. At the basis of the SCF analysis one has to choose the geometry of the system (below we make use of a one-gradient spherical coordinate system and a two-gradient cylindrical one, see figure 2) and one must specify the number of molecules in this volume. The micelle that is constructed in this geometry is pinned with its center of mass to a well-defined coordinate. This occurs without the need to restrict the

translational degrees of individual molecules; only the translational entropy of the micelle as a whole is ignored by this pinning. Hence, instead of a hidden parameter $\mathcal{N}$, we have (typically) exactly one (explicit) micelle in the system. The associated thermodynamic potential for this micelle, which can be accurately evaluated in the SCF calculation, is given by ϵ_m and differs from ε because the former has no translational degrees of freedom. The difference between the two can thus be seen as the entropy that is lost in the SCF pinning procedure:

$$\varepsilon - \varepsilon_m = k_B T \ln \phi_m \tag{25}$$

Here $-k_B \ln \phi_m$ is (in dilute solutions) the translational entropy of the micelle (k_B is the Boltzmann constant), while ϕ_m is the volume fraction of micelles in the system. From this equation we can interpret ε as the (excess) chemical potential associated to the presence of micelles. Above we already mentioned that this excess chemical potential must be zero (this follows also from the mass action law for self-assembly) and thus the micelle volume fraction $\phi_m = \exp -\varepsilon_m / k_B T$. For this it is evident that for relevant systems $\varepsilon_m > 0$.

The characteristic function in a SCF calculations is the Helmholtz energy, $F = \varepsilon_m + \sum_i n_i \mu_i$ is (when the number of molecules is specified) and this follows from the partition function, *i.e.,* $F = -k_B T \ln Q$. Let the system be composed of $i = 1, \cdots, I$, linear molecules having segments with ranking numbers $s = 1, \cdots, N_i$. These molecules are composed of a limited set of segment types referred to by X or Y, where, *e.g.,* $X = A, B, C, ...$ It is convenient to define chain architecture parameters $\delta_{i,s}^X$. These quantities assume the value unity when segment s of molecule i is of type X and are zero otherwise. The set of $\delta_{i,s}^X$ completely specifies the molecules in terms of its composition.

Here we use the SCF model making use of the discretisation scheme of Scheutjens and Fleer.[135,136] In this approach both the macromolecules are assumed to be composed of a discrete set of segments and the space is represented by a lattice, that is, a discrete set of coordinates. The segments and lattice sites match, which means that on each site exactly one segment (or monomeric molecules) can be placed. Here we will illustrate the method by focusing on the one-gradient spherical coordinate system, and trust that the extension to the two-gradient cylindrical coordinate system is clear. In this lattice we distinguish spherical lattice layers referred to by $r = 1, \cdots, r_m$. In this geometry the number of lattice sites per layer L grows quadratically with the layer r, *i.e.* $L(r) \propto r^2$. In each layer we will employ a (local) mean-field approximation and focus on the volume fractions $\varphi_X(r) = n_X(r)/L(r)$, where n_X is the number of sites occupied by segments of type X. This approximation thus ignores the exact position of the segments in a layer, but allows for gradients in composition between layers.

Within the mean-field approximation it is impossible to account accurately for the pair interactions (in contrast to simulations). Instead, it is assumed that the segments feel an external potential $u_X(r)$. Because this potential is not fixed, but (as we will see) is a function of the local distributions, we refer to such potential as being self-consistent. For each segment type X we thus have a pair of distribution functions $\{\varphi(r), u(r)\}$. The free energy is formally given by:

$$F(\{\varphi\},\{u\},u') = -k_BT\ln Q(\{u\}) - \sum_r L(r)\sum_X u_X(r)\varphi_X(r) \tag{26}$$

$$+F^{\text{int}}(\{\varphi\}) + \sum_r L(r)u'(r)(\sum_X \varphi_X(r) - 1))$$

where u' is the Lagrange multiplier originating from the requirement that all lattice sites are occupied, *i.e.,* $\sum_X \varphi_X(r) = 1$, $\forall r$. The first term of this free energy shows that we can compute the partition function in "potential" space. The second term of equation 7.2 transforms this result back into the experimentally relevant "concentration" space. The interactions that are present in the system must be (re)added, hence, the interaction term F^{int}. This free energy functional need to be at an extreme with respect to its variables; in fact we need to look for saddle points. When for F^{int} a Flory Huggins-like counting of the interactions is implemented, the minimisation with respect to the volume fractions gives

$$\frac{\partial F}{\partial \varphi_X(r)} = -L(r)u_X(r) + \frac{\partial F^{\text{int}}}{\partial \varphi_X(r)} + L(r)u'(r) = 0 \tag{27}$$

Within a Flory-Huggins type interaction free energy, the Bragg-Williams approximation is used. Flory-Huggins interaction χ parameters give the strength of the interactions (negative for attraction and positive for repulsion):

$$\frac{1}{k_BT}\frac{\partial F^{\text{int}}}{\partial \varphi_X(r)} = L(r)\sum_Y \chi_{XY}\left(\langle\varphi_Y(r)\rangle - \varphi_Y^b\right) \tag{28}$$

where φ_Y^b is the volume fraction of segments of type Y in the bulk (far from the micelle where no volume fraction gradients are present, *i.e.,* near $r = r_m$). The angular brackets denote a three-layer average:

$$\langle\varphi(r)\rangle = \lambda(r,r-1)\varphi(r-1) + \lambda(r,r)\varphi(r) + \lambda(r,r+1)\varphi(r+1) \tag{29}$$

Obviously, the *a priori* site probabilities λ add up to unity, *i.e.,*

$\sum_{r'=r-1,r,r+1} \lambda(r,r') = 1$. They further must obey an internal balance equation $L(r)\lambda(r,r+1) = L(r+1)\lambda(r+1,r)$. For $r \to \infty$ $\lambda(r,r+1) = \lambda(r,r-1) = \frac{1}{3}$. With equation 28 we can compute the segment potentials $u[\varphi]$ from the volume fractions.

Maximisation of the free energy F (equation 7.2) with respect to the segment potentials leads to the complementary equation $\varphi[u]$:

$$\frac{\partial F}{\partial u_X(r)} = \frac{-k_B T \partial \ln Q}{\partial u_X(r)} - L(r)\varphi_X(r) = 0 \tag{30}$$

Here the partition function Q may be decomposed into single-chain partition functions q_i: $Q = \Pi_i q^{n_i}/n_i!$, where n_i is the number of molecules of type i in the system. This formal way to compute the volume fraction $\varphi_X(r)$ as given by equation 30 is correct for any chain model, even for self-avoiding chains. Above we have mentioned that we are going to account for interactions on the Bragg-Williams level. At this level the exact positions of the segments are lost and therefore the chain model does not necessarily need to be self-avoiding. Following Scheutjens and Fleer we use a freely-jointed chain model for which a very efficient computational route is available that implements equation 30.

In this approach the volume fraction of segment s of molecule i at coordinate r is computed from the combination of two complementary Green's functions, which specify the combined statistical weights of the possible conformations of complementary chain fragments:

$$\varphi_i(r,s) = \frac{n_i}{q_i} \frac{G_i(r,s|1)G_i(r,s|N)}{G_i(r,s)} \tag{31}$$

In this equation the single-chain partition function $q_i = \sum_r L(r)G_i(r,1|N)$ is interpreted as the overall statistical weight to find molecule i in the system. In equation 31, $G_i(r,s)$ is the (free) segment weighting factor for segment s, which is given by the Boltzmann equation $G_i(r,s) = \exp -\frac{u_i(r,s)}{k_B T}$. The endpoint distribution functions (Green's functions) $G_i(r,s|1)$ and $G_i(r,s|N)$ follow from the free segment distribution functions through two complementary propagator equations:

$$G_i(r,s|1) = G_i(r,s)\,\langle G_i(r,s-1|1)\rangle \tag{32}$$

$$G_i(r,s|N) = G_i(r,s)\,\langle G_i(r,s+1|N)\rangle \tag{33}$$

which are started by $G_i(r,1|1) = G_i(r,1)$ and $G_i(r,N|N) = G_i(r,N)$, respectively. The angular brackets indicate a similar averaging as in equation 29. We note that the segment potentials are found from $u_i(r,s) =$

$\sum_X \delta_{i,s}^X u_X(r)$. Similarly,

$$\varphi_X(r) = \sum_i \sum_s \varphi_i(r,s)\delta_{i,s}^X \tag{34}$$

The volume fractions of all components in the bulk also obey the incompressibility constraint $\sum_X \varphi_X^b = 1$ and its evaluation is facilitated by using $n_i/q_i = \varphi_i^b/N_i$.

The saddle point of the free energy is found by a numerical procedure which is stopped when its parameters are self-consistent. This means that the same segment potentials both follow from, and determine the volume fractions, and *vice versa* that the volume fractions both follow from and determine the segment potentials. The numerical procedure is not stopped until all parameters have a numerical accuracy of 7 significant digits, while obeying the incompressibility condition 33. Subsequently, the Helmholtz energy is evaluated accurately and from this all other thermodynamical quantities follow. For example, the chemical potentials of all components are evaluated from the volume fractions in the bulk. Hence, the grand potential $\varepsilon_m = F - \sum_i \mu_i n_i$ is easily computed.

The results of SCF calculations accurately obey the Gibbs-Duhem equation that relates the grand potential to the chemical potential:

$$d\varepsilon_m = -\sum_i g_i d\mu_i \tag{35}$$

where the aggregation number, g_i, equals

$$g_i = \frac{1}{N_i}\sum_r L(r)\left(\varphi_i(r) - \varphi_i^b\right) \tag{36}$$

The critical micellisation concentration (CMC) is identified from the criterion that $\varepsilon_m(g)$ has a maximum value;[137,138] where $\sum_i g_i\mu_i$ is minimised; *i.e.*, $\sum_i g_i d\mu_i = 0$. The volume fraction of micelles and, hence, the volume available per micelle $V/\mathcal{N}$ (where V is the volume of the system) can be estimated from equation 25.

It appears useful to introduce a composition variable as the ratio p^c of negative to positive polymer in the system.

$$p^x = \frac{\varphi_{AB}^x N_A}{\varphi_C^x N_C} \tag{37}$$

where φ is the overall volume ratio (that is, both contributions from associated and non-associated polymers in the system) and N is the degree of polymerisation. In the calculations we have reasonably easy access to the charge ratio in the bulk p^b and to a ratio that exist in micelles p^m. These ratios are very often not the same, that is, the charge ratio in the bulk may differ strongly from that in micelles. Of course below the CMC there are

no micelles and $p^c = p^b$. In general however we would have for micellar solutions,

$$p^c = \frac{\varphi^b_{AB} N_A V + \mathcal{N} g_{AB} N_A}{\varphi^b_C N_C V + \mathcal{N} g_C N_C} \tag{38}$$

One of the complications in using this equation is the appearance of V and $\mathcal{N}$. Although these can be estimated from using 25, we typically avoid using 38.

At the first appearance of micelles (theoretical CMC), the concentration of the micelles is typically very low and hence the overall polymer concentrations still equal the polymer concentrations in the bulk: $p^c \approx p^b$. On the other hand, when the majority of the polymers is in the micelles, that is, well above the CMC, we can ignore the contribution of the polymers in the bulk and

$$p^c \approx p^m = \frac{g_{AB} N_A}{g_C N_C} \tag{39}$$

The focus of the current study is to compare calculations to experiments. In experimental conditions, we used a typical concentration of polymers of 1 g L^{-1} which implies approximately $\phi \approx 10^{-4}$. As the CMC is much lower, we conclude that most of the material is in micelles. Without mentioning otherwise we shall approximate $p^c \approx p^m$. This approximation is typically good as long as the system is well below the CMI. We say that we have a "balanced" system, or system with balanced charge stoichiometry when $p^c = 1$. Experimentally, such balanced systems can easily be made by choosing the composition accordingly. Hence, below (or near) the CMC we can impose p^b in the bulk but far above the CMC we can impose p^m in the micelles, respectively.

7.3. Model and Parameters

7.3.1. The coordinate systems

Two different coordinate systems were used: 1) a one-gradient spherical and 2) a two-gradient cylindrical one.

The one-gradient system was used for the "empty" micelle, and for the lysozyme globule, respectively. In this one-gradient lattice, there are spherical lattice layers referred to by $r = 1, \cdots, r_m$, where $r_m = 80$ (see figure 2a). In each layer the volume fractions $\varphi_X(r) = n_X(r)/L(r)$ (where n_X is the number of sites occupied by segments of type X) are determined using the mean-field approximation.[139–141] This approximation allows for gradients in segment composition between layers. The micelle that is constructed in this geometry is pinned with its center of mass to $r = 0$. In figure 2a the

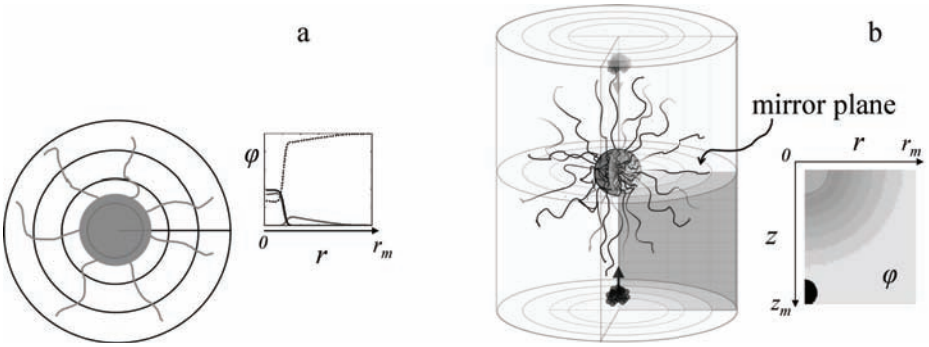

FIGURE 2. Schematic representation of **a)** one-gradient spherical coordinate system ($r = 1, ..., r_m$) and **b)** two-gradient cylindrical coordinate system $(z, r) = (1, ..., z_m, 1, ..., r_m)$. Both in **a)** and **b)** schematic interpretation of the way the molecules are organised is shown pictorially as well as in terms of a radial volume fraction **a)** or equal density grey scale plot **b)**. The mirror plane is indicated by an arrow.

coordinate system and the radial volume fraction $\varphi_x(r)$ are illustrated.

The two-gradient system is used to study micelles in the presence of proteins. In this system the pair of coordinates (z, r) is used, where $z = 1, ..., z_m$ (where $z_m = 60$) is along the axis of the cylinder and $r = 1, ..., r_m$ (where $r_m = 50$) is the radial coordinate (see figure 2b). Now $\varphi_x(z, r) = n_x(z, r)/L(r)$ is the local volume fraction at coordinate (z, r) and the volume fractions are presented as equal density contour plots.

In the two-gradient calculations the center of mass of the micelle is at the symmetry plane pinned at $z = 1, r = 1$ (see figure 2b). As a consequence of this pinning procedure the calculation deals with half a micelle only. By considering the mirror image (as is depicted in figure 2b), the volume fractions of the various segments of the whole micelle can be determined. In our approach we "push" one lysozyme-like object, which has a central amino acid X (see figure 3) at position $(z^*, 1)$, into such micelle by lowering the number of z^* in steps. The same happens for the mirror image and hence we obtain information about the simultaneous insertion of two lysozyme-like objects into one micelle. A typical density contour plot of the calculated part of the micelle is given in figure 2b. In figure 11, however, we will present the mirror images and present a full cross section through the micelle. The plane of this cross section contains the two mentioned pinning positions.

In SCF calculations the lattice length should be such that the individual segments of the polymers fit in. One of the components in our calculations is a protein. The average size of amino acids is estimated to be around 0.6 nm.[142,143] Therefore we have chosen this value as the lattice length (ℓ) in

our calculations. The length also fixes the conversion from volume fractions to (molar) concentrations. For monomeric species the conversion factor is approximately 10.

The dimensions of the lattice volume are fixed by the value r_m in the spherical coordinate system and the set (r_m, z_m) for the cylindrical one. Typically r_m and z_m values were chosen such that the bulk volume fractions prevailed, but small enough so that the calculation times did not become too high. Also the lattice volume is small enough so that, to a good approximation, the majority of the polymer molecules that are in the calculation volume did assemble in the micelle and a negligible part of it remained in the bulk layers (this facilitates the calculations).

7.3.2. The molecules

We encounter up to six different molecular species in our SCF calculations:
(1) The homopolymer which is positively charged (homopolyelectrolyte), mimicking $PDMAEMA_{150}$ (poly(N,N dimethylaminoethyl methacrylate)). This polymer was modeled as a linear chain, having 150 monomers (C).
(2) The diblock copolymer, mimicking PAA_{42}-$PAAm_{417}$ (poly(acrylic acid)-*block*-poly(acryl amide)) consists of two blocks, a negatively charged block which consisted of 40 monomers (A) and a neutral hydrophilic block (B), containing 400 monomers.
(3) The protein molecule was modeled as a linear polymer (see figure 3). Amino acids were defined as monomers being either positively charged K =H, K, and R; negatively charged Z =D, and E; polar P =S, T, Y, C, N, and Q; or non-polar N =G, A, V, L, I, F, M, P, and W (here the letters refer to the commonly used one-letter abbreviations of amino acids, see, *e.g.,* biochemistry textbooks). These monomers were placed in the same amino acid sequence as in lysozyme. In water this lysozyme-like molecule collapses to a sort of molten globule.
(4 and 5) are the small ions Cl^- and Na^+, that are used to control the electrostatic interactions.
(6) is the monomeric solvent mimicking water (W).

7.3.3. Interaction parameters

Recently, using SCF theory, a model was proposed to study polyelectrolyte complex micelles.[134] The model featured two (symmetric) diblock copolymer types, A_nB_m and C_nB_m, in a non-selective solvent, *i.e.*, for which the Flory-Huggins (FH) parameters with the solvent χ_{SA}, χ_{SB}, χ_{SC} were near the theta-value, *i.e.,* $\chi \approx 0.5$. Self-assembly was shown to occur when the $\chi_{AC} << 0$. It was argued that this attraction between A and C can mimic the electrostatic attraction between two oppositely charged segments as these occur in polyelectrolyte complex micelles. We refer to this as the

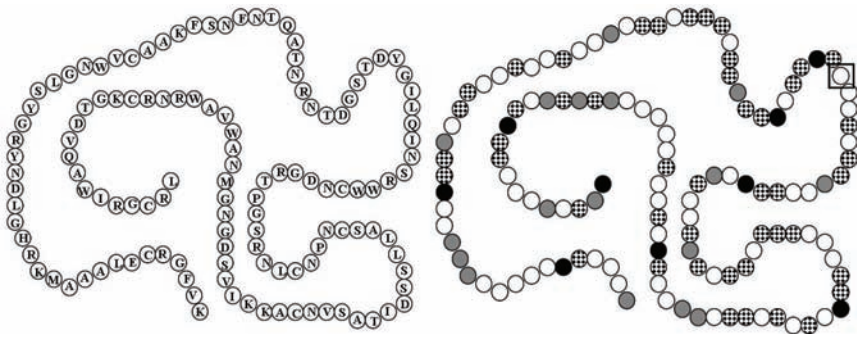

FIGURE 3. Sequence of lysozyme and its translation to the segments of our model: N=white, P= checkerboard, K= grey and Z=black. The "translation" of amino acids to segments is given in the text. The □ indicates, the amino acid G (here referred to as X), which was pinned in the two-gradient calculations to a coordinate $(z^*, 1)$.

correlation attraction. The B-block is the corona chain which accumulates as a well-solvated polymer brush is formed around the (less swollen) core forming chains A and C. In this model the two polymers had identical block lengths, which helped the theoretical analysis of self-assembly enormously. However, it was shown (only as an example) that stable micelles also form in a mixture of homopolymer A_{N_A} with diblock copolymer $C_{N_C}B_{N_B}$, where N_A is the length (in number of segments) of block A, *etc.,* and that such micelles have a larger aggregation number than in the binary diblock copolymer system. The reason for this is obvious, as the growth of the micelles is stopped by the crowding of chains in the corona. When there is just one type of diblock copolymer in the system, the number of such corona chains per A-C contact is lower when a homopolymer-diblock copolymer system is used, than in the case of two diblock copolymers.

In the present study we make use of a slightly adjusted parameter set. The reason for using a more detailed set of parameters is to tune the model to the experimental data. It is illustrative to discuss the differences between the "old" and current set of parameters. As starting point for the calculations in this study, "old" Flory-Huggins parameters were chosen for the current A_{40}-B_{400}, C_{150} system. Specifically, for the correlation attraction parameter between the charged block of the diblock copolymer and the homopolymer $\chi_{AC} = -3$ was chosen. The Flory-Huggins (FH) parameters with the solvent (W) for the different segments are all set to the theta-value $\chi_{WA} = \chi_{WB} = \chi_{WC} = 0.5$.

The radial volume fraction profile of a typical micelle obtained by these interaction parameters close to the CMC while the system is electrostatically balanced, is shown in figure 4. As the focus here is on micelles near the

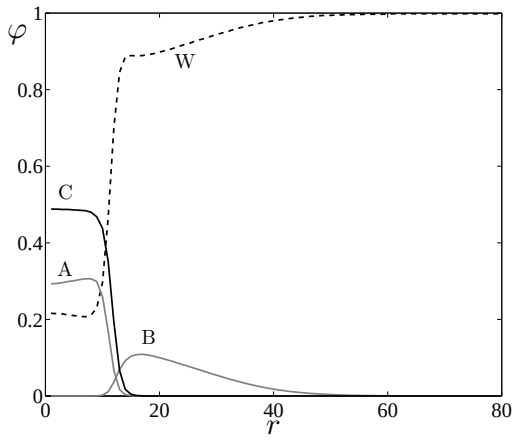

FIGURE 4. Radial volume fraction profile of a micelle near the CMC, consisting C_{150} and A_{40}-B_{400} with equal bulk concentrations of φ of solvent (W), homopolymer (C), soluble block (B) and charged block (A) of the diblock copolymer. The FH-interaction parameters are $\chi_{AC} = 3$ and $\chi_{WA} = \chi_{WB} = \chi_{WC} = 0.5$. These micelles contain approximately 40 diblock copolymers and 20 homopolymers.

CMC it is reasonable to implement the (balancing) constraint $p^c = p^b = 1$, that is, the bulk charge concentrations of the two different components are kept the same. In figure 4 the radial volume fraction profiles of the different components (A, B, C and W) are plotted as function of the layer number (r). As expected segment A and C are mainly found in the core of the micelle (layer number $1-12$). The corona forming segment B is found from layer number $12-45$. The amount of water W in the core of the micelle is ≈ 0.2, this amount increases from layer number $12-45$ and becomes close to unity outside the micelle. The core corona-interface is rather sharp (a few lattice lengths).

Because of the strong negative χ_{AC} value ($\chi_{AC} = -3$), the system tries to optimise the number of AC contacts (which occurs locally when $\varphi_A = \varphi_C$). However, the compositional asymmetry between the two polymers: linear polymer (C_{150}) *versus* diblock copolymer (A_{40}-B_{400}), clearly prevents the perfect realisation of charge stoichiometry $p^m = 1$ in the micelle. In the core, the homopolymer is clearly favoured over the diblock copolymer, when the bulk concentrations are chosen such that the ratio between homopolymer and diblock copolymer in the bulk is unity ($p^b = 1$). The corona-forming block B hinders the accumulation of diblock copolymers and the A block being much shorted than the C chain also opposes balanced micelles $p^m = 1$. For the current parameter set $p^m < 1$ persists

also at higher micelle concentration and we decided to restore the balance somewhat by choosing $\varphi_{WC} = 0.2$. Improving the solvent quality of C reduces the partitioning of the homopolymer in the micelles. It further increases the overall water-content of the micelle, and indirectly, reduces the driving force for micelle formation.

Using $\chi_{WC} = 0.2$, micelles were formed that were significantly closer to "charge stoichiometry" than the micelle shown in figure 4. The aggregation number of these micelles was still rather high in comparison to the experimental data. To decrease the aggregation numbers, the interaction between water and the corona-forming block χ_{WB} was slightly reduced to 0.45. The improved solvent quality of the corona block B strengthens the stopping mechanism of the micellar growth. The interactions between the charged segments of the homopolymer and diblock copolymer with the corona-forming block were unchanged with respect to the "old" parameter set ($\chi_{AB} = \chi_{BC} = 0.5$). To reduce the number of different interaction parameter values, the simple ions were given the same interaction parameters as the like-charged segments of the polymers, *i.e.,* with other segments (y) ($\chi_{Ay} = \chi_{Cl^-y}$ and $\chi_{Cy} = \chi_{Na^+y}$). As a result, specific ionic effects are ignored.

As mentioned, the lysozyme-like molecule is built up from four different segments: Non-polar (N), Polar (P), positively charged (K) and negatively charged (Z) (see figure 3). The charged amino acids were given the same interaction parameters with segments (y) as the like charged polymer segments and simple ions: ($\chi_{Zy} = \chi_{Ay} = \chi_{Cl^-y}$ and $\chi_{Ky} = \chi_{Cy} = \chi_{Na^+y}$). The polar segments were given the same interaction parameters as the corona forming block ($\chi_{By} = \chi_{Py}$). The non-polar segments N of the protein globule are very important for the structure. Their strong hydrophobicity leads to strong repulsion between the solvent and these segments which we capture by $\chi_{NW} = 4$. As there are many hydrophobic segments we observe a collapse of the linear chain to a single protein-like globule. The Flory-Huggins interaction parameter between the polar and charged segments with the non-polar segments is set to $\chi_{NK} = \chi_{NZ} = \chi_{NP} = 2.5$. The relatively good solvent quality for P ($\chi_{WP} = 0.45$), causes these water-soluble segments to be mainly found at the surface of the molten globule.

The current Flory-Huggins interaction parameters are collected in table 1. In this table it can be seen that no more than five different groups of segments have been defined: solvent (W), non polar (N), positively charged (C, K and Na^+), negatively charged (A, Z and Cl^-) and water soluble (B and P).

Table 1: Flory-Huggins interaction parameters

χ	**W**	**N, X**	**C, K, Na^+**	**A, Z, Cl^-**	**B, P**
W	0	4	0.2	0.5	0.45
N, X	4	0	2.5	2.5	2.5
C, K, Na^+	0.2	2.5	0	-3	0.5
A, Z, Cl^-	0.5	2.5	-3	0	0.5
B, P	0.45	2.5	0.5	0.5	0

7.4. Results and Discussion

7.4.1. One-Gradient results

In figure 4 the volume fraction profiles for a micelle near the CMC with constraint $p^b = 1$ was shown. However, comparison or predictions with experiments calls for micelles that exist at much higher concentrations. More specifically, in corresponding experiments we work at polymer concentrations of approximately 1 g L^{-1}. Assuming that most polymers are in the micelles, this leads to a micelle volume fraction $\varphi_m \approx 10^{-4}$. Using equation 25, we find that we should focus on micelles with a grand potential $\varepsilon_m \approx 9.2\ k_BT$. It will be clear that under these conditions and for an asymmetric system *e.g.,* a homopolymer and a diblock copolymer, the ratio between the polymers in the micelle p^m is very different from that in the bulk p^b (equation 37), and the approximation $p^c \approx p^m$ may be more appropriate. Because of the asymmetry between the charged blocks, we cannot simply impose $p^m = 1$. Hence, we need an appropriate strategy to compute relevant micelle compositions. This strategy is explained further on; anticipating results, we will argue that $p^c = p^m = 0.85$ corresponds to a most likely composition. We will first show a typical radial volume fraction profile (in figure 5) for such a system and then discuss its thermodynamic stability in figure 6. In both figures we used a salt concentration of $\varphi_{salt} = 0.001$.

In figure 5 the radial volume fraction distribution of the different segments for the "optimal" micelle ($p^c = 0.85$ is imposed, the volume fraction of micelles is $\varphi_m = 10^{-4}$ and the ionic strength is $\varphi_{salt} = 10^{-3}$), with the interaction parameters of table 1 are presented. It can be seen that both the volume fraction of the interacting part of the diblock copolymer (A) and the homopolymer (C) are maximal in the core of the micelle. The volume fraction of the homopolymer (≈ 0.39) is still higher than the volume fraction of the diblock copolymer (≈ 0.35), but the ratio between these volume fractions is much closer to unity than in figure 4. Outside the core the highest volume fraction of the soluble block of the diblock copolymer (B)

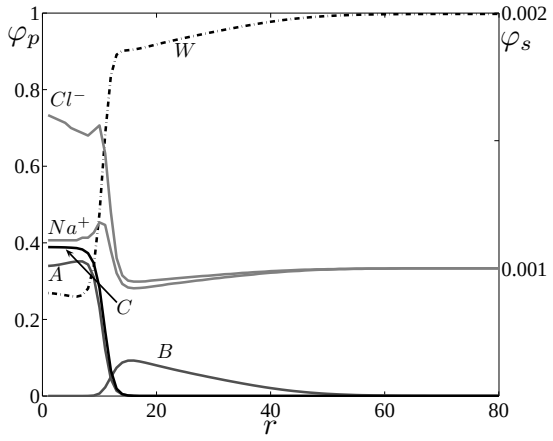

FIGURE 5. Radial volume fraction φ_p of Water (W), homopolymer (C), soluble diblock copolymer (B) and charged diblock copolymer (A) (left y-axis) and radial volume fraction φ_s of Cl^- and Na^+ (right y-axis) as a function of the layer number r, $\varphi^b_{salt} = 0.001$. Data presented are for: $p^c = p^m = 0.85$ (see figure 7), volume fraction of micelles is $\varphi_m = 10^{-4}$.

is found.

From these volume fractions one can determine the radius of gyration (Rg) of the core and the corona by taking the first moment:

$$Rg = \sqrt{\frac{\sum_r L(r) r^2 (\varphi(r) - \varphi^b)}{\sum_r L(r)(\varphi(r) - \varphi^b)}} \tag{40}$$

where $\varphi(r)$ and φ^b are the volume fractions at layer r and in the bulk, respectively. As an estimation of the Rg_{core} we used the equation 40 with $\varphi = \varphi_C$; taking into account the lattice length of 0.6 nm, this results in $Rg_{core} \approx 5.4$ nm. Since for a sphere with homogeneous density $Rg^2 = \frac{3}{5}R^2$, the core radius is estimated by $R_{core} \approx 7$ nm. We may estimate the hydrodynamic radius R^h of the micelle by using the volume fraction of the terminal B segment of the copolymer in equation 40. By doing so we find $R^h \sim Rg_{micelle} \approx 26$ nm. For the experimental micelles approximately the same radii are found, namely $R_{core} \approx 11$ nm and $R_h \approx 27$ nm (chapter 6).

The volume fractions of water (W) and small ions (Cl^- and Na^+) are also shown in figure 5. The volume fraction of water is minimal in the core of the micelle and increases in the outward direction; outside the micelle the volume fraction of water is unity as expected. Please note that the y-axis of

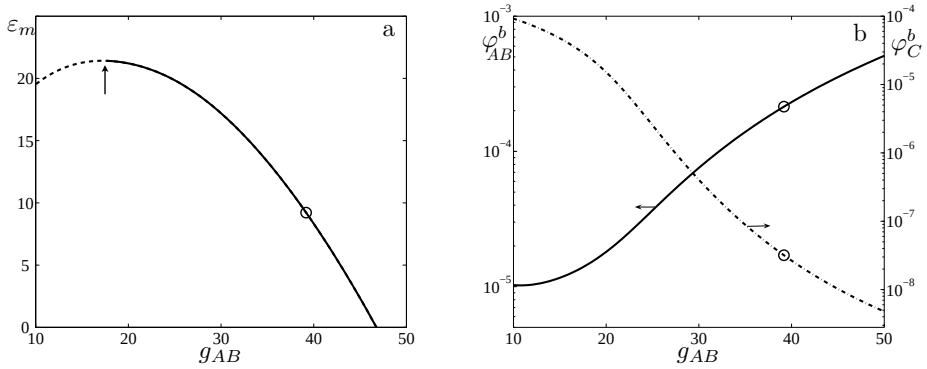

FIGURE 6. **a)** Grand potential ε_m in units of k_BT as a function of the aggregation number of copolymers (g_{AB}) and **b)** φ^b_C (dashed line) and φ^b_{AB} (solid line) on a logarithmic scale as a function of the aggregation number (g_{AB}). The circles in both figures point to the micellar system for which the radial profiles were shown in figure 5. Here the constraint $p^c = p^m = 0.85$ is used and $\varphi_{salt} = 0.001$ and $\varphi_m = 10^{-4}$. Micelles indicated by the dashed line (left of the arrow) in **a)** are instable.

the small ions Cl^- and Na^+ is found on the right hand side of the diagram. The amount of Cl^- ions in the core is a bit higher than that of Na^+ ions. This is because Cl^- is attracted to the (positively charged) homopolymer, which is slightly in excess in the core. This indicates that the micelle tends to approach charge neutrality. At the core-corona interface both volume fractions of the ions have a small maximum. This indicates adsorption, and is a consequence (induced by the chosen parameter set) of the presence of an interfacial tension between the core and the corona. By accumulating at the core-corona interface the ions reduce the unfavourable core-corona contacts and lower the interfacial tension.

Proper stability curves for micelles feature a grand potential (ε_m) as function of the aggregation number (g_{AB}) with a maximum. For thermodynamic stability, however, we must require that $\varepsilon_m > 0$ but also $\frac{\partial \varepsilon_m}{\partial g_{AB}} < 0$. In figure 6a it can be seen (arrow) that, insisting on the constraint $p^c = 0.85$ even near the CMC, the smallest stable micelles have $g_{AB} \approx 17$ where the corresponding grand potential is 22 k_BT. This implies that the volume fraction of micelles near the CMC is very low: $\phi_m \approx 2 \times 10^{-10}$. Such low concentrations are difficult to study by experimental techniques. In our experiments the micellar concentration is much higher, namely 1 g L^{-1}, and the value of $\varepsilon_m \approx 9.2\ k_BT$, which corresponds to a volume fraction of micelles of $\varphi = 10^{-4}$, is experimentally more relevant. In figure 6a the system with this grand potential is indicated with a circle, the aggregation number

of this micelle is about twice the value of the smallest stable micelle, namely $g_{AB} \approx 39$.

The corresponding volume fractions of the homopolymer φ_C^b and diblock copolymer φ_{AB}^b in the bulk as function of the aggregation number (g_{AB}) are presented in 6b, on a logarithmic scale. Here again, the selected micelle (shown in figure 5) is also indicated by a circle. In this figure it can directly be seen that close to the CMC ($g_{AB} \approx 17$), $\varphi_{AB}^b \approx \varphi_C^b$, so that p^b is close to unity, as was imposed as a constraint in figure 4. An increase in aggregation number induces an asymmetry in the bulk: φ_C^b decreases much more than φ_{AB}^b. This indicates that the composition of the micelle and the bulk strongly depend on the micelle concentration. For the micelle of our interest, indicated by $\circ$, ($\varphi_m = 10^{-4}$, $p^m = 0.85$ and $\varphi_{salt} = 0.001$), in the bulk $\varphi_{AB}^b \gg \varphi_C^b$ and $p^b \approx 10^4$.

When the number of contacts between the oppositely charged groups of the polymers (AC) is maximal, in the ideal case, the ratio between the number of homopolymers (C_{150}) and diblock copolymers (A_{40}-B_{400}) should be 4:15. However, since we are dealing with an asymmetric system this ratio may be hard to get, as was already discussed in figure 5. From figure 6 we calculated that for micelles with $\varphi = 10^{-4}$, the aggregation numbers were $g_{AB} \approx 39$ and $g_C \approx 12$. These calculations were performed at fixed homopolymer to diblock copolymer ratio in the system. We still need to justify this particular choice. In figure 7a it is presented how this ratio was determined.

The key idea is to focus on systems with a *fixed* volume fraction of micelles. For this we have chosen the experimental value, *i.e.*, $\varphi_m = 10^{-4}$. This concentration of micelles can occur for a range of g_{AB} and g_C values, each representing micelles at a different p^c-value. There are various ways to present the results. We choose to show the aggregation number of diblock copolymers (g_{AB}) as function of the ratio p^c between the diblock copolymer and homopolymer (see equation 39) in the system in figure 7. We emphasise that we are far from the CMC and thus $p^c \approx p^m$. In figure 7a a maximum is found for the aggregation number (g_{AB}) as a function of p^c. This maximum is interpreted as the micelle with optimal (preferred) composition.[31] The maximum is found at $p^c = 0.85$. The motivation for this choice is that for "optimal" conditions the aggregation number should be larger than for suboptimal conditions (at fixed micelle concentration). The corresponding ratio between homopolymer and diblock copolymer was used in al subsequent calculations, hence in figures 5 and 6, but also for later figures.

Results presented in figure 7a have an experimental counterpart, even though in experiments it is virtually impossible to vary the composition in the system at fixed micelle concentration. Nevertheless, a maximum as function of the ratio between homopolymer and diblock copolymer is indeed observed in experiments. The experimental technique of choice to

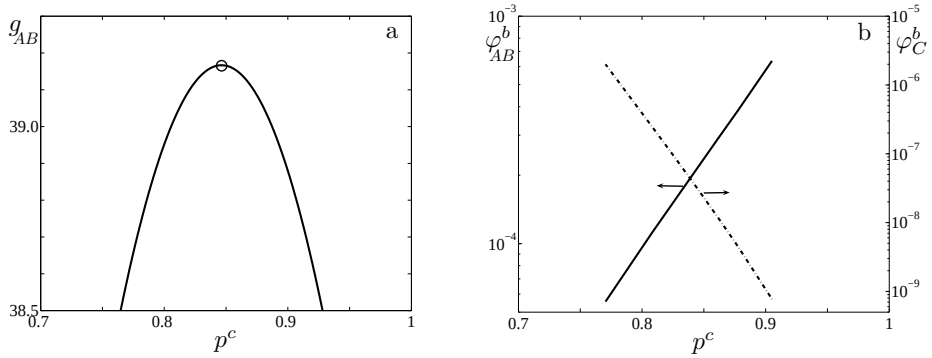

FIGURE 7. **a)** Aggregation number (g_{AB}) as function of the diblock copolymer/homopolymer ratio (p^c) and **b)** φ^b_C (dashed line) and φ^b_{AB} (solid line) on a logarithmic scale as function of p^c, $\varphi_{salt} = 0.001$. In all calculations the volume fraction of micelles is fixed to $\varphi_m = 10^{-4}$.

study the polyelectrolyte complex micelle formation is a Light Scattering (LS) titration. During a LS-titration measurement, a solution containing polyelectrolytes with given charge is titrated to a solution containing oppositely charged macromolecules. After every titration step the light scattering intensity is measured and presented as function of the composition F^- ($F^- = \frac{p^c}{p^c+1} \approx \frac{p^m}{p^m+1}$). Typically, intensity *versus* composition ($I(F^-)$)plots have a maximum at the optimal micellar composition. Because the mass of the scattering objects is maximal at this composition, it is assumed that the polyelectrolyte complex micelles have the optimal ratio between the oppositely charged macromolecules. Typically, one expects that, experimentally, $p^m \approx 1$, but small deviations have been observed.[144] Our results show that $p^m < 1$ is indeed probable.

For all the systems with fixed micelle concentration, not only the grand potential, but also the two bulk volume fractions are known. Corresponding to the data of figure 7a, φ^b_{AB} and φ^b_C *versus* g_{AC} are presented in figure 7b on log-lin coordinates. At $p^c = 0.85$ the volume fraction of diblock copolymer is approximately 10^4 times higher than the concentration of homopolymers in the bulk. Again, the large value of p^b is expected because of the molecular asymmetry in the system. The diblock copolymer is hindered to accumulate in the micelle by its B-block. In other words, it is hard to increase the amount of diblock copolymers to levels comparable to that of the C polymer to optimise the AC contacts. This simply implies that in order to have $p^m \approx 1$, the concentration of free diblock copolymers in solution must be relatively high (compared to that of the homopolymer). Extrapolating this result to the experimental situation suggests that during

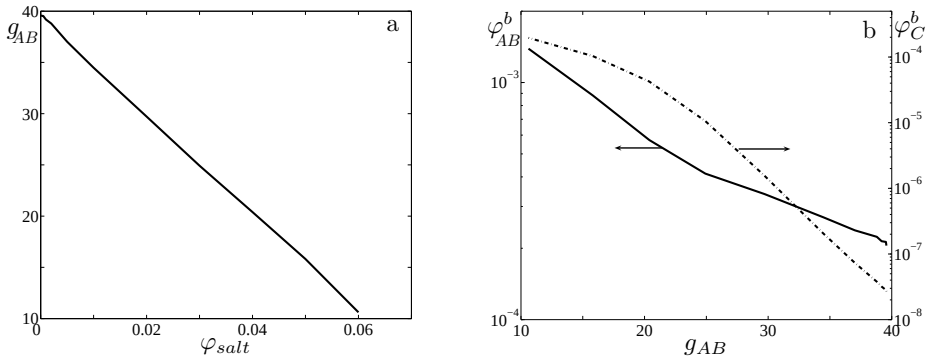

FIGURE 8. **a)** Aggregation number (g_{AB}) as function of the salt concentration and **b)** dashed line is φ^b_C and solid line is φ^b_{AB} on a logarithmic scale as function of the aggregation number. The micelle concentration was $\varphi_m = 10^{-4}$ and the calculations were performed at $p^c = 0.85$.

a LS-titration, the concentration of free diblock copolymers in solution can be much higher than that of the homopolymer. Whether the total amount of copolymer in the bulk becomes so high that one underestimates the amount of (co)polymers in the micelles will depend strongly on the strength of the driving force (*e.g.,* the ionic strength).

From our experiments we gained some information about the disintegration process of the micelles upon the addition of salt. Increasing the salt concentration weakens the electrostatic attraction between the oppositely charged molecules. Light scattering titrations where salt is titrated to the micelles, and SANS measurements at different salt concentrations, revealed that the scattering intensity and aggregation number decrease upon increasing ionic strength. Because the charge density of the protein molecules is lower than the charge density of the polyelectrolytes, a two-step disintegration process has been proposed. First, the protein molecules are released (at ≈ 0.12 M NaCl) and then the micelles disintegrate (at ≈ 0.5 M NaCl). It was therefore chosen to try to find additional proof for the salt-induced release (see chapter 5).

In figure 8 a few characteristics of the polymer micelles as function of the salt concentration are shown. Again, the ratio between homopolymer and diblock copolymer was fixed at the optimal value, *i.e.,* $p^c = 0.85$. Obviously, insisting on $p^c = 0.85$ is an approximation; for each ionic strength, a different optimal composition may exist. Hence, by fixing $p^c = 0.85$ we ignore such compositional drift; however, it is expected to be significant only around the CMI. The choice to fix p^c is a pragmatic one, as it keeps the computational efforts within reasonable bounds. The salt concentration

was varied per calculation and the aggregation numbers of the micelles were determined at fixed micelle concentration ($\varphi_m = 10^{-4}$). In figure 8a one can see that g_{AB}, and thus g_C, decreases (p_m is constant) linearly as function of the salt concentration, which was also found in experiments (chapter 5). Another consequence is that the CMC increases with increasing ionic strength (result not shown). With increasing ionic strength also the maximum of $\varepsilon_m(g_{AB})$ decreases gradually. At some threshold ionic strength it appears that the maximum of $\varepsilon_m(g_{AB})$ drops below our selected value of $\varepsilon_m = 9.2\ k_BT$ (where $\varphi_m = 10^{-4}$). We concluded that for this polymer concentration we have reached the critical ionic strength *i.e.,* the CMI. A further increase of the ionic strength will only give micelles in the system if the polymer concentration is raised. In other words, we have reached a condition where the micelles rather suddenly cease to form. For our selected p^m, the highest salt concentration where stable micelles still exist is $\varphi_{salt} \approx 0.06$. Under these conditions, the micelles have a very low aggregation number; it is only $\frac{1}{4}$ of that at the low ionic strength cases.

In figure 8b the corresponding bulk concentrations of the homopolymer and diblock copolymer are presented as function of the aggregation number g_{AB}. In this diagram it is seen that the bulk concentrations are a very strong function of aggregation number and hence of the ionic strength. With decreasing driving force (increasing ionic strength) the concentration of the homopolymer can increase by several orders of magnitude. At the same time the copolymer concentration increases by just a factor of 10. Hence, p^b goes from a very small value towards unity. Indeed, at low aggregation numbers *i.e.,* at high ionic strength, the concentration of diblock copolymers and homopolymers in the bulk is almost the same and approaches the overall concentration of polymers in the system. This is indicative of approaching the CMC, or more precisely, the CMI, the salt concentration above which no micelles are detected (chapter 5 and 6).

7.4.2. The protein "Lysozyme"

The lysozyme molten globule was placed in an one-gradient coordinate system and the radial volume distributions of the different monomers were calculated. Figure 9 presents the volume fractions φ of the different segments of the protein molecule from layer 1-8. These profiles are typical for a molten globule. In this figure one can see that the volume fraction of the non-polar segments, N, is highest in the center of the molecule. The water-soluble segments (P, K and Z) are found in a broad interfacial zone of the protein-like object. In the sequence of lysozyme $\#Z \neq \#K \neq \#P$, therefore the integrated values of the volume fraction distributions of these segments are different. The amount of water in the center of the object is very low (as expected), due to the choice $\chi_{WN} = 4$, and increases when the number of non-polar segments decreases, *i.e.,* at larger r-values.

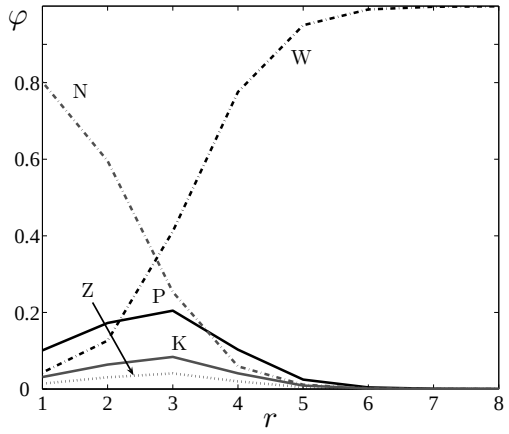

FIGURE 9. Radial volume fraction φ of water (W), non-polar segments (N), polar segments (P), negatively charged segments (Z) and the positively charged segments K of the lysozyme-like object as function of the layer number r

From figure 9, the size of the lysozyme-like molecule can be estimated. Using equation 40, the radius of gyration of the protein molecule was calculated: 2.1 nm. Assuming a homogeneous sphere one can infer a hydrodynamic radius around 2.7 nm; the hydrodynamic radius for lysozyme reported in literature is 2.1 nm.[145]

Due to the discrete nature of the lattice with a cell size (ℓ) of 0.6 nm (corresponding to the segment size), we loose information about the protein globule at length scales smaller than ℓ. Hence, the SCF model is a rather rough way to account for compact globular proteins. Nevertheless, the modeling captures the nature of protein as unimolecular micelles in a reasonable way. The hydrophobic segments and hydrophilic segments show significant overlap of their distributions. This must be attributed to the coupling of the primary amino-acid sequence to the overall globule topology.

7.4.3. Protein insertion in the polyelectrolyte complex micelle

In this section we will consider the interaction between polymer micelles and protein-like molecules, modeled in a two-gradient coordinate system. In the absence of the protein-like molecule, the structure of the micelle in the cylindrical coordinate system is essential identical to that of the spherical coordinate system. Also, the grand potential and the bulk concentrations of its constituents match in both coordinate systems. So, the results obtained from the spherical coordinate system can directly be used to select relevant situations in the computationally challenging cylindrical coordinate system.

Again, we will focus on the optimal micelle system, *i.e.* the micelle with $p^c = 0.85$ that exists at a micelle concentration $\varphi_m = 10^{-4}$ suspended in a salt concentration of $\varphi_{salt} = 10^{-3}$.

As explained in the parameter section, one protein-like object and half of the micelle were placed inside a two-gradient coordinate system (see figure 2) (the other half -its mirror image- is present on the other side of the boundary). One of the non-polar segments, somewhere in the middle of lysozyme-like molecule was pinned (segment X, in table 1 and indicated by $\square$ in figure 3) to a specified coordinate $(z^*, 1)$ and the center of mass of the micelle is in all cases at $(1, 1)$. For each specified position z^* of the protein molecule, we can compute the relevant thermodynamic potential

$$F^{po}(z^*) = F - \sum_i \mu_i n_i \tag{41}$$

where F is the system's Helmholtz energy and the summation over i runs over all mobile components, that includes the two polymers (homopolymer and copolymer), the ions and water. It excludes the protein-like object itself because we have fixed this molecule to be with segment X at z^*. The partial open free energy F^{po} thus includes both the grand potential ε_m (more precisely: half the grand potential) of the micelles (because the other half is outside the volume) as well as the chemical potential of the protein-like molecule. Our main interest is in F^{po} as a function of z^*. Systematic variation of the z^* coordinate leads to the free energy of interaction (potential of mean force) of a single protein-micelle pair, $\Delta F(z^*)$:

$$\Delta F(z^*) = F(z^*) - F(\infty) \tag{42}$$

which is presented in figure 10. During the calculations the aggregation numbers of diblock copolymer $g_{AB} = 39$ and homopolymer $g_{AB} = 12$ were effectively kept constant, and the salt concentration was fixed to $\varphi_{salt} = 0.001$ as well. In figure 11 we present the volume fraction distributions as contour plots through a cross section of the micellar systems, where the protein was pinned at four different positions (a-d in figure 10). Since in these viewgraphs cross sections through the whole micelle are presented, there are two protein-like objects seen in these figures (both the protein and its mirror image).

When the protein-like molecule is outside of the micelle, (or in the periphery of the corona), the free energy of interaction is to good approximation constant and close to zero ($z^* = 20-55$). The reason for the absence of a repulsive force in the periphery of the corona is that the volume fraction of B is very low there. Therefore, there are very few contacts between B and the protein-like object. Moreover, for $\chi_{WB} = 0.45$ the second virial coefficient (v), associated with the corona-solvent interaction, is relatively

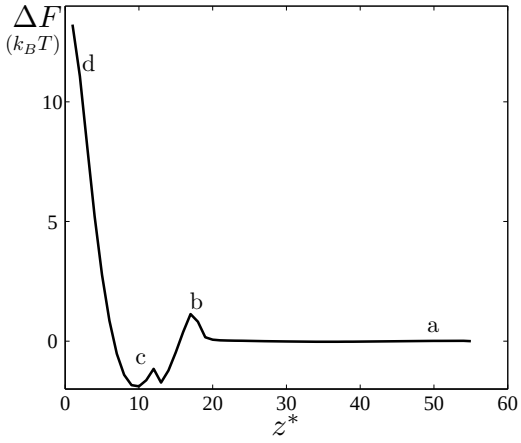

FIGURE 10. The free energy of interaction (in units of k_BT) of a micellar system interacting with a lysozyme-like molecule pinned at z^* minus that when the lysozyme-like molecule is in the bulk ($z^* = \infty$), ΔF, as function of the pinning position (z^*). In these calculations the ratio between homopolymer and diblock copolymer in the micelles was kept fixed to $p^c = 0.85$, $\varphi_m = 10^{-4}$, this means that the aggregation numbers of the micelle were fixed as well. The salt concentration was $\varphi_{salt} = 0.001$. The cross section through the whole micelle at position of a-d can be found in figure 11.

low ($v = 1 - 2\chi_{WB} = 0.1$). As a result the osmotic pressure in the corona remains relatively low. In such situation it is not too expensive to push an object into the outer corona. The free energy of insertion increases when $z^* < 20$, and has a maximum when segment X is pinned at position 17. The first idea is that the increase of the free energy is due to the higher concentration of corona chains in this region and thus the insertion against a locally higher osmotic pressure is starting to be significant. To get more detailed insight in what happens we need the distributions of the molecules in the micelle; we will return to this issue once we have discussed these.

Pushing the lysozyme beyond $z^* = 17$ into the micelle decreases the free energy. Interestingly, there is a pronounced minimum at position 10, which is at core-corona interface. The irregular change of the free energy of interaction near the minimum proves that there are a number of different contributions to the free energy of interaction which give a subtle change of ΔF (which remain unidentified as yet). Pushing the lysozyme-like object further into the core of the micelle results in an unexpected and dramatic increase in free energy. This non-trivial result can more easily be explained once some typical distributions have been discussed.

In figure 11 we show the two-gradient volume fraction distributions of

the micelle + lysozyme at four different pinning positions: 50, 17, 10 and 2 (figure 11a-d) as contour plots. In figure 11a, the core (as well as the corona) remains spherical (as expected); the protein molecule is still outside the micelle. Also, the micelle has its unperturbed structure (see figure 5; in figure 11a we also have drawn short vertical lines in the contour plot of which the corresponding volume fractions are given in the legend). In figure 10 we saw that the free energy has a local maximum at layer $z^* = 17$, the corresponding contour plot is figure 11b. It can be seen that the core is now slightly elongated in the axial (z)-direction. Close inspection of the profiles shows that the elongation of the core is due to a rearrangement of the A segments (charged block of the diblock copolymer) that try to optimise contacts with both the homopolymer (present in the core) and the protein-like object (both have a same charge, opposite to that of the A block). Such "bridging" leads to a deformed core.

Figure 11c shows the contour plot for the case when the lysozyme is pinned at position $z^* = 10$, which is in the core-corona interface. From figure 10 we know that this is the energetically most favourable position. Now the shape of the core is again close to spherical. Hence, the reduction of the free energy by going from $z^* = 17$ to $z^* = 10$ is in part the recovery of the elastic deformation of the core. As the interfacial tension is finite, there must be a gain in interfacial free energy accompanied by the adsorption process. In order to estimate this contribution separately we need to evaluate the effective surface tension of the core-corona interface. At present we do not know how to obtain this quantity accurately. To a first approximation, however, we can take the depth of the interaction curve and use the cross-section area of the protein to find an estimate of the surface tension. We then find the fairly reasonable value of $\gamma \approx 1.2$ mN/m. Note that because we treat the protein molecule as a molten globule (see figure 3) it is possible for the molecule to adjust its conformation to the most favourable shape. It should also be realised that in experiments globular proteins have rotational freedom which will also enable them to find the most favourable situation.

In figure 10 it can be seen that it is energetically unfavourable to push the lysozyme molecule further into the core of the micelle. In fact, the molecule is forced into the core by the pinning of X. The corresponding two-gradient volume fraction distributions of the micelle and lysozyme-like molecule can be found in figure 11d, where $z^* = 2$. We, surprisingly, see that the protein-like object simply refuses to go into the core; instead most of the protein segments remain at the core-corona interface. In this figure one can see that both the morphology of the core as well as the structure of the lysozyme-like molecule have changed dramatically when the grafting segment X is put near the center of the core. The core now, is flattened in the z-direction. This is understood because there is a force acting on the

protein towards the center of the core, and as the proteins remain interfacial, the force is balanced by the deformation of the core. Obviously, this non-spherical shape is a very unfavourable situation. How can it be that the protein-like molecule remains at the core-corona interface while the position of X is near the center? An answer can be found from figure 11d, where in the core two dark spots are seen; these are the pinned segments X. In addition, there is a tether going from $z^* = 2$ to the main part of the protein at the core-corona interface (this is more difficult to see, because the tether is smeared). Obviously, it is costly to pull a tether out of the protein, but it is even more costly to bring the entire protein into the core. Both the deformed core and the structural changes of the protein are consistent with the free energy increase that is observed in figure 10.

One may argue that the fundamental reason why a protein-like molecule refuses to go inside the center is that its mirror-image is preventing it to do so. This would be a reasonable explanation if the two lysozyme molecules would indeed repel each other strongly (as they do experimentally under reasonable conditions). Therefore reference calculations were performed in order to quantify the pair interaction between two lysozyme-like objects (not shown). From these calculations we learned that these protein-like objects in fact do not repel each other. The reason is that the long range electrostatic effects which in the experimental situation is responsible for the repulsion, is replaced by short-range interactions only. Indeed, in the present model the two lysozyme molecules tend to stick to, rather than repel each other. Hence, an unfavourable pair interaction is not an explanation for the increase in free energy observed in figure 10. Apparently, the lysozyme molecule is not wetted by the core components. To deform the shape of the core and to push the homopolymers and diblock copolymers (slightly) away from the center are sufficient to explain the repulsive part of ΔF.

We haste to mention that in the experiments there is no constraining force on the position of one of the amino acids of lysozyme and thus we cannot directly use the free energy curve to compute the equilibrium distribution of the proteins inside the polymer micelle. However, the calculations strongly suggest that proteins will very likely be positioned in the core-corona interface and that there is an energy barrier separating the bound state of the protein (at the core-corona interface) and the unbound one (floating freely in solution).

Let us return to the local maximum found at $z^* = 17$. In a mean-field theory one may anticipate that the phenomena that were discussed, *i.e.,* the work against the osmotic pressure (increasing with decreasing z^*) and the elastic deformation of the core (increasing with increasing z^*), may have resulted in a first-order like transition, with meta-stable branches in $\Delta F(z^*)$. This does not occur in the present system. Possibly, the reason for this is

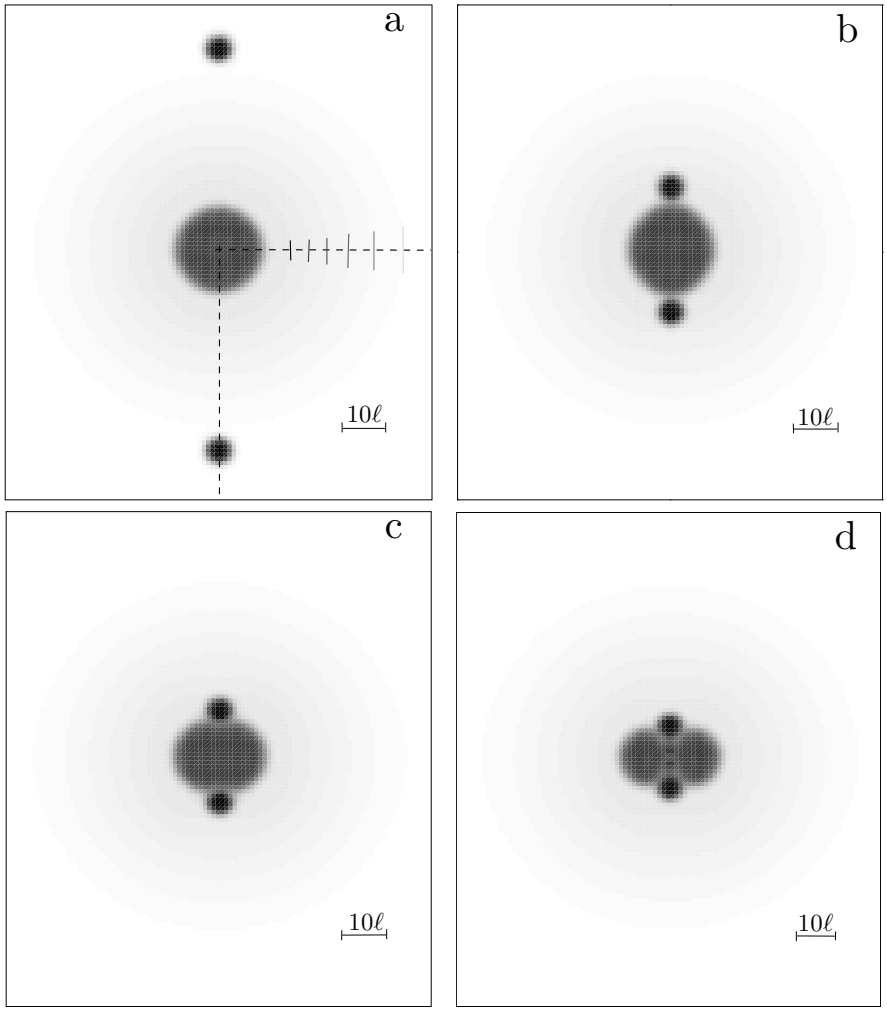

FIGURE 11. Two-gradient volume fraction distributions of a micelle with on both sides in the z-direction a protein-like molecule is pinned **a)** lysozymes pinned with the X-segment at $z^* = |50|$, **b)** lysozyme pinned at $z^* = |17|$, **c**) lysozymes pinned at $z^* = |10|$ and **d)** lysozyme pinned at $z^* = |2|$. In figure **a** the volume fraction of diblock copolymer at the respective vertical lines from the core to the outside are: 0.09, 0.075, 0.006, 0.045, 0.03 and 0.015. The scale bar indicates 10 lattice sites.

that the lengths of the polymers that form the micelle were too short for this. We do not exclude, however, that on a mean-field level the transition between bound and unbound states becomes a true transition in the appropriate thermodynamic limit (very long chains). High barriers between bound and unbound states would be of practical interest obviously.

The final question to be addressed is whether, upon increasing the ionic strength, the protein-like objects are released, and whether (or not) this occurs before the micelles disintegrate. To obtain relevant predictions we have recorded the depth of the free energy of interaction ΔF_{min} as function of the salt concentration. Again we focus on the optimal micelle composition $p^c = 0.85$ and keep the micelle volume fraction $\varphi_m = 10^{-4}$. Referring to figure 8a and b, we know that in this system both the aggregation numbers and the bulk concentrations depend on the salt concentration used. To calculate the depth of the free energy ($\Delta F(z^*)$) as a function of the salt concentration, these features have been implemented as constraints. This means that for a given calculation of $\Delta F(z^*)$ not only the ionic strength, but also the corresponding bulk volume fractions of all polymers were specified. This means that the aggregation numbers could relax to the values reported in figure 8, both in the presence and in the absence of the protein-like molecule.

The first issue is to localise the minimum in the interaction curve. Clearly as the aggregation number changes, it is conceivable that the minimum position of F^* shifts. It was found, however, that the position of the minimum free energy did not change; it remained located at $z^* = 10$ for all salt concentration. Using this result, the absolute value of the free energy of interaction $|\Delta F(10)|$, which is the difference in free energy of the micellar system with the protein-like molecule at $z^* = 10$ and at $z^* = \infty$, was determined as function of the salt concentration. The results of these calculations are presented in figure 12.

Based on light- and neutron scattering measurements as function of the salt concentration it was proposed that first the enzymes are gradually released and then the micelles disintegrate. In figure 12 it can be seen that the free energy difference is constant ($\approx 1.9\ k_BT$) up to a salt concentration of 10^{-3}. $|\Delta F(10)|$ decreases with ionic strength when $\varphi_{salt} > 10^{-3}$. At $\varphi_{salt} \approx 0.04$ it is less than k_BT, which indicates that the accumulation of the lysozyme-like object must have decreased by a factor of approximately 2.5. This salt concentration is clearly lower than the salt concentration at which the micelles disappear (see figure 8a and b). Hence, this suggests that most of the lysozyme-like objects are released before the micelles fall apart. From figure 8a and b it became also clear that the aggregation number of the micelles decreases as function of the ionic strength, indicating that, apart from the enzyme release, also homopolymer and diblock copolymers are released. All these results are consistent with the experimental results.

In figure 12 we also present the ionic strength dependence of the interfacial tension between water and a macroscopic A_{40} + C_{150} complex phase. Up to an ionic strength of $\approx 2 \times 10^{-2}$ the free energy of interaction ($|\Delta F(10)|$) and the interfacial tension follow the same trend. Above $\varphi_{salt} = 2 \times 10^{-2}$ the decrease in the free energy of interaction is more

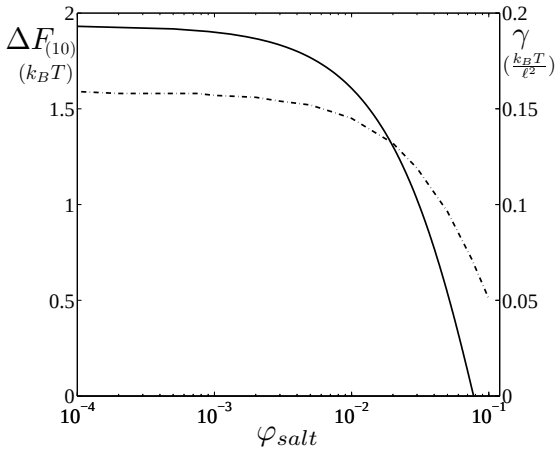

FIGURE 12. Absolute value of the free energy of interaction of a lysozyme-like object pinned at layer $z^* = 10$ (left y-axis and solid line), from the center of the micelle, $|\Delta F(10)|$ (in units of k_BT) as a function of the salt concentration. The ionic strength dependence of the bulk concentrations of the homopolymer and diblock copolymer were taken from the results of figure 8b. The volume fraction of micelles is fixed to $\varphi_m = 10^{-4}$. Ionic strength dependence of the interfacial tension of a A_{40} + C_{150} complex (right y-axis, dashed line) in units k_BT per lattice length squared (ℓ^2) .

pronounced than the decrease in the interfacial tension. This correlation between the free energy of interaction and the interfacial tension indicates that the protein-like object is not wetted by the core-forming phase and therefore has its most favourable conformation in the core-corona interface. The difference in shape, upon comparing the interfacial tension and free energy of interaction at $\varphi_{salt} > 2 \times 10^{-2}$, may be due to the curvature of the micelle, which was not taken into account in our reference calculations, where we just considered a macroscopic (flat) interface. Also, in our reference calculations we only used the charged block of the diblock copolymer, contributions of the hydrophilic uncharged block B to the interfacial tension in the core-corona interface were thus ignored.

At this stage it is of interest to elaborate shortly on how the calculations compare to corresponding experimental data. We have estimated, from SANS data, the typical aggregation number of the three different components and the amount of water in the core, for a micelle concentration of $\varphi_m \approx 10^{-4}$. The aggregation number of the homopolymer and diblock copolymer in the calculations are 12 and 39, respectively; we pushed 2 lysozyme molecules into these micelles. The experimental micelles contain on

average 8 homopolymers, 29 diblock copolymers and 2 lysozyme molecules (chapter 6). Because we deliberately tuned our Flory-Huggins parameters such that these numbers are comparable, we can hardly argue that this is an independent result. However, we can say that the calculations are helpful for giving insight into the experimental system, *e.g.,* in giving structural information.

A key disparity between the experimental data and the model predictions is the amount of water in the core of the micelles. For the experimental micelle the volume fraction of water in the core is estimated to be as high as 0.92; similar volume fractions of water were found for micelles consisting of PAA_{42}-$PAAm_{417}$ and $P2MVP_{209}$.[64] For the determination of the amount of water in these polyelectrolyte complex micelles, several assumptions have to be made and it is expected that the error is between 10 and 15%. The volume fraction of water in the model micelle is only ≈ 0.30 and thus well outside the uncertainty range of the experiments. In mean field calculations it is possible to increase the water concentration in the core of the micelles. However, to do so, the strength of the correlation attraction has to be increased to very (unreasonably) high values, while the solvent quality χ_{AW} and $\chi_{CW} \ll 0$. Calculations in this region of parameter space were exceedingly difficult. Here we clearly see a limitation of the Bragg-Williams approximation.

The calculations, nevertheless, give new insights and truly contribute in explaining experimental findings. For the experimental micelle it is for instance known that homopolymer needs to be in excess of like charged protein in order to obtain stable micelles. The above results now may give a clue why this is the case. An explanation may be that the optimal place for a protein is in the core-corona interface. When the protein is in excess, there is not enough interface available for the protein and the structures that are formed have a tendency to disintegrate. In previous work we have found that micelles, where the molar ratio between $PDMAEMA_{150}$ and lysozyme was 13:87, were unstable (chapter 2). Small Angle Neutron Scattering measurements of these structures could not be interpreted using the standard model for a micelle of a (homogeneous) core surrounded by a dilute corona. The preference of proteins to be in the core-corona interface was not considered and may be an explanation for the instability of these micelles and the difficulties in explaining the neutron data.

7.5. Conclusions

Self-consistent field modeling is presented which is targeted to identify the main physical characteristics of protein insertion in polyelectrolyte complex micelles. Predictions were, when possible, confronted with experimental data. The attractive interactions between the oppositely charged species are treated on the Flory-Huggins short-range interaction level. Our polyelectrolyte complex micelles consist of homopolymers and diblock copolymers, which means that the system is composition-wise asymmetric. The model allowed flexibility in adjusting the appropriate Flory-Huggins interaction parameters such that the model polyelectrolyte complex micelle truely resembles experimental ones. We have analysed the charge stoichiometry of the polyelectrolyte complex core, and argue that the optimal charge ratio between diblock and homopolymer is slightly lower than unity, *i.e.*, $p^c = 0.85$.

For most of our results, we fixed our attention to micelles with this optimal ratio and to systems where the micelle concentration and salt concentration were fixed ($\varphi_m = 10^{-4}$ and $\varphi_{salt} = 0.001$) as well. First, a one-gradient spherical coordinate system was used and calculations were performed to characterise the polyelectrolyte complex micelle and the lysozyme-like objects separately. Subsequently, the micelle was pinned with its center of mass in a two-gradient cylindrical coordinate system and the lysozyme-like object was pushed into the micelle along the cylinder's axis. The free energy as function of the distance to the core has a minimum of $\approx -2\ k_BT$ in the core-corona interface, indicating that this position is favourable in comparison to the bulk or the corona. A dramatic increase in free energy is observed when the lysozyme-like object is pushed into the center of the core, showing that the protein-like molecule strongly prefers the core-corona interface. Importantly, we found that there is a free energy barrier between the bound (protein is at the core-corona interface) and unbound (protein is free in solution) state of the protein. The height of this barrier is determined jointly by the work against the osmotic pressure and the work to deform the core.

The stability of the micelles in terms of ionic strength, was determined and compared to experimental results. First, the aggregation number of the polyelectrolyte complex micelle decreased as function of the ionic strength and at $\varphi_{salt} \approx 0.06$ the critical micelle ionic strength (CMI) is found for micelles where $p^m = p^c = 0.85$ and $\varphi_m = 10^{-4}$. From calculations in the two-gradient coordinate system, where the free energy of the unbound state (protein is outside micelle) is compared to the bound state (protein is at the core-corona interface), it can be derived that the well depth of the protein/micelle potential of mean force decreases strongly upon increasing the ionic strength, well before the micelles themselves vanish. Hence, the proteins loose affinity for the micelles with increasing ionic strength. This

salt-induced release was also concluded from the experimental data.

Chapter 8

Effects of polyelectrolyte complex micelles and their components on the enzymatic activity of lipase

Abstract.
The enzymatic activity of *Hℓ*-lipase embedded in complexes of poly-2-methylvinylpyridinium-*co*-polyethylene oxide ($P2MVP_{41}$-PEO_{205}) and polyacrylic acid (PAA_{139}) is studied as function of the PAA_{139} + $P2MVP_{41}$-PEO_{205} complex composition. The measurements revealed that there are several factors that influence the enzymatic activity. When incorporated in micelles, the activity of lipase is increased, which suggests that the micelles favour the active state. The activity may further increase because the substrate is drawn to the micelles. It is found that the presence of PAA_{139} alone also increases the enzymatic activity somewhat. Increasing of the ionic strength decreases the enzymatic activity in all systems. However, at ionic strengths where the micelles are disintegrated (> 0.5 M), the activity of lipase in the presence of both polyelectrolytes is still higher than the activity of free lipase. At 0.7 M NaCl it was found that lipase in the presence of (just) $P2MVP_{41}$-PEO_{205} is more active than lipase without this additive.

submitted to Biomacromolecules

8.1. Introduction

Enzymes are biocatalysts. Their biological activity, *i.e.,* their ability to catalyse specific reactions, is strongly related to their shape and structure. Most enzymes that are active in aqueous environment have their catalytic center at the surface; in this way their active site is accessible to substrate molecules in the solvent. There are also water-soluble enzymes that catalyse reactions of water-insoluble substrates; *e.g.,* lipases belong to this group of enzymes. Lipases catalyse the hydrolysis of esterbonds in, *e.g.,* triacylglycerols to fatty acids. For most lipases their shape is such that their rather hydrophobic catalytic center is covered by a lid.[146,147] In a water-rich environment this lid is mainly closed and the lipase molecules are biologically inactive. Lid opening occurs in the presence of a hydrophobic/hydrophilic interface. The exact mechanism of the lid opening depends on the type of lipase. For the lipase used in this study, which is from *Humicola ℓanuginosa* (*Hℓ*-lipase), the lid-containing part of the enzyme is somewhat hydrophobic. When this side interacts with a hydrophobic interface,[148] the lid opens and the lipase assumes its active form. Because of this interfacial induction of the enzymatic activity, such lipases are called to be interfacially active.[149]

The interfacial activation of *Hℓ*-lipase also depends on the surface curvature. For unilaminar vesicles with a diameter of 100 nm the closed form is favoured. However, smaller unilaminar vesicles with a diameter of 40 nm induce the active form of the enzyme molecule.[150,151] From these studies it is also known that the negative charge on the surface of the vesicles favours the open state. An explanation for this activation is that the so-called hinge around the lid contains the positively charged amino acids arginine and lysine. Therefore, the lid opening is expected to be partly electrostatically controlled.[151,152]

In this chapter, the enzymatic activity of lipase in polyelectrolyte complex micelles is investigated. The polyelectrolyte complex micelles consist of positively charged diblock copolymers (poly-2-methylvinylpyridinium-*co*-polyethylene oxide ($P2MVP_{41}$-PEO_{205})) and negatively charged homopolymers (polyacrylic acid (PAA_{139})). A method was developed to incorporate negatively charged lipase molecules in these micelles. First, the lipase is mixed with the negatively charged homopolymer. Subsequently, this mixture is added to a diblock copolymer solution. If the ratio between the positively and negatively charged groups is about unity (this is called the preferred micellar composition: PMC), (almost) electroneutral micelles are formed with lipase molecules incorporated somewhere in the core of the micelles. Away from the PMC, soluble complexes are also formed, which have an excess charge and are therefore not considered as (electroneutral) micelles. From previous work it is known that stable structures are formed when the ratio between homopolymers and protein molecules is such that the homopolymer is in excess (chapter 2). In this study we therefore fix the

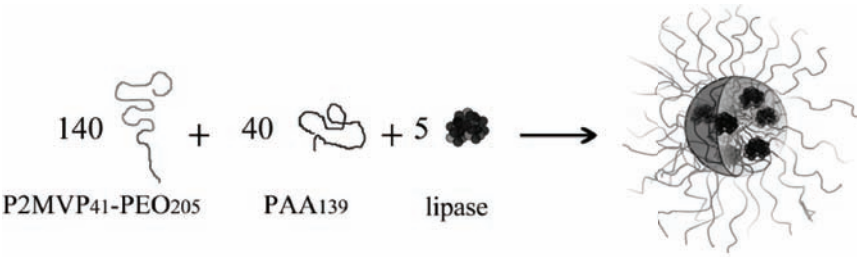

FIGURE 1. Artistic impression of the formation of a polyelectrolyte complex micelle with lipase in the core. Aggregation numbers were derived by SANS (chapter 5)

homopolymer-to-lipase ratio at 9:1.

Detailed characterisation of the micelles has been performed using Light Scattering (LS) titrations and Small Angle Neutron Scattering (SANS) experiments (chapter 5). From these measurements the size and aggregation numbers of the micelles could be estimated. The micelles have a core radius of ≈ 14 nm and a hydrodynamic radius of ≈ 23 nm. Each micelle contains approximately 140 diblock copolymers, 40 homopolymers and 5 lipase molecules. The amount of water in the core is estimated to be 83% (chapter 5). A schematic sketch of such a micelle is given in figure 1.

The behaviour of these micelles has been studied as a function of the salt concentration. Since the components of the micelles are hold together by electrostatic forces, the strength of the resulting attraction can be tuned by changing the salt concentration. It was found that both the core radius and the scattering intensity decreased upon the addition of salt, indicating a loss of mass from the core. Assuming this loss is solely due to the release of lipase molecules, we could conclude that all the enzyme molecules will be released at a salt concentration of 0.12 M NaCl (chapter 5).

The interesting question is whether incorporation in the micelles influences the enzymatic activity of lipase. For polyelectrolyte complex micelles, consisting of a negatively charged diblock copolymer and lysozyme, it was found that the enzymatic activity of lysozyme increased when it was incorporated in the micelles.[37] To study the effect of the micelles on the activity of lipase two types of experiments were designed: experiment A and experiment B.

In experiment A the enzymatic activity of free lipase is compared to the enzymatic activity of incorporated lipase. As a control, the influence of the mere presence of normal polyelectrolyte complex micelles (consisting of PAA_{139} and $P2MVP_{41}$-PEO_{205} only) on the activity of free lipase was checked. Furthermore, the effect of adding extra normal micelles on the activity of incorporated lipase was investigated. If substrate molecules accumulate in polyelectrolyte complex micelles, the reaction rate of lipase in

this system will be lower than in the system without extra micelles.

In experiment B, the influence of the polyelectrolyte composition on the enzymatic activity was studied. In this experiment the molar ratio between lipase and PAA_{139} was kept constant (at 1:9) and the amount of $P2MVP_{41}PEO_{205}$ was varied. The enzymatic activity of lipase in complexes having seven different complex compositions around the PMC was compared to the activity of free lipase. This experiment was also performed at five different salt concentrations (0, 0.1, 0.3, 0.5 and 0.7 M NaCl), to check whether the afore mentioned salt-induced release would also affect the activity.

8.2. Experimental

8.2.1. Materials.

The lipase used in this study was Lipolase™, derived from the fungus *Humicola ℓanuginosa*, was a kind gift from Novozymes (Bagsvaerd, Denmark). The homopolymer used was Poly(acrylic acid)$_{139}$ (Polymer Source Inc., Canada), M_w = 10000 g mol^{-1}, PDI= 1.15; when fully charged this anion contains 139 charges. The positively charged diblock copolymer Poly(2-methylvinyl pyridinium iodide)$_{41}$-*block*-Poly(ethylene oxide)$_{205}$, was obtained by quarternisation of Poly(2-vinyl pyridinium)$_{41}$-*block*-Poly(ethylene oxide)$_{205}$), PDI= 1.05, purchased from Polymer Source *Inc.,* Canada, and using the following protocol. In a typical reaction, 1 g of diblock copolymer containing P2VP was dissolved in 35 mL DMF. Iodomethane (3 mL) was added, and the reaction was stirred under nitrogen flux for 48h at 60 °C. Ether (110 mL) was added to precipitate the polymer (add until no more precipitation occurs). The precipitate was filtered and washed with ether (5 × 10 mL) to yield a light yellow powder. (After each washing step the polymeric product was less yellow, less sticky, and more powdery). Subsequently, the polymer was placed in an oven at 50 °C to dry overnight. The mass after quarternisation was 19100 g mol^{-1}.

8.2.2. Sample preparation.

Solutions of the macromolecules were prepared in a 3.5 mM phosphate buffer at pH 7. The pH of these solutions was adjusted to 7 with NaOH or HCl after dissolving the macromolecules.

8.2.3. Enzymatic Activity Measurements.

Two types of enzymatic activity measurements were performed. First, the activity of free lipase, lipase in micelles, lipase with micelles and lipase in micelles with micelles were determined (experiment A). In this experiment four different lipase concentrations were studied, 0.1, 0.2, 0.3 and 0.4 mg L^{-1}. The compositions of the lipase-filled and normal micelles (consisting

of just P2MVP$_{41}$-PEO$_{205}$ and PAA$_{139}$) were determined by light scattering titrations using the previously described protocol (chapter 5). For the systems with lipase-containing micelles and lipase with normal micelles, the concentration of polyelectrolyte complex micelles was approximately the same. For the system where lipase was in micelles and extra micelles were added, the concentration of lipase-filled and normal micelles was the same *i.e.,* the total concentration of micelles was approximately twice as high in comparison to the other systems.

In the second experiment (experiment B) the activity of lipase as function of the complex composition was measured. Here, it was chosen to compare the activities of 7 different compositions to the activity of free lipase. The composition of the system (F^-) is defined by:

$$F^- = \frac{[n_-]}{[n_-] + [n_+]} \tag{43}$$

in this equation $[n_-]$=c_-N_- refers to the total negative charge concentration, and $[n_+]$=c_+N_+ is the total positive charge concentration; c_i is the molar concentration of species i, and the number of chargeable groups per chain on the polyelectrolytes is denoted as N_i. The compositions chosen were $F^- = 0.25$, 0.375, 0.5 (PMC), 0.625, 0.75,0.875 and 1. The ratio between the negatively charged homopolymer and negatively charged lipase was fixed at 9:1 and the different compositions were obtained by varying the amount of positively charged diblock copolymer. These measurements were performed at 5 different salt concentrations: 0, 0.1, 0.3, 0.5 and 0.7 M NaCl. The lipase concentrations in these measurements were 0.1, 0.2, and 0.4 mg L^{-1}.

The enzymatic activities were measured in 96-well plates. These plates were designed in such a way that all the measurements of experiment A were measured on the same plate. For experiment B five plates were prepared; the salt concentration was varied per plate. Every well was filled with 50 μL of sample. The substrate used was paranitrophenol-butyrate (pnp-butyrate), purchased from Sigma. Lipase hydrolyses the ester bond yielding butyric acid and paranitrophenol (pnp), the latter substance has a yellow color. Pnp-butyrate (5 μL) was dissolved in 5.3 mL 2-isopropanol. From this mixture 0.5 mL was added to 3.5 mM phosphate buffer (pH= 7, and containing 0, 0.1, 0.3, 0.5, 0.7 M NaCl, depending on the measurement). Per well 150 μL of this mixture was added yielding a pnp-butyrate concentration of 0.1 mM per well.

The enzymatic activities were measured using a Molecular Devices Spectramax plus plate reader. The change in absorbance at 405 nm was followed for 30 minutes. The absorbance was measured every 15 seconds. In view of initial irregularities in the enzymatic conversion, it was decided to select the concentration of para-nitrophenol formed after 9 minutes as a measure for the lipase activity, rather than the initial slopes of the absorption *versus*

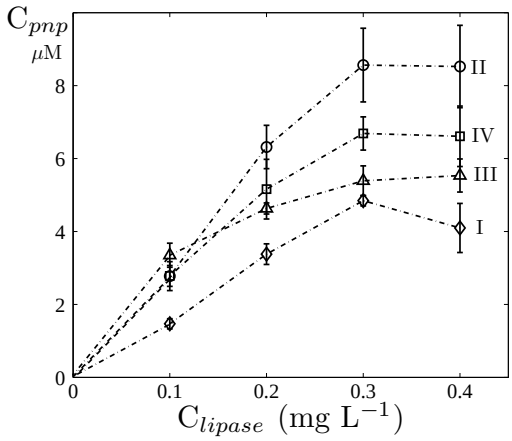

FIGURE 2. Activity as function of lipase concentration for ∘ free lipase (I), △ free lipase with micelles (III), ⋄ lipase in micelles plus extra micelles (IV) and □ lipase in micelles (II).

time. The concentration of para-nitrophenol was calculated by applying Lambert-Beer's law, using 18,000 cm^{-1} M^{-1} as the molar extinction of pnp.[153] Results are presented as an average of triplicate experiments together with their standard deviation.

8.3. Results

8.3.1. Experiment A.

In experiment A four different systems were studied: (I) free lipase, (II) lipase in micelles, (III) free lipase with normal polyelectrolyte complex micelles and (IV) lipase in micelles with extra normal polyelectrolyte complex micelles. These four systems enabled comparison between the activity of (free) lipase in buffer (I) with the activity of lipase incorporated in micelles (II). It may be that lipase interacts with normal polyelectrolyte complex micelles (consisting of P2MVP$_{41}$-PEO$_{205}$ and PAA$_{139}$ only) and therefore the activity of lipase in the presence of normal micelles is determined (III). The paranitrophenol butyrate, the substrate of lipase used in the assay, is rather hydrophobic and may accumulate in the micelles. In system (IV) we therefore add extra micelles to lipase-containing micelles. When the substrate accumulates in the micelles, the reaction rate in (IV) will be lower than that of the system containing lipase-filled micelles only (II). Determination of the optimal micellar composition for both lipase-filled and normal micelles was done using light scattering titrations. These experiments are elaborately discussed in chapter 5 and will therefore not be presented here.

In figure 2 the activity of lipase in the various systems at four different

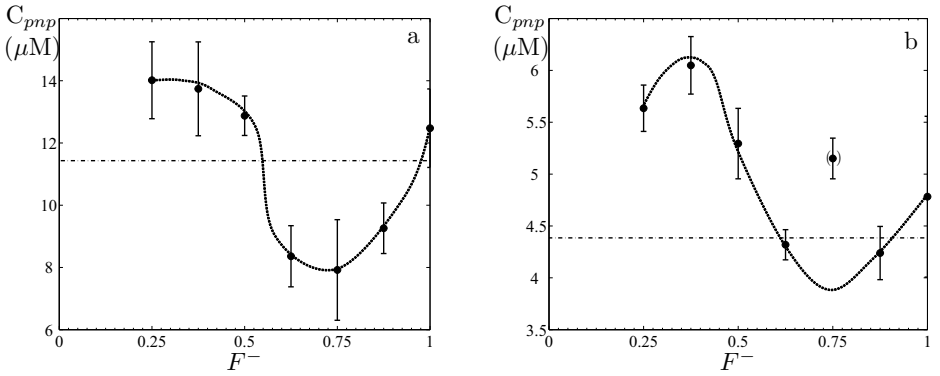

FIGURE 3. Lipase activity as function of the complex composition F^- for **a)** samples with a lipase concentration of 0.4 mg L^{-1} and **b)** 0.1 mg L^{-1}. The lines indicate the activity of free lipase at the respective concentrations, the error in the activity of free lipase was 11% for 0.4 mg L^{-1} and 8% for 0.1 mg L^{-1}.

concentrations are shown. In the range $C < C_{lipase} < 0.3$ mg L^{-1}, C_{pnp} is nearly proportional to C_{lipase}; this implies the activity is constant in this range, and given by the slope. The four different systems (I, II, III and IV) have different activities as function of lipase concentration (see figure 2). The lowest activity was found for free lipase (I). An increase of the activity is observed when normal micelles are added (III). The activity of a solution containing both lipase-filled and normal micelles (IV) is higher than the activity of free lipase together with normal micelles (III). The highest activity is found for micelle bound lipase (II). At $C_{lipase} = 0.3$ mg L^{-1} the activity of system II is almost twice as high of I. At 0.1 mg L^{-1} lipase the difference between the activity of lipase in the four different systems is less pronounced than at the higher concentrations.

8.3.2. Experiment B.

Here, we investigate the enzymatic activity as function of the complex composition. At $F^- = 1$, the system only contains the negatively charged components *i.e.,* PAA_{139} and lipase. Upon increasing the concentration of $P2MVP_{41}$-PEO_{205}, soluble polyelectrolyte complexes are initially formed that are negatively charged ($F^- = 0.875$, 0.75 and 0.625). At $F^- = 0.5$, solutions contain near-neutral polyelectrolyte complex micelles with lipase molecules incorporated in the core. At $F^- = 0.375$ and 0.25, the positive charges are in excess in complexes.

The results of these measurements are presented in figures 3a and b. In figure 3a the lipase concentration is 0.4 mg L^{-1} and in figure 3b the lipase

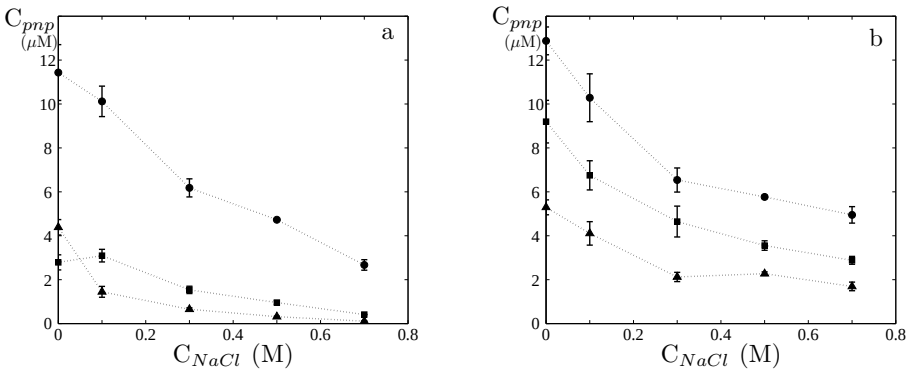

FIGURE 4. Concentration of pnp formed after 9 minutes for **a)** free lipase and **b)** lipase in micelles as function of the salt concentration. For lipase concentrations of: • 0.4, ■ 0.2 and ▲ 0.1 mg L^{-1}

concentration is 0.1 mg L^{-1}. In both figures the dashed lines indicate the activity of free lipase at the respective concentrations. At first sight, the shapes of the activity *versus* F^- curves for the two lipase concentrations are not the same. However, on close inspection, only the activity at $F^- = 0.75$ is different; for 0.1 mg L^{-1} the activity is much higher. For the other compositions the same trend is followed: the highest activity is found at $F^- = 0.25$ or 0.375, followed by a decrease in activity from $F^- = 0.375$ to 0.75 and subsequently an increase in activity is found for $F^- = 0.75$ to 1. This trend is indicated by a dotted line. It appears from these results that the activity is predominantly enhanced in the cationic-to-neutral range, and suppressed in the anionic range. Surprisingly, the activity is slightly enhanced where only PAA_{139} and lipase are present ($F^- = 1$).

Previous work revealed, that upon raising the NaCl concentration to $\approx$ 0.12 M NaCl, lipase is entirely released, and that further increase of the NaCl concentration to $\approx$ 0.5 M leads to disintegration of the micelles. Therefore, the activity of lipase as function of the salt concentration was also considered. The results of these measurements are presented in figure 4a and b, for free lipase and incorporated lipase, respectively. In figure 4a the activity of free lipase is plotted as a function of the salt concentration. The activity was determined for three different lipase concentrations: 0.1, 0.2 and 0.4 mg L^{-1}.

Both for free lipase (figure 4a) and for lipase-filled micelles (figure 4b) a decrease of the enzymatic activity is found upon increasing salt concentration. However, the activity reduction is different for free lipase and incorporated lipase: the decrease in activity for free lipase is more dramatic. Especially at the two lowest lipase concentrations (0.1 and 0.2 mg L^{-1}) and

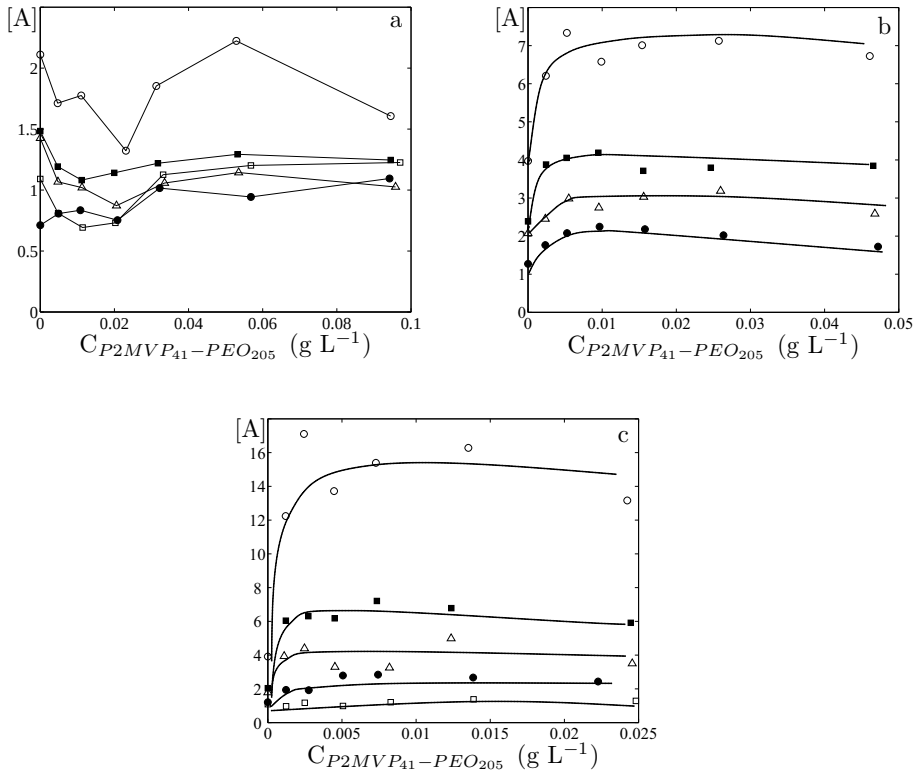

FIGURE 5. Normalised activity ([A]) for **a)** 0.4 mg L^{-1}, **b)** 0.2 mg L^{-1} and **c)** 0.1 mg L^{-1} lipase as function of the diblock copolymer concentration ($C_{P2MVP_{41}-PEO_{205}}$) for five different salt concentrations: □ 0 M, • 0.1 M, △ 0.3 M, ■ 0.5 M and ○ 0.7 M NaCl. Here, [A] is defined as the activity of lipase at the respective composition F^- and at a certain salt concentration, divided by the activity of free lipase at this salt concentration. Lines are meant as guides to the eye.

at 0.7 M NaCl, the activity was almost completely suppressed. In contrast, lipase maintains substantial activity in the presence of the two polyelectrolytes, even in 0.7 M NaCl.

The lipase activity as function of the complex composition was studied at five different salt concentrations. The results of these measurements are shown in figure 5a, b, and c, for 0.4, 0.2 and 0.1 mg L^{-1} lipase, respectively. In this figure the activity, normalised with respect to the free lipase at the same salt concentration [A], is plotted as function of the diblock copolymer ($P2MVP_{41}$-PEO_{205}) concentration. The corresponding complex compositions are $F^- = 1$, 0.875, 0.75, 0.625, 0.5, 0.375 and 0.25. Presenting the

data in this way (rather than as function of F^-) helps to demonstrate the effect of the polymer concentration on the enzymatic activity of lipase. The data of figures 3 and 4 are again used to construct figure 5 (*e.g.,* the lowest curves in figure 5a and c are the same data as in figure 3a and b). At 0.5 and 0.7 M NaCl, it is expected that the polyelectrolyte complex micelles have disintegrated (chapter 5), *i.e.,* that there are only free polymers in solution. In figure 5a and c the five different data sets shown are at the five different salt concentrations (0, 0.1, 0.3, 0.5 and 0.7 M NaCl); in figure 5b the results for 0 M NaCl are not shown, because the data were unreliable.

In figure 5a, the normalised activities of 0.4 mg L^{-1} lipase are shown. For $0 - 0.5$ M NaCl, the activity of lipase at different complex compositions (here expressed by the concentration of P2MVP$_{41}$-PEO$_{205}$) is approximately the same as for free lipase, since the normalised activity is about unity. At 0.7 M NaCl the normalised activity becomes significantly higher than unity.

At lower lipase concentrations, *i.e.,* 0.2 and 0.1 mg L^{-1}, similar trends are observed for the normalised activity [A] with varying complex composition, see figure 5b and c. At $F^- = 1$ the activity is lowest, and about the same as the activity of free lipase. Then, when P2MVP$_{41}$-PEO$_{205}$ is added, the activity increases, and levels off at higher concentration of diblock copolymer. At higher salt concentration, there is a remarkable difference between the activity of free lipase, and that of lipase in the presence of polyelectrolytes. At 0.7 M NaCl, the activity of lipase (for the lowest lipase concentration 0.1 mg L^{-1}) in the presence of both polymers is approximately 16 times higher than the activity of free lipase (see figure 5c).

8.4. Discussion

The set of experiments described in this study provides detailed information on conditions that influence the enzymatic activity. The data show that the influence of incorporation of lipase in polyelectrolyte complex micelles on its enzymatic activity is complex and not easily interpreted. It seems that several factors influence the activity simultaneously. Let us try to point out the effects caused by these factors one by one.

8.4.1. The effect of polyelectrolyte complex micelles.

In experiment A, the effect of incorporation of lipase in polyelectrolyte complex micelles was studied. The results of these measurements are presented in figure 2. From the four systems studied, free lipase (I) has the lowest enzymatic activity. In the presence of polyelectrolyte complex micelles (III), lipase is more active, hence the presence of the micelles somehow influences the enzymatic activity in a positive way.

If we compare the activity of free lipase with the activity of lipase incorporated in polyelectrolyte complex micelles (system I *versus* system II), it is obvious that the incorporation has a very positive effect on the enzymatic activity. Apparently, incorporation in the polyelectrolyte complex micelles somehow favours the active form of lipase.

The enzymatic activity of incorporated lipase (II) decreases when extra normal polyelectrolyte complex micelles (without lipase) are added (IV). This experiment has been performed to figure out whether there is an attraction between the substrate and the micelles. The observed decrease in activity when extra micelles are added indicates that the substrate interacts with or accumulates in the micelles. This may also be the explanation why the activity of incorporated lipase is highest. The substrate and lipase "find" each other in the micelles. Moreover, when the accumulation of substrate occurs in the PEO-corona this may well explain the increase in activity of lipase in the presence of polyelectrolyte complex micelles (III). However, it may also be that the substrate accumulates in the core of the micelles and then this explanation would not apply.

8.4.2. The effect of complex composition.

It is interesting that the incorporation of lipase in polyelectrolyte complex micelles has a positive effect on the enzymatic activity. However, the results of experiment A do not fully explain why the activity is higher. Studying the lipase activity as function of the complex composition F^- may provide more information about the effect of the presence of polyelectrolytes and polyelectrolyte complexes. When P2MVP$_{41}$-PEO$_{205}$ is added to a mixture of lipase and PAA$_{139}$ (molar ratio is 1:9), first polyelectrolyte complexes are formed, and then, close to charge neutralisation, polyelectrolyte complex micelles are formed. As function of the complex composition F^- a clear trend is observed (see figure 3). Starting at $F^- = 1$, the lipase activity first decreases and has a minimum at $F^- = 0.75$; subsequently, the activity increases and is maximal at $F^- = 0.375 - 0.25$. Hence, the activity of lipase strongly depends on the complex composition. In the range $F^- = 0.875 - 0.625$ it is expected that the solution contains negatively charged polyelectrolyte complexes, rather than micelles. At these compositions a lower enzymatic activity is measured, compared to activity of free lipase. At $F^- = 0.75$ the lowest activity is found. Increasing the amount of diblock copolymer induces the formation of the micelles, and at $F^- = 0.625$ part of the lipase molecules will be incorporated in electroneutral micellar structures.

It has been discussed in the introduction that the interfacial activation of *Hℓ*-lipase depends on the surface curvature. The closed, inactive, form is favoured when unilaminar vesicles with a diameter of 100 nm are present in the system; smaller unilaminar vesicles with a diameter of 40 nm induce

the active form of the enzyme molecule.[150,151] The micelles in this study have a core diameter of ≈ 28 nm and a hydrodynamic diameter of ≈ 46 nm (chapter 5), which means that the curvature of the micelles is similar to that of the 40 nm versicles. By studying the enzymatic activity as function of the composition, an effect of surface curvature may be probed. Polyelectrolyte complexes, consisting of a few polymer molecules, do not have a well-defined curvature but when micelles are formed, the curvature becomes more defined. The increase in activity from $F^- = 0.625 - 0.5$ may perhaps be explained by the increase in radius due to micelle formation. Another explanation may be that, unlike in the micelles, the substrate does not accumulate in the polyelectrolyte complexes, resulting in a lower enzymatic activity at compositions $F^- = 0.875 - 0.625$.

The highest activity is not found at $F^- = 0.5$ where one expects electroneutral polyelectrolyte complex micelles, but at a composition where the positively charged diblock copolymer $P2MVP_{41}$-PEO_{205} is in excess (at $F^- = 0.375$ and 0.25). At these compositions part of the lipase molecules may be released. The activity being higher at $F^- = 0.375$ and 0.25 could indicate that the diblock copolymer as a whole, or one of its blocks, influences the conformation of lipase molecules.

8.4.3. The effect of salt.

Previous scattering experiments indicated that upon increasing salt concentration lipase is released before the micelles disintegrate. Therefore, the activity of lipase is studied as function of the salt concentration. The data for the lipase-filled micelles cannot be readily interpreted in terms of this salt-induced release of lipase. We have seen that the activity of both lipase-filled micelles and lipase with normal micelles is enhanced compared to the activity of free lipase (see figure 2). This makes it hardly possible to discriminate between lipase in, and lipase with (but outside) polyelectrolyte complex micelles. In figure 4a and b the activity of free lipase (figure 4a) and the activity of "incorporated" lipase (figure 4b) is presented as function of the salt concentration.

The activity of lipase in both the free and the incorporated state is lower at higher NaCl concentration. For free lipase the decrease in activity is more pronounced than for incorporated lipase, especially for the higher NaCl concentrations (0.5 and 0.7 M NaCl). It is known that an increase in ionic strength favours the closed, inactive state of lipase.[154] At these salt concentrations it is expected that the polyelectrolyte complex micelles are disintegrated due to screening of the charges on the polymers (chapter 5). Yet, at 0.7 M NaCl, the activity of lipase in presence of polyelectrolytes is remarkably higher than the activity of free lipase. This suggests that the presence of the polymers has a positive effect on the enzymatic activity of lipase even though electrostatic interactions would be expected to

be screened.

In figure 5a, b, and c, the enzymatic activity of lipase at different compositions and salt concentrations is presented. It was chosen to plot the data as function of the diblock copolymer concentration instead of against F^-. Presenting the data in this way facilitates to demonstrate the effect of the polymer concentration on the enzymatic activity of lipase. Moreover, at 0.5 and 0.7 M NaCl, we have evidence that the polyelectrolyte complex micelles have fallen apart (chapter 5), *i.e.,* there are only free polymers in solution.

The change in activity for the highest concentration of lipase compared to the activity of free lipase, as function of salt, is practically zero for $C_{NaCl} = 0 - 0.5$ M (see figure 5a). At 0.7 M NaCl the lipase activity in presence of the polymers is enhanced with respect to the activity of free lipase. For the lower concentrations (see figure 5b and c) a more pronounced effect is observed: the normalised activity strongly increases as function of the ionic strength.

8.4.4. The effect of the presence of polymers.

In figure 3 it was observed that at $F^- = 1$ the activity of lipase is higher, compared to the activity of free lipase. At this composition only negatively charged macromolecules (and no polyelectrolyte complexes) are present in the solution. Negatively charged molecules are known to favour the active form of lipase.[151,155] The presence of the negatively charged PAA_{139} may thus explain the increased activity at this composition. The reason is that electrostatic interaction between negatively charged species and positively charged arginines and lysines in the lid region favours the lid opening of lipase.[156] The enzymatic activity of an NaCl-free solution containing 0.1 mg L^{-1} lipase at $F^- = 1$ is higher than the activity of lipase at $F^- = 1$ in the presence of salt. This may be explained by the screening of the charges on the negatively charged homopolymer and thereby reducing its positive effect on the conformation of lipase. Such electrostatically controlled lid opening may also explain why the activity at compositions $F^- = 0.875 - 0.625$ is lower; at these compositions PAA_{139} forms polyelectrolyte complexes with the positively charged homopolymer so that it becomes less available for an interaction with the positively charged amino acids around the lid of lipase.

The increase in activity of lipase in the presence of normal polyelectrolyte complex micelles (system III, experiment A), could be due to the presence of the PEO in the corona of the micelles. However, the data in figure 5a and c, where the normalised activity [A] was presented as function of the diblock copolymer concentration, did not show a very pronounced increase in activity upon increasing diblock copolymer concentration (and thus PEO concentration) at 0 M NaCl. Additional activity measurements of lipase in the presence of free PEO revealed that there was no influence of

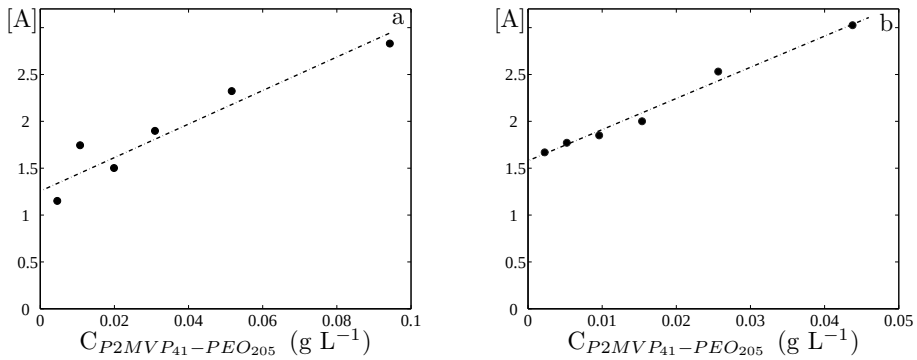

FIGURE 6. Normalised activity of lipase at 0.7 M NaCl in the presence as function of the $P2MVP_{41}$-PEO_{205} concentration for **a)** 0.4 mg L^{-1} and **b)** 0.2 mg L^{-1} lipase.

PEO on the lipase activity (data not shown). At higher salt concentrations ($0.1 - 0.7$ M NaCl), there is a clear difference in activity of free lipase and lipase in the presence of both PAA_{139} and $P2MVP_{41}$-PEO_{205} (figures 5b and c). At $0.1 - 0.5$ M NaCl it is expected that these polymers are present in either polyelectrolyte complexes or polyelectrolyte complex micelles (depending on the complex composition). At 0.7 M NaCl these complexes have disintegrated, due to electrostatic screening of the charges on the polymers. The equilibrium of polyelectrolytes in complexes (or complex micelles) *versus* free polyelectrolytes depends on the salt concentration. This suggests that the presence of free polymers in solution somehow influences the activity of lipase and may have an effect on the conformation of the enzyme.

To check whether the activity of lipase is indeed affected by the diblock copolymer alone, the activity measurements and in the presence of $P2MVP_{41}$-PEO_{205} have been performed at 0.7 M NaCl. This salt concentration was chosen because it is known that all the polyelectrolyte complexes have fallen apart, so that the homopolymer and diblock copolymer are free in solution. The experiment at 0.7 M NaCl was repeated with the same concentrations of diblock copolymer that were used in experiment B. The results for 0.2 and 0.4 mg L^{-1} lipase are shown in figure 6. From these figures it can be seen that the lipase activity increases as function of the $P2MVP_{41}$-PEO_{205} concentration.

Apparently, the presence of the diblock copolymer (despite of the high ionic strength) influences the activity of lipase. This effect is more pronounced at the lower concentrations of lipase. At 0.4 mg L^{-1} lipase, the activity of free lipase and lipase in, or in the presence of, polyelectrolytes/ polyelectrolyte complexes/ polyelectrolyte complex micelles (depending on the composition) is approximately the same for salt concentrations up to

0.5 M NaCl (see figure 5a). At these concentrations it may be that lipase-lipase bimolecular aggregates which consist of two open lipase molecules are present in the system.[157] At lower concentrations the equilibrium between bimolecular lipase aggregates and free lipase molecules may shift to free lipase molecules and these single lipase molecules have a closed conformation in a water-rich environment.[146,147]

In figure 7 some possible scenarios concerning the influence of the polymers on the enzymatic activity are sketched. When no polymers are present, lipase at low concentrations, will mostly be present in its closed inactive state (a). At higher concentrations bimolecular aggregates may be formed (a').[157] When the negatively charged homopolymer is present in the solution, it electrostatically interacts with the positively charges amino acids in the region around the active site. This may induce the open active form of lipase (b). Also the positively charged diblock copolymer may induce the active state of lipase (c). In the region around the lid, there are also negatively charged amino acids present. There is a clear effect of an increase in activity at higher salt concentration of diblock copolymer. Although there are no electrostatic attraction between the diblock copolymer and lipase at 0.7 M NaCl, somehow, the active form in promoted when $P2MVP_{41}$-PEO_{205} is present (c).

As a final point of this discussion we would like to address the effect of polyelectrolyte complex micelles on the activity of lipase. From the measurements in experiment A and B there are strong indications that lipase in the micelles is present in its active form. The interface between the core and corona may induce interfacial activation of $H\ell$-lipase. Self consistent field calculations revealed that the energetically most favourable place for a protein-like structure is in the core-corona interface (chapter 7). If the core-corona interface induces the open conformation of lipase, it may explain, together with our finding that the substrate has a tendency to accumulate in the micelles, why the activity of lipase is higher when it is present in the micelles (figure 7d) .

8.5. Conclusions

The active site of $H\ell$-lipase is covered by a lid. This lid can be opened by several factors. It was found that the activity of lipase incorporated in polyelectrolyte complex micelles was enhanced in comparison to free lipase. This indicates that the micelles induce the open, active state of lipase. Moreover, it was found that the substrate accumulates in the micelles and this may further influence the enzymatic activity.

$H\ell$-lipase in buffer is mainly present in its closed, inactive conformation. The equilibrium towards the open, active state can also be altered by the separate components of the micelles. It was found that in the presence

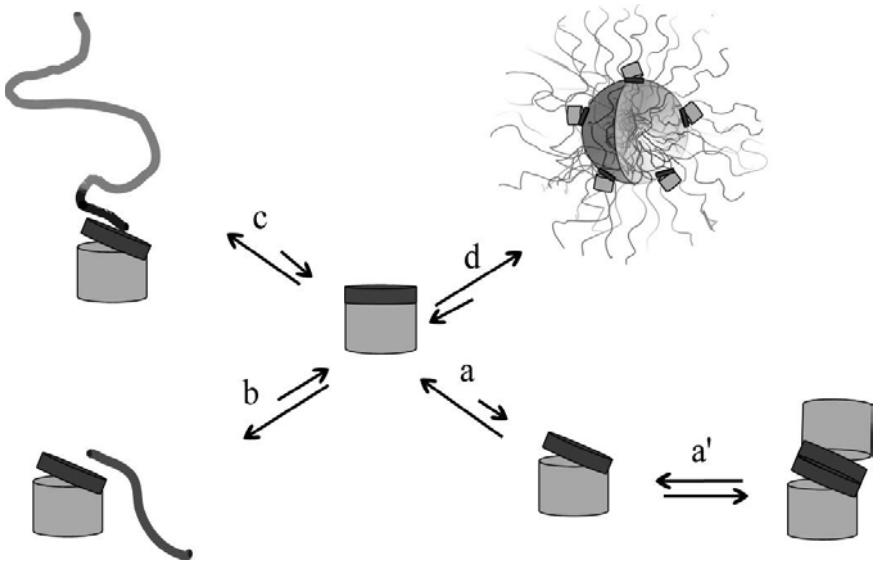

FIGURE 7. Simple sketch of different situations which influence the equilibrium between the closed and open conformation of $H\ell$-lipase. **a)** Equilibrium between closed and open form in solution. **a')** Equilibrium between single lipase and bimolecular aggregates. **b)** Equilibrium between lipase and lipase + PAA_{139}. **c)** Equilibrium between lipase and lipase + $P2MVP_{41}$-PEO_{205}. **d)** Equilibrium between free lipase and lipase in micelles.

of negatively charged homopolymer (PAA_{139}) the enzymatic activity was higher in comparison to the activity of free lipase, indicating that the open conformation was favoured. When salt was added, the activity of free lipase and that of lipase with PAA_{139} were approximately the same, suggesting that the electrostatic attraction between the negatively charged homopolymer and positively charged amino acids was responsible for the opening of the lid.

Changing the polyelectrolyte complex composition by addition of the positively charged diblock copolymer $P2MVP_{41}$-PEO_{205} also affects the enzymatic activity. At compositions where PAA_{139} is in excess, the enzymatic activity is lower, which may be caused by the formation of soluble complexes of the three components. The concentration of free PAA_{139} becomes lower and the favourable electrostatic attraction between lipase and PAA_{139} disappears. At compositions where lipase is present in the polyelectrolyte complex micelles the activity increases.

In all systems the enzymatic activity of lipase decreases upon increasing ionic strength. The decrease of the activity of free lipase is more pronounced than that of lipase incorporated in the micelles or in the presence of both polyelectrolytes. Also a clear effect of the lipase concentration is observed.

At lower lipase concentrations the decrease of the enzymatic activity is more dramatic. This suggests that the presence of polyelectrolytes and other lipase molecules favour the open conformation of lipase.

Acknowledgements
The authors would like to thank the Laboratory of Food Microbiology for using their Molecular Devices Spectramax plus plate-reader for our enzymatic activity measurements.

Chapter 9

General Discussion

9.1. Introduction

This thesis is entitled "Polyelectrolyte Complex Micelles as Wrapping for Enzymes." In this research several aspects of these polyelectrolyte complex micelles have been addressed. The conclusion of chapter 2 was that instead of two-components (enzymes and diblock copolymers), three-components (enzymes, diblock copolymers and homopolymers) are needed for stable micelles to be formed. Sofar, three-component polyelectrolyte complexes have hardly been investigated.

In chapter 3, an issue concerning three-component complexes has been addressed, namely that the three components can be mixed in three different ways. An important conclusion of chapter 3 is that different preparation protocols may result in different final structures. To understand this pathway dependency, insight in the interactions between the three components is required.

In three-component micelles there are three types of interactions: the interaction between the enzyme and the positively charged polymer, the interaction between the enzyme and the negatively charged polymer and the interaction between the negatively and positively charged polymers. The latter interaction is the most important one with respect to the final structure, and the relaxation behaviour of the polyelectrolyte complexes (see chapter 3).

For food and pharma applications one is allowed to only use polyelectrolytes that are food-grade or bio-compatible. If one would like to use these polyelectrolytes as wrapping for enzymes it may be useful to predict the relaxation behaviour, and *e.g.,* check whether sample history will be an issue. In this chapter we discuss whether it is possible to estimate the relaxation behaviour of polyelectrolyte complexes from physicochemical principles and how one can influence or control the relaxation behaviour.

In the following we will first discuss the above mentioned three types of interactions, starting with the interactions between the enzymes and the polyelectrolytes. Then we focus on polyelectrolyte complex formation. It has been tried to construct a scheme to predict polyelectrolyte complex relaxation behaviour from the available (mainly polyelectrolyte multilayer) literature. The discussion of this literature and the construction of the scheme form the second part of this General Discussion. At the end of this

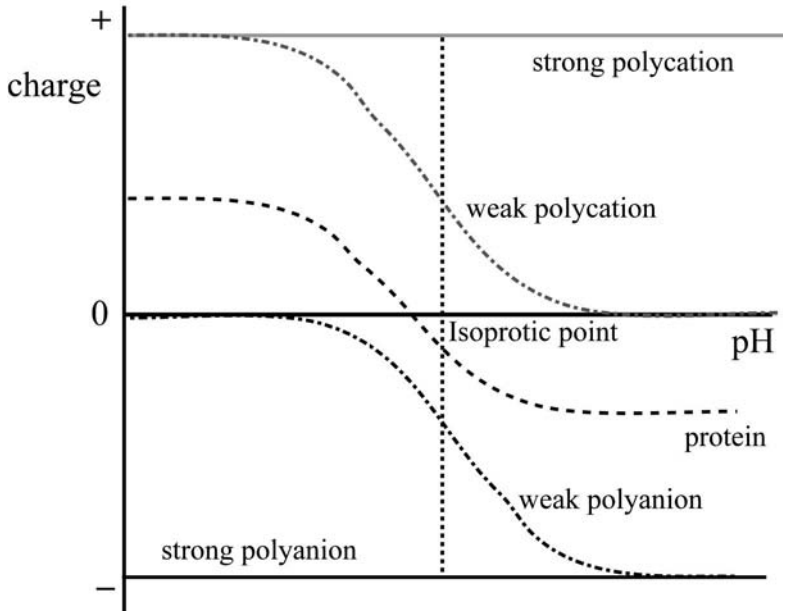

FIGURE 1. Charge of weak and strong polyelectrolytes, and proteins as function of the pH.

chapter we return to the applications of these protein-containing polyelectrolyte complexes, that were mentioned in chapter 1.

9.2. Polyelectrolyte complexes with proteins.

Proteins may be regarded as a special type of weakly charged polyelectrolytes, with a low charge density and a charge sign that is dependent on the pH. This makes the pH a very important tuning parameter for the interaction strength. In figure 1 the charge as function of the pH for strong and weak polyelectrolytes and proteins is depicted. In this paragraph we focus on the charge of the protein as function of the pH.

It can be seen that at low pH all protein molecules are positively charged; they become negatively charged at pH values above their iso-electric point (the point where the number of positive charges is equal to the number of negative charges). This means that in principle electrostatically driven complex formation occurs with negatively charged polyelectrolytes below the iso-electric point and with positively charged polyelectrolytes above their iso-electric point.

In the pH-interval around the iso-electric point it has been observed that protein molecules and *like*-charged polyelectrolytes are able to form complexes.[59,158–162] A huge debate can be found in literature about the reason why this occurs. There are basically two explanations. The first

explanation is related to "patchiness," the second to "charge regulation."

The "patchiness proponents" state that protein molecules have regions on their interface that contain an excess of charge that is opposite to the net charge of the protein molecule. The complexes that are formed are between these patches and the polyelectrolyte.[158–160,162].The "charge regulation supporters" say that either the protein molecule and/or the polyelectrolyte molecule can adjust its or their charge such that they become oppositely charged.[59] Most likely both mechanisms apply, but their relative contributions strongly depend on the protein molecule used.

By using both a negatively and a positively charged polyelectrolyte as wrapping for enzymes, it possible to obtain complexes in a very broad pH regime (see figure 1), and one circumvents the whole issue about patchiness and charge regulation. Incorporation of enzymes in complexes of two oppositely charged polyelectrolytes in this sense a very easy and promising method, the only thing one needs to be aware of is in what order the molecules are mixed.

9.3. The broader context of polyelectrolyte complex formation

In this thesis two types of micelles, consisting of different polyelectrolytes, are studied. In chapter 3 it has been discussed that sample history may be very important. For one of the micelles, mixing the components in different ways, yielded different structures. It is useful to predict *a priori*, whether for a certain oppositely charged polyelectrolyte couple, the way of mixing matters. Therefore, a relaxation behaviour prediction scheme has been constructed (figure 6). In the following, first, the relaxation behaviour of polyelectrolyte complexes in general will be discussed. Subsequently, we will discuss polyelectrolyte multilayer formation. The two different growth regimes found for multilayer formation, *i.e.,* linear and exponential, are a very good example of differences in relaxation behaviour of polyelectrolyte complexes. The predictive scheme for relaxation behaviour is mainly based on this literature and will be discussed at the end of this section.

9.3.1. Polyelectrolyte complex relaxation

Polyelectrolyte complex formation is fundamentally an ion exchange process where polymer-counterion pairs are replaced by polymer-polymer ion pairs (see chapter 1, figure 2).[61,163] This means that polyelectrolyte complex formation involves release of small ions and is therefore largely entropically driven. The reversibility of this ion exchange process influences the relaxation time of the polyelectrolyte complex formation. The relaxation time of polyelectrolyte complex formation consists of two steps. The first step is the

formation of initial aggregates of the oppositely charged macromolecules. The rate of this step is determined by the rate of collisions between the compounds. Thus, it is diffusion controlled and depends on the concentration of the polyelectrolytes and the temperature. The second step is the rearrangement of these initial aggregates towards their equilibrium state, via polyelectrolyte exchange reactions between the chains or with free polyelectrolytes in the solution.[72,73] This second step is not driven any more by the release of small ions, so that the remaining driving force is much smaller. The period of time which is needed for these polyelectrolyte exchange reactions depends on the molecular properties of the polyelectrolytes, *i.e.,* their hydrophobicity,[65,76] pH-dependency of their charge and charge density, and chain length. Solvent properties as pH, the salt concentration and the nature of the counterions furthermore determine the rate of rearrangement of the initial aggregates (we will come back to this later; see figure 4 for a sketch of this process).

In terms of relaxation time the following classification may be made: (a) (instantaneous) equilibrium, (b) observable relaxation behaviour and (c) quenched. The time of an experiment determines to which class a system belongs. Equilibrium will be found when the relaxation time (τ) is shorter than the experimental time scale (τ_{exp}). When τ and τ_{exp} are approximately the same relaxation is observable during the experiment. An example of a system that belongs to this class are the micelles consisting of PAA_{42}-$PAAm_{417}$ and $PDMAEMA_{150}$ (chapter 3). Systems belonging to the third class, *e.g.,* the micelles consisting of quaternised $P2MVP_{41}$-PEO_{205} and PAA_{139} (chapter 3), are kinetically quenched for a period of at least a week.

One can imagine that a certain distance between oppositely charged groups is required in order to make rearrangement within a complex possible. The association energy between a polyelectrolyte couple determines its stability and its ability to reorganise,[90] thus controlling the relaxation time of the system. This is reflected in the enthalpy of polyelectrolyte complex formation $\Delta_f H$.[86] This enthalpy arises from the change in potential energy associated with the inter-ionic distances:

$$\Delta_f H = \Delta_f \left(\sum_{ij} \frac{e^2}{4\pi\varepsilon r_{ij}}\right) \tag{44}$$

where r_{ij} is the distance between the charged groups of the oppositely charged polymers. Factors influencing this distance, *e.g.,* salt and pH, thus influence the enthalpy. When the (averaged) distance between the charged groups decreases during complexation, $\Delta_f H$ is negative. This situation will, *e.g.,* be found at low salt, where the ion pairs in the complex are tight.

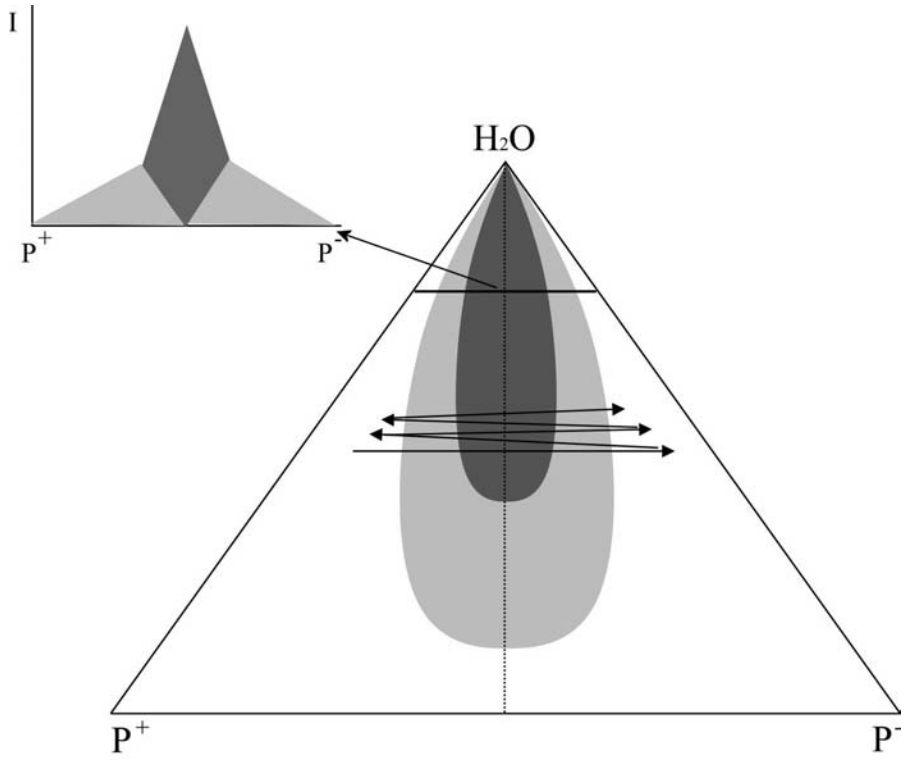

FIGURE 2. Pase diagram of polyelectrolyte complex formation and its relation to $I(F^-)$ plots. The dark grey areas indicate stoichiometric complexes; the light grey areas indicate soluble complexes. The arrows indicate the "walking through" the phase diagram when multilayers are prepared (slightly exaggerated).

9.3.2. Linear *versus* exponential multilayer growth

Polyelectrolyte multilayer formation is a specific kind of polyelectrolyte complex formation. Here, a charged surface is exposed, in an alternating fashion, to a solution containing polyanions and to a solution containing polycations (or *vice versa*). Because of this simple procedure, several aspects of polyelectrolyte complex formation could be studied. It is rather easy to extract information on the relaxation behaviour of polyelectrolyte complexes from the polyelectrolyte multilayer literature. But let us first consider what happens during multilayer formation.

In figure 2 the phase diagram of two oppositely charged polyelectrolytes (P^+ and P^-) is presented together with an $I(F^-)$ plot (see preceding chapters) . During a light scattering composition titration, one starts with a solution containing like charged macromolecules to which oppositely charged macromolecules are titrated. Hence, the system moves through the phase diagram once. When multilayers are prepared, one starts with a solution

containing one type of polyelectrolyte. Then the surface is rinsed to remove the excess material. Subsequently, it is exposed to a solution containing oppositely charged macromolecules. Then the surface is rinsed again, *etc.,*. This means that during the multilayer build-up the system passes through the phase diagram several times (see arrows in figure 2).

In chapter 3 it was found that the reversibility of the complex formation is system dependent. This has been studied by preforming titrations, starting from both ends of the composition axis ($F^- = 0$ and $F^- = 1$, respectively). Whether reversible micelle formation is observed depends on the relaxation rate of the polyelectrolyte complex and the experimental timescale. Considering the fact that one goes through the phase diagram upon polyelectrolyte multilayer build-up, one may realise that in order to have stable multilayers, the relaxation time of the system should at least be of the same order as the experimental timescale, because when the relaxation time is is shorter than the experimental time scale, the system (since it repeatedly leaves the 2-phase region) prefers forming polyelectrolyte complexes in solution rather than multilayers.[62,84,87,114]

For polyelectrolyte multilayers differences in the mode of relaxation behaviour show up as differences in growth, *i.e.,* linear and exponential growth. For linear growth the thickness increment is constant with each sequential polyelectrolyte addition. For exponential growth, all polyions of a certain kind in the layer can participate in complex formation (reservoir effect), so that the thickness increment (dh) becomes proportional to the thickness h ($dh \sim h$).[85]

In order to explain the difference between linearly growing films and exponentially growing films a mechanism based on the inward and outward diffusion of polyelectrolytes was proposed.[81,164] Because vertical diffusion of polyelectrolytes within a multilayer has been observed,[85] a model was proposed that is based on this in- and outward diffusion throughout the film of at least one of the polyelectrolytes.[82]

The growth behaviour may be controlled by mixing a weak and a strong polyelectrolyte of the same charge (to form one layer). In this case two growth regimes are found: first an exponential growth and then, from a certain point on, a linear growth. The characteristic feature of the transition is that the growth rate in the linear regime is smaller than in the exponential growth regime. This is explained by supposing that the number of chains diffusing out of the film during the cycle time becomes constant.[83]

Mixing of a like-charged weak and strong polyelectrolyte is not the only case of transition from one to another growth regime. Such a transition is also found for two weakly charged polyelectrolytes from a certain layer number on (it was found from $\approx$ layer 12 on).[165,166] This exponential-to-linear transition resulted in a new model, the three zone model, which is no longer based on the diffusion of polyelectrolytes in and out the film.[166]

The first zone (I) is the zone in closest contact to the substrate surface and the behaviour is mainly determined by the properties of the surface. Increasing the number of layers leads to a zone where the diffusion process occurs and the film grows exponentially, the third zone (III). From a certain layer on the film undergoes a restructuring of the bottom layers of the third zone. This restructuration zone is referred to as the second zone (II). This zone hinders the diffusion process and the third zone reaches a constant thickness.[166] In the linear growth regime the thickness increment of the polyanion/polycation deposition step is independent of the molecular weight of the polyelectrolytes. Diffusion of high molecular weight polymers is restricted to the upper part of the film, whereas low molecular weight polymers can diffuse into and through the entire film.[166] Hence, the extent to which film components are mobile is crucial for the relaxation process.

9.3.3. Complex formation between two strongly charged polyelectrolytes.

In the previous sections it has been discussed that differences in relaxation behaviour arise from distances between charges on the polyelectrolytes, and that the two different growth regimes in multilayer formation are manifestations of differences in relaxation behaviour in polyelectrolyte complex formation. In the following, the influence of the nature of the charge (*i.e.,* whether it is permanent (strong), or titratable (weak)), on the relaxation behaviour will be considered. We first discuss complex formation between two strongly charged polyelectrolytes, and then the complex formation between two weakly charged polyelectrolytes. Based on this, the mechanism of complex formation between a strong and weak polyelectrolyte is estimated. These aspects are used for the construction of figure 6. In literature several interesting aspects of complex formation between weak and strong polyelectrolytes are discussed, but we prefer not to include them in this general discussion.

The complex formation between two strongly charged polyelectrolytes was first studied by Fuoss *et al.,*. They found that colloidal precipitates were formed upon mixing two oppositely charged polyelectrolytes.[167] These complexes formed rapidly, and essentially stoichiometric compositions were obtained. Michaels[168] found that complexes formed of two strongly charged polyelectrolytes were nearly perfectly stoichiometric. The composition of the precipitate was independent of the relative proportions in which the polymers were mixed, and of the order of addition. The same phenomenon is found in multilayers consisting of two strongly charged polyelectrolytes. Within the multilayers stoichiometry is obeyed; only the surface bears a considerable excess charge.[87] Polymer charges balance each other without the requirement for additional counterions.[87]

For poly(styrene sulfonate)(PSS) and a cationic strongly charged random copolymer with varying charge density, the influence of charge density on the polyelectrolyte multilayer formation has been studied.[78–80] We have used the charge densities of these studies in our prediction scheme. Please note that in the scheme, these numbers are only used as an approximation; no hard conclusions should be drawn from them. These numbers may vary for different types of oppositely charged polyelectrolytes. In the scheme different scenarios are depicted by the letters a-j; sketches of these situations can be found in figure 3a-d, 4e-g and 5h-k.

It was discovered that a minimum charge density is required for the formation of polyelectrolyte multilayers. For strong polyelectrolytes four different regimes are distinguished. When the charge density is too low, $< 14\%$, no multilayers are formed (see figure 3a). Between 14% and 50% thin multilayers were formed. From 50% to 75% an increase in multilayer thickness is found upon increasing the charge density, with a maximum at 75%. Above 75% the thickness decreases slightly with increasing charge density.[61,77,78,80] It was also observed that below a charge density of 70% the adsorption stops after a certain number of addition cycles.[169]

An explanation for this behaviour is, that between 14% and 50% multilayer formation is most likely not primarily driven by electrostatic attraction, since salt does not influence its formation, its thickness and its surface roughness.[79,80] These multilayers form through other interactions *e.g.,* hydrogen bonding, hydrophobic interactions or Van der Waals interactions (see figure 3b).

When electrostatic interactions are responsible for the multilayer formation, first an increase in thickness is seen ($\approx$ 50 to 75%), because more polyelectrolytes can be adsorbed upon increasing charge density, but also since they are not fully charged the uncharged material also requires some space (see figure 3c). From a certain charge density on ($\approx$ 75%) the multilayer thickness decreases slightly, because the polymers adsorb in a more flat conformation. At a certain charge density, a polyelectrolyte starts to stretch, since the like charges on the polymer repel each other. This stretching is a function of the charge density and is responsible for the decrease in multilayer thickness,[61,77,78] because the distance (r_{ij}) between the oppositely charged polyelectrolytes decreases (see figure 3d).

The molecular characteristics of polyelectrolytes mainly determine the polymer mobility in the multilayer.[170] Decreasing the degree of charge enhances the mobility of the polyelectrolytes. Intrinsic backbone stiffness hinders interpenetration of polymers and the formation of complexes. Hydrophilicity promotes the swelling and softening in water, and enhances the mobility.[170] The lateral mobility of the polyelectrolytes within the multilayer is controlled by the strength between the polymers in neighboring layers and the swelling characteristics.[170] The interactions may be further

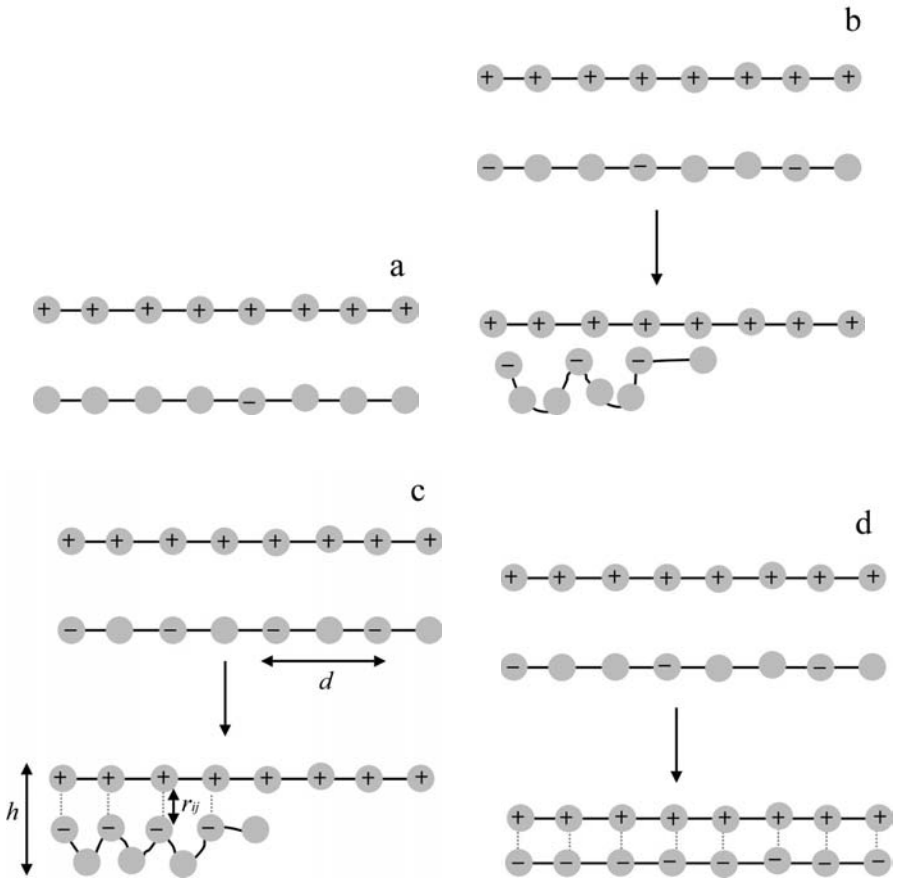

FIGURE 3. Polyelectrolyte complex formation between two oppositely charged, strong polyelectrolytes, with varying charge densities. The letters a-d represent the situations in figure 6. In the meaning of r_{ij}, d and h in figure **c)** is explained in the text in section 9.3.6.

tuned by the addition of salt to pre-made multilayers, increasing the salt concentration and the type of salt;[170] we will return to the influence of salt on polyelectrolyte complex formation later in this chapter.

It was also found that a certain molar mass is required for multilayer formation. Low molar mass ($5-10$ kDa) polyelectrolytes rather form polyelectrolyte complexes in solution.[74] This may indicate a higher mobility of the polyelectrolytes due to a different balance between the entropy gain of counterion release and the entropy gain of having free chains or soluble complexes in solution. In other words, the length of a polyelectrolyte chain is important since the number of charged groups on the chain determines how many counterions can be released.

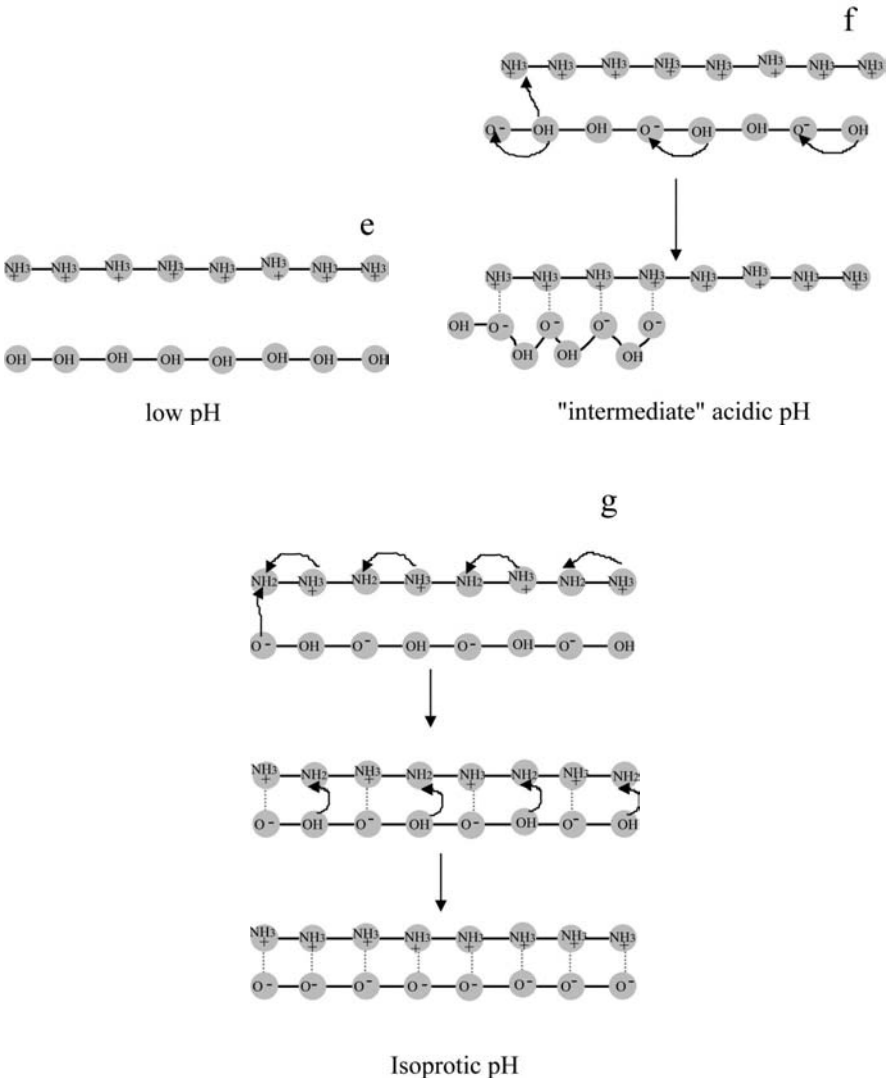

FIGURE 4. Polyelectrolyte complex formation between two oppositely charged, weak polyelectrolytes as function of the pH. Increasing the pH will affect the charge density on the polycation. The letters e-g represent the situations in figure 6.

9.3.4. Complex formation between two weakly charged polyelectrolytes.

The complexation behaviour of two weakly charged polyelectrolytes seems rather complicated, because the charge density of the two polyelectrolytes depends not only on the pH of the solution, but also on the interactions between the polyelectrolytes. Weakly charged polyelectrolytes are able to

take up or release protons, this equilibrium is changed in the presence of oppositely charged polyelectrolytes. The complexity arises when two weakly charged polyelectrolytes are used for the complex formation. This is because they can influence each other's dissociation behaviour.[67–71,171] The acid-base equilibrium shifts are layer-dependent and the dissociation levels off to a constant deviation from the dilute solution values,[67] resulting in shifts of the effective pK_{anion} and pK_{cation} of the polyelectrolytes. The degree of protonation can be measured by potentiometric titrations and by measured shifts in the pK's.

When the pH is fixed and the salt concentration is low, three different regimes are observed.[69] The first regime, where one of the polyelectrolytes is very weakly charged, is found at high and low pH (see figure 1). In this regime the degree of protonation, *i.e.,* the charge density, of one of the polyelectrolytes is very low and the degree of protonation for the other polyelectrolyte is maximal (see figure 4e). At low pH polyanions, *e.g.,* PAA, is known to form hydrogen bonds and adsorption of polyelectrolytes at low pH can be ascribed to hydrogen bond formation.[172]

The second regime is found at pH values where one polyelectrolyte is almost fully charged and one is becoming charged (see figure 1). This regime may directly be compared to the situation where one polyelectrolyte has a charge density between 14 and 50% described for the strongly charged polyelectrolytes; at low pH the anion has a low charge density and the cation is fully charged; at high pH the opposite is the case (see figure 4f). Under these conditions protons are able to jump between and along the molecules; thereby changing the net charge on the polyelectrolytes. In this regime thick multilayers are found.[69]

Thin multilayers are found in the third regime, when the pH equals the average pK ($pH = \frac{1}{2}(pK_{anion} + pK_{cation})$). This point is called the isoprotic point and is indicated by a line in figure 1. This pH regime is favourable for the multilayer formation[61,69,84] as well as polyelectrolyte complex micelle formation[173] (see figure 4g).

The salt concentration has no detectable influence on the acid-base equilibria of the multilayer films[67] or complexes in solution.[71] However, increasing the ionic strength in the intermediate pH-regime, may induce the formation of soluble complexes. In this case, overshoots, followed by desorption of the multilayer are observed,[84] indicating that the relaxation time is shorter than the experimental timescale. In this situation the grey areas, which represent soluble complexes and stoichiometric complexes in figure 2, become narrower with respect to the vertical symmetry plane.

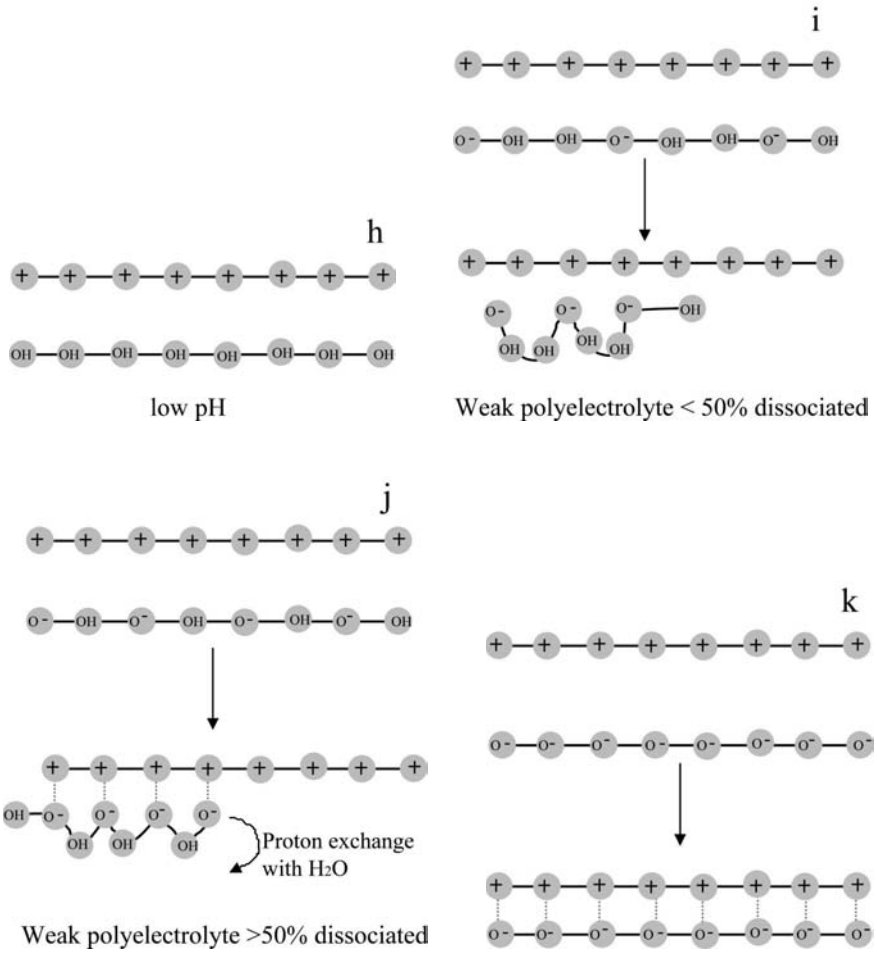

FIGURE 5. Polyelectrolyte complex formation between a weak polyanion and a strong polycation as function of the pH. For a weak polycation and a strong polyanion the same will happen when one starts at basic pH. The letters h-k represent the situations in figure 6.

9.3.5. Complex formation between a weakly and a strongly charged polyelectrolytes.

The complex formation between a strongly and weakly charged polyelectrolyte can, to a first approximation, be estimated from the complex formation between two strongly charged polyelectrolytes and two weakly charged polyelectrolytes, described above. By changing the pH, the charge density of the weak polyelectrolyte is altered. Therefore, the behaviour will resemble the four scenarios described in the section about strongly charged polyelectrolytes. However, since we are dealing with a weak polyelectrolyte,

proton exchange with water may also influence the dissociation equilibrium *i.e.,* charge adjustment of the weak polyelectrolyte may occur. The trend that is observed can therefore be explained, but the percentages used here are not better than rough estimates.

If we take a strong polycation and weak polyanion, at low pH, no complex formation occurs, since then the polyanion is uncharged (see figure 1). For a weak polycation and a strong polyanion, this regime is found at high pH. This situation is sketched in figure 5h.

Subsequently, at pH values where the weakly charged polyelectrolyte is for $< 50\%$ dissociated the situation can be compared to the second regime for weak polyelectrolytes and the situation where one strong polyelectrolyte has a charge density between 14 and 50% (see figure 5i).

At pH values where the weak polyelectrolyte is dissociated between $\approx 50 - 75\%$, similar behaviour will be observed as for the strongly charged polyelectrolytes of which one has a charge density between $50 - 75\%$ (see figure 5j). When the weak polyelectrolyte is fully dissociated the behaviour will be similar to the case where one is dealing with two fully charged strong polyelectrolytes or two weakly charged polyelectrolytes at the isoprotic point. This is sketched in figure 5k.

How to use the relaxation behaviour prediction scheme?
The different scenarios described above are put together in the relaxation behaviour prediction scheme (figure 6). By the use of this scheme, the relaxation behaviour of any oppositely charged polyelectrolyte couple can be estimated. As typical experimental timescale one should use ≈ 1 hour, the typical polyelectrolyte concentration is $1 - 5$ g L^{-1} and one of the polyelectrolytes should have ≈ 150 charges. As typical ionic strength one should have ≤ 10 mM in mind. It works rather simply. Begin at START and answer the questions. The scenarios of the letters a-j are sketched and can be found in figure 3a-d, 4e-g and 5h-k. Below, the points indicated in the scheme are discussed one by one:

(1.) When two hydrophobic oppositely charged polyelectrolytes are used, quenched structures will be obtained; typically $\tau \gg \tau_{exp}$ because of the strong hydrophobic interactions between the polyelectrolytes.
(2.) The charge density of the polyelectrolytes is too low, no complexes will form.
(3.) The charge density on the polyelectrolytes is very low. If complexes are formed it is very likely that the origin of the interactions between the polyelectrolytes is both electrostatic and non-electrostatic (hydrophobic, H-bond formation, Van der Waals interactions *etc.,*). The relaxation behaviour of this complex formation may strongly depend on the temperature.

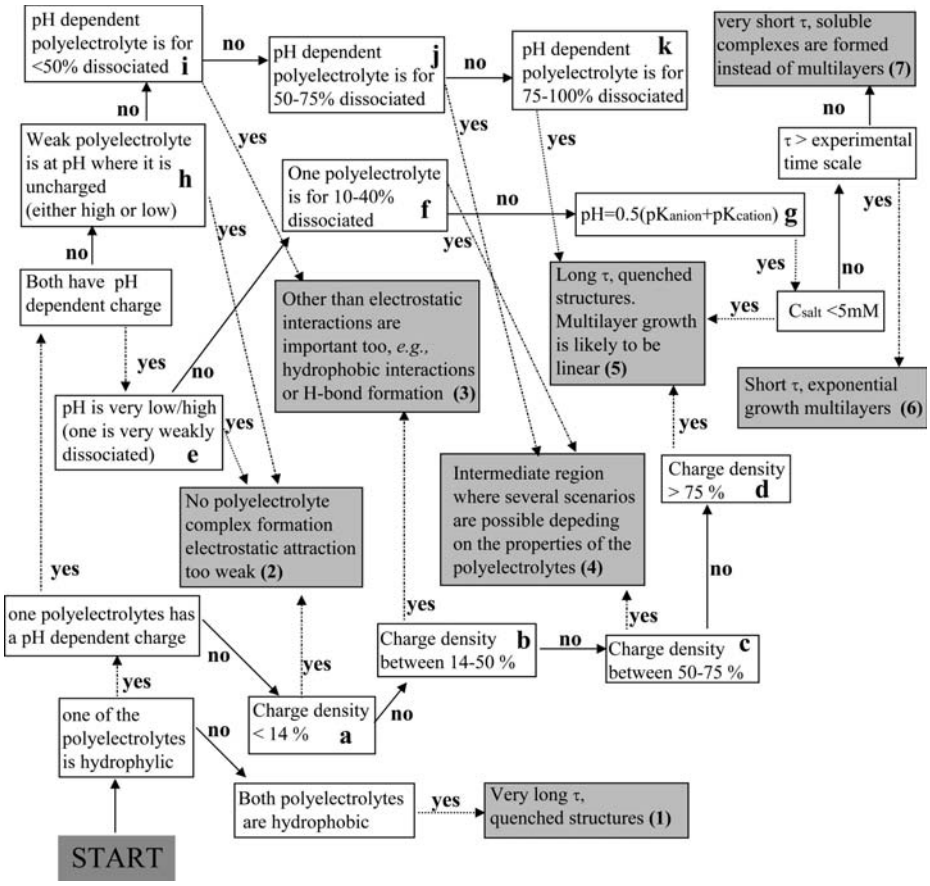

FIGURE 6. Relaxation behaviour prediction scheme. Begin at START and answer the questions, you will end up at a certain number. In the text you can find additional information about the relaxation time and ways to influence it. The situations a-j are sketched and can be found in figure 3, 4 and 5

(4.) The relaxation behaviour of the system is hard to predict. For weak polyelectrolytes, small changes in pH may influence the relaxation behaviour. The molecular properties of the polyelectrolytes are very important.

(5.) In this case $\tau > \tau_{exp}$; at low salt concentration the distance between the charges of the polyelectrolytes is very small and kinetically quenched structures may be obtained.

(6.) Using this polyelectrolyte couple one probably finds $\tau \approx \tau_{exp}$. For multilayers exponential growth will be observed, polyelectrolyte complexes will behave like the PAA_{42}-$PAAm_{417}$ micelles that are elaborately discussed in this thesis (see chapter 2, 3 and 6).

(7.) For these oppositely charged polyelectrolytes $\tau \leq \tau_{exp}$, which means that this under these conditions liquid-liquid phase separation (also known as complex coacervation) may occur.

9.3.6. Changing the relaxation behaviour.

For polyelectrolyte multilayers there are three distances that are important for the relaxation behaviour. These distances are sketched in figure 3c. The first distance is that between the polyelectrolytes; in figure 3c this distance is called r. The second distance is that between the charged groups of a polyelectrolyte, indicated by d in figure 3c. This distance is related to the charge density of the polyelectrolyte. Both distances, together with the amount of swelling of a polyelectrolyte,[88] determine the thickness of the multilayer h. By changing one of these distances the relaxation rate may be influenced. The charge density of the polyelectrolytes or the pH influences d. In the following it will be discussed how one can influence or control r_{ij}.

It has been said that the relaxation behaviour prediction scheme can be used for low ionic strength ($\leq$ 10 mM). By increasing the ionic strength the relaxation behaviour may be influenced. In chapter 5 and 6 the salt-induced disintegration of the two different polyelectrolyte complex micelles that were under consideration in this thesis, are discussed. It has been observed that the salt-induced disintegration of the kinetically quenched P2MVP$_{41}$-PEO$_{205}$ + PAA$_{139}$ micelles differed from the salt-induced disintegration of the PAA$_{42}$-PAAm$_{417}$ + PDMAEMA$_{150}$ micelles.

Let us first consider the complex formation at low ionic strength. It has been discussed that the relaxation rate of complex formation consists of two steps: first the formation of the polyelectrolyte complexes and second the rearrangement of these complexes to their equilibrium state. Here, we discuss the difference in relaxation rate between two weak and two strong polyelectrolytes during the second step. A sketch of the energy required to break one ion pair and form a new pair is given in figure 7. It should be realised that here only two polyelectrolyte molecules are drawn and that for a polyelectrolyte complex many polyelectrolytes may be involved.

In figure 7 it can be seen that for two strong polyelectrolytes (left hand side) the energy barrier of breaking one ion pair is high compared to the energy barrier of breaking an ion pair when two weakly charged polyelectrolytes are involved (right hand side). This difference is due to the ability of protons to jump from one polyelectrolyte to the other. This means that the energy for two weakly charged polyelectrolytes to rearrange is related to the difference in pK's of the charged groups. For strong polyelectrolytes it costs the full electrostatic energy.

In figure 8a and b the stability diagrams for polyelectrolyte complexes that belong to the "observable relaxation behaviour" and "quenched" class are presented as function of the ionic strength. The difference between these

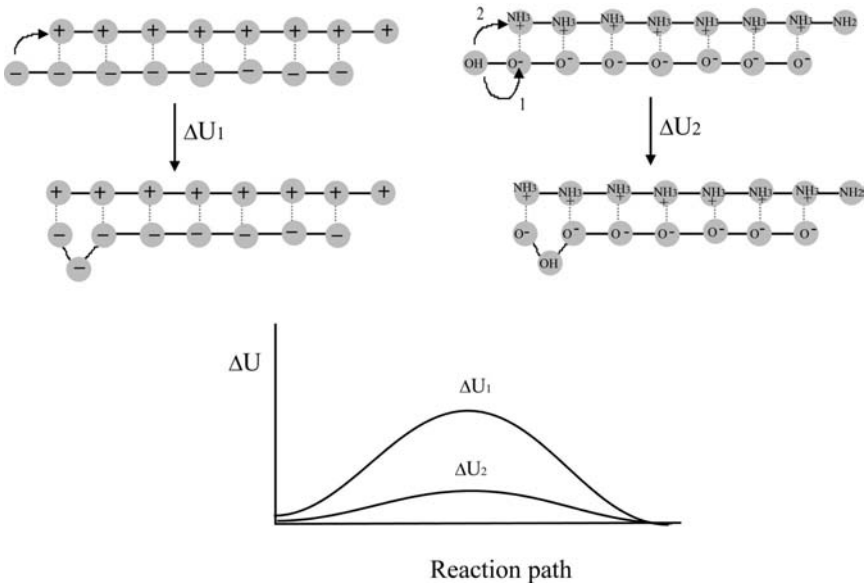

FIGURE 7. Difference in energy of breaking of polyelectrolyte exchange reactions of oppositely charged strong polyelectrolytes and two oppositely charged weak polyelectrolytes at low salt concentration.

two stability diagrams is the appearance of a liquid or a solid phase. In chapter 6 it has been discussed that for PAA_{42}-$PAAm_{417}$ + $PDMAEMA_{150}$ micelles at a certain ionic strength a critical point is found. When instead of a diblock copolymer a homopolymer of ≈ 42 PAA units would have been used, at this ionic strength a liquid phase may have formed. The $P2MVP_{41}$-PEO_{205} + PAA_{139} micelles were kinetically quenched throughout the whole salt titration. For this system no liquid phase was found.

Salt ions can help the polyelectrolyte complex to rearrange in a similar way as protons do (see figure 7). One can imagine that when the salt concentration is increased, it becomes "cheaper" to break an ion pair, because the salt ions can, like protons, also disrupt an ion pair. For multilayers, added salt screens the intramolecular electrostatic repulsion in this upper layer, allowing for more loop formation of the polyelectrolytes at the surface.[87] Therefore, an increase in distance (r_{ij}) between the oppositely charged groups of the polyelectrolytes is found. This results in an increase of the multilayer thickness at higher salt concentration. The internal structure of multilayers may be further disordered when the external ionic strength is increased. Due to the presence of additional external charge at the surface, *e.g.,* due to salt, both perpendicular interdiffusion (for adsorbing polymer) and parallel interdiffusion (for smoothing the surface) takes place at the multilayer surface.[115] Addition of salt to pre-made multilayers shows that

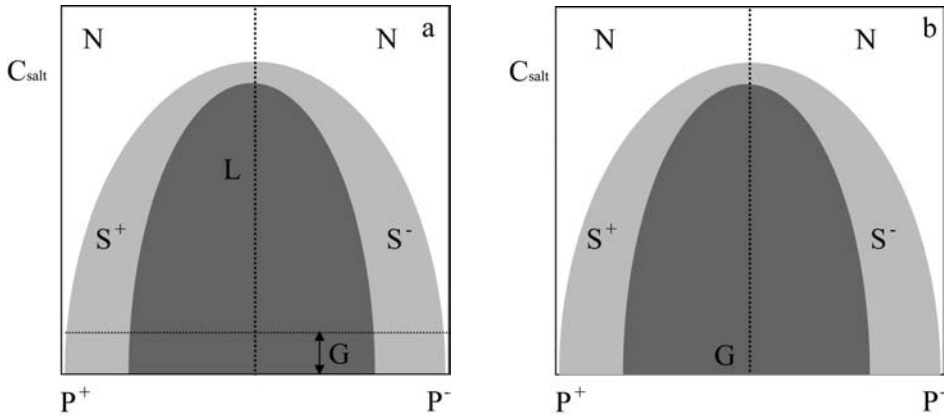

FIGURE 8. Schematic representation of the stability diagram of **a)** polyelectrolyte complexes of which $\tau \approx \tau_{exp}$ and **b)** polyelectrolyte complexes $\tau > \tau_{exp}$ as function of the ionic strength. On the horizontal axis is the composition of the mixture given. On the vertical axis is the salt concentration. The L region indicates a liquid state, and the G region the glassy (quenched) state; S indicates soluble polyelectrolyte complexes, and in the N region, no complexation occurs. Figure **a)** is a slight modification of the diagram proposed by Kovacevic *et al.,*[84]

the swelling is dependent on the composition of the multilayer. The surface roughness decreases after a brief annealing period in high salt.[174]

Increasing the ionic strength may change the relaxation behaviour of the polyelectrolyte complex formation. With this in mind, one can imagine that upon increasing salt concentration, for kinetically quenched polyelectrolyte complexes, situations 6 and 7 in the relaxation behaviour prediction scheme may be reached. The salt concentration at which this happens will depend on the molecular properties of the polyelectrolytes.

In principle, any oppositely charged polyelectrolyte couple is able to form a liquid phase. This may seem in conflict with our findings for the $P2MVP_{41}$-PEO_{205} + PAA_{139} micelles in chapter 5 and figure 8b. However, whether one finds this liquid phase depends on the concentration of the polyelectrolytes. The concentration of micelles studied in chapter 5 was 1 g L^{-1} (DLS). At this concentration we have found that micelles dissolve at a certain ionic strength. When the concentration of both polyelectrolytes is increased, the complexes dissolve at a higher ionic strength. It means that by increasing both the ionic strength and the polyelectrolyte concentration, one will enter the region of the phase diagram where this liquid phase is formed. However, one may have to use very high concentrations of polyelectrolytes.

The liquid-liquid phase separation of oppositely charged polyelectrolytes

is called complex coacervation and was first reported by Bungenberg de Jong.[19] It was found that in protein-polyelectrolyte systems of stoichiometric charge ratio, in addition to formation of solid-like complexes, separation in two liquid-like phases is reported. Since two oppositely charged polyelectrolytes form this *liquid* phase, the equilibration time of such a complex should be very short. Furthermore, this implies that the phase forms independent of the way of mixing these two polyelectrolytes. In literature several systems are called complex coacervates, but it is not entirely clear whether they really are liquid(-like).

Complex Coacervation and Biology

In the Permian era, which was 200 million years ago, the marine salt concentration was 0.15 M (nowadays it is 0.6 M). In this era the earth suffered from major climate changes. At the end of this era almost all life on earth vanished, which is known as the "greatest extinction of all." One idea why this happened is that the salt concentration decreased below 0.15 M. This happened after an ice age when salt was precipitated. Increasing the temperature resulted in the melting of the ice, and the salt concentration decreased.[175] The first organisms that suffer from such a decrease in salt concentration are the single cellular organisms living in water, *e.g.,* plankton. Because the salt concentration around them decreased, their inner salt concentration decreased too. As a result, the electrostatic interactions between the charged macromolecules in their cytosol became stronger, their mobility ceased, and they died. Because, *e.g.,* phytoplankton is autotrophic and produces oxygen, the amount of oxygen on earth decreased.[176] This resulted in oceanic anoxia. Since most animals need oxygen, and since for many organisms their food disappeared, animals died as well.

This indicates that a certain ionic strength is needed to optimise the interactions between the charged macromolecules in biological systems, such as in the cytosol. In chapter 2 and 5 it has been discussed that the electrostatic attraction between polyelectrolytes and proteins is screened beyond an ionic strength of $\approx$ 0.12 M NaCl (*ie.,* close to 0.15 M); similar observations are reported in literature.[36,177] In chapter 7 it has been discussed that an enzyme-like molecule, for thermodynamic reason, preferably resides in the core-corona interface; it is very unfavourable to go inside the core.

It is known that the macromolecule concentration inside the cellular fluid is of order 200 g L^{-1}.[178–180] This seems in conflict with the above mentioned observations. One may wonder how it is possible for so many different macromolecules to coexist in such a crowded environment.

Perhaps the key to the understanding of the extremely complicated, but very efficient, machinery in cells is the relaxation behaviour of the macromolecules which it contains. This would imply that the physiological conditions, *i.e.,* $C_{salt} \approx$ 0.15 M and pH= 7.4, allow for a certain mobility of

the macromolecules present in the cytosol. The pH of 7.4 is very interesting since this is, for most natural polyacids and polybases, about equal to $\frac{1}{2}(pK_{anion}+pK_{cation})$, which was found to be a condition, very sensitive, towards the addition of salt.[84] Hence, the relaxation behaviour of polyelectrolytes under these circumstances becomes highly sensitive to fluctuations. These conditions may be crucial for reaching such high concentrations of macromolecules, as are found in the cytosol.

In this context it is not entirely surprising that the enzymatic activity of lipase is improved when it is incorporated in the complexes or in the presence of polyelectrolytes (see chapter 8). In the literature several examples can be found where the activity of enzymes incorporated in polyelectrolyte complexes was studied. In all cases the enzymes remained active and in most cases the activity was influenced by the incorporation in polyelectrolyte complexes.[94,181–188]

In his book "The Origin of Life," Oparin launched the interesting idea that complex coacervates play an important role in the coming into existence of life.[189] In an aqueous environment colloids can interact to form a separate phase, which is dense in colloids. This dense phase may have been the pre-structure of a cell or cellular components such as mitochondria. Could Oparin be right?

9.4. Possible Applications and Future Research

In the General Introduction (chapter 1) possible applications of enzyme-containing micelles were mentioned. As conclusion of this General Discussion we would like to consider the applicability of these micelles and what research has to be done in order to make them applicable.

The first point which was addressed in chapter 1 was the protection of (an) enzyme(s) in a mixture of different enzymes. As a specific example "laundry detergents" were discussed. With the knowledge obtained during this PhD project, it is very likely that in laundry detergents the micelles will fall apart. Laundry detergents contain high concentrations of surfactants, which may be charged. There is a fair chance that these components disintegrate the micelles because they are rather fragile structures.

When the activity of lysozyme was studied using a *Micrococcus lysodeikitus* assay, (*Micrococcus lysodeikitus* are bacteria, their cell walls are lysed by the lysozyme. The turbidity of the solutions is measured as a function of time.) it was found that components of the bacteria destroyed the micelles. This indicates that the micelles are rather sensitive to the presence of other molecules.

The concept of protecting enzymes using micelles can therefore only be applied when the substrate or product does not destroy the micelles. Moreover, the salt concentration should not be too high.

The increase in the enzymatic activity of lipase incorporated in polyelectrolyte complex micelles and in the presence of polyelectrolytes (chapter 8), is very promising for biotechnology. However, because the micelles are rather fragile structures and above 0.12 M NaCl the enzymes are released, it may be better to use a macroscopic complex coacervate phase, instead of micelles.

The use of polyelectrolyte complex micelles as wrapping for functional ingredients may be possible. To make the micelles applicable for food-pharma applications, polymers should be used that are harmless to our body. Incorporation of enzymes or other functional proteins in bio-degradable polyelectrolyte complex micelles may have several applications. One could think of food-additives; the acid environment in the stomach will disintegrate the micelles and release the enzymes. Incorporation of therapeutic proteins in polyelectrolyte complex micelles may enhance the stability of a drug, allowing to prolong the life-time of a formulation. Whenever such a formulation comes in contact with body fluids, at physiological conditions ($C_{salt} \approx 0.15$ M), the enzymes will be released.

Several aspects of using protein-filled polyelectrolyte complex micelles as medicine still have to be investigated. For instance, the equilibrium between free and incorporated enzymes should be studied. It would be interesting to determine whether the structure of an enzyme changes upon incorporation. Also the thermal stability of enzymes in micelles is an interesting topic to study.

In this thesis it was also tried to better understand the dynamics and thermodynamics of polyelectrolyte complex formation. In chapter 3 the relaxation behaviour of polyelectrolyte complex micelles was considered. The Self-consistent field calculations (chapter 7) helped us to understand experimental results. However, there are still aspects that are not (yet) fully understood and it is definitely worthwhile to further study the theoretical aspects of polyelectrolyte complex formation.

A polyelectrolyte complex micelle consisting of three-components is a very simplified model of a molecular crowded system. The knowledge obtained by studying enzymes in these structures may give some insight in the biological behaviour of proteins in cells. From an evolutionary point of view it may be interesting to investigate whether complex coacervates played a relevant role in the coming into existence of life.

Because micelles are rather small in comparison to cells, it would be better to use systems with micrometer dimensions. By studying three (two oppositely charged polyelectrolytes and enzymes) component systems at high concentrations in microfluidic devices, knowledge will be obtained on the

behaviour of enzymes in a molecularly crowded environment (*e.g.,* ≈ 100 g L^{-1}). By using fluorescent substrates, fluorescence spectroscopy techniques, such as CSLM (confocal scanning laser microscopy) and FCS (fluorescence correlation spectroscopy), one should be able to study the enzymatic activity. The use of fluorescent proteins will give information about the dynamics of proteins in such crowded environments. As model of a cell, this system may be further improved by increasing the number of components. Here, one could also think of polysaccharides and other components, such as RNA, that are encountered in cells.

Summary

During this PhD-project the applicability of polyelectrolyte complex micelles as "wrapping" for enzymes has been explored. Several aspects of this interdisciplinary topic have been addressed. The approach was as follows: first, the preparation protocol of the micelles was studied (chapter 2-4), followed by the stability of the micelles against disintegration by salt (chapter 5 and 6). In chapter 7 self consistent field calculations were performed to obtain information about the free energy associated with the incorporation of enzymes in polyelectrolyte complex micelles. The information gathered in these seven chapters was very useful for the interpretation of the enzymatic activity of lipase incorporated in these micelles. The results of that study are reported in chapter 8. In this summary the main findings are discussed per chapter.

Micelle preparation
In chapter 2 the formation, structure and stability of lysozyme-filled polyelectrolyte complex micelles was considered. The scattering techniques were used to study these aspects. From the light scattering composition titrations it became clear that the formation of micelles consisting of lysozyme and PAA_{42}-$PAAm_{417}$ was irreversible. Dilution of the lysozyme solution with the like charged homopolymer $PDMAEMA_{150}$ resulted in intensity *versus* composition ($I(F^-)$) plots that became more and more symmetrical upon increasing the amount of homopolymer. The stability of the micelles towards salt was enhanced by increasing the amount of homopolymer.

Information about the structure of the micellar core was obtained from small angle neutron scattering. The shape of the micelles changed from ellipsoidal, for complexes consisting of only diblock copolymer and lysozyme, to spherical for micelles where the homopolymer was in excess. The findings of chapter 2 are schematically summarised in figure 1. A further advantage of the addition of homopolymer is that the amount of enzymes in the core can be controlled.

From chapter 2 it thus became clear that for stable protein-containing micelles three different macromolecules are needed: a diblock copolymer, a homopolymer and a protein molecule. This gives rise to the question that was addressed in chapter 3: when you have three components, does is matter how you mix them? In order to answer this question two different systems were studied: one, containing a positively charged protein (lysozyme), a positively charged homopolymer ($PDMAEMA_{150}$) and a negatively charged diblock copolymer (PAA_{42}-$PAAm_{417}$) and another one containing a negatively charged protein (α-lactalbumin), a negatively charged homopolymer (PAA_{139}) and a positively charged diblock copolymer ($P2MVP_{41}$-PEO_{205}).

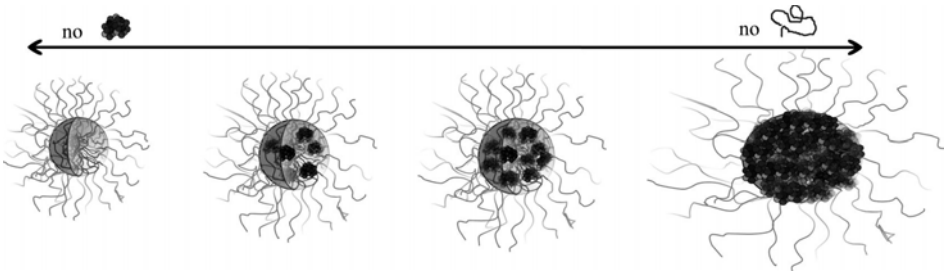

FIGURE 1. Overview of the micelles that can be made by changing the homopolymer to protein ratio.

Two types of light scattering measurements were used: light-scattering composition titrations, starting from both sides of the composition axis F^- (at $F^- = 0$ and $F^- = 1$). These measurements give information about the reversibility of the complex formation. It was found that the position of the maximum is direction-dependent for both systems. The shapes of the $I(F^-)$ plots of the lysozyme-containing system were similar for both directions, whereas the shapes of the respective $I(F^-)$ plots of the α-lactalbumin-containing system where remarkably different.

The second type of light scattering measurement was size relaxation at fixed composition ($F^- = 0.5$). For these measurements solutions containing the three different macromolecules were mixed in three different ways. The light scattering intensity and size of the micelles was followed in time. The light scattering intensity and hydrodynamic radius of the lysozyme-containing system became the same (independent of sample history) in 2 days. The results for the α-lactalbumin-containing system did not change in a period of a week.

The most important lesson of chapter 3 is that it does matter how one prepares the micelles. Therefore, one needs to stick to one preparation protocol in order to make a fair comparison between different measurements. This sample history is definitely something to keep in mind when one is interested in studying the enzymatic activity of enzymes incorporated in polyelectrolyte complex micelles.

The polyelectrolyte complex micelles studied in chapter 2 and 3 contained like-charged homopolymers and proteins (and oppositely charged diblock copolymer). In principle it should be possible to also prepare micelles containing oppositely charged homopolymers and proteins (diblock copolymer having the same sign as the protein). Chapter 4 is about micelles consisting of the latter combination of macromolecules. It was found that using an oppositely charged homopolymer and protein, a second maximum was observed in the $I(F^-)$ plot. A precipitate of the protein and homopolymer

may be responsible for this second maximum.

Chapter 2-4 yield three important observations that one has to take in to account when making protein-containing micelles:

1. The homopolymer should be in excess, in order to obtain stable micelles.
2. Always use a like charged homopolymer and protein, to avoid complex formation between the protein and homopolymer.
3. Be aware of sample history *i.e.,* different preparation protocols may result in different micellar objects.

Micelles and salt

All polyelectrolyte complexes disintegrate above a certain salt concentration. This makes studying these micelles as function of the salt concentration very relevant, *e.g.,* pharmaceutical applications require a certain stability towards changes in ionic strength. The salt-induced disintegration of the two different kinds of micelles (discussed in chapter 3), was studied using LS-titrations and Small Angle Neutron Scattering (chapter 5 and 6). In chapter 5 the negatively charged enzyme was lipase (other than in chapter 3 where α-lactalbumin was used), since that was the enzyme of our choice to perform enzymatic activity measurements (chapter 8).

The light scattering salt titrations and Small Angle Neutron Scattering data for the lipase containing micelles (polymers: PAA_{139} and $P2MVP_{41}$-PEO_{205}) revealed that with increasing salt concentration, the volume of the core decreased, but the hydrodynamic radius remained constant. A linear relationship was found between I_0 (SANS) and the volume of the core of the micelles. This relationship suggests that upon addition of salt molecules are leaving the micelles. Because the enzyme molecules have a lower charge density than the polymers these molecules are expected to be released first. When we assume that only lipase molecules are expelled from the core, at 0.12 M NaCl, all lipase molecules are released.

The salt-induced disintegration process for the lysozyme-filled micelles (consisting of $PDMAEMA_{150}$ and PAA_{42}-$PAAm_{417}$) is discussed in chapter 5. The disintegration process of these micelles was slightly different from that of the lipase containing micelles. For the lysozyme containing system both the hydrodynamic radius and the core radius decreased upon the addition of salt. It indicates that, unlike the lipase-containing micelles, the lysozyme-containing micelles are strongly affected by changes in the ionic strength. This can be explained by the difference in relaxation rate between the two micellar systems (discussed in chapter 3).

For both systems the aggregation numbers and water content could be

derived from the neutron scattering data. Results are summarised in table 1.

Table 1: Overview of the properties of the micelles

	lipase-filled micelles	lysozyme-filled micelles
R_h (nm)	23	29
R_{core} (nm)	13.8	10.9
# homopolymers	40	8
# diblock copolymers	140	29
# protein molecules	5	2
amount of water	83%	92%

SCF-calculations

The results obtained in chapter 2-6 do not answer the question whether it is thermodynamically favourable for a protein molecule to be in the micelles. This question is very difficult to answer experimentally; therefore Self Consistent Field (SCF) calculations were performed. The electrostatic attraction in these calculations was mimicked by short-range attractive interactions using a strongly negative Flory-Huggins parameter. The protocol used in these calculations was rather complicated, because our micelles are an asymmetric system as they consist of a homopolymer and diblock copolymer. Therefore an asymmetric Flory-Huggins interaction parameter set had to be used. As a consequence the stoichiometry, *i.e.,* the charge ratio of the homopolymer and diblock copolymer, p^c, of the core of the micelles was not unity. This ratio had to be fixed; we set $p^c = 0.85$. Other quantities that were fixed were the micellar volume fraction and the salt concentration. Here, values were chosen that mimicked the experimental conditions.

The free energy as function of the distance to the core has a minimum of $\approx -2\ k_BT$ in the core-corona interface, indicating that this position is favourable in comparison to either the bulk or the corona. A dramatic increase in free energy is observed when the lysozyme-like object is pushed into the center of the core, showing that the protein-like molecule strongly prefers the core-corona interface.

From calculations in the two-gradient coordinate system, where the free energy of the unbound state (protein is outside micelle) is compared to the bound state (protein is at the core-corona interface), it can be derived that the well depth of the protein/micelle potential of mean force decreases

strongly upon increasing the ionic strength, well before the micelles themselves vanish. Hence, the proteins loose affinity for the micelles with increasing ionic strength. This salt-induced release was also concluded from the experimental data in chapter 5.

Lipase activity

Chapter 8, deals with the enzymatic activity of Hℓ-lipase. The active site of this type of lipase is covered by a lid. Several external factors are known to induce lid opening or lid closure. This makes unraveling the influence of incorporation in polyelectrolyte complex micelles on the enzymatic activity quite a challenge.

In our approach first the enzymatic activity of lipase was compared to the activity of lipase incorporated in the micelles and it was found that the activity of lipase in the micelles is higher. The enzymatic activity in a system where extra polyelectrolyte complex micelles (with no lipase in the core) was added to a solution containing lipase-filled micelles, was lower than the activity of only lipase-filled micelles. This suggests that the substrate accumulates in the micelles.

As function of the complex composition (F^-), a clear trend in the enzymatic activity was observed. Starting at $F^- = 1$, having only lipase and PAA_{139} in the system, the enzymatic activity was higher compared to the activity of free lipase. From $F^- = 0.875-0.625$ the activity is lower than the activity of free lipase. At the preferred micellar composition ($F^- = 0.5$) and in systems where the diblock copolymer was in excess ($F^- = 0.375 - 0.25$) the activity was higher than the activity of free lipase. An explanation for this trend may be that the negativity charged diblock copolymer favours the open state of the enzyme. When diblock copolymer is added, PAA_{139} + $P2MVP_{41}$-PEO_{205} complexes are formed. The negatively charged diblock copolymer may then not have this favourable interaction with lipase, and as a consequence the activity decreases. From a certain composition on micelles are formed, it was already seen that in these micelles the enzymatic activity of lipase is higher. Combined with the results obtained for the activity as function of the composition, an explanation may be that the surface curvature of the micelles favours the active form. The soluble complexes found at compositions $F^- = 0.875 - 0.625$, may not have a well-defined curvature.

The enzymatic activity was further measured as function of the ionic strength. It was found that for both free lipase and lipase "incorporated" in micelles, the enzymatic activity decreased. Surprisingly, the decrease in activity of free lipase was more dramatic than the decrease in activity of lipase in the presence of polyelectrolytes. Additional measurements at 0.7

M NaCl and P2MVP$_{41}$-PEO$_{205}$ revealed that lipase in the presence the diblock copolymer is more active.

Samenvatting van: Polyelectrolyt Complex Micellen als verpakkingsmateriaal voor Enzymen

Enzymen zijn moleculen die specifieke chemische reacties katalyseren. De moleculen waar ze mee reageren heten *substraat*. Soms is het wenselijk om enzymen te beschermen. Deze moleculen zijn namelijk nogal gevoelig voor veranderingen in hun omgeving, zoals temperatuursschommelingen en veranderingen in de zoutconcentratie of de pH. Een manier om enzymen te beschermen is door ze in te pakken. In dit onderzoek is bekeken of polyelectrolyt complex micellen een geschikt verpakkingsmateriaal voor enzymen zijn.

Polyelectrolyt complex micellen bestaan uit tenminste 2 soorten moleculen die een tegengestelde lading hebben. Deze moleculen noemen we polyelectrolyten. Bovendien is het belangrijk dat aan tenminste een van die moleculen een stuk zit wat ongeladen is. Deze moleculen, met een ongeladen en een geladen blok, worden diblok copolymeren genoemd. Wanneer oplossingen van deze moleculen met elkaar worden gemengd, dan vormen de tegengesteld geladen gedeelten van de moleculen een polyelectrolyt complex, want plus en min trekken elkaar aan en vormen de *kern* van het deeltje. In zo'n complex zitten x deeltjes met een positieve lading en y deeltjes met een negatieve lading, omdat het aantal positieve ladingen gelijk moet zijn aan het aantal negatieve ladingen. Het ongeladen gedeelte van de diblok copolymeren willen niet in de kern zitten en steken naar buiten. Zo ontstaan vanzelf een soort bolletjes met haren aan de buitenkant, al deze haren samen vormen de *corona* van het deeltje. De nu gevormde deeltjes worden polyelectrolyt complex micellen genoemd (zie figuur 1).

Deze polyelectrolyt complex micellen zijn maar heel klein, ze hebben namelijk een straal van ongeveer 25 nanometer (0.000025 millimeter). Omdat ze zo klein zijn moet je speciale meettechnieken gebruiken om ze te kunnen detecteren. In dit proefschrift hebben we vooral gebruik gemaakt van lichtverstrooiing en neutronenverstrooiing. Meer informatie over deze technieken is te vinden in hoofdstuk 1.

Het inpakken van enzymen

Waarom denken we dat deze micellen een geschikt inpakmateriaal zouden kunnen zijn? Enzymen hebben vaak ook een lading. Dat betekent dat ze in principe spontaan ingepakt kunnen worden wanneer ze met een tegengesteld geladen diblok copolymeer worden gemengd. In hoofdstuk 2 hebben we dat (ook) gedaan, maar we waren niet helemaal tevreden met de deeltjes die gevormd werden. Naar schatting zitten er namelijk zo'n 1000 enzymen in

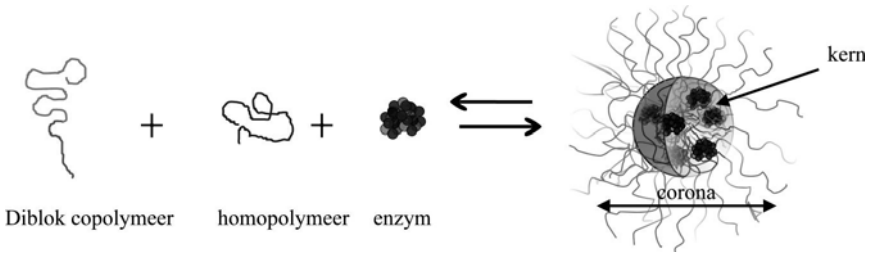

FIGUUR 1. De verschillende componenten van een polyelectrolyt complex micel.

een deeltje. Wanneer we willen kijken of de enzymen substraat kunnen omzetten, kan dat lastig worden omdat de enzymen midden in de micel moeilijk te bereiken zijn.

We hebben dit probleem opgelost door extra geladen polymeren met dezelfde lading als het enzym toe te voegen. Deze polymeren noemen we homopolymeren. Hierdoor wordt de hoeveelheid enzym per micel kleiner. Een belangrijk resultaat van deze studie is dat de beste deeltjes worden gevormd wanneer je verhoudingsgewijs meer homopolymeren dan enzymen hebt.

De conclusie van hoofdstuk 2 is dat voor optimale deeltjes er drie soorten moleculen nodig zijn: diblok copolymeren, homopolymeren en enzymen. In hoofdstuk 3 hebben we onderzocht of het uitmaakt in welke volgorde de polymeren en de enzymen gemengd worden. Het kan namelijk zijn dat de optimale inpakmethode afhangt van de manier waarop de moleculen gemengd worden. Dit bleek voor sommige combinaties van diblok copolymeren en homopolymeren inderdaad het geval te zijn.

Tot nu toe is besproken dat om optimale deeltjes te krijgen er drie verschillende moleculen nodig zijn: een homopolymeer en enzym met dezelfde lading en een tegengesteld geladen diblok copolymer. Het is misschien ook mogelijk om deeltjes te maken die bestaan uit een diblok copolymeer en een enzym met dezelfde lading en een homopolymeer met een tegengestelde lading. Dit is onderzocht, en beschreven in hoofdstuk 4.

Het blijkt dat deze tweede manier van inpakken niet zo goed gaat. Wat er namelijk kan gebeuren is dat de homopolymeer en het enzym, die in dit geval een tegengestelde lading hebben, ook complexen kunnen vormen. Die complexen zijn veel groter dan de micellen en die zakken naar de bodem.

Er zijn dus een aantal dingen waar je rekening mee moet houden als je enzymen wilt inpakken in polyelectrolyt complex micellen:

1. Gebruik een overmaat van homopolymeer
2. Zorg ervoor dat de homopolymeer en het enzym hetzelfde ladingsteken hebben

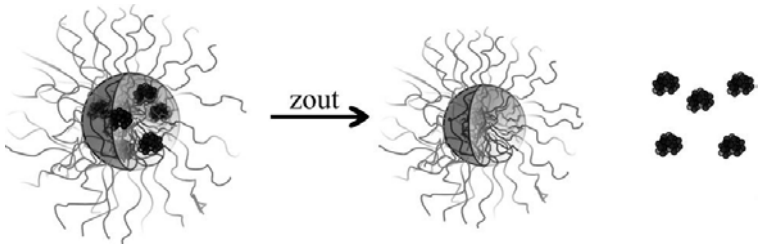

FIGUUR 2. Het uitpakken van enzymen.

3. Hou er rekening mee dat de volgorde waarop je de drie soorten moleculen mengt van invloed kan zijn op het eindresultaat

Het uitpakken van enzymen

Als je enzymen kunt inpakken, wil je ook weten of je ze weer uit kunt pakken. Nou, is het zo dat de plakkracht tussen tegengesteld geladen polyelectrolyten afhangt van de zoutconcentratie. Als de zoutconcentratie verhoogd wordt, wordt de plakkracht minder sterk, totdat boven een bepaalde zoutconcentratie er zelfs geen polyelectrolyt complexen meer gevormd kunnen worden. Dit betekent dus, dat door de zoutconcentratie te verhogen, de micellen uit elkaar vallen en de enzymen uitgepakt worden.

Dit is onderzocht en de resultaten van deze studies zijn te vinden in hoofdstuk 5 en 6. De technieken die gebruikt zijn voor dit onderzoek zijn licht- en neutronenverstrooiing. We hebben gevonden dat de manier waarop de enzymen uitgepakt worden vrij bijzonder is. De enzymen worden namelijk eerst uit de micel losgelaten, bij een zoutconcentratie van ongeveer 0.12 M NaCl. Bij een zoutconcentratie van ongeveer 0.5 M NaCl vallen de micellen uitelkaar. Dit uitpakproces is schematisch weergegeven in figuur 2.

TABEL 1. OVERZICHT VAN DE MICELEIGENSCHAPPEN

	micellen met lipase	micellen met lysozyme
$R_{kern+corona}$ (nm)	23	29
R_{kern} (nm)	13.8	10.9
# homopolymeren	40	8
# diblok copolymeren	140	29
# enzyme moleculen	5	2
hoeveelheid water	83%	92%

Een leuke bijkomstigheid van de neutronenverstrooiingsexperimenten is dat je ook kan bepalen hoeveel moleculen er in de micellen zitten. Dit hebben we gedaan voor micellen die lysozyme bevatten en micellen die lipase bevatten. De gegevens voor deze twee verschillende deeltjes zijn samengevat in tabel 1.

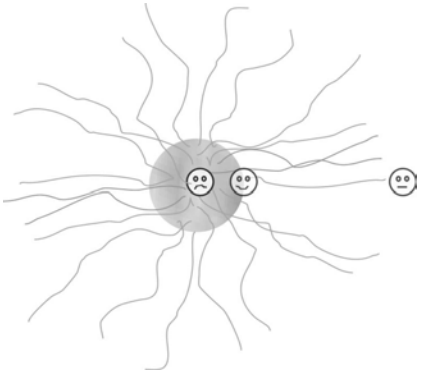

FIGUUR 3. Waar het enzym zich het gelukkigst voelt.

Waar zit het enzym het liefst?
In hoofdstuk 7 is onderzocht waar het enzym zich in de micel bevindt. Omdat het vrijwel onmogelijk is om dit met experimenten in het lab uit te zoeken, hebben we gebruik gemaakt van computerberekeningen. Voor deze berekeningen hebben we eerst, in het rekenprogramma een micel laten vormen door de homopolymeren en diblok copolymeren te definiëren. Daarna hebben we een lysozyme molecuul gedefinieerd. Vervolgens hebben we een halve micel genomen en daar 1 lysozyme molecuul ingeduwd en hebben we gemeten hoeveel energie het kost om een lysozyme molecuul in de halve micel te duwen. Deze berekeningen hebben duidelijk gemaakt dat het eiwit molecuul het niet leuk vindt om de kern van de micel in te gaan; hij zit veel liever in het grensvlak tussen de kern en de corona (zie figuur 3).

Dit resultaat hadden we eigenlijk niet verwacht, maar het verklaart wel dat je een bepaalde hoeveelheid homopolymeer nodig hebt om stabiele deeltjes te krijgen. Als je namelijk te weinig homopolymeer gebruikt is er niet genoeg grensvlak om alle enzymen in kwijt te kunnen. Als het enzym zich in het grensvlak tussen de kern en de corona bevindt, is het ook logisch dat bij het toevoegen van zout aan deze deeltjes het enzym het eerst uit de micel gaat.

Lipase activiteit
Het laatste hoofstuk gaat over de enzymactiviteit van lipase. Deze activiteit is bestudeerd in en met micellen, in polyelectrolyt complexen en met de afzonderlijke componenten van de micellen. De lipase die voor deze metingen gebruikt is lijkt een beetje op een pedaalemmer. Als de klep openstaat dan kan de lipase een substraat omzetten, met de klep open is lipase dus actief.

Er zijn verschillende manieren waarop de klep van de pedaalemmer geopend kan worden. Wanneer lipase alleen in oplossing is en de concentratie laag is, staat z'n klep over het algemeen dicht. Wanneer de lipase concentratie hoog is, kunnen twee lipase moleculen zo aan elkaar plakken

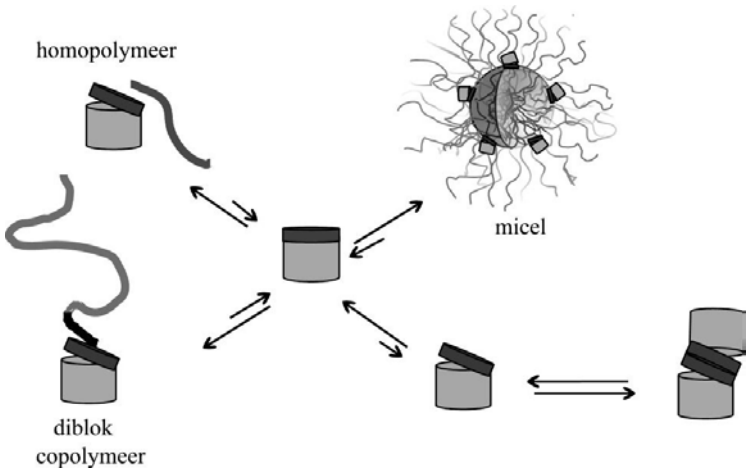

FIGUUR 4. Hoe de verschillende componenten en de micellen de klep van lipase kunnen openen.

dat de klep open gaat staan.

Wij hebben ontdekt dat in de polyelectrolyt complex micellen de klep openstaat. Maar ook dat de klep geopend kan worden in de aanwezigheid van de afzonderlijke polyelectrolyten. De negatief geladen polyelectrolyt opent de klep bij een lage zoutconcentratie; de positief geladen polyelectrolyt opent de klep juist bij een hoge zoutconcentratie. Het openen van de klep in de verschillende situaties is weergegeven in figuur 4.

Bibliography

1. Qasba, P. K. and Kumar, S. *Critical Reviews in Biochemistry and Molecular Biology* **32**(4), 255–306 (1997).
2. Whitcomb, D. C. and Lowe, M. E. *Digestive Diseases and Sciences* **52**(1), 1–17 (2007).
3. Pieroni, G., Gargouri, Y., Sarda, L., and Verger, R. *Advances in Colloid and Interface Science* **32**(4), 341–378 (1990).
4. Zoungrana, T. and Norde, W. *Colloids and Surfaces B-Biointerfaces* **9**(3-4), 157–167 (1997).
5. Zhao, X. S., Bao, X. Y., Guo, W. P., and Lee, F. Y. *Materials Today* **9**(3), 32–39 (2006).
6. Deere, J., Magner, E., Wall, J. G., and Hodnett, B. K. *Journal of Physical Chemistry B* **106**(29), 7340–7347 (2002).
7. Vinu, A., Murugesan, V., and Hartmann, M. *Journal of Physical Chemistry B* **108**(22), 7323–7330 (2004).
8. Vinu, A., Murugesan, V., Tangermann, O., and Hartmann, M. *Chemistry of Materials* **16**(16), 3056–3065 (2004).
9. Chong, A. S. M. and Zhao, X. S. *Catalysis Today* **93-95**, 293–299 (2004).
10. Deere, J., Magner, E., Wall, J. G., and Hodnett, B. K. *Chemical Communications* (5), 465–466 (2001).
11. Ballauff, M. *Progress in Polymer Science* **32**, 1135–1151 (2007).
12. Wittemann, A. and Ballauff, M. *Analytical Chemistry* **76**(10), 2813–2819 (2004).
13. Haupt, B., Neumann, T., Wittemann, A., and Ballauff, M. *Biomacromolecules* **6**(2), 948–955 (2005).
14. Wittemann, A., Haupt, B., and Ballauff, M. *Zeitschrift Fur Physikalische Chemie-International Journal of Research in Physical Chemistry and Chemical Physics* **221**(1), 113–126 (2007).
15. Gummel, J., Boue, F., Deme, B., and Cousin, F. *Journal of Physical Chemistry B* **110**(49), 24837–24846 (2006).
16. Gummel, J., Cousin, F., and Boue, F. *Journal of the American Chemical Society* **129**, 5806–5807 (2007).
17. Gummel, J., Boue, F., Clemens, D., and Cousin, F. *Soft Matter* **4**, 16–53–1664 (2008).
18. Cousin, F., Gummel, J., Ung, D., and Boue, F. *Langmuir* **21**(21), 9675–9688 (2005).

19. Bungenberg de Jong, H. *Complex colloid systems*, volume 2 of *Colloid Science*. (1949).
20. de Kruif, C. G., Weinbreck, F., and de Vries, R. *Current Opinion In Colloid & Interface Science* **9**(5), 340–349 (2004).
21. Weinbreck, F., Tromp, R. H., and de Kruif, C. G. *Biomacromolecules* **5**(4), 1437–1445 (2004).
22. Schmitt, C., Sanchez, C., Desobry-Banon, S., and Hardy, J. *Critical Reviews In Food Science And Nutrition* **38**(8), 689–753 (1998).
23. Harada, A. and Kataoka, K. *Macromolecules* **28**(15), 5294–5299 (1995).
24. Kabanov, A. V., Bronich, T. K., Kabanov, V. A., Yu, K., and Eisenberg, A. *Macromolecules* **29**(21), 6797–6802 (1996).
25. Cohen Stuart, M. A., Besseling, N. A. M., and Fokkink, R. G. *Langmuir* **14**(24), 6846–6849 (1998).
26. Harada, A. and Kataoka, K. *Macromolecules* **31**(2), 288–294 (1998).
27. Harada, A. and Kataoka, K. *Langmuir* **15**(12), 4208–4212 (1999).
28. Goldberg, M., Langer, R., and Jia, X. Q. *Journal of Biomaterials Science-Polymer Edition* **18**(3), 241–268 (2007).
29. Gibbs, B. F., Kermasha, S., Alli, I., and Mulligan, C. N. *International Journal Of Food Sciences And Nutrition* **50**(3), 213–224 (1999).
30. Kataoka, K., Harada, A., and Nagasaki, Y. *Advanced Drug Delivery Reviews* **47**(1), 113–131 (2001).
31. van der Burgh, S., de Keizer, A., and Cohen Stuart, M. A. *Langmuir* **20**(4), 1073–1084 (2004).
32. Hofs, B., Voets, I. K., Keizer, A. d., and Cohen Stuart, M. A. *Physical Chemistry Chemical Physics* **8**, 4242–4251 (2006).
33. Voets, I. K., de Keizer, A., de Waard, P., Frederik, P. M., Bomans, P. H. H., Schmalz, H., Walther, A., King, S. M., Leermakers, F. A. M., and Cohen Stuart, M. A. *Angewandte Chemie-International Edition* **45**(40), 6673–6676 (2006).
34. Voets, I. K., de Keizer, A., Cohen Stuart, M. A., and de Waard, P. *Macromolecules* **39**(17), 5952–5955 (2006).
35. van der Burgh, S., Fokkink, R., de Keizer, A., and Cohen Stuart, M. A. *Colloids And Surfaces A-Physicochemical And Engineering Aspects* **242**(1-3), 167–174 (2004).
36. Harada, A. and Kataoka, K. *Journal Of The American Chemical Society* **121**(39), 9241–9242 (1999).
37. Harada, A. and Kataoka, K. *Journal Of Controlled Release* **72**(1-3), 85–91 (2001).
38. Harada, A. and Kataoka, K. *Journal Of The American Chemical Society* **125**(50), 15306–15307 (2003).
39. Yuan, X. F., Harada, A., Yamasaki, Y., and Kataoka, K. *Langmuir* **21**(7), 2668–2674 (2005).

40. Yuan, X. F., Yamasaki, Y., Harada, A., and Kataoka, K. *Polymer* **46**(18), 7749–7758 (2005).
41. Wakebayashi, D., Nishiyama, N., Itaka, K., Miyata, K., Yamasaki, Y., Harada, A., Koyama, H., Nagasaki, Y., and Kataoka, K. *Biomacromolecules* **5**(6), 2128–2136 (2004).
42. Wakebayashi, D., Nishiyama, N., Yamasaki, Y., Itaka, K., Kanayama, N., Harada, A., Nagasaki, Y., and Kataoka, K. *Journal Of Controlled Release* **95**(3), 653–664 (2004).
43. Jaturanpinyo, M., Harada, A., Yuan, X. F., and Kataoka, K. *Bioconjugate Chemistry* **15**(2), 344–348 (2004).
44. Berret, J. F. *Journal Of Chemical Physics* **123**(16) (2005).
45. Berret, J. F., Schonbeck, N., Gazeau, F., El Kharrat, D., Sandre, O., Vacher, A., and Airiau, M. *Journal Of The American Chemical Society* **128**(5), 1755–1761 (2006).
46. Berret, J. F., Sehgal, A., Morvan, M., Sandre, O., Vacher, A., and Airiau, M. *Journal Of Colloid And Interface Science* **303**(1), 315–318 (2006).
47. Berret, J. F., Yokota, K., and Morvan, M. *Soft Materials* **2**(2-3), 71–84 (2004).
48. Taton, D., Wilczewska, A., and Destarac, M. *Macromolecular Rapid communication* **22**, 1497–1503 (2001).
49. Chalikian, T. V., Totrov, M., Abagyan, R., and Breslauer, K. J. *Journal of Molecular Biology* **260**(4), 588–603 (1996).
50. van der Veen, M., Norde, W., and Cohen Stuart, M. *Colloids And Surfaces B-Biointerfaces* **35**(1), 33–40 (2004).
51. Salomaa, P., Schaleger, L. L., and Long, F. A. *Journal Of The American Chemical Society* **86**(1), 1– (1964).
52. Glatter, O. *Journal Of Applied Crystallography* **10**(OCT1), 415–421 (1977).
53. Glatter, O. *Journal Of Applied Crystallography* **12**(APR), 166–175 (1979).
54. Glatter, O. and Kratky, O. *Small Angle X-ray Scattering.* Academic Press, (1982).
55. Biesheuvel, P. M. and Cohen Stuart, M. A. *Langmuir* **20**(7), 2785–2791 (2004).
56. Ullner, M. and Jonsson, B. *Macromolecules* **29**(20), 6645–6655 (1996).
57. Biesheuvel, P. M., Lindhoud, S., de Vries, R., and Cohen Stuart, M. A. *Langmuir* **22**(3), 1291–1300 (2006).
58. Berret, J. F., Herve, P., Aguerre-Chariol, O., and Oberdisse, J. *Journal Of Physical Chemistry B* **107**(32), 8111–8118 (2003).
59. de Vos, W. M., Biesheuvel, P. M., de Keizer, A., Kleijn, J. M., and Cohen Stuart, M. A. *Langmuir* **24**(13), 6575–6584 (2008).
60. Decher, G. *Science* **277**(5330), 1232–1237 (1997).

61. von Klitzing, R. *Physical Chemistry Chemical Physics* **8**(43), 5012–5033 (2006).
62. Sukhishvili, S. A., Kharlampieva, E., and Izumrudov, V. *Macromolecules* **39**(26), 8873–8881 (2006).
63. Voets, I. K., de Keizer, A., Cohen Stuart, M. A., Justynska, J., and Schlaad, H. *Macromolecules* **40**(6), 2158–2164 (2007).
64. Voets, I. K., van der Burgh, S., Farago, B., Fokkink, R., Kovacevic, D., Hellweg, T., de Keizer, A., and Cohen Stuart, M. A. *Macromolecules* **40**, 8476–8482 (2007).
65. Hofs, B., de Keizer, A., and Cohen Stuart, M. A. *Journal of Physical Chemistry B* **111**(20), 5621–5627 (2007).
66. Galisteo, F. and Norde, W. *Colloids and Surfaces B-Biointerfaces* **4**(6), 389–400 (1995).
67. Burke, S. E. and Barrett, C. J. *Langmuir* **19**(8), 3297–3303 (2003).
68. Burke, S. E. and Barrett, C. J. *Pure and Applied Chemistry* **76**(7-8), 1387–1398 (2004).
69. Shiratori, S. S. and Rubner, M. F. *Macromolecules* **33**(11), 4213–4219 (2000).
70. Yoo, D., Shiratori, S. S., and Rubner, M. F. *Macromolecules* **31**(13), 4309–4318 (1998).
71. Petrov, A. I., Antipov, A. A., and Sukhorukov, G. B. *Macromolecules* **36**(26), 10079–10086 (2003).
72. Zintchenko, A., Rother, G., and Dautzenberg, H. *Langmuir* **19**(6), 2507–2513 (2003).
73. Bakeev, K. N., Izumrudov, V. A., Kuchanov, S. I., Zezin, A. B., and Kabanov, V. A. *Macromolecules* **25**(17), 4249–4254 (1992).
74. Sui, Z. J., Salloum, D., and Schlenoff, J. B. *Langmuir* **19**(6), 2491–2495 (2003).
75. Wong, J. E., Rehfeldt, F., Hanni, P., Tanaka, M., and Klitzing, R. V. *Macromolecules* **37**(19), 7285–7289.
76. Itano, K., Choi, J. Y., and Rubner, M. F. *Macromolecules* **38**(8), 3450–3460 (2005).
77. Steitz, R., Jaeger, W., and von Klitzing, R. *Langmuir* **17**(15), 4471–4474 (2001).
78. Glinel, K., Moussa, A., Jonas, A. M., and Laschewsky, A. *Langmuir* **18**(4), 1408–1412 (2002).
79. Voigt, U., Jaeger, W., Findenegg, G. H., and Klitzing, R. V. *Journal of Physical Chemistry B* **107**(22), 5273–5280 (2003).
80. Schoeler, B., Kumaraswamy, G., and Caruso, F. *Macromolecules* **35**(3), 889–897 (2002).
81. Lavalle, P., Gergely, C., Cuisinier, F. J. G., Decher, G., Schaaf, P., Voegel, J. C., and Picart, C. *Macromolecules* **35**(11), 4458–4465 (2002).

82. Lavalle, P., Picart, C., Mutterer, J., Gergely, C., Reiss, H., Voegel, J. C., Senger, B., and Schaaf, P. *Journal of Physical Chemistry B* **108**(2), 635–648 (2004).
83. Hubsch, E., Ball, V., Senger, B., Decher, G., Voegel, J. C., and Schaaf, P. *Langmuir* **20**(5), 1980–1985 (2004).
84. Kovacevic, D., van der Burgh, S., de Keizer, A., and Cohen Stuart, M. A. *Langmuir* **18**(14), 5607–5612 (2002).
85. Lavalle, P., Vivet, V., Jessel, N., Decher, G., Voegel, J. C., Mesini, P., and Schaaf, P. *Macromolecules* **37**, 1159–1162 (2004).
86. Laugel, N., Betscha, C., Winterhalter, M., Voegel, J. C., Schaaf, P., and Ball, V. *Journal of Physical Chemistry B* **110**(39), 19443–19449 (2006).
87. Schlenoff, J. B., Ly, H., and Li, M. *Journal of the American Chemical Society* **120**(30), 7626–7634 (1998).
88. Schonhoff, M., Ball, V., Bausch, A. R., Dejugnat, C., Delorme, N., Glinel, K., Klitzing, R. V., and Steitz, R. *Colloids and Surfaces a-Physicochemical and Engineering Aspects* **303**(1-2), 14–29 (2007).
89. Farhat, T., Yassin, G., Dubas, S. T., and Schlenoff, J. B. *Langmuir* **15**(20), 6621–6623 (1999).
90. Jaber, J. A. and Schlenoff, J. B. *Langmuir* **23**(2), 896–901 (2007).
91. Glinel, K., Prevot, M., Krustev, R., Sukhorukov, G. B., Jonas, A. M., and Mohwald, H. *Langmuir* **20**(12), 4898–4902 (2004).
92. Halthur, T. J. and Elofsson, U. M. *Langmuir* **20**(5), 1739–1745 (2004).
93. Park, J. M., Muhoberac, B. B., Dubin, P. L., and Xia, J. L. *Macromolecules* **25**(1), 290–295 (1992).
94. Caruso, F. and Schuler, C. *Langmuir* **16**(24), 9595–9603 (2000).
95. Kaibara, K., Okazaki, T., Bohidar, H. B., and Dubin, P. L. *Biomacromolecules* **1**(1), 100–107 (2000).
96. Madene, A., Jacquot, M., Scher, J., and Desobry, S. *International Journal of Food Science and Technology* **41**(1), 1–21 (2006).
97. Wei, W. *International Journal of Pharmaceutics* **185**(2), 129–188 (1999).
98. Taluja, A., Youn, Y. S., and Bae, Y. H. *Journal of Materials Chemistry* **17**, 4002–4014 (2007).
99. Solaro, R. *Journal of Polymer Science Part a-Polymer Chemistry* **46**, 1–11 (2008).
100. Silva, J. L. and Weber, G. *Annual Review of Physical Chemistry* **44**, 89–113 (1993).
101. Scharnagl, C., Reif, M., and Friedrich, J. *Biochimica Et Biophysica Acta-Proteins and Proteomics* **1749**(2), 187–213 (2005).
102. Ai, H., Jones, S. A., and Lvov, Y. M. *Cell Biochemistry and Biophysics* **39**(1), 23–43 (2003).

103. Ichikawa, S., Iwamoto, S., and Watanabe, J. *Bioscience Biotechnology and Biochemistry* **69**(9), 1637–1642 (2005).
104. Antipov, A. A. and Sukhorukov, G. B. *Advances in Colloid and Interface Science* **111**(1-2), 49–61 (2004).
105. Allen, C., Maysinger, D., and Eisenberg, A. *Colloids and Surfaces B-Biointerfaces* **16**(1-4), 3–27 (1999).
106. Gaucher, G., Dufresne, M. H., Sant, V. P., Kang, N., Maysinger, D., and Leroux, J. C. *Journal of Controlled Release* **109**(1-3), 169–188 (2005).
107. Nishiyama, N. and Kataoka, K. *Pharmacology and Therapeutics* **112**(3), 630–648 (2006).
108. Bae, Y., Nishiyama, N., and Kataoka, K. *Bioconjugate Chemistry* **18**(4), 1131–1139 (2007).
109. Bae, Y., Nishiyama, N., Fukushima, S., Koyama, H., Yasuhiro, M., and Kataoka, K. *Bioconjugate Chemistry* **16**(1), 122–130 (2005).
110. Bae, Y., Jang, W. D., Nishiyama, N., Fukushima, S., and Kataoka, K. *Molecular Biosystems* **1**(3), 242–250 (2005).
111. Oishi, M., Sasaki, S., Nagasaki, Y., and Kataoka, K. *Biomacromolecules* **4**(5), 1426–1432 (2003).
112. Kono, K., Kawakami, K., Morimoto, K., and Takagishi, T. *Journal of Applied Polymer Science* **72**(13), 1763–1773 (1999).
113. Duinhoven, S., Poort, R., Vandervoet, G., Agterof, W. G. M., Norde, W., and Lyklema, J. *Journal Of Colloid And Interface Science* **170**(2), 351–357 (1995).
114. Izumrudov, V., Kharlampieva, E., and Sukhishvili, S. A. *Macromolecules* **37**(22), 8400–8406 (2004).
115. Jomaa, H. W. and Schlenoff, J. B. *Macromolecules* **38**(20), 8473–8480 (2005).
116. Nicolai, T., Pouzot, M., Durand, D., Weijers, M., and Visschers, R. W. *Europhysics Letters* **73**(2), 299–305 (2006).
117. Postmus, B. R., Leermakers, F. A. M., and Cohen Stuart, M. A. *Langmuir* **24**, 1930 – 1942 (2008).
118. Aswal, V. K., Goyal, P. S., Kohlbrecher, J., and Bahadur, P. *Chemical Physics Letters* **349**(5-6), 458–462 (2001).
119. Hiraoka, K., Shin, H., and Yokoyama, T. *Polymer Bulletin* **8**(7-8), 303–309 (1982).
120. Fischer, H., Polikarpov, I., and Craievich, A. F. *Protein Science* **13**(10), 2825–2828 (2004).
121. Berret, J. F., Yokota, K., Morvan, M., and Schweins, R. *Journal of Physical Chemistry B* **110**(39), 19140–19146 (2006).
122. Pignol, D., Ayvazian, L., Kerfelec, B., Timmins, P., Crenon, I., Hermoso, J., Fontecilla-Camps, J. C., and Chapus, C. *Journal Of Biological Chemistry* **275**(6), 4220–4224 (2000).

123. Chaniotakis, N. A. *Analytical and Bioanalytical Chemistry* **378**(1), 89–95 (2004).
124. Schmitt, C., Bovay, C., and Frossard, P. *Journal of Agricultural and Food Chemistry* **53**(23), 9089–9099 (2005).
125. Serefoglou, E., Oberdisse, J., and Staikos, G. *Biomacromolecules* **8**(4), 1195–1199 (2007).
126. Rehfeldt, F., Steitz, R., Armes, S. P., von Klitzing, R., Gast, A. P., and Tanaka, M. *Journal of Physical Chemistry B* **110**(18), 9177–9182 (2006).
127. Velev, O. D., Kaler, E. W., and Lenhoff, A. M. *Biophysical Journal* **75**(6), 2682–2697 (1998).
128. Yin, N. W. and Chen, K. Q. *Polymer* **45**(11), 3587–3594 (2004).
129. Zhulina, E. B. and Borisov, O. V. *Macromolecules* **35**(24), 9191–9203 (2002).
130. Siyam, T. *Designed Monomers and Polymers* **4**(2), 107–168 (2001).
131. Gurdag, G. and Cavus, S. *Polymers for Advanced Technologies* **17**(11-12), 878–883 (2006).
132. Yan, Y., de Keizer, A., Stuart, M. A. C., Drechsler, M., and Besseling, N. A. M. *Journal of Physical Chemistry B* **112**(35), 10908–10914 (2008).
133. Lindhoud, S., Norde, W., and Cohen Stuart, M. A. *Journal of Physical Chemistry B* **113**(16), 5431–5439 (2009).
134. Voets, I. K. and Leermakers, F. A. M. *Physical Review E* **78**(6) (2008).
135. Scheutjens, J. and Fleer, G. J. *Journal of Physical Chemistry* **83**(12), 1619–1635 (1979).
136. Scheutjens, J. and Fleer, G. J. *Journal of Physical Chemistry* **84**(2), 178–190 (1980).
137. Besseling, N. A. M. and Stuart, M. A. C. *Journal of Chemical Physics* **110**(11), 5432–5436 (1999).
138. Sprakel, J., Leermakers, F. A. M., Stuart, M. A. C., and Besseling, N. A. M. *Physical Chemistry Chemical Physics* **10**(34), 5308–5316 (2008).
139. Jodar-Reyes, A. B. and Leermakers, F. A. M. *Journal of Physical Chemistry B* **110**(12), 6300–6311 (2006).
140. Leermakers, F. A. M. and Scheutjens, J. *Journal of Colloid and Interface Science* **136**(1), 231–241 (1990).
141. Leermakers, F. A. M., Wijmans, C. M., and Fleer, G. J. *Macromolecules* **28**(9), 3434–3443 (1995).
142. Zhulina, E. B. and Leermakers, F. A. M. *Biophysical Journal* **93**(5), 1452–1463 (2007).
143. Zhulina, E. B. and Leermakers, F. A. M. *Biophysical Journal* **93**(5), 1421–1430 (2007).
144. van der Burgh, S. *Complex Coacervate Core Micelles in Solution and at Interfaces (PhD thesis).* (2004). PhD thesis.

145. Eberstein, W., Georgalis, Y., and Saenger, W. *Journal of Crystal Growth* **143**(1-2), 71–78 (1994).
146. Cygler, M. and Schrag, J. D. *Lipases, Part A* **284**, 3–27 (1997).
147. Svendsen, A., Clausen, I. G., Patkar, S. A., Borch, K., and Thellersen, M. *Lipases, Part A* **284**, 317–340 (1997).
148. Noinville, S., Revault, M., Baron, M. H., Tiss, A., Yapoudjian, S., Ivanova, M., and Verger, R. *Biophysical Journal* **82**(5), 2709–2719 (2002).
149. Martinelle, M., Holmquist, M., and Hult, K. *Biochimica Et Biophysica Acta-Lipids and Lipid Metabolism* **1258**(3), 272–276 (1995).
150. Cajal, Y., Busquets, M. A., Carvajal, H., Girona, V., and Alsina, M. A. *Journal of Molecular Catalysis B-Enzymatic* **22**(5-6), 315–328 (2003).
151. Hedin, E. M. K., Hoyrup, P., Patkar, S. A., Vind, J., Svendsen, A., and Hult, K. *Biochemistry* **44**(50), 16658–16671 (2005).
152. Berg, O. G., Cajal, Y., Butterfoss, G. L., Grey, R. L., Alsina, M. A., Yu, B. Z., and Jain, M. K. *Biochemistry* **37**(19), 6615–6627 (1998).
153. deRuyter, P., Kuipers, O. P., Beerthuyzen, M. M., vanAlenBoerrigter, I., and deVos, W. M. *Journal of Bacteriology* **178**(12), 3434–3439 (1996).
154. Brzozowski, A. M., Savage, H., Verma, C. S., Turkenburg, J. P., Lawson, D. M., Svendsen, A., and Patkar, S. *Biochemistry* **39**(49), 15071–15082 (2000).
155. Cajal, Y., Svendsen, A., Girona, V., Patkar, S. A., and Alsina, M. A. *Biochemistry* **39**(2), 413–423 (2000).
156. Holmquist, M., Norin, M., and Hult, K. *Lipids* **28**(8), 721–726 (1993).
157. Palomo, J. M., Fuentes, M., Fernandez-Lorente, G., Mateo, C., Guisan, J. M., and Fernandez-Lafuente, R. *Biomacromolecules* **4**(1), 1–6 (2003).
158. Ladam, G., Gergely, C., Senger, B., Decher, G., Voegel, J. C., Schaaf, P., and Cuisinier, F. J. G. *Biomacromolecules* **1**(4), 674–687 (2000).
159. Wittemann, A. and Ballauff, M. *Physical Chemistry Chemical Physics* **8**(45), 5269–5275 (2006).
160. Seyrek, E., Dubin, P. L., Tribet, C., and Gamble, E. A. *Biomacromolecules* **4**(2), 273–282 (2003).
161. Leermakers, F. A. M., Ballauff, M., and Borisov, O. V. *Langmuir* **23**(7), 3937–3946 (2007).
162. Czeslik, C., Jackler, G., Steitz, R., and von Grunberg, H. H. *Journal of Physical Chemistry B* **108**(35), 13395–13402 (2004).
163. Bucur, C. B., Sui, Z., and Schlenoff, J. B. *Journal of the American Chemical Society* **128**(42), 13690–13691 (2006).
164. Picart, C., Mutterer, J., Richert, L., Luo, Y., Prestwich, G. D., Schaaf, P., Voegel, J. C., and Lavalle, P. *Proceedings of the National Academy of Sciences of the United States of America* **99**(20), 12531–12535

(2002).
165. Porcel, C., Lavalle, P., Ball, V., Decher, G., Senger, B., Voegel, J. C., and Schaaf, P. *Langmuir* **22**(9), 4376–4383 (2006).
166. Porcel, C., Lavalle, P., Decher, G., Senger, B., Voegel, J. C., and Schaaf, P. *Langmuir* **23**(4), 1898–1904 (2007).
167. Fuoss, R. M. and Sadek, H. *Science* **110**(2865), 552–554 (1949).
168. Michaels, A. S. *Industrial and Engineering Chemistry* **57**(10), 32–40 (1965).
169. Voigt, U., Khrenov, V., Thuer, K., Hahn, M., Jaeger, W., and von Klitzing, R. *Journal of Physics-Condensed Matter* **15**(1), S213–S218 (2003).
170. Nazaran, P., Bosio, V., Jaeger, W., Anghel, D. F., and von Klitzing, R. *Journal of Physical Chemistry B* **111**(29), 8572–8581 (2007).
171. Xie, A. F. and Granick, S. *Macromolecules* **35**(5), 1805–1813 (2002).
172. Izumrudov, V. and Sukhishvili, S. A. *Langmuir* **19**(13), 5188–5191 (2003). I.
173. Lindhoud, S., de Vries, R., Norde, W., and Cohen Stuart, M. A. *Biomacromolecules* **8**(7), 2219–2227 (2007).
174. Dubas, S. T. and Schlenoff, J. B. *Langmuir* **17**(25), 7725–7727 (2001).
175. Kunz, W., Nostro, P. L., and Ninham, B. W. *Current Opinion in Colloid and Interface Science* **9**(1-2), 1 – 18 (2004).
176. Wignall, P. B. and Twitchett, R. J. *Science* **272**(5265), 1155–1158 (1996).
177. Honglei Zhang, A. S. J.-M. G. R. C. *Macromolecular Symposia* **251**(1), 25–32 (2007).
178. Burg, M. B. *Cellular Physiology and Biochemistry* **10**(5-6), 251–256 (2000).
179. Minton, A. P. *Journal of Cell Science* **119**(14), 2863–2869 (2006).
180. Ellis, R. J. *Trends in Biochemical Sciences* **26**(10), 597–604 (2001).
181. Zaitsev, S. Y., Gorokhova, I. V., Kashtigo, T. V., Zintchenko, A., and Dautzenberg, H. *Colloids And Surfaces A-Physicochemical And Engineering Aspects* **221**(1-3), 209–220 (2003).
182. Onda, M., Lvov, Y., Ariga, K., and Kunitake, T. *Biotechnology and Bioengineering* **51**(2), 163–167 (1996).
183. Onda, M., Ariga, K., and Kunitake, T. *Journal of Bioscience and Bioengineering* **87**(1), 69–75 (1999).
184. Caruso, F., Trau, D., Mohwald, H., and Renneberg, R. *Langmuir* **16**(4), 1485–1488 (2000).
185. Hamlin, R. E., Dayton, T. L., Johnson, L. E., and Johal, M. S. *Langmuir* **23**(8), 4432–4437 (2007).
186. Jessel, N., Atalar, F., Lavalle, P., Mutterer, J., Decher, G., Schaaf, P., Voegel, J. C., and Ogier, J. *Advanced Materials* **15**(9), 692–695 (2003).

187. Leguen, E., Chassepot, A., Decher, G., Schaaf, P., Voegel, J. C., and Jessel, N. *Biomolecular Engineering* **24**(1), 33–41 (2007).
188. Jin, W., Shi, X. Y., and Caruso, F. *Journal of the American Chemical Society* **123**(33), 8121–8122 (2001).
189. Oparin, A. I. *The origin of life*. New York: Dover (1952) (first published in 1938), (1924).

List of Publications

This dissertation:

- Saskia Lindhoud, Willem Norde and Martien Cohen Stuart: **Effects of polyelectrolyte complex micelles and their components on the enzymatic activity of lipase**, *submitted to Biomacromolecules*
- Saskia Lindhoud, Lenny Voorhaar, Renko de Vries, Ralf Schweins, Martien Cohen Stuart and Willem Norde: **Salt-induced Disintegration of Lysozyme-containing polyelectrolyte complex micelles**, *accepted in Langmuir*
- Saskia Lindhoud, Willem Norde, Martien Cohen Stuart and Frans Leermakers: **SCF calculations of protein incorporation in polyelectrolyte complex micelles**, *submitted to Physical Review E*
- Saskia Lindhoud, Willem Norde and Martien Cohen Stuart: **Reversibility and Relaxation Behaviour of Polyelectrolyte Complex Micelle Formation**, *The Journal of Physical Chemistry B*, 113(15), 5431-5439, 2009
- Saskia Lindhoud, Renko de Vries, Ralf Schweins, Martien Cohen Stuart and Willem Norde: **Salt-induced Release of Lipase from Polyelectrolyte Complex Micelles**, *Soft Matter*, 5, 242-250, 2009
- Saskia Lindhoud, Renko de Vries, Willem Norde and Martien Cohen Stuart: **Structure and Stability of Complex Coacervate Core Micelles with Lysozyme**, *Biomacromolecules*, Volume 8, 7, 2219-2227, 2007

Other work:

- Hans Tromp and Saskia Lindhoud: **Arrested segregative phase separation in capillary tubes**, *Physical Review E*, Volume 74, 3, 2006
- Maarten Biesheuvel, Saskia Lindhoud, Renko de Vries and Martien Cohen Stuart: **Phase behaviour of mixtures of oppositely charged protein nanoparticles at asymmetric charge ratios**, *Physical Review E*, Volume 74, 3, 2006
- Maarten Biesheuvel, Saskia Lindhoud, Renko de Vries and Martien Cohen Stuart: **Phase behaviour of mixtures of oppositely charged nanoparticles: Heterogeneous Poisson-Boltzmann cell model applied to lysozyme and succinylated lysozyme**, *Langmuir*, Volume 22, 3, 1291-1300, 2006

Dankwoord

Net als bij de aftiteling van een film, hoort bij het eind van een proefschrift ook een soort aftiteling, namelijk het dankwoord. Gedurende mijn bijna vier jaar durende onderzoek hebben veel mensen mij bijgestaan en daar ben ik hen dankbaar voor. Natuurlijk begin je zo'n aftiteling met de meest belangrijke personen die hebben bijgedragen aan de totstandkoming van dit proefschrift.

Martien, ik bewonder je inzicht in de wetenschap en de inspirerende manier waarop je AIO's begeleidt. Bedankt voor je hulp, de goede discussies en de vrijheid die je me gegeven hebt in het uitvoeren van mijn onderzoek. Willem, het was fijn om met je over mijn onderzoek te praten, je kritische opmerken hebben mij vaak aan het denken gezet en hebben tot nieuwe ideeën en inzichten geleidt. Ook vond ik het heel speciaal om samen met jou naar Japan te gaan. Frans, met je enthousiasme sleep je iedereen mee. Van ons gezamenlijke werk heb ik enorm veel geleerd en het heeft ons nieuwe inzichten gegeven. Ook vond ik het leuk om met jou de Polyamphi Summer School te organiseren en ben ik blij dat je me overtuigd hebt om Latex te gebruiken. Renko, bedankt voor je hulp bij het uitvoeren en analyseren van de neutronenverstrooiingsmetingen. Remco, ik wil jou in het bijzonder bedanken, het goede onderhoud van de lichtverstrooiiers was essentieel voor het slagen van mijn onderzoek.

Ik heb genoten van de verschillende buitenlandse reizen en met name de AIO reis naar Zweden en Denemarken. Ik wil alle andere AIO's bedanken voor de gezellige tijd, maar een aantal in het bijzonder. Bart, het was leuk om met jou een kamer te delen. Bas 'Syntheseman' Hofs, ik vond het heel gezellig om met jou Praag onveilig te maken. Joris, je was een gezellige buurman en ik heb veel om, en met je gelachen, het is fijn dat er iemand is die net zo'n dirty mind heeft als ik. Agata and Paulina, you were great roommates and Paulina, thanks for accompanying me to Grenoble.

Lenny en Sjoerd, ik vond het leuk om jullie te begeleiden met jullie afstudeervak. Ik wens jullie alle goeds toe voor de toekomst.

Niet alleen op wetenschappelijk gebied is Fysko een leuke plek om te werken, ook de goede sfeer heeft enorm bijgedragen aan het plezier in mijn werk. De gezellige koffie en lunch pauzes, de labuitjes ga ik zeker missen. Ik wil iedereen van Fysko bedanken voor de geweldige tijd. Josie, ik wil jou in het bijzonder bedanken voor je interesse, steun en je wijze lessen. Mara en Anita, bedankt voor jullie gezelligheid en hulp.

Natuurlijk wil ik ook al mijn vrienden en familie en nieuwe familie bedanken voor hun steun. Johannes, bedankt voor het doorlezen van mijn introductie en samenvatting. Peter en Teuntje, en Simon en Corinne, ik wil jullie bedanken voor al jullie steun. Het was en is allemaal niet zo gemakkelijk en ik hoop dat het in de toekomst wat makkelijker wordt voor ons allemaal. Peter en Simon, ik vind het geweldig en heel speciaal dat jullie mijn paranimfen willen zijn en ik wil jullie veel succes wensen met het afronden van jullie proefschrift.

Lieve Wiebe, voor jou zijn de laatste regels. Ik wil je zowel bedanken voor de eerste twee jaar van mijn promotie toen je nog gewoon een leuke collega was als voor de afgelopen twee jaar, toen je wat meer werd dan dat. Het is fijn dat iemand begrijpt waar je precies mee bezig bent. Bedankt voor al je steun en advies. Ik hoop dat we wat minder zware en onzekere tijden tegemoet gaan en dat onze gezamenlijke promotie daar het begin van is.

Saskia

Levensloop

Saskia Lindhoud werd op 2 April 1982 geboren in Lundazi, Zambia. In 2000 nam ze haar diploma, behaald aan het Gymnansium Celeanum te Zwolle, in ontvangst. Datzelde jaar begon ze aan de studie Moleculaire Wetenschappen aan Wageningen Universiteit. Haar eerste afstudeervak werd uitgevoerd aan het laboratorium voor Biofysica. Met behulp van Electron Spin Resonantie werd geprobeerd om dynamische informatie te krijgen over gespinlabelde peptiden van een vacuolar ATP-ase. Tijdens haar tweede aftudeervak, uitgevoerd aan het Laboratorium voor Fysische Chemie en Kolloïdkunde, werd de interactie tussen twee tegengesteld geladen lysozyme moleculen bestudeerd. Haar stage voerde Saskia uit bij NIZO Food Research in Ede. Hier bestudeerde ze het fasegedrag van gelatine en dextraan in capilairen. September 2005 studeerde ze af, met als specialisatie Fysiche Chemie. Oktober van dat jaar begon ze aan haar promotie-onderzoek aan het Laboratorium voor Fysische Chemie en Kolloïdkunde. Dit onderzoek resulteerde in het proefschrift met de titel: Polyelectrolyte Complex Micelles as Wrapping for Enzymes.

Overview of completed training activities

Discipline specific activities

Polyamphi Summer school, Chodova Plana, Czeck Republic, 2005*
Winter school, Han-sur-Lesse, Belgium, 2006
Summer School: scattering methods, Bombannes, France, 2006
Prague meetings on macromolecules, Prague, Czeck Republic, 2006
SONS Networking Activity Workshop, Prague, Czeck Republic, 2006*
UT symposium on NanoBio Integration, Tokyo, Japan 2006†
JSPS Core-to-Core meeting," Kyoto, Japan 2006*
Colloquium University of Tokyo, Japan 2006*
Winter school, Han-sur-Lesse, Belgium, 2007
RPK-B: Polymer Physics, Utrecht, the Netherlands 2007
Student conference, Ven, Sweden, 2007*
Polyamphi Summer school, Biezenmortel, the Netherlands, 2007
Dutch Polymer Days, Lunteren, the Netherlands, 2008*
Liquid Matter Conference, Lund, Sweden, 2008†
ECIS, Cracow, Poland, 2008*
Dutch Polymer Days, Lunteren, the Netherlands, 2009*
Colloquium Laboratory of Biosensors and Bioelectronics, ETH Zürich, 2009*
Colloquium Laboratory of Complex Materials, ETH Zürich, 2009*
Colloquium Nizo Food research Ede, 2009*
IACIS, New York, USA, 2009*
Gordon Research Conference, Waterville ME, USA, 2009†
* =oral contribution, † = poster

General Courses

Personal competence, time management and project planning, WUR, 2004
Symposium "Women in Chemistry," NWO, 2008
Learning how to use the computer program "Latex"
Introduction to Summer school organisation and management, 2007

Optional courses and activities

Work group meetings 2005-2009
Colloquia 2005-2009
PhD-study trip Sweden and Denmark, 2007
Introduction to Summer school organisation and management, 2007